

Photoactivatable Sensors for Detecting Mobile Zinc

Jacob M. Goldberg,^{†,§} Fang Wang,^{†,§} Chanan D. Sessler,[†] Nathan W. Vogler,[‡] Daniel Y. Zhang,[†] William H. Loucks,[†] Thanos Tzounopoulos,[‡] and Stephen J. Lippard*,[†]

[†]Department of Chemistry, Massachusetts Institute of Technology, 77 Massachusetts Avenue,
Cambridge, MA 02139, United States

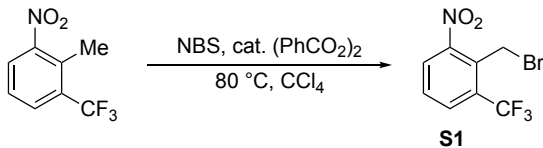
[‡]Pittsburgh Hearing Research Center, Department of Otolaryngology, University of Pittsburgh, 3501 Fifth
Avenue, Pittsburgh, Pennsylvania 15261, United States

General Materials and Methods.

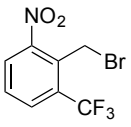
Reagents were purchased from commercial sources and used as received. Zinpyr-1 (ZP1) and the diacetylated derivative DA-ZP1 were synthesized as previously described.¹⁻² NMR spectra were acquired on a 400 MHz Bruker AVANCE-400 spectrometer. ¹H NMR chemical shifts are reported in ppm relative to that of SiMe₄ (δ = 0.00) and were referenced internally to residual solvent peaks.³ Low-resolution electrospray mass spectra were acquired on an Agilent 1100 Series LC/MSD Trap spectrometer. High-resolution mass spectra were acquired on a Bruker Daltonics APEXIV 4.7 tesla Fourier transform ion cyclotron resonance mass spectrometer at the MIT Department of Chemistry Instrumentation Facility. Compounds were purified using Agilent 1200 Series HPLC systems fitted with multi-wavelength detectors and automated fraction collectors using a C18 reverse stationary phase (Zorbax-SB C18 columns: preparative, 7 μ m, 21.2 \times 250 mm; semi-preparative, 5 μ m 9.4 \times 250 mm; and analytical, 5 μ m, 4.6 \times 250 mm) and a mobile phase composed of two solvents (A: H₂O + 0.1% (v/v) CF₃CO₂H; B: CH₃CN + 0.1% (v/v) CF₃CO₂H). UV-visible spectra were recorded on a Varian Cary 50 Bio UV-visible spectrophotometer. Fluorescence measurements were made with a Photon Technologies International 4L-format scanning spectrofluorometer equipped with a temperature-controlled, 4-position sample turret. Quartz cuvettes with 1.00 cm path lengths were used for all spectroscopic measurements. Milli-Q purified water with resistivity of at least 18 M Ω ·cm⁻¹ was used to prepare all buffers. Aqueous buffers were treated with Chelex® resin according to the manufacturer's instructions prior to use.

Chemical Synthesis.

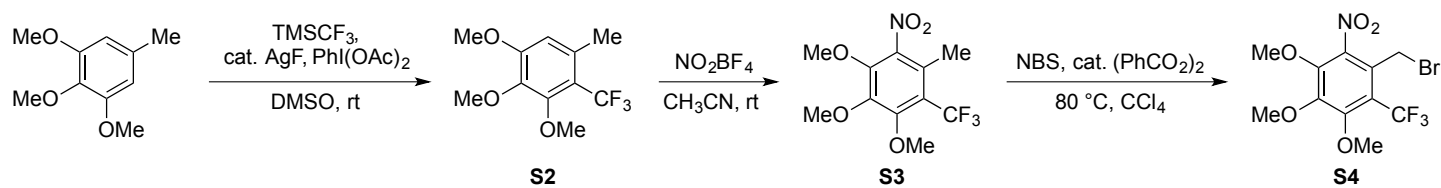
Scheme S1. Synthesis of 2-(bromomethyl)-1-nitro-3-(trifluoromethyl)benzene (**S1**).



2-(Bromomethyl)-1-nitro-3-(trifluoromethyl)benzene (**S1**)

 In a 50 mL round-bottom pressure vessel, 2-methyl-1-nitro-3-(trifluoromethyl)benzene (1026 mg, 5.00 mmol), *N*-bromosuccinimide (NBS, 797 mg, 5.50 mmol), and benzoyl peroxide (61 mg, 0.25 mmol) were mixed with CCl₄ (30 mL). The reaction was heated at 80 °C (oil bath temperature) in ambient light. Additional NBS (445 mg, 0.5 equiv) was added at 24 h. Another portion of NBS (223 mg, 0.25 equiv) was added at 48 h. After 72 h, the solvent was evaporated under vacuum and the crude product was purified by column chromatography (EtOAc:hexanes = 1:8 to 1:6). A colorless oil was obtained (951 mg, 67% yield). ¹H NMR (400 MHz, CDCl₃) δ 8.06 (dd, J = 8.2, 0.9 Hz, 1H), 7.94 (d, J = 8.0 Hz, 1H), 7.63 (tq, J = 8.1, 0.8 Hz, 1H), 4.93 (s, 2H). ¹⁹F NMR (376 MHz, CDCl₃) δ -59.4 (s, 3F). EI-MS(+) *m/z* calcd for [M]⁺ 283, found 283. Spectroscopic data are consistent with reported values.⁴

Scheme S2. Synthesis of 1-(bromomethyl)-3,4,5-trimethoxy-2-nitro-6-(trifluoromethyl)benzene (**S4**).



1,2,3-Trimethoxy-5-methyl-4-(trifluoromethyl)benzene (**S2**)

Anhydrous DMSO (36 mL) was added through a syringe to a Schlenk flask containing 3,4,5-trimethoxytoluene (3.28 g, 18.0 mmol), $\text{PhI}(\text{OAc})_2$ (11.6 g, 36.0 mmol), and AgF (571 mg, 4.50 mmol). TMSCF_3 (5.31 mL, 36.0 mmol) was added to the flask dropwise. The slightly exothermic reaction was stirred under an inert atmosphere for 12 h. The reaction was mixed with brine (100 mL) and EtOAc (30 mL). The mixture was then filtered and the solid was washed with EtOAc (15 mL). The organic phase was isolated and the aqueous phase was extracted with EtOAc (30 mL \times 3). The combined organic phase was washed with brine (30 mL \times 3) and dried over MgSO_4 . The solvent was evaporated under vacuum. The crude product was purified by column chromatography ($\text{EtOAc:hexanes} = 1:8$). A slightly yellow oil was obtained (2.65 g, 59% yield). ^1H NMR (400 MHz, CDCl_3) δ 6.49 (s, 1H), 3.91 (s, 3H), 3.88 (s, 3H), 3.85 (s, 3H), 2.43 (qd, $J_{\text{H-F,through space}} = 3.5$ Hz, $J_{\text{H-H,through space}} = 0.5$ Hz, 3H). ^{19}F NMR (376 MHz, CDCl_3) δ -54.8 (q, $J_{\text{H-F,through space}} = 3.5$ Hz, 3F). EI-MS(+) m/z calcd for $[\text{M}]^+$ 250, found 250. Spectroscopic data are consistent with reported values.⁵

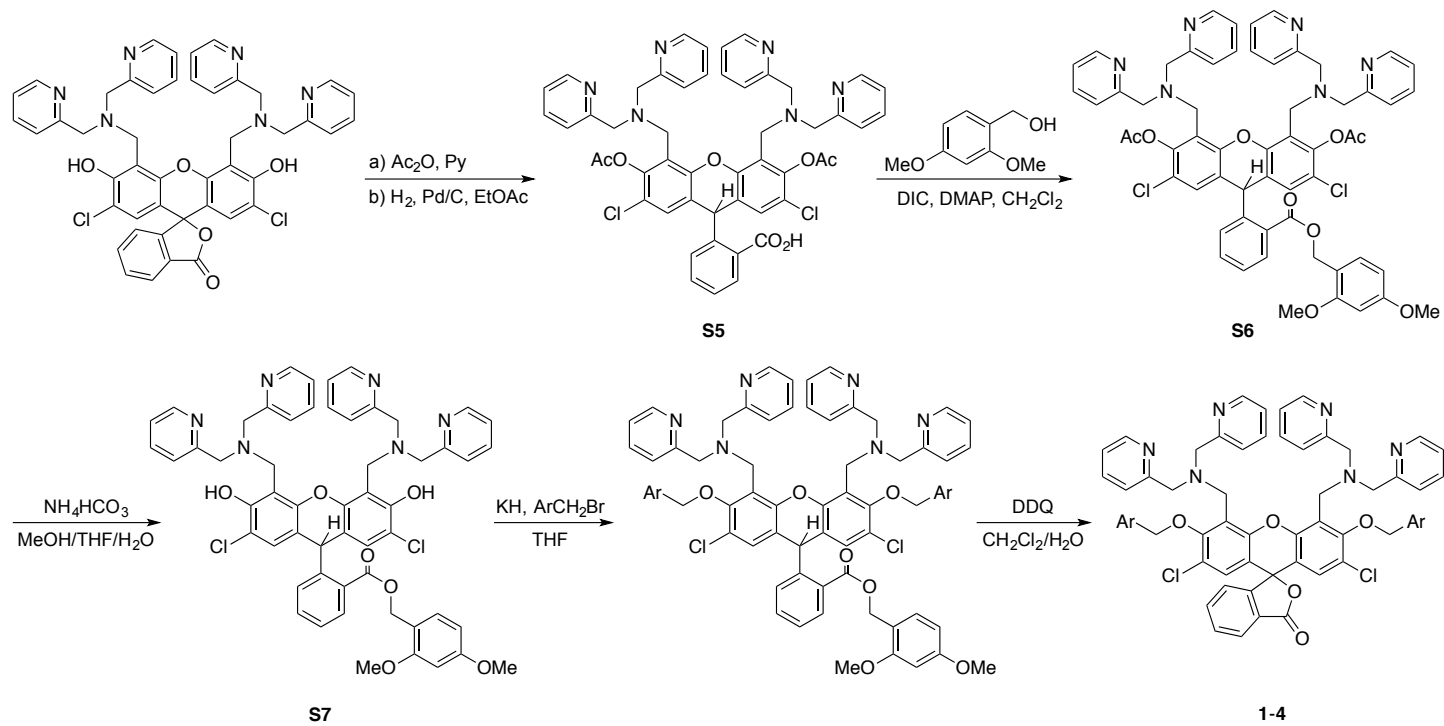
1,2,3-Trimethoxy-5-methyl-4-nitro-6-(trifluoromethyl)benzene (**S3**)

In a glovebox, NO_2BF_4 (1.11 g, 8.40 mmol) was added in one portion to 1,2,3-trimethoxy-5-methyl-4-(trifluoromethyl)benzene (**S2**, 1.75 g, 7.00 mmol) in anhydrous CH_3CN (70 mL). The reaction was stirred at room temperature for 30 min. The reaction mixture was removed from the glovebox and quenched with H_2O (100 mL). The mixture was extracted with CH_2Cl_2 (50 mL \times 3). The organic phase was dried over MgSO_4 . The crude product was purified by column chromatography ($\text{EtOAc:hexanes} = 1:8$). A white solid was obtained (378 mg, 18% yield). ^1H NMR (400 MHz, CDCl_3) δ 4.02 (s, 3H), 3.94 (s, 3H), 3.91 (s, 3H), 2.28 (q, $J_{\text{F-H,through space}} = 3.0$ Hz, 3H). ^{13}C NMR (101 MHz, CDCl_3) δ 155.4 (q, $^3J_{\text{C-F}} = 1.7$ Hz), 148.0, 145.4, 143.9, 124.8 (q, $^3J_{\text{C-F}} = 1.6$ Hz), 123.8 (q, $^1J_{\text{C-F}} = 275.5$ Hz), 119.0 (q, $^2J_{\text{C-F}} = 29.6$ Hz), 62.4, 62.2 (q, $J_{\text{C-F,through space}} = 0.9$ Hz), 61.3, 14.6 (q, $J_{\text{C-F,through space}} = 4.6$ Hz). ^{19}F NMR (376 MHz, CDCl_3) δ -55.0 (q, $J_{\text{F-H,through space}} = 2.9$ Hz, 3F). EI-MS(+) m/z calcd for $[\text{M}]^+$ 295, found 295.

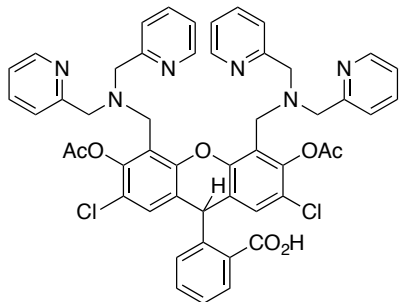
1-(Bromomethyl)-3,4,5-trimethoxy-2-nitro-6-(trifluoromethyl)benzene (S4)

In a 150 mL round bottom pressure vessel, 1,2,3-trimethoxy-5-methyl-4-nitro-6-(trifluoromethyl)benzene (**S3**, 354 mg, 1.20 mmol), NBS (214 mg, 1.20 mmol), and benzoyl peroxide (9.7 mg, 0.04 mmol) were mixed with CCl_4 (60 mL). The reaction was heated at 80 °C (oil bath temperature) in ambient light. Additional NBS (642 mg, 3.0 equiv) was added in three equal portions at 24 h, 48 h, and 72 h. After 96 h, the solvent was evaporated under vacuum and the crude product was purified by column chromatography (EtOAc:hexanes = 1:8). A white solid was obtained (181 mg, 40% yield). The starting material was recovered as a white solid (195 mg, 55% recovered). ^1H NMR (400 MHz, CDCl_3) δ 4.47 (q, $J_{\text{F}-\text{H},\text{through space}} = 1.0$ Hz, 2H), 4.04 (s, 3H), 3.98 (s, 3H), 3.95 (s, 3H). ^{13}C NMR (101 MHz, CDCl_3) δ 155.9 (q, $^3J_{\text{C}-\text{F}} = 1.6$ Hz), 148.6, 147.8, 143.4, 123.8 (q, $^3J_{\text{C}-\text{F}} = 1.2$ Hz), 123.4 (q, $^1J_{\text{C}-\text{F}} = 275.9$ Hz), 118.7 (q, $^2J_{\text{C}-\text{F}} = 30.1$ Hz), 62.6, 62.3 (q, $J_{\text{C}-\text{F},\text{through space}} = 0.8$ Hz), 61.3, 21.5 (q, $J_{\text{C}-\text{F},\text{through space}} = 5.3$ Hz). ^{19}F NMR (376 MHz, CDCl_3) δ -55.2 (s, 3F). EI-MS(+) m/z calculated for $[\text{M}]^+$ 373, found 373.

Scheme S3. Synthesis of Protected Sensors (**1-4**).



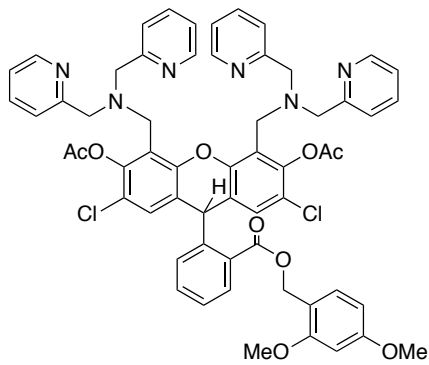
2-(3,6-Diacetoxy-4,5-bis((bis(pyridin-2-ylmethyl)amino)methyl)-2,7-dichloro-9H-xanthen-9-yl)benzoic acid (S5)



DA-ZP1 (1.09 g, 1.20 mmol) was dissolved in EtOAc (250 mL). The mixture was degassed with N₂ for 15 min. A portion of Pd/C (250 mg, 10 wt %) was added and the reaction was stirred under an H₂ atmosphere for 24 h. Additional Pd/C (500 mg) was added in two equal portions at 24 h and 48 h. After 72 h, the reaction was monitored by ESI-MS to confirm completion of the reduction.

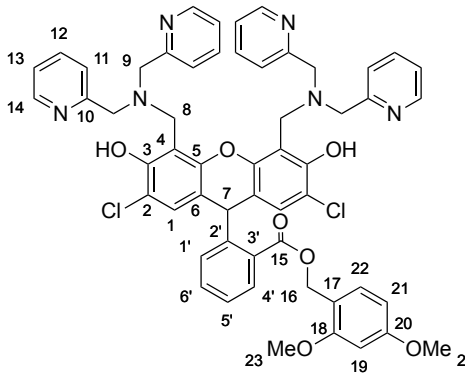
The reaction mixture was flushed with N₂ and filtered through Celite. The filtrate was then filtered through a 0.2 µm PTFE syringe filter. The solvent was removed under vacuum to give a slightly pink foam (1.09 g, 100%). The solid was used directly in the next step without further purification. MS (ESI+): *m/z* calcd for [M+H]⁺ 909.3, found 909.3.

4,5-Bis((bis(pyridin-2-ylmethyl)amino)methyl)-2,7-dichloro-9-(2-(((2,4-dimethoxybenzyl)oxy)carbonyl)-phenyl)-9H-xanthene-3,6-diyl diacetate (S6)



purification. MS (ESI+): *m/z* calcd for [M+H]⁺ 1059.3, found 1059.4.

2,4-Dimethoxybenzyl 2-(4,5-bis((bis(pyridin-2-ylmethyl)amino)methyl)-2,7-dichloro-3,6-dihydroxy-9H-xanthen-9-yl)benzoate (S7)



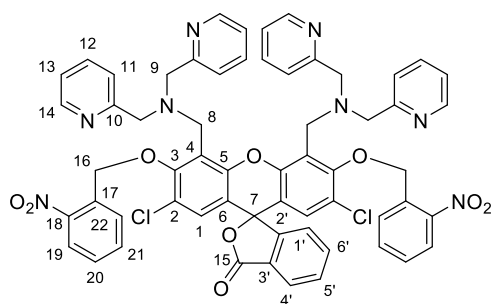
Compound S6 (ca. 1.20 mmol, crude) was dissolved in a mixture of THF (120 mL) and MeOH (60 mL). An aqueous solution of NH₄HCO₃ (1.93 g, 24.4 mmol, in 60 mL of H₂O) was then added. The reaction was stirred in the dark at room temperature and monitored by ESI-MS. Deacetylation was complete after 3 days. The organic solvents were removed with a rotavap. The crude product in water was dissolved in CH₃CN (ca. 350 mL) and purified by preparative HPLC using solvent gradeint 1 (Table S1). Fractions containing the desired product (*t_R* = 11.2 min) were combined and lyophilized to give a light orange solid (61 mg, 51%). ¹H NMR (400 MHz, CD₃CN) δ 8.67 (d, *J* = 5.6 Hz, 4H), 8.10 (t, *J* = 7.8 Hz, 4H), 7.71 (dd, *J* = 7.9, 1.4 Hz, 1H), 7.68 (d, *J* = 8.2 Hz, 4H), 7.63 (t, *J* = 6.7 Hz, 4H), 7.41 (td, *J* = 7.7,

1.4 Hz, 1H), 7.32 – 7.24 (m, 2H), 6.99 (d, J = 8.5 Hz, 1H), 6.70 (s, 2H), 6.50 (s, 1H), 6.49 (dd, J = 8.0, 3.6 Hz, 1H), 5.72 (s, 1H), 5.23 (s, 2H), 4.37 (s, 8H), 4.17 (pseudo q, AB system, J = 13.6 Hz, 4H), 3.76 (s, 3H), 3.72 (s, 3H). ^{13}C NMR (101 MHz, CD₃CN) δ 168.9, 162.7, 160.1, 155.2, 152.7, 148.7, 146.5, 144.6, 144.3, 133.3, 132.6, 132.0, 131.2, 130.5, 130.2, 128.0, 126.7, 126.1, 117.6, 116.9, 116.8, 112.8, 105.4, 99.3, 63.7, 58.0, 56.3, 56.0, 49.7, 38.8. ESI-MS(+) m/z calcd for [M+H]⁺ 975.3, found 975.2.

General procedure for preparation of 1 and other derivatives.

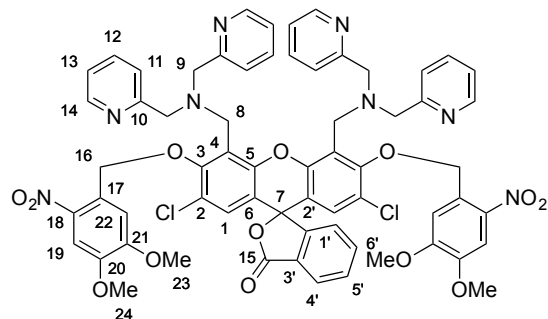
In an anaerobic glovebox, potassium hydride (7.6 mg, 0.192 mmol) was added to a Schlenk flask containing a solution of **S7** (31.2 mg, 0.032 mmol) in THF (4 mL). The reaction was stirred at room temperature for 30 min before the addition of *o*-nitrobenzyl bromide (34.6 mg, 0.320 mmol). The reaction flask was wrapped with aluminum foil and the reaction was stirred overnight. The reaction was monitored by ESI-MS(+) to confirm the formation of the desired product (m/z calcd for [M+H]⁺ = 1245.4, found 1245.5). The Schlenk flask was removed from the glovebox and attached to a manifold. The reaction was quenched with water (0.1 mL) and the solvent was evaporated. The crude product was stirred with CH₂Cl₂/H₂O (3.0 mL/0.6 mL). A portion of 2,3-dichloro-5,6-dicyano-1,4-benzoquinone (DDQ, 72.6 mg, 0.320 mmol) was added and the reaction was stirred at room temperature in the dark for 24 h. The organic solvent was evaporated and the residue was dissolved in CH₃CN/H₂O (27 mL/27 mL). Insoluble material was removed by filtration through a 0.2 μm PTFE syringe filter. The crude product was purified by preparative and semi-preparative HPLC using the solvent gradients indicated below. Fractions containing the desired compound were combined and lyophilized.

4',5'-Bis((bis(pyridin-2-ylmethyl)amino)methyl)-2',7'-dichloro-3',6'-bis((2-nitrobenzyl)oxy)-3H-spiro[isobenzofuran-1,9'-xanthen]-3-one (1)



This compound was prepared by using **S7** (0.032 mmol) and *o*-nitrobenzyl bromide (0.32 mmol) according to the general procedure. The crude material was purified by preparative HPLC using solvent gradient 2 (Table S1). Further purification by semi-preparative HPLC using solvent gradient 3 (Table S1) afforded a slightly yellow solid (19.7 mg, 56% yield). UV (CH₃CN) $\varepsilon_{254} = 45,500 \text{ M}^{-1} \cdot \text{cm}^{-1}$. ^1H NMR (400 MHz, CD₃CN) δ 8.49 (dd, J = 5.2, 0.7 Hz, 4H), 8.14 (dd, J = 8.2, 1.2 Hz, 2H), 8.05 (d, J = 7.9 Hz, 2H), 8.02 (dt, J = 7.7, 0.9 Hz, 1H), 7.90 – 7.72 (m, 8H), 7.61 (pseudo dt, J = 8.2, 1.4 Hz, 2H), 7.42 (d, J = 7.9 Hz, 4H), 7.38 (dd, J = 7.0, 6.0 Hz, 4H), 7.22 (d, J = 7.7 Hz, 1H), 6.73 (s, 2H), 5.40 (s, 4H), 4.32 (pseudo dd, J = 20.7, 12.7 Hz, 4H), 4.26 (s, 8H). ^{13}C NMR (101 MHz, CD₃CN) δ 169.1, 157.3, 156.3, 151.5, 150.0, 147.9, 146.2, 141.9, 136.9, 135.3, 133.7, 131.9, 130.0, 129.8(0), 129.7(8), 127.5, 126.6, 125.9, 125.4, 125.0, 124.9, 124.6, 122.3, 117.7, 81.6, 73.1, 59.3, 50.2. ESI-HRMS(+) m/z calcd for C₆₀H₄₇Cl₂N₈O₉⁺ [M+H]⁺ 1093.2838, found 1093.2819.

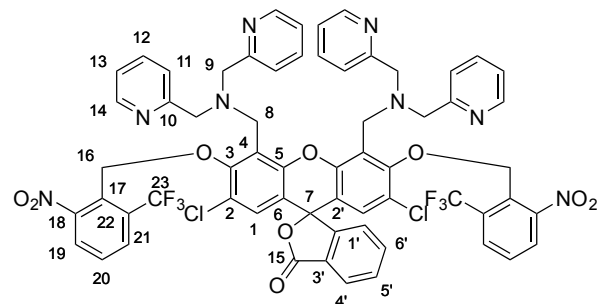
4',5'-Bis((bis(pyridin-2-ylmethyl)amino)methyl)-2',7'-dichloro-3',6'-bis((4,5-dimethoxy-2-nitrobenzyl)oxy)-3H-spiro[isobenzofuran-1,9'-xanthen]-3-one (2)



This compound was prepared by using S7 (0.040 mmol) and 4,5-dimethoxy-2-nitrobenzyl bromide (0.40 mmol) according to the general procedure. The crude material was purified by preparative HPLC using solvent gradient 4 (Table S1). Further purification by semi-preparative HPLC using solvent gradient 5 (Table S1) afforded a slightly yellow solid (21.8 mg, 45% yield). UV (CH_3CN)

$\epsilon_{254} = 55,300 \text{ M}^{-1}\cdot\text{cm}^{-1}$ and $\epsilon_{300} = 14,700 \text{ M}^{-1}\cdot\text{cm}^{-1}$. ^1H NMR (400 MHz, CD_3CN) δ 8.48 (br dd, $J = 5.3, 0.7 \text{ Hz}$, 4H), 8.02 (d, $J = 7.7 \text{ Hz}$, 1H), 7.89 (td, $J = 7.8, 1.5 \text{ Hz}$, 4H), 7.87 (td, $J = 7.9, 1.1 \text{ Hz}$, 1H, overlap with H12), 7.77 (td, $J = 7.6, 0.8 \text{ Hz}$, 1H), 7.71 (s, 2H), 7.45 (s, 2H), 7.44 (d, $J = 8.5 \text{ Hz}$, 4H), 7.41 (ddd, $J = 6.4, 1.9, 0.8 \text{ Hz}$, 4H), 7.23 (d, $J = 7.7 \text{ Hz}$, 1H), 6.74 (s, 2H), 5.35 (s, 4H), 4.36 (d, $J = 12.6 \text{ Hz}$, 1H), 4.33 (pseudo dd, AB system, $J = 12.6, 7.3 \text{ Hz}$, 4H) 4.28 (d, $J = 2.0 \text{ Hz}$, 8H), 3.96 (s, 6H), 3.94 (s, 6H). ^{13}C NMR (101 MHz, CD_3CN) δ 169.1, 157.0, 156.4, 155.0, 151.5, 150.0, 149.5, 145.8, 142.4, 140.3, 136.9, 131.9, 129.9, 128.4, 127.5, 126.6, 125.7, 125.2, 124.9, 124.6, 122.2, 117.7, 111.4, 109.1, 81.6, 73.3, 59.1, 57.2, 57.1, 50.2. ESI-HRMS(+) m/z calcd for $\text{C}_{64}\text{H}_{55}\text{Cl}_2\text{N}_8\text{O}_{13}^+ [\text{M}+\text{H}]^+$ 1213.3260, found 1213.3290.

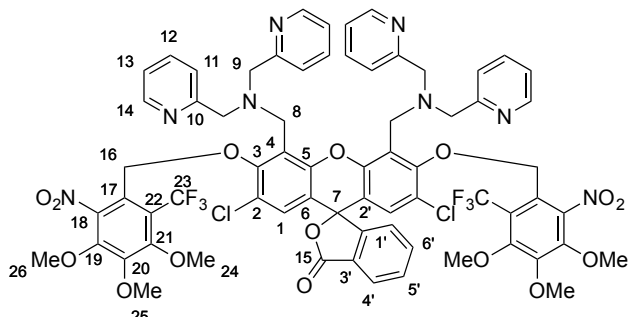
4',5'-Bis((bis(pyridin-2-ylmethyl)amino)methyl)-2',7'-dichloro-3',6'-bis((2-nitro-6-(trifluoromethyl)benzyl)oxy)-3H-spiro[isobenzofuran-1,9'-xanthen]-3-one (3)



This compound was prepared by using S7 (0.040 mmol) and 2-(bromomethyl)-1-nitro-3-(trifluoromethyl)benzene (0.40 mmol) according to the general procedure. The crude material was purified by preparative HPLC using solvent gradient 6 (Table S1) to afford a slightly yellow solid (27.7 mg, 56% yield). UV (CH_3CN) $\epsilon_{254} = 39,900 \text{ M}^{-1}\cdot\text{cm}^{-1}$. ^1H NMR (400 MHz, CD_3CN)

δ 8.53 (d, $J = 4.7 \text{ Hz}$, 4H), 8.05 – 8.04 (m, 4H), 8.00 (d, $J = 7.7 \text{ Hz}$, 1H), 7.90 (td, $J = 7.8, 1.5 \text{ Hz}$, 4H), 7.87 (dd, $J = 7.7, 1.0 \text{ Hz}$, 1H), 7.80 (t, $J = 8.1 \text{ Hz}$, 2H), 7.77 (t, $J = 7.6 \text{ Hz}$, 1H), 7.45 (dd, $J = 6.7, 6.0 \text{ Hz}$, 4H), 7.32 (d, $J = 7.9 \text{ Hz}$, 4H), 7.16 (d, $J = 7.7 \text{ Hz}$, 1H), 6.59 (s, 2H), 5.45 (pseudo dd, AB system, $J = 12.8 \text{ Hz}$, 4H), 4.14 (s, 8H), 4.08 (pseudo dd, AB system, $J = 14.0, 12.3 \text{ Hz}$, 4H). ^{13}C NMR (101 MHz, CD_3CN) δ 168.9, 157.3, 156.1, 152.5, 151.1, 149.8, 145.8, 142.4, 136.9, 132.0, 131.9, 131.3 (q, $^3J_{\text{C}-\text{F}} = 5.7 \text{ Hz}$), 130.8 (q, $^2J_{\text{C}-\text{F}} = 31.2 \text{ Hz}$), 129.9, 129.4 (C17 and C19), 127.6, 126.6, 125.3, 125.2, 124.8, 124.3 (q, $^1J_{\text{C}-\text{F}} = 274.0 \text{ Hz}$), 123.9, 121.9, 117.7, 81.3, 69.1 (q, $J_{\text{C}-\text{F}}$, through space = 2.5 Hz), 58.7, 50.20. ^{19}F NMR (376 MHz, CD_3CN) δ –58.9 (s, 6F). ESI-HRMS(+) m/z calcd for $\text{C}_{62}\text{H}_{45}\text{Cl}_2\text{F}_6\text{N}_8\text{O}_9^+ [\text{M}+\text{H}]^+$ 1229.2585, found 1229.2595.

4',5'-Bis((bis(pyridin-2-ylmethyl)amino)methyl)-2',7'-dichloro-3',6'-bis((3,4,5-trimethoxy-2-nitro-6-(trifluoromethyl)benzyl)oxy)-3H-spiro[isobenzofuran-1,9'-xanthen]-3-one (4)



This compound was prepared by using **S7** (0.040 mmol) and 1-(bromomethyl)-3,4,5-trimethoxy-2-nitro-6-(trifluoromethyl)benzene (0.40 mmol) according to the general procedure. The reaction mixture was purified by preparative HPLC using solvent gradient 7 (Table S1) to obtain a slightly yellow solid (16.7 mg, 30% yield). UV (CH_3CN) $\epsilon_{254} = 22,200 \text{ M}^{-1}\cdot\text{cm}^{-1}$ and $\epsilon_{300} = 3,570 \text{ M}^{-1}\cdot\text{cm}^{-1}$. ^1H NMR (400 MHz, CD_3CN) δ 8.53 (d, $J = 4.9 \text{ Hz}$, 4H), 8.00 (d, $J = 7.7 \text{ Hz}$, 1H), 7.91 (td, $J = 7.7, 1.1 \text{ Hz}$, 4H), 7.88 (t, $J = 7.6 \text{ Hz}$, 1H), 7.77 (t, $J = 7.6 \text{ Hz}$, 1H), 7.44 (pseudo t, $J = 6.4 \text{ Hz}$, 4H), 7.32 (d, $J = 7.9 \text{ Hz}$, 4H), 7.11 (d, $J = 7.6 \text{ Hz}$, 1H), 6.58 (s, 2H), 5.15 (pseudo dd, AB system, $J = 13.1, 8.7 \text{ Hz}$, 4H), 4.15 (s, 8H), 4.11 (pseudo dd, $J = 12.1, 9.0 \text{ Hz}$, 4H), 4.02 (s, 6H), 3.98 (s, 6H), 3.96 (s, 6H). ^{13}C NMR (101 MHz, CD_3CN) δ 168.9, 157.5, 156.8 (q, $^3J_{\text{C}-\text{F}} = 1.7 \text{ Hz}$), 156.1, 151.2, 149.7, 149.4, 148.9, 145.8, 144.0, 142.3, 136.9, 131.9, 129.9, 127.5, 126.6, 125.1(5), 125.1(4), 124.7, 124.5 (q, $^1J_{\text{C}-\text{F}} = 275.1 \text{ Hz}$), 123.9, 123.5 (q, $^3J_{\text{C}-\text{F}} = 1.3 \text{ Hz}$), 121.8, 119.3 (q, $^2J_{\text{C}-\text{F}} = 30.0 \text{ Hz}$), 117.6, 81.3, 69.4 (q, $J_{\text{C}-\text{F,through space}} = 5.7 \text{ Hz}$), 63.4, 63.0 (q, $J_{\text{C}-\text{F,through space}} = 0.7 \text{ Hz}$), 62.1, 58.9, 50.4. ^{19}F NMR (376 MHz, CD_3CN) δ -55.3 (s, 6F). ESI-HRMS(+) m/z calcd for $\text{C}_{68}\text{H}_{57}\text{Cl}_2\text{F}_6\text{N}_8\text{O}_{15}^+$ $[\text{M}+\text{H}]^+$ 1409.3219, found 1409.3254

Table S1. HPLC Solvent Gradients.

Gradient	Time (min)	% Solvent B	Gradient	Time (min)	% Solvent B
1	0	25	5	0	10
	2.5	45		5	55
	12.5	55		13	64
	15	100		14	100
	17	100		15	100
	19	0		17	10
	20	0			
2	0	20	6	0	10
	3	50		3	55
	16	63		15	67
	19	100		16	100
	20	100		17	100
	22	20		19	10
	23	20		20	10
3	0	10	7	0	10
	3	60		3	65
	8	65		14	76
	10	100		15	100
	10.5	100		17	10
	12	10		18	10
	13	10			
4	0	25	8	0	10
	3	55		5	10
	16	68		30	100
	16.5	100		33	100
	17.5	100		36	10
	19.5	25		40	10
	20.5	25			

Spectroscopy.

Concentrated stock solutions of each sensor were prepared in DMSO and stored as frozen aliquots at -80 °C. Extinction coefficients were determined in CH₃CN by dissolving lyophilized samples of each sensor in known volumes of CD₃CN (~700 μL) and diluting a small aliquot of each solution (2.000 μL) to 2.000 mL with CH₃CN. Absorption spectra of the dilute solutions were recorded at 25 °C. For compounds **1-3**, a known amount of DMF (~4 μL) was added to each of the CD₃CN stock solutions. For compound **4**, an aliquot (25 μL) of a stock solution of known concentration of CH₂Cl₂ in CD₃CN (~180 mM) was added to the sample. ¹H NMR spectra were collected with 30 s relaxation delay times.⁶ The concentration of each sensor stock solution was determined by integrating ¹H NMR peaks of the sensor and comparing them to those arising from the DMF or CH₂Cl₂ standard. These data were used to calculate the following extinction coefficients: for compound **1**, $\epsilon_{254} = 45,500 \text{ M}^{-1}\cdot\text{cm}^{-1}$; for compound **2**, $\epsilon_{254} = 55,300 \text{ M}^{-1}\cdot\text{cm}^{-1}$ and $\epsilon_{300} = 14,700 \text{ M}^{-1}\cdot\text{cm}^{-1}$; for compound **3**, $\epsilon_{254} = 39,900 \text{ M}^{-1}\cdot\text{cm}^{-1}$; for compound **4**, $\epsilon_{254} = 22,200 \text{ M}^{-1}\cdot\text{cm}^{-1}$ and $\epsilon_{300} = 3,570 \text{ M}^{-1}\cdot\text{cm}^{-1}$. For cuvette studies, sensors were irradiated with a 4 W 254 nm compact light source (UVP; UVGL-25 p/n 95-0021-12) or a custom-made 380 nm light source consisting of nine 5 mm 20 mW LED bulbs (Super Bright LEDs, Inc.; p/n RL5-UV0230-380). Both light sources were mounted above a stir plate at a distance of ~5 cm away from the cuvette.

Photocleavage of each of the protected sensors was evaluated by comparing absorption and fluorescence spectra of each molecule before and after irradiation with 254 or 380 nm light in the presence and absence of ZnCl₂, as well as by collecting analytical HPLC traces at each time point. For all experiments, the buffer was 50 mM PIPES, 100 mM KCl, pH 7.0. A typical sample consisted of buffer (200 μL), water (1200 μL), acetonitrile (600 μL), and sensor (1.0 μL, final conc. 3 μM). Samples were stirred for ~1 min. The fluorescence emission spectrum of each sample was recorded from 500 – 650 nm, with an excitation wavelength of 490 nm. Background-corrected absorption spectra were also collected at a scan rate of 600 nm/min. An aliquot (50 μL) of each sample was removed for analytical HPLC analysis using solvent gradient 8 (Table S1). Samples were irradiated at either 254 nm or 360 nm for an interval of 15 s. Fluorescence and absorption spectra were collected and another aliquot (50 μL) was removed for HPLC analysis. This procedure was repeated until 90 s of total irradiation time was reached, at which point the irradiation interval was increased to 30 s and then 60 s. The experiment was stopped after 180 or 240 s of total irradiation time. Samples were irradiated in either the absence or presence of ZnCl₂ (10 μM final conc.). For the samples irradiated in the absence of ZnCl₂, a small amount of ZnCl₂ (~1 μL) was added to give a final concentration of 10 μM after the final irradiation period. Fluorescence and absorption spectra were then obtained. After all of the spectroscopic data had been collected, tris(2-pyridylmethyl)amine (TPA; 20 μM final conc.) was added to every sample. Each sample was stirred for 10 min, after which time fluorescence and absorption spectra were recorded. For all measurements, the step size was 1 nm. The integration time was 0.5 s. The slit width was 2 nm. The temperature was 298 K. In the course of

the irradiation experiment, mono-protected intermediates were observed during HPLC analysis of the irradiated samples. Although we were unable to collect a sufficient amount of material for NMR spectroscopic characterization, the mono-protected compounds do not absorb at 520 nm, which suggests that they exist in non-fluorescent lactone forms.

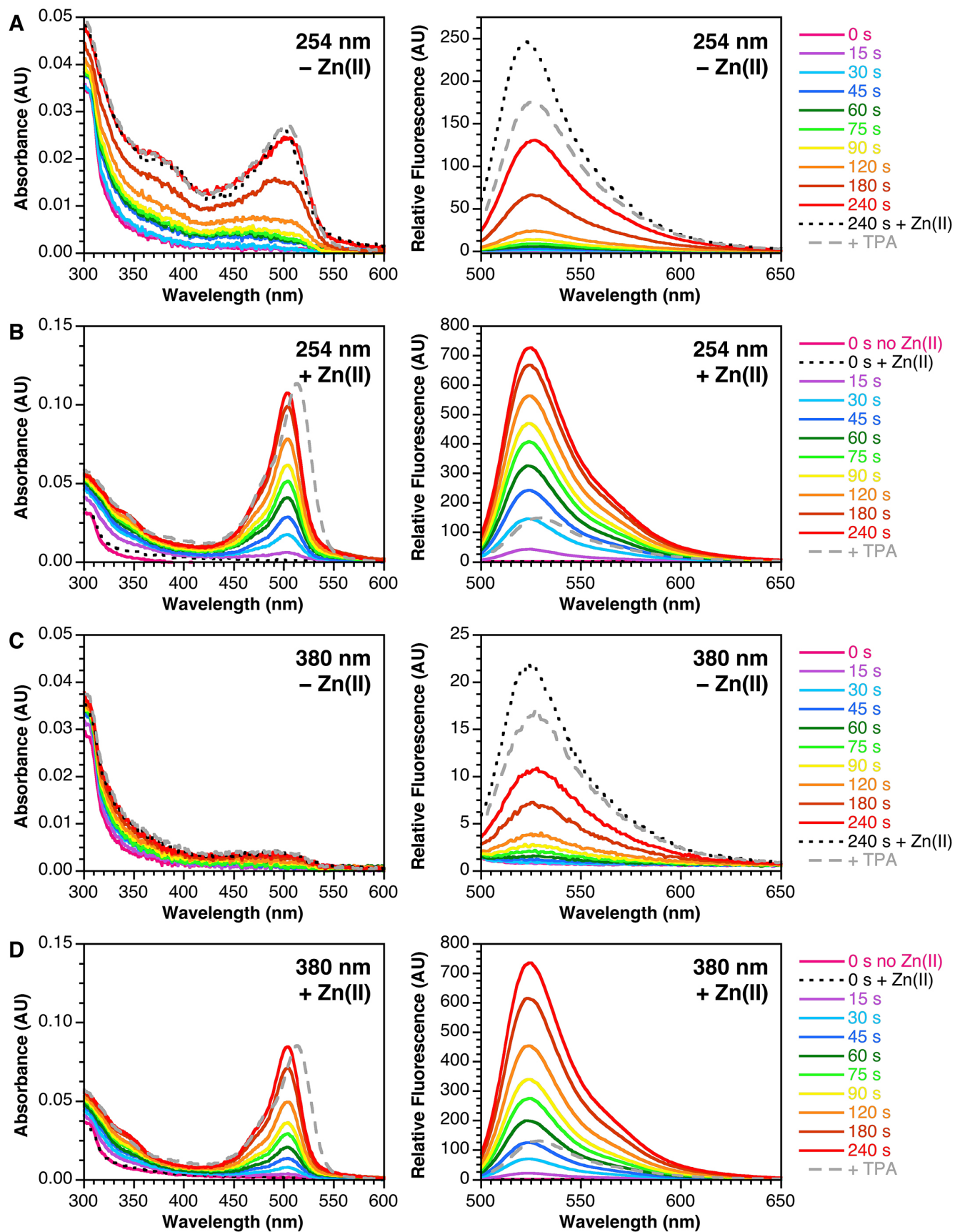


Figure S1. Absorption (left) and fluorescence (right) spectra of **1** after irradiation with 254 nm (A,B) or 380 nm (C,D) light for varying intervals of time in the absence (A,C) and presence (B,D) of ZnCl_2 , as indicated.

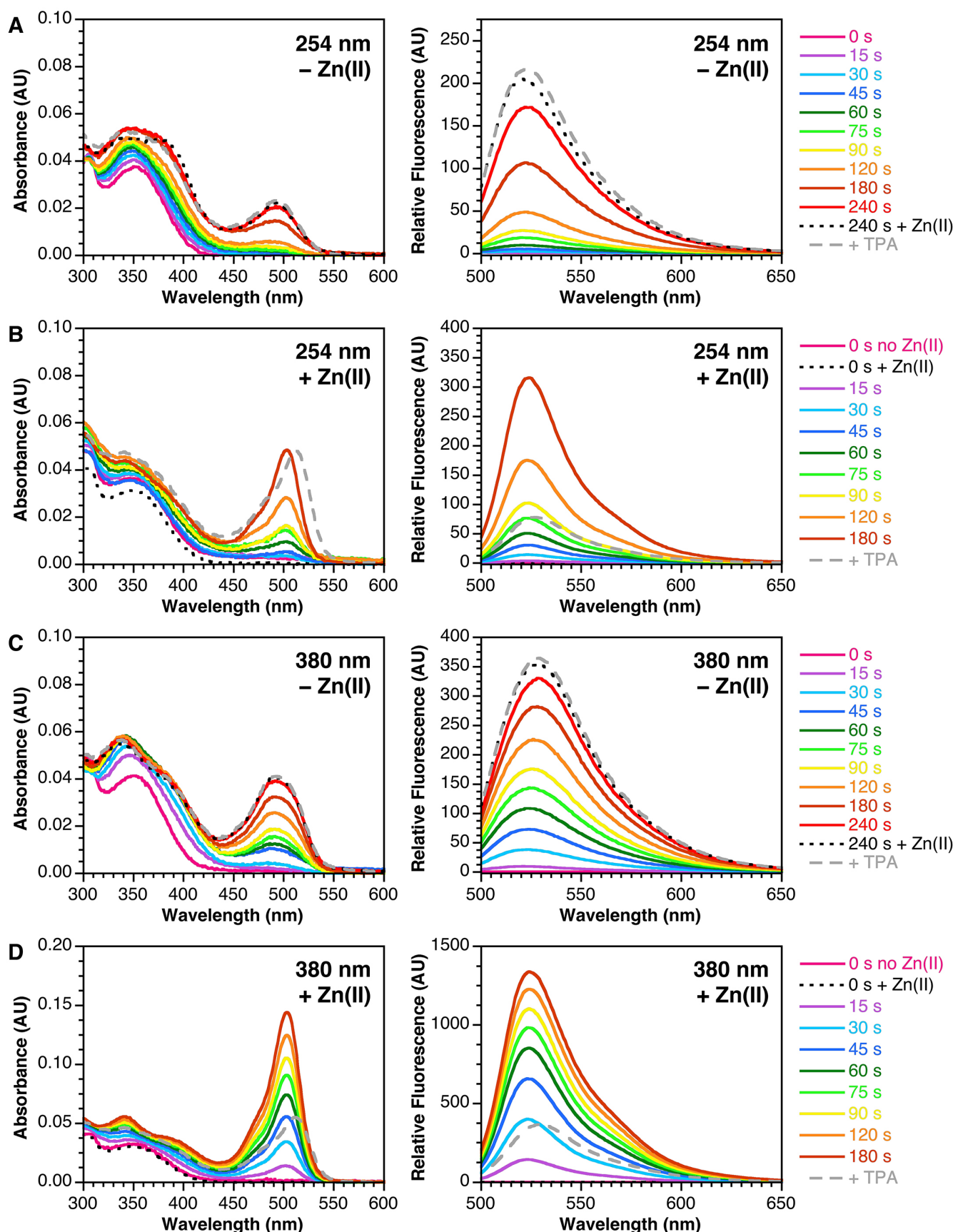


Figure S2. Absorption (left) and fluorescence (right) spectra of **2** after irradiation with 254 nm (A,B) or 380 nm (C,D) light for varying intervals of time in the absence (A,C) and presence (B,D) of ZnCl_2 , as indicated.

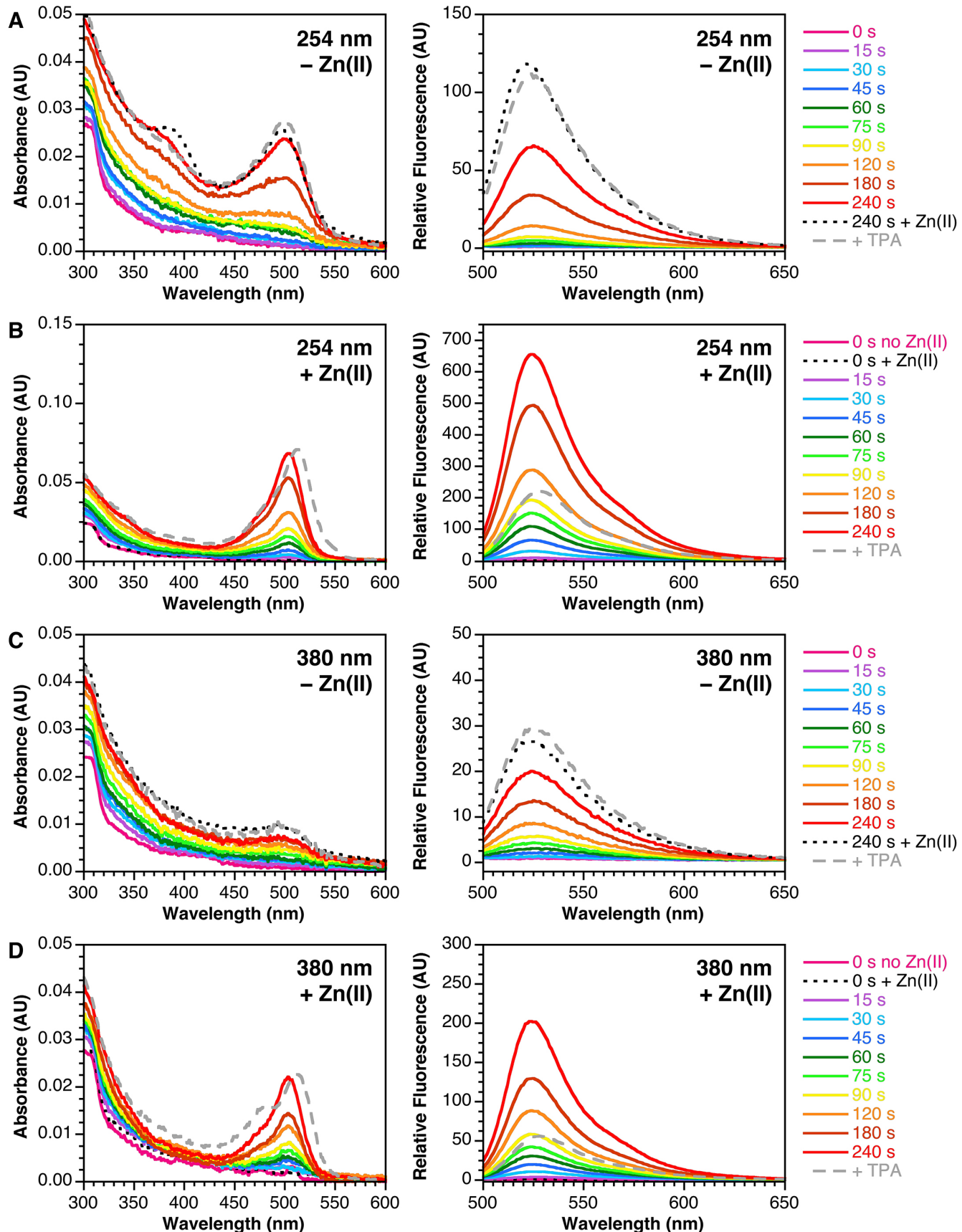


Figure S3. Absorption (left) and fluorescence (right) spectra of **3** after irradiation with 254 nm (A,B) or 380 nm (C,D) light for varying intervals of time in the absence (A,C) and presence (B,D) of ZnCl_2 , as indicated.

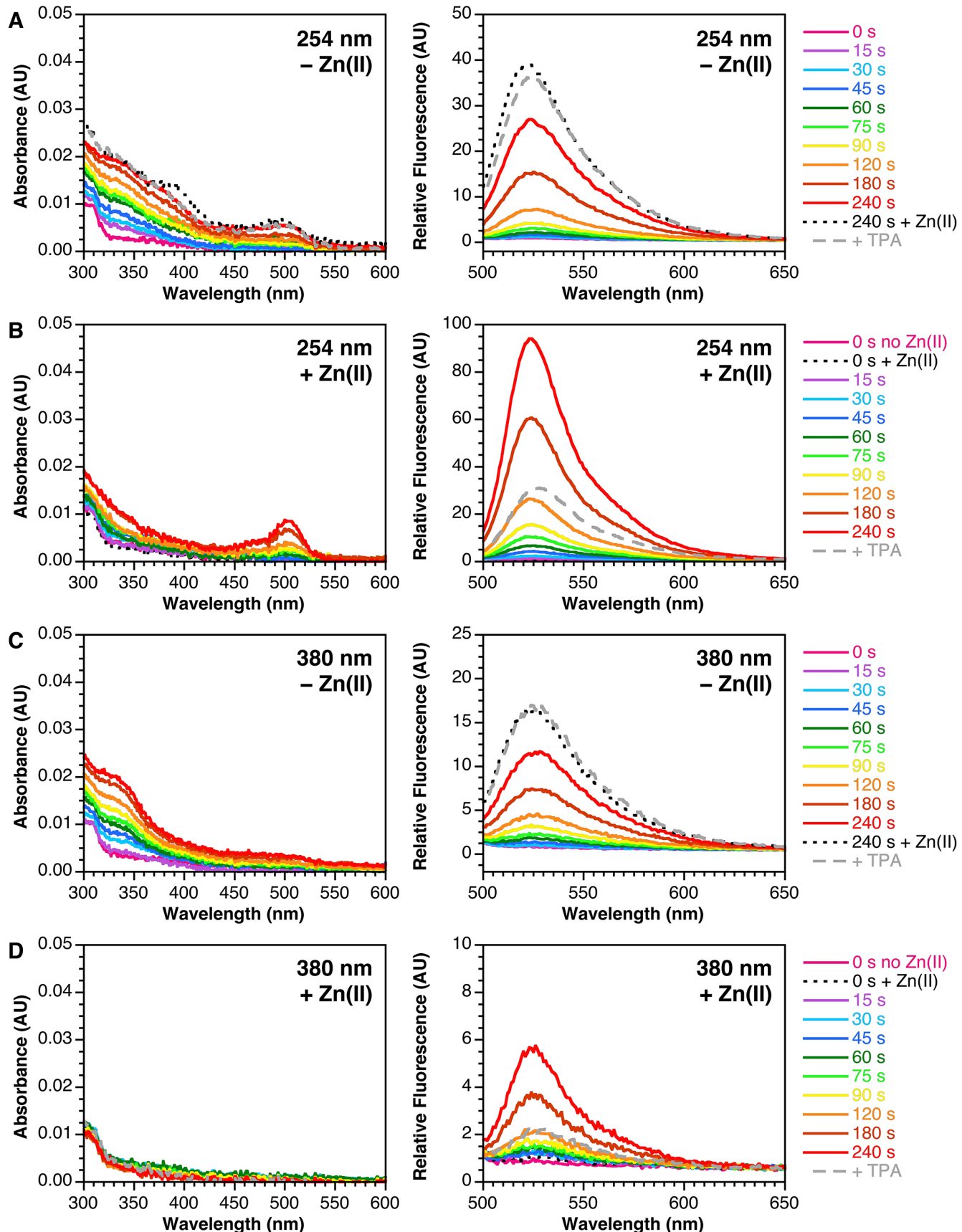


Figure S4. Absorption (left) and fluorescence (right) spectra of **4** after irradiation with 254 nm (A,B) or 380 nm (C,D) light for varying intervals of time in the absence (A,C) and presence (B,D) of ZnCl_2 , as indicated.

Table S2. Integrated relative fluorescence turn-on after intervals of irradiation of sensors **1-4** in the absence of ZnCl₂. The corresponding emission spectra are shown in panels A and C (right) in Figures S1-S4.

	254 nm				380 nm			
	1	2	3	4	1	2	3	4
0 s	1.0	1.0	1.0	1.0	1.0	1.0	1.0	1.0
15 s	1.1	1.1	1.1	1.1	1.0	5.1	1.1	1.0
30 s	1.4	1.7	1.2	1.2	1.0	18	1.2	1.1
45 s	2.1	3.0	1.5	1.4	1.2	34	1.7	1.2
60 s	3.2	4.9	2.1	1.7	1.3	51	2.2	1.5
75 s	4.6	8.8	3.1	2.1	1.6	68	2.8	1.7
90 s	6.7	12	4.3	2.8	1.9	84	3.6	2.1
120 s	11	22	7.3	4.4	2.4	109	4.9	2.8
180 s	29	48	17	8.7	3.9	137	7.5	4.3
240 s	58	79	31	15	5.6	160	11	6.3
+ Zn(II)	103	92	54	21	9.8	173	14	8.5
+ TPA	79	99	52	20	8.2	177	16	8.9

Table S3. Integrated relative fluorescence turn-on after intervals of irradiation of sensors **1-4** in the presence of ZnCl₂. The corresponding emission spectra are shown in panels B and D (right) in Figures S1-S4.

	254 nm				380 nm			
	1	2	3	4	1	2	3	4
initial	1.0	1.0	1.0	1.0	1.0	1.0	1.0	1.0
0 s + Zn(II)	1.0	1.0	1.2	1.1	0.8	1.1	1.1	1.1
15 s	16	3.1	4.9	1.2	7.8	54	2.3	1.2
30 s	55	9.5	14	1.6	24	152	5.2	1.2
45 s	92	19	28	2.3	44	256	8.6	1.2
60 s	124	31	45	3.3	70	337	13	1.3
75 s	157	46	63	4.7	96	394	17	1.3
90 s	182	62	80	6.6	120	446	23	1.4
120 s	223	106	120	11	162	505	35	1.5
180 s	269	193	208	24	224	560	50	2.1
240 s	295	-	280	36	271	-	78	2.9
+ TPA	65	53	101	14	52	165	24	1.6

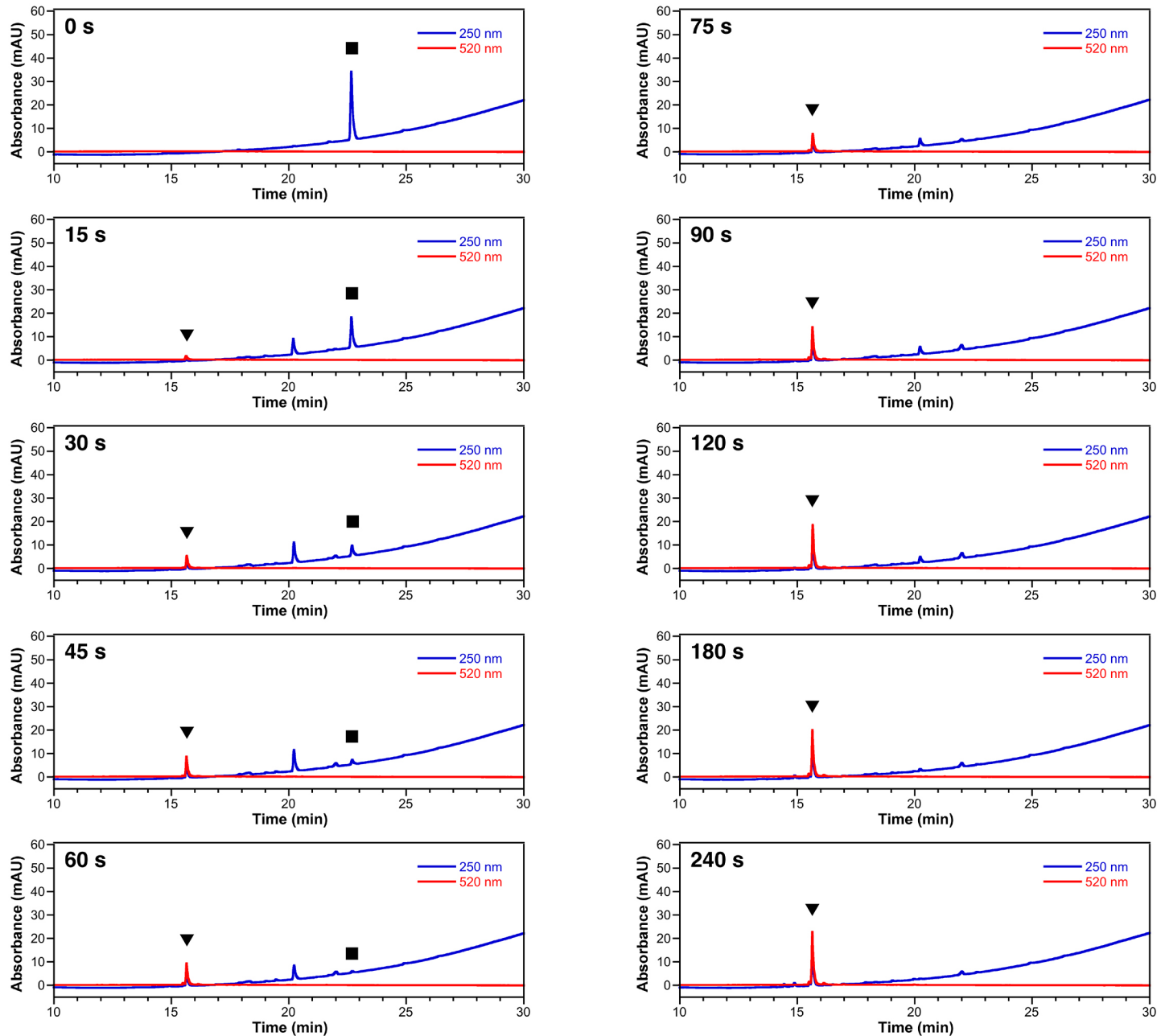


Figure S5. HPLC chromatograms of **1** after irradiation with 254 nm light for varying intervals of time, as indicated, in the presence of 10 μM ZnCl_2 . Absorbance monitored at 250 nm (blue) and 520 nm (red). Peaks corresponding to **1** and ZP1 are identified with squares and triangles, respectively. Solvent gradients are given in text.

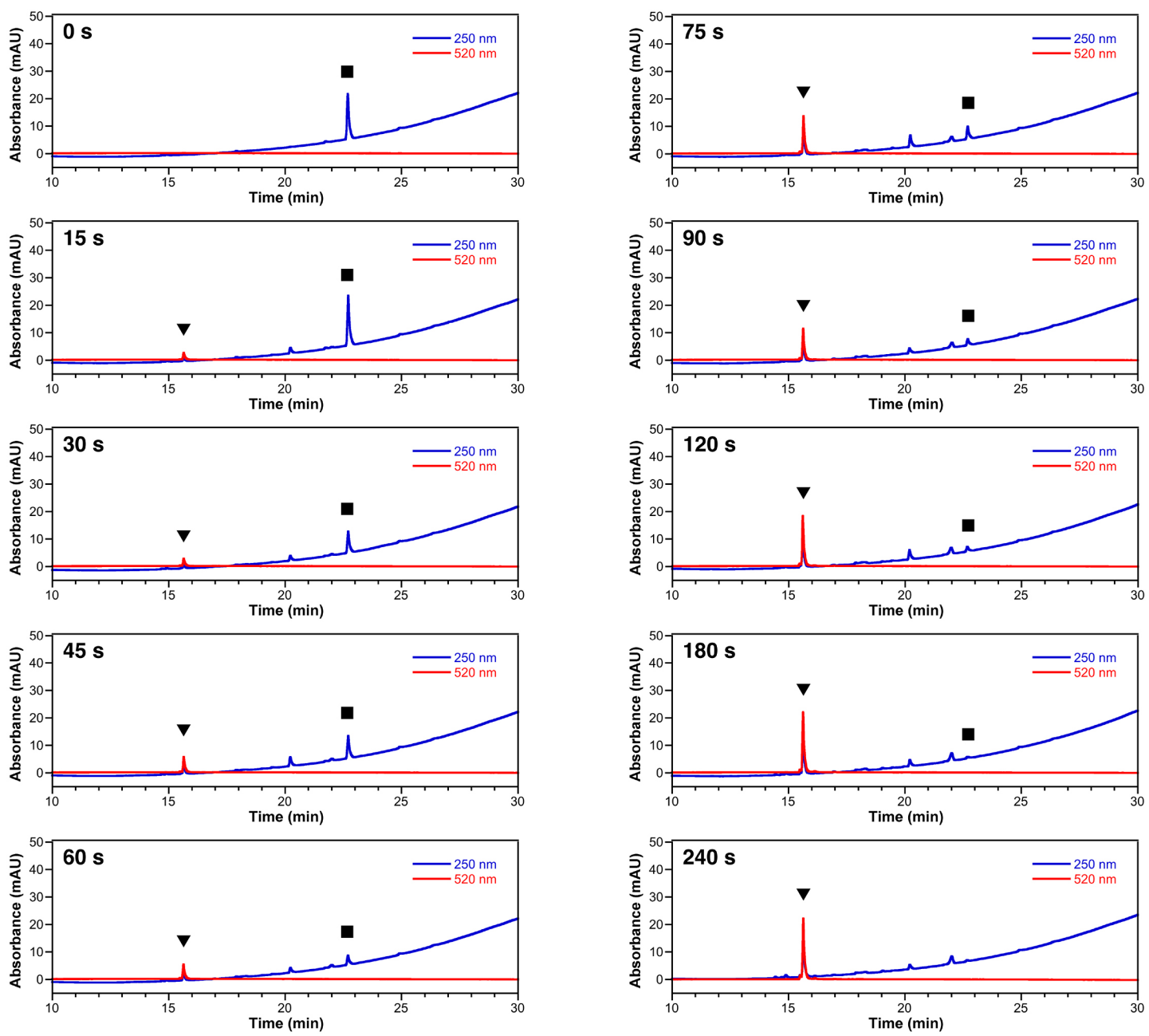


Figure S6. HPLC chromatograms of **1** after irradiation with 380 nm light for varying intervals of time, as indicated, in the presence of 10 μM ZnCl_2 . Absorbance monitored at 250 nm (blue) and 520 nm (red). Peaks corresponding to **1** and ZP1 are identified with squares and triangles, respectively. Solvent gradients are given in text.

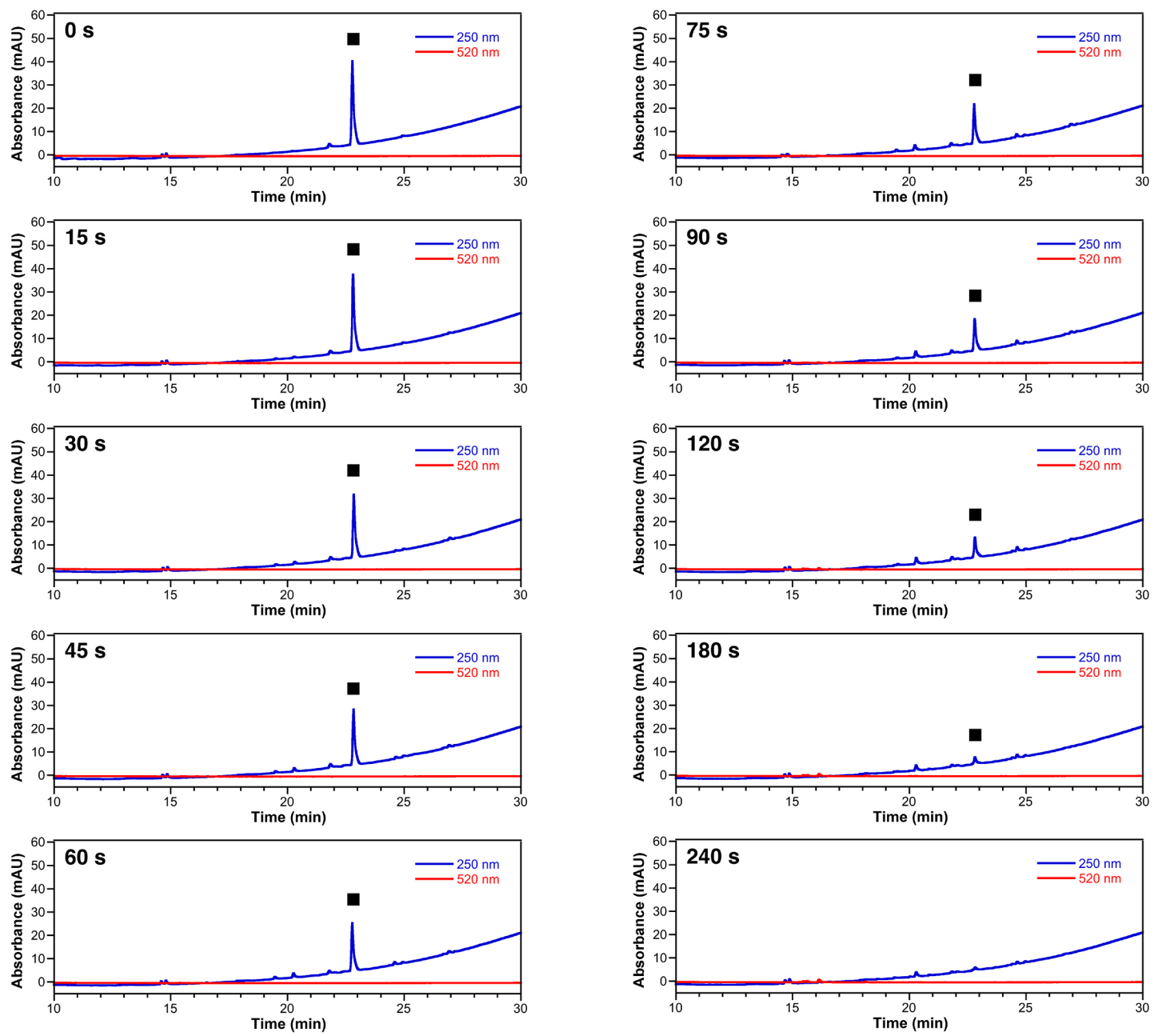


Figure S7. HPLC chromatograms of **1** after irradiation with 254 nm light for varying intervals of time, as indicated. Absorbance monitored at 250 nm (blue) and 520 nm (red). Peaks corresponding to **1** are identified with squares. Solvent gradients are given in text.

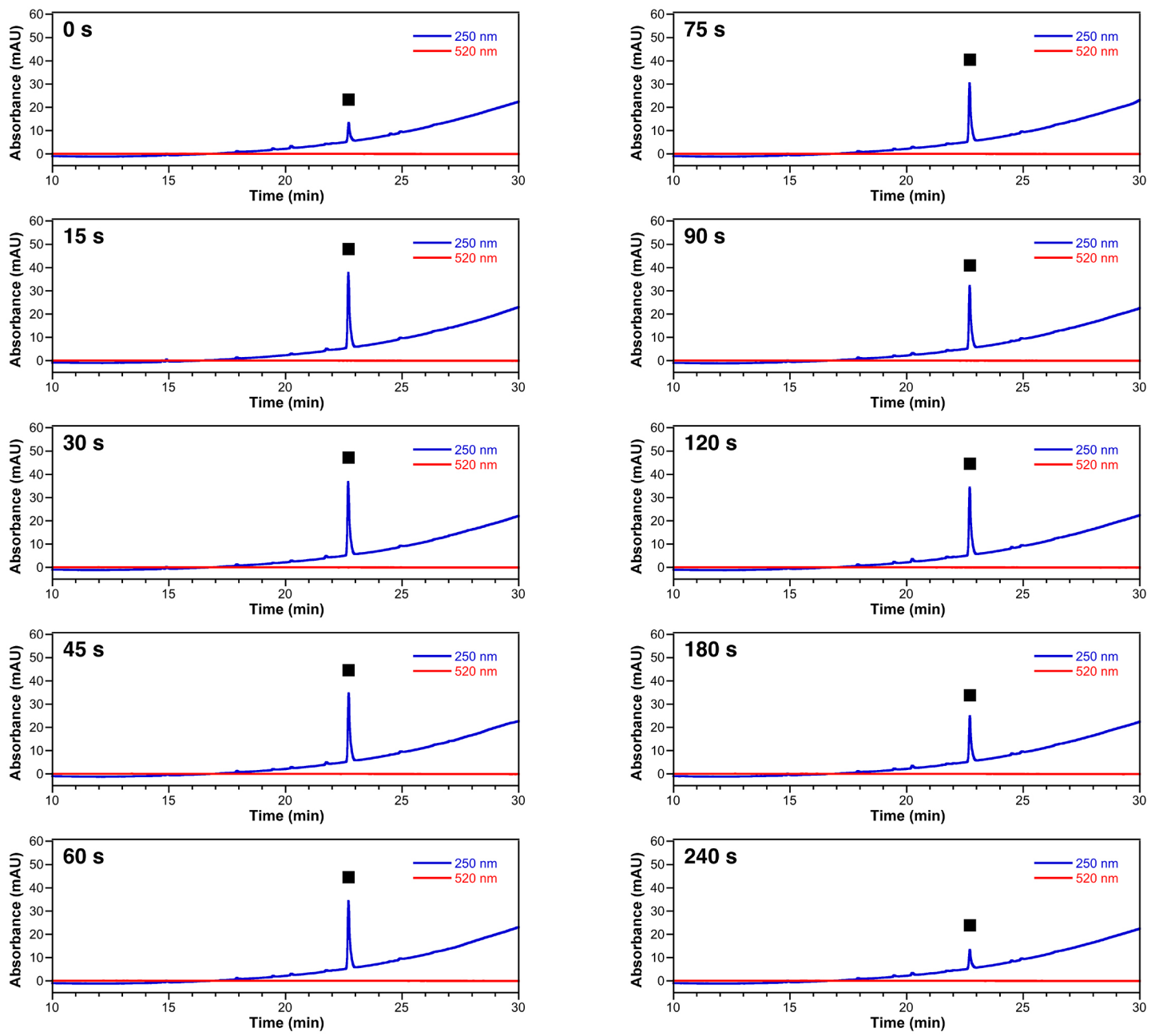


Figure S8. HPLC chromatograms of **1** after irradiation with 380 nm light for varying intervals of time, as indicated. Absorbance monitored at 250 nm (blue) and 520 nm (red). Peaks corresponding to **1** are identified with squares. Solvent gradients are given in text.

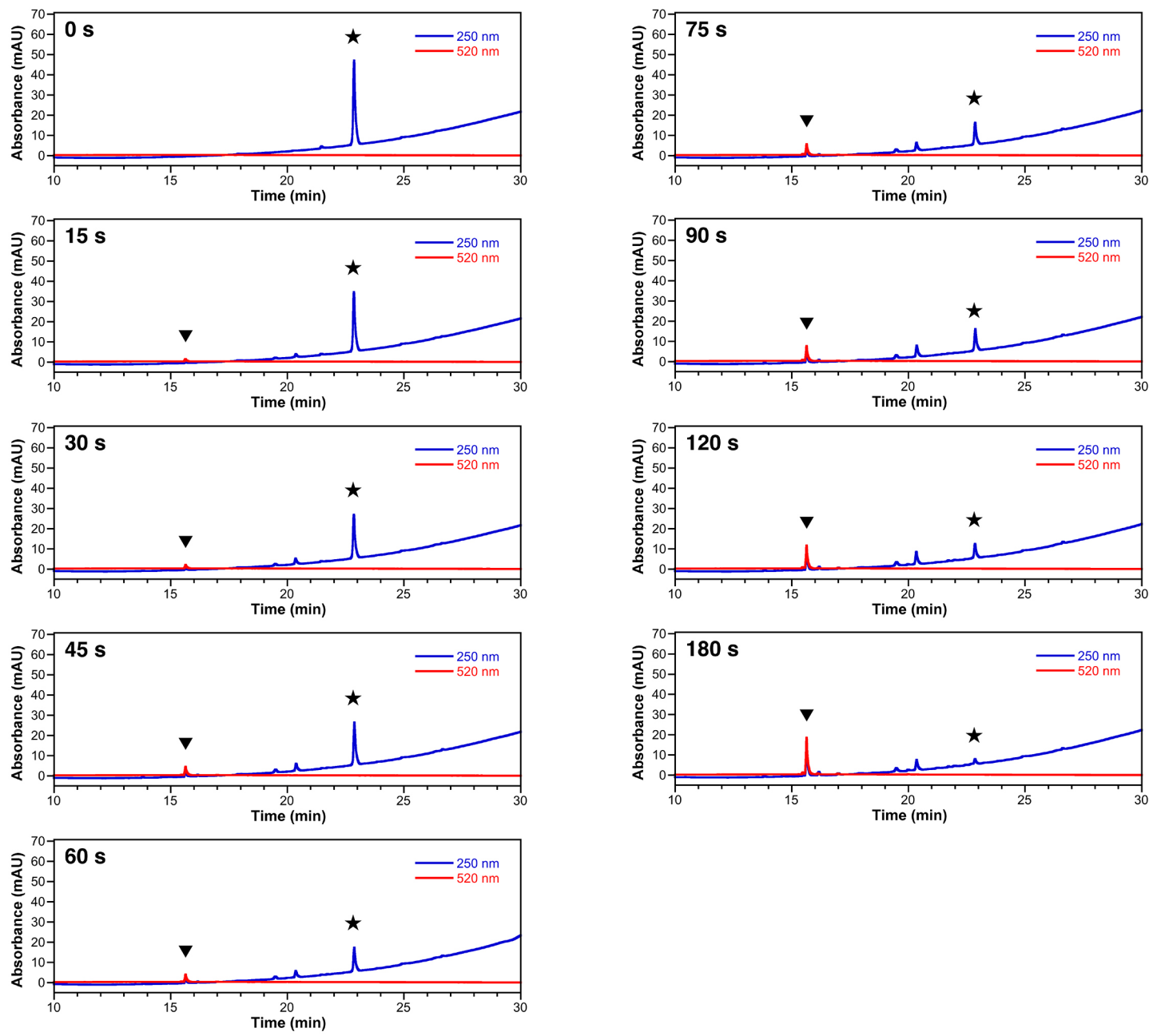


Figure S9. HPLC chromatograms of **2** after irradiation with 254 nm light for varying intervals of time, as indicated, in the presence of 10 μ M $ZnCl_2$. Absorbance monitored at 250 nm (blue) and 520 nm (red). Peaks corresponding to **2** and ZP1 are identified with stars and triangles, respectively. Solvent gradients are given in text.

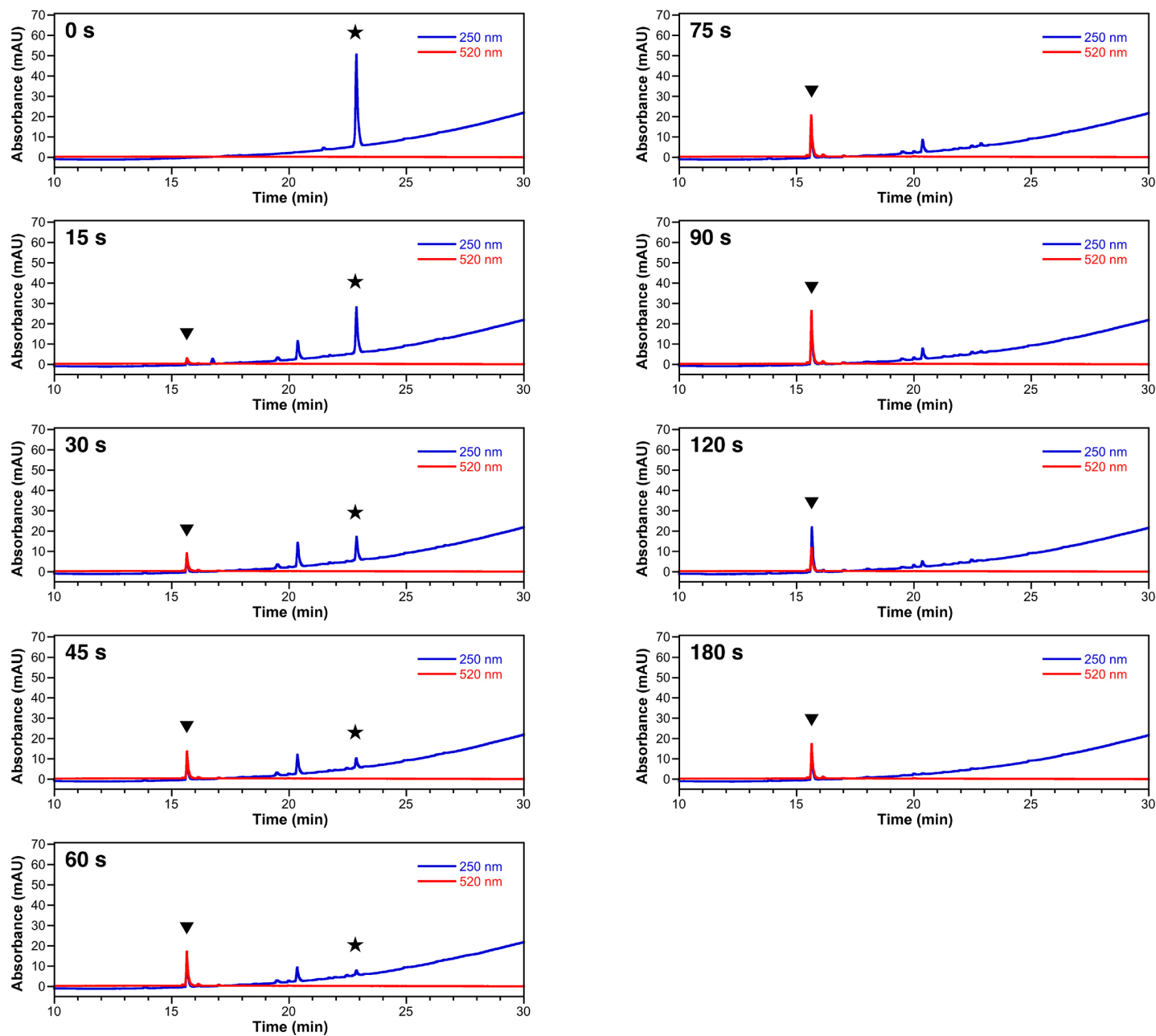


Figure S10. HPLC chromatograms of **2** after irradiation with 380 nm light for varying intervals of time, as indicated, in the presence of 10 μ M $ZnCl_2$. Absorbance monitored at 250 nm (blue) and 520 nm (red). Peaks corresponding to **2** and ZP1 are identified with stars and triangles, respectively. Solvent gradients are given in text.

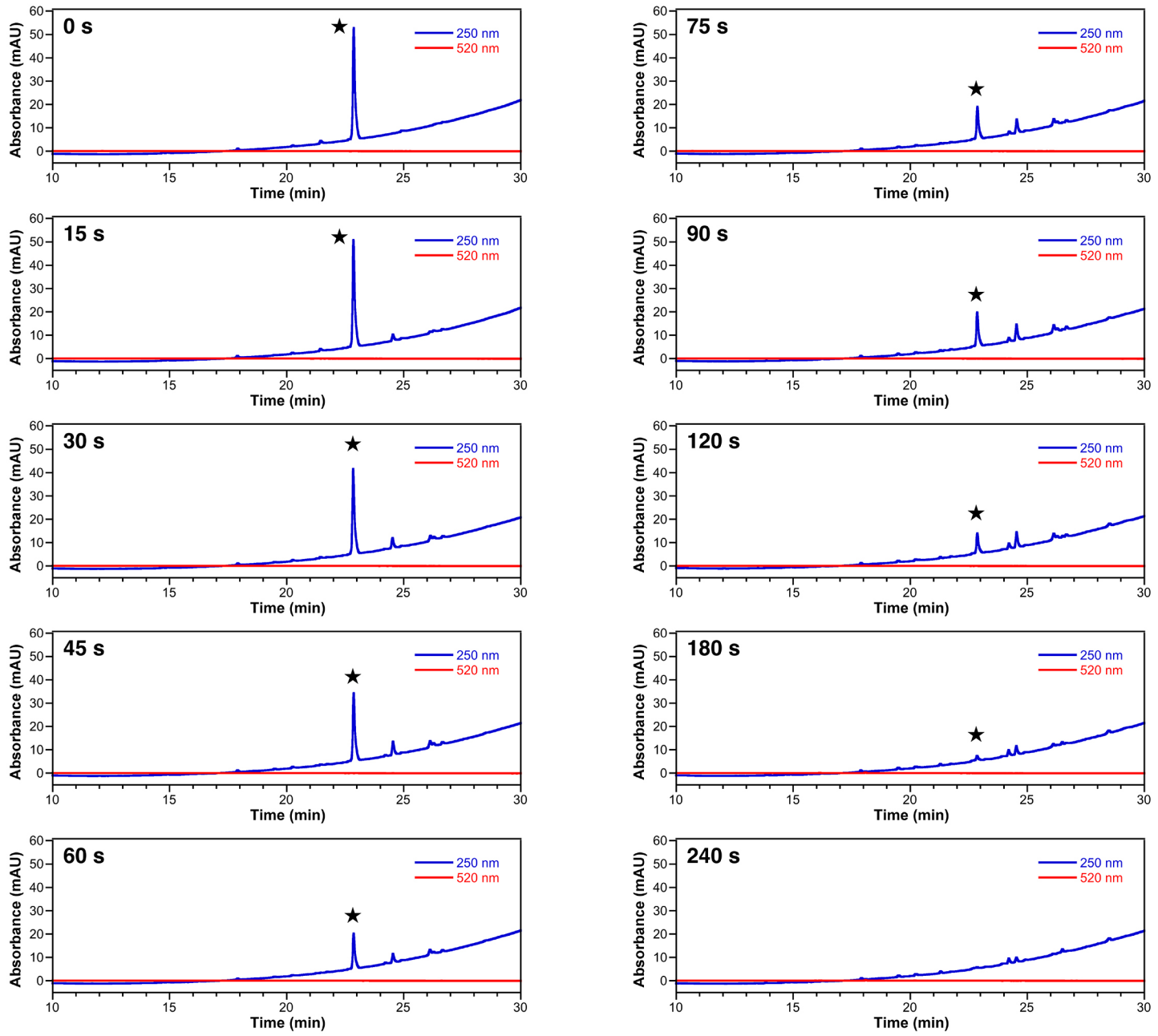


Figure S11. HPLC chromatograms of **2** after irradiation with 254 nm light for varying intervals of time, as indicated. Absorbance monitored at 250 nm (blue) and 520 nm (red). Peaks corresponding to **2** are identified with stars. Solvent gradients are given in text.

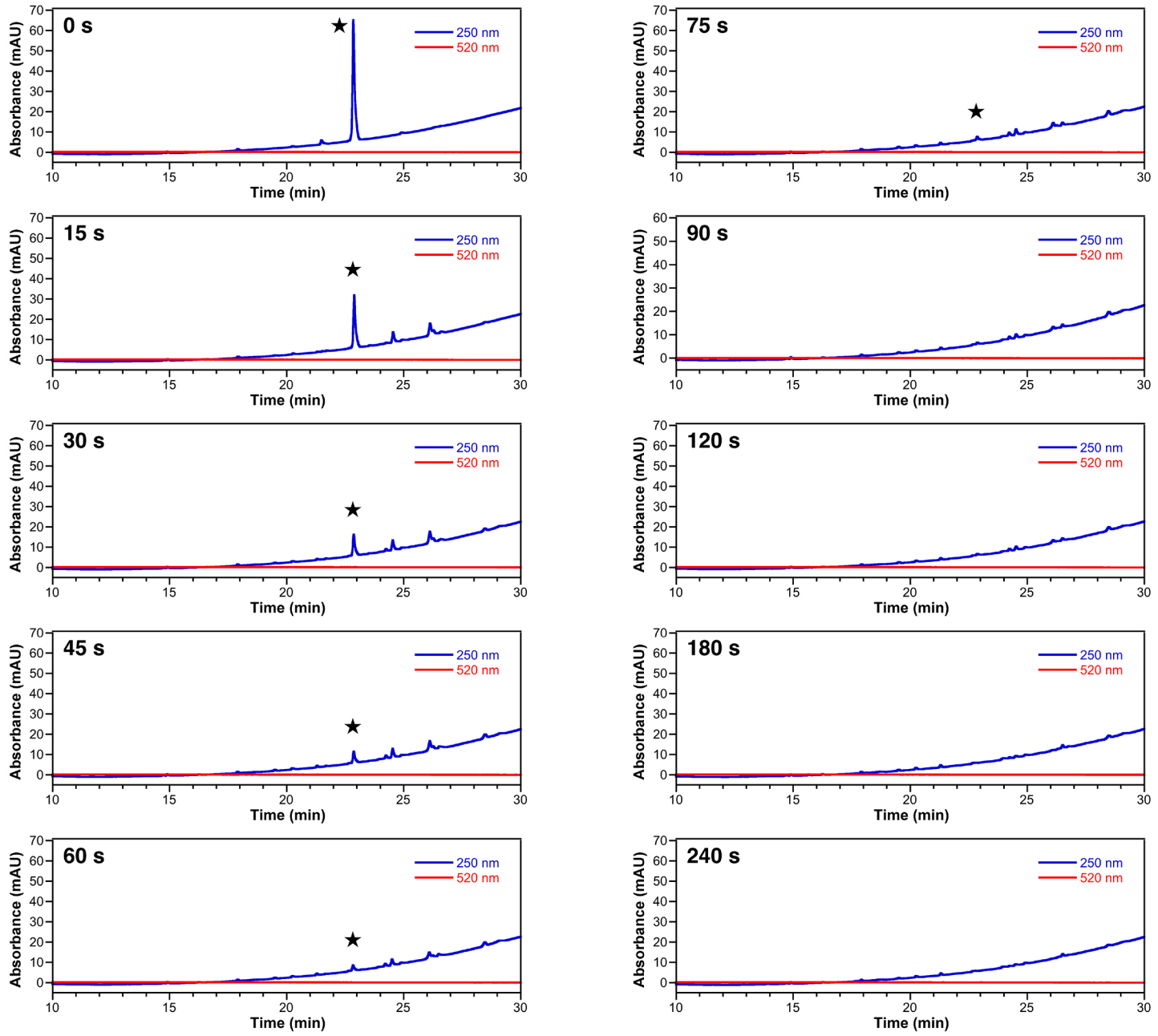


Figure S12. HPLC chromatograms of **2** after irradiation with 380 nm light for varying intervals of time, as indicated. Absorbance monitored at 250 nm (blue) and 520 nm (red). Peaks corresponding to **2** are identified with stars. Solvent gradients are given in text.

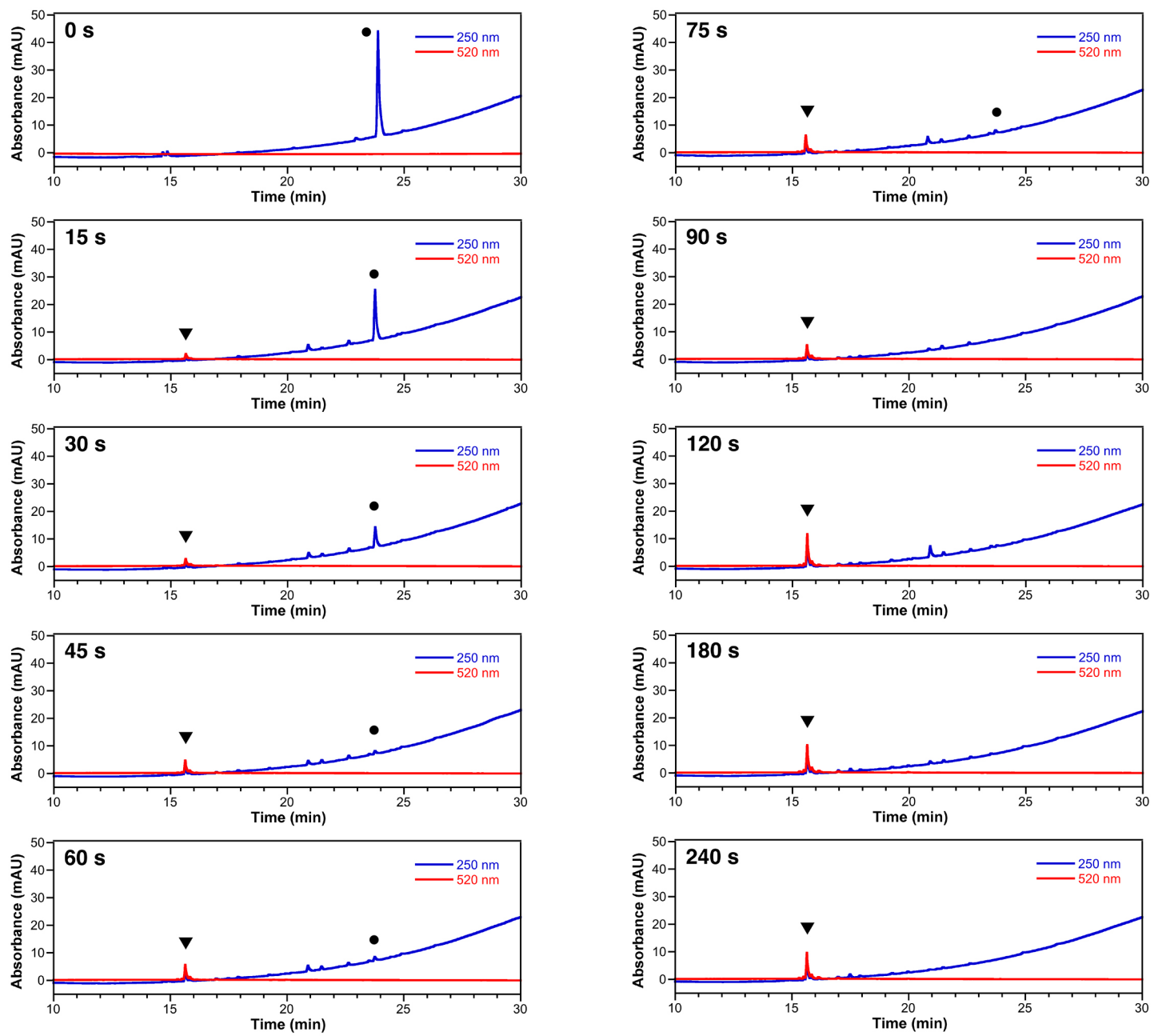


Figure S13. HPLC chromatograms of **3** after irradiation with 254 nm light for varying intervals of time, as indicated, in the presence of 10 μM ZnCl_2 . Absorbance monitored at 250 nm (blue) and 520 nm (red). Peaks corresponding to **3** and ZP1 are identified with circles and triangles, respectively. Solvent gradients are given in text.

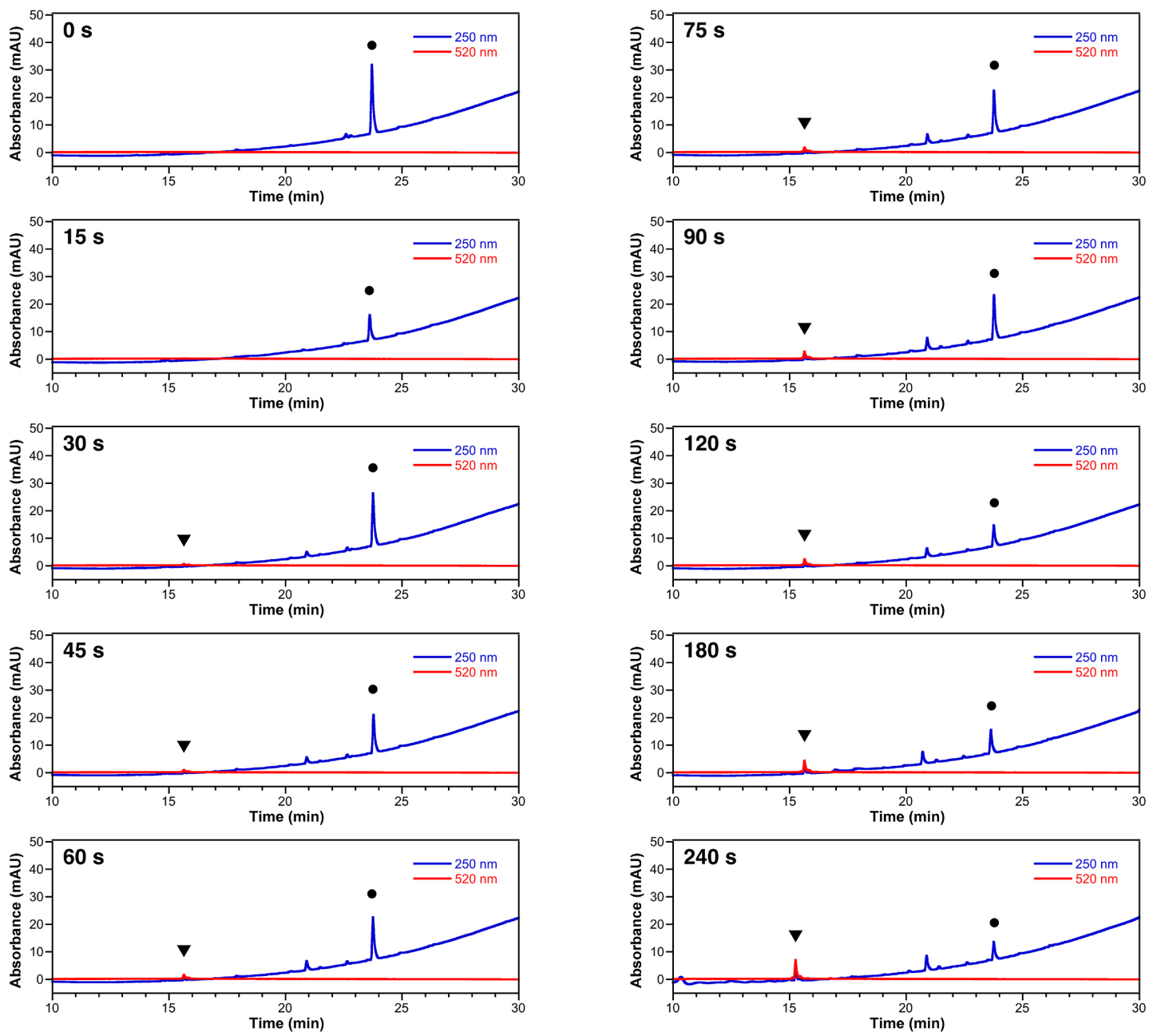


Figure S14. HPLC chromatograms of **3** after irradiation with 380 nm light for varying intervals of time, as indicated, in the presence of 10 μM ZnCl_2 . Absorbance monitored at 250 nm (blue) and 520 nm (red). Peaks corresponding to **3** and ZP1 are identified with circles and triangles, respectively. Solvent gradients are given in text.

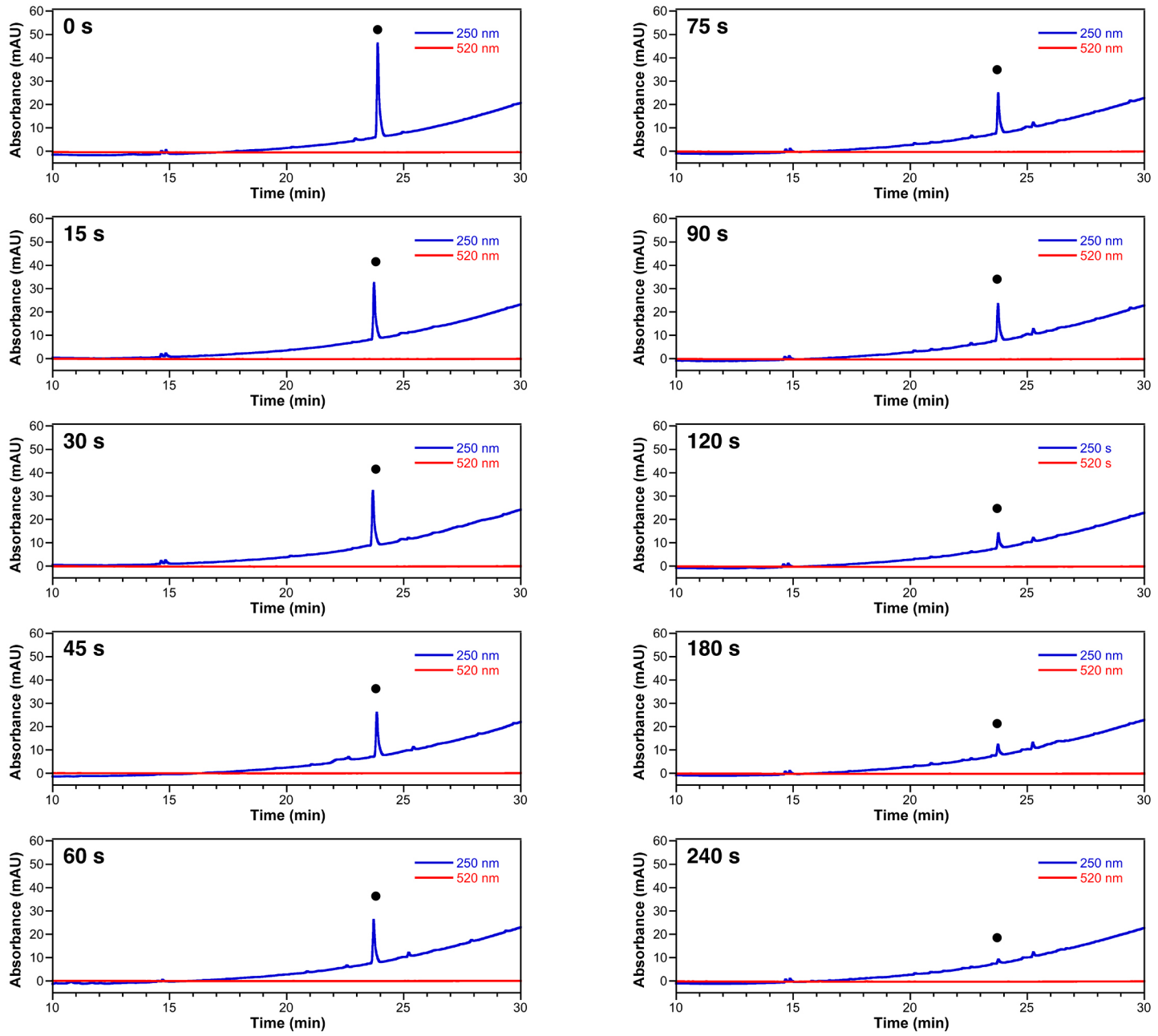


Figure S15. HPLC chromatograms of **3** after irradiation with 254 nm light for varying intervals of time, as indicated. Absorbance monitored at 250 nm (blue) and 520 nm (red). Peaks corresponding to **3** are identified with circles. Solvent gradients are given in text.

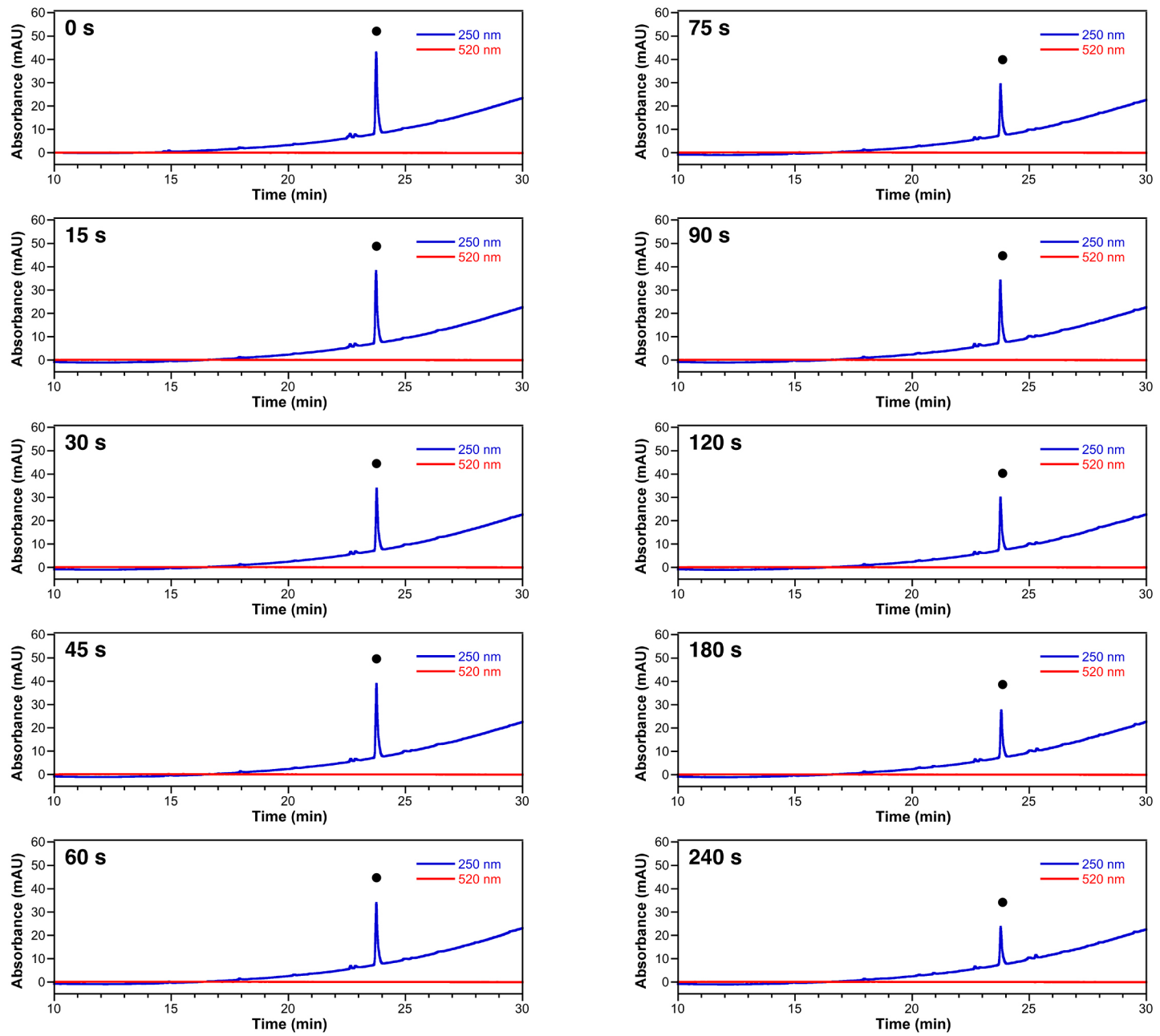


Figure S16. HPLC chromatograms of **3** after irradiation with 380 nm light for varying intervals of time, as indicated. Absorbance monitored at 250 nm (blue) and 520 nm (red). Peaks corresponding to **3** are identified with circles. Solvent gradients are given in text.

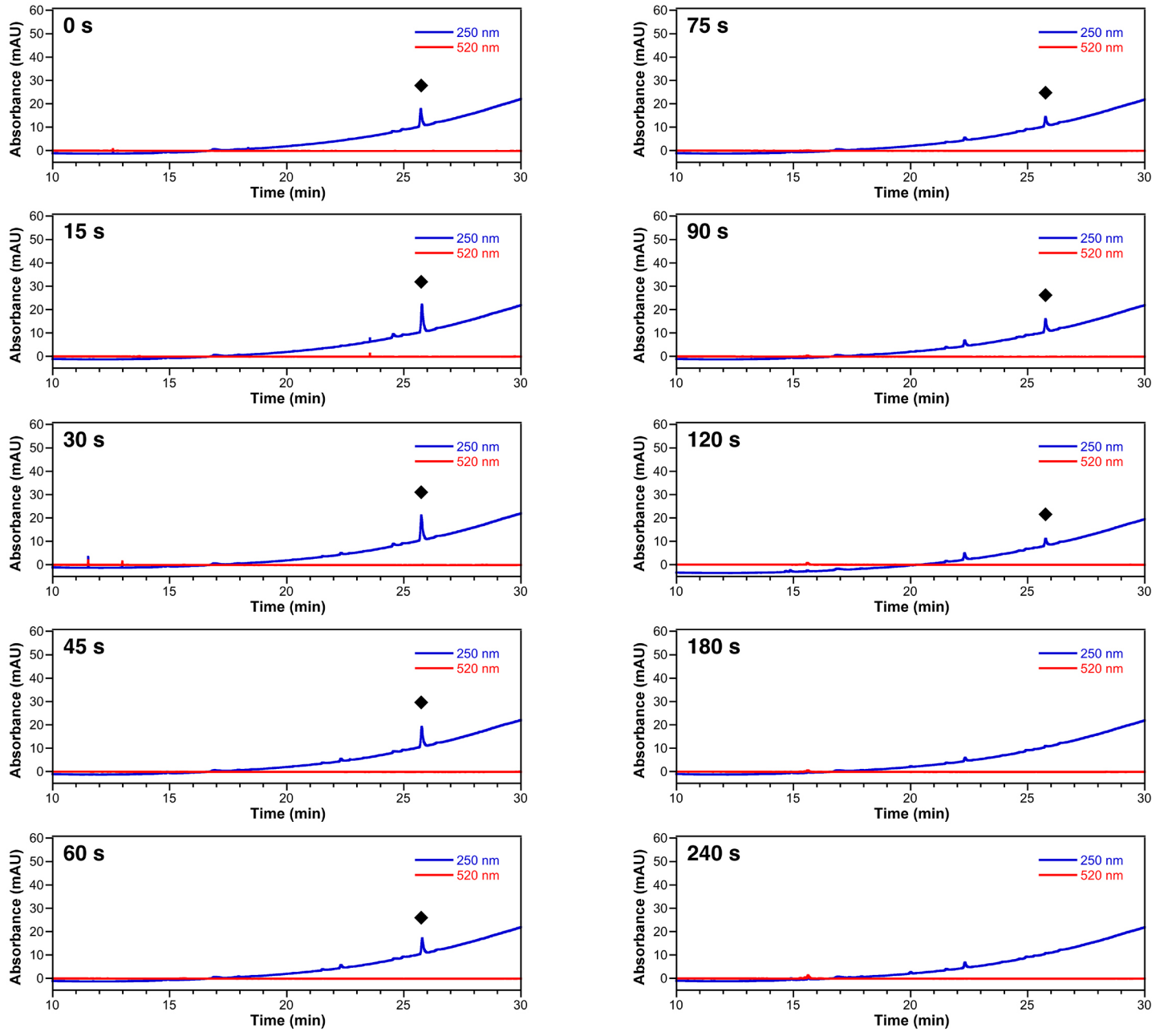


Figure S17. HPLC chromatograms of **4** after irradiation with 254 nm light for varying intervals of time, as indicated, in the presence of 10 μM ZnCl_2 . Absorbance monitored at 250 nm (blue) and 520 nm (red). Peaks corresponding to **4** are identified with diamonds. Solvent gradients are given in text.

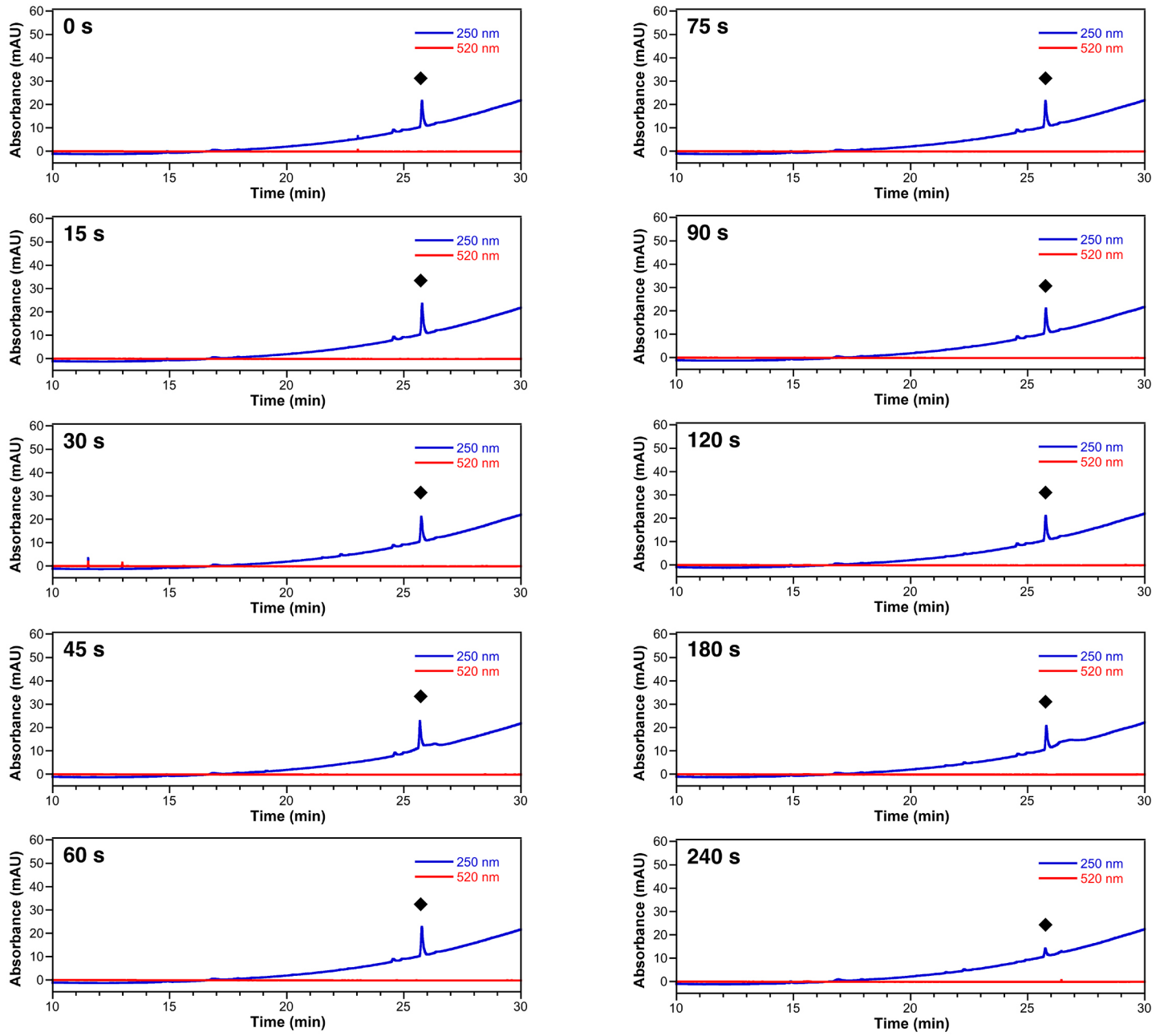


Figure S18. HPLC chromatograms of **4** after irradiation with 380 nm light for varying intervals of time, as indicated, in the presence of 10 μM ZnCl_2 . Absorbance monitored at 250 nm (blue) and 520 nm (red). Peaks corresponding to **4** are identified with diamonds. Solvent gradients are given in text.

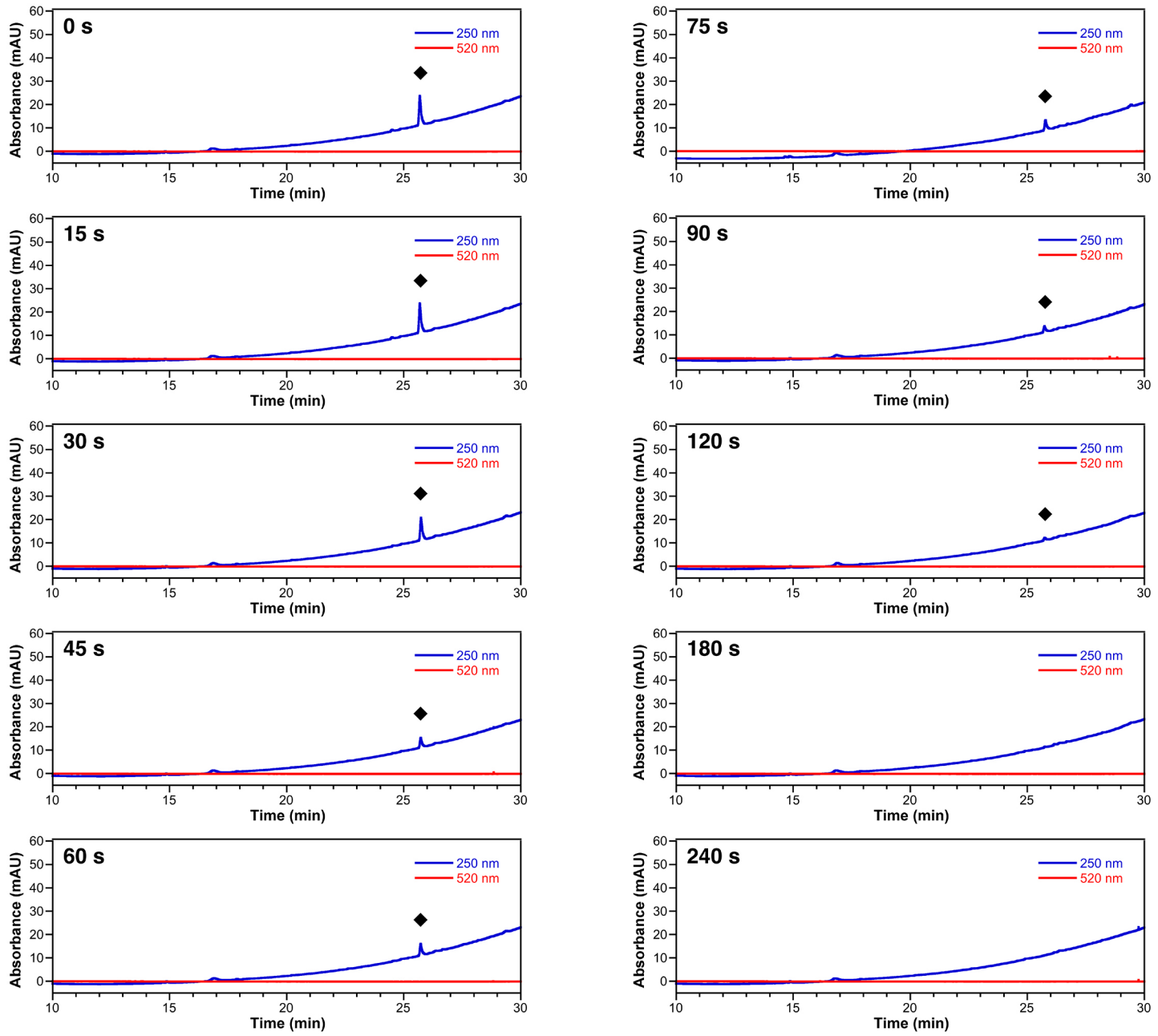


Figure S19. HPLC chromatograms of **4** after irradiation with 254 nm light for varying intervals of time, as indicated. Absorbance monitored at 250 nm (blue) and 520 nm (red). Peaks corresponding to **4** are identified with diamonds. Solvent gradients are given in text.

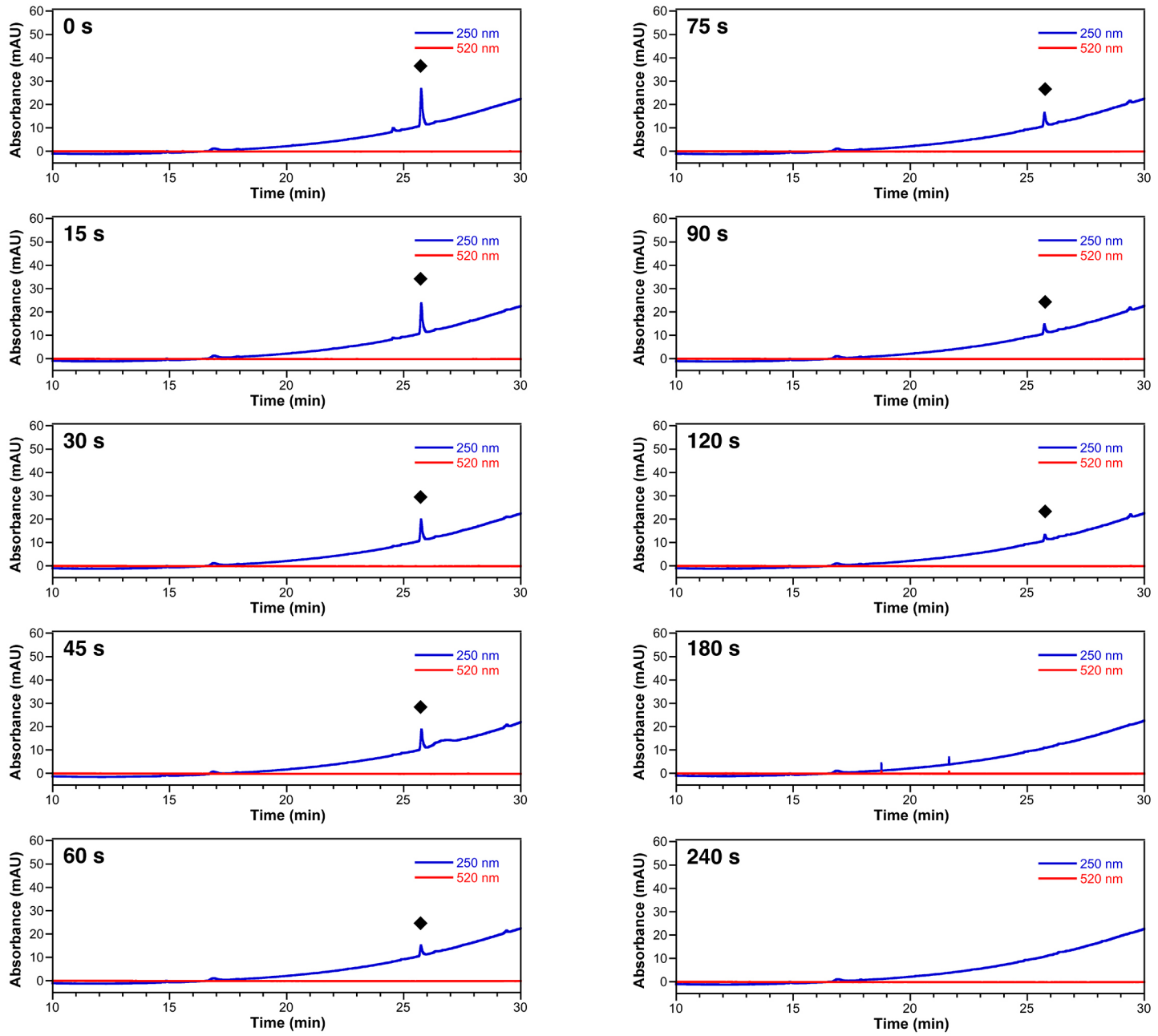


Figure S20. HPLC chromatograms of **4** after irradiation with 380 nm light for varying intervals of time, as indicated. Absorbance monitored at 250 nm (blue) and 520 nm (red). Peaks corresponding to **4** are identified with diamonds. Solvent gradients are given in text.

pH Dependence of the Zinc Response.

The fluorescence of **3** was measured in buffers of various pH values. The following buffers were prepared and treated with Chelex® resin according to the manufacturer's protocols: 50 mM potassium acetate, 100 mM KCl, pH 4.0; 50 mM potassium acetate, 100 mM KCl, pH 5.0; 50 mM PIPES, 100 mM KCl, pH 6.0; 50 mM PIPES, 100 mM KCl, pH 7.0; 50 mM Tris, 100 mM KCl, pH 8.0. A typical sample consisted of 1999 μ L buffer and 1 μ L sensor (final conc. 0.5 μ M). Samples were allowed to stir for ~1 min. The fluorescence emission spectrum from 500 – 650 nm of each sample was recorded with an excitation wavelength of 490 nm. The step size was 1 nm. The integration time was 0.2 s. The slit widths were 3 nm and the temperature was 298 K. Samples were irradiated for 60 s with 254 nm light. The fluorescence of each sample was measured again. Samples were also irradiated in the presence of zinc, in which case a 2.0 μ L aliquot of ZnCl₂ (final conc. 20 μ M) was added to each sample after the initial measurement, but before the 60 s irradiation. All experiments were conducted in triplicate. The integrated emission spectra of the sensor before (F_0) and after (F) irradiation were used to calculate the fluorescence turn-on.

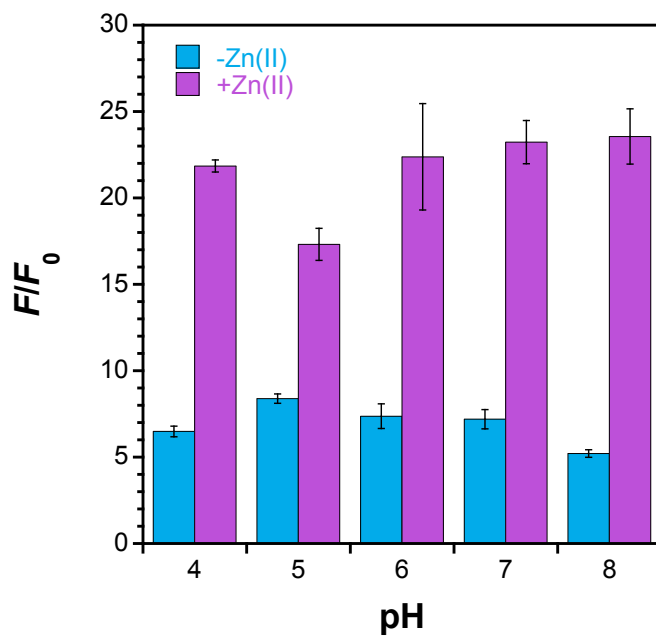


Figure S21. Integrated fluorescence turn-on of **3** in buffers of various pH values after 60 s irradiation with 254 nm light in the presence (purple) and absence (blue) of 20 μ M ZnCl₂, as described in the text. Error bars are standard error.

Metal Selectivity Studies.

Aqueous stock solutions of metal chloride salts were analytically prepared at the following concentrations: 0.80 M CaCl₂ and MgCl₂; 0.020 M CdCl₂, CoCl₂, CuCl₂, MnCl₂, NiCl₂, and ZnCl₂. A fresh stock solution of **3** (1.0 mM) in DMSO was also prepared. The buffer was 50 mM PIPES, 100 mM KCl, pH 7.0. Samples were prepared in triplicate and consisted of buffer (1999 μ L) and sensor (1.0 μ L, final conc. 0.5 μ M). Samples were stirred for ~1 min. The fluorescence of each sample was recorded with an excitation wavelength of 490 nm. Emission spectra were collected from 500 – 650 nm. An aliquot (2.0 μ L) of the appropriate metal chloride stock solution was added for a final concentration of 20 or 800 μ M metal ion. After 1 min of stirring, fluorescence spectra were recorded. Samples were irradiated for 60 s at 254 nm and fluorescence measurements were obtained. For all measurements, the step size was 1 nm. The integration time was 0.2 s. The excitation and emission monochromators were gated with 3 nm slits. The temperature was 298 K. The integrated emission spectra of the sensor before (F_0) and after (F) irradiation were used to calculate the fluorescence turn-on. All experiments were conducted in triplicate.

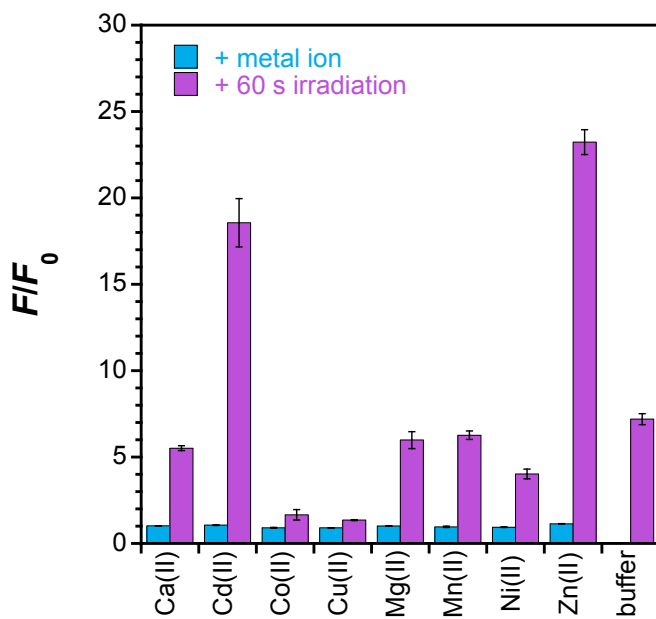


Figure S22. Integrated fluorescence turn-on of **3** upon addition of selected metal chloride salts (blue bars) and after subsequent irradiation with 254 nm light for 60 s (purple bars), as described in the text. Error bars are standard error.

Cell Culture and Imaging Experiments.

HeLa cells (ATTC; CCL-2) were cultured in Dulbecco's Modified Eagle Medium (DMEM) supplemented with 10% heat-deactivated fetal bovine serum (FBS) and 1% penicillin/streptomycin. The cultures were incubated in a humidified atmosphere with 5% CO₂ at 37 °C. Approximately 48 h before imaging, HeLa cells were plated in glass bottom imaging dishes coated with poly-D-lysine (MatTek; 35 mm dishes, No. 1.5 coverslip, 14 mm glass diameter).

Concentrated (1 mM) stock solutions of the sensor in DMSO were prepared and stored as frozen aliquots at -80 °C. A solution of 20% Pluronic® F-127 (Sigma-Aldrich) in DMSO (w/v) was prepared and stored at room temperature. Immediately before each imaging experiment, a 1 µL aliquot of the sensor stock solution was combined with an equal volume of the Pluronic® F-127 stock solution and mixed gently in a microcentrifuge tube. Dye free DMEM (1 mL) was added to the tube and the resulting solution was mixed thoroughly by pipetting up and down several times. The medium in the imaging dishes was replaced with this solution and the dishes were returned to the incubator. After 15 min, the solution was removed and the cells were washed with phosphate buffered saline (PBS: 0.144 g·L⁻¹ KH₂PO₄, 0.795 g·L⁻¹ Na₂HPO₄, 9.00 g·L⁻¹ NaCl; 2 mL × 3). A fresh portion of dye free DMEM (1 mL) was added to the dish and the cells were imaged.

Imaging was performed using a Zeiss Axiovert 200M inverted epifluorescence microscope fitted with a Hamamatsu EM-CCD digital camera C9100, a MS200 XY Piezo Z stage, and a 63× oil immersion objective. The light source was an X-Cite 120 metal halide lamp (EXFO). Zeiss standard filter sets 49 (excitation G 365 nm; beam splitter FT 395 nm; emission BP 445/50 nm) and 38 HE (excitation BP 470/40 nm; beam splitter FT 495 nm; emission BP 525/50 nm) were used to activate the caged sensors and visualize ZP1, respectively. The microscope was operated with Volocity software (version 6.01). Cells were maintained at 37 °C and under a humidified 5% CO₂ atmosphere with an on-stage incubator. Regions of interest (ROI) were identified using differential interference contrast (DIC) microscopy. DIC images were acquired (14 ms exposure time) of each ROI. Fluorescence images were acquired with the Zeiss 38 HE standard green channel filter set and a 300 ms exposure time. The cells were irradiated with UV light using the Zeiss standard filter set 49 for 15 s and the lowest intensity setting for the EXFO lamp. After a 1 min resting period, images of the green channel fluorescence were recorded with a 300 ms exposure time. A solution of warm dye free DMEM (1 mL; ~37 °C) containing 20 µM ZnCl₂ and 40 µM sodium pyrithione was gently added to the imaging dish and the cells were allowed to incubate on the microscope stage for 5 min. An additional set of fluorescence images was acquired. A solution of tris(2-pyridylmethyl)amine (TPA; 2 µL of a 20 mM stock solution in DMSO) in warm dye free DMEM (1 mL, 37 °C) was carefully added to the imaging dish and the cells were allowed to incubate on the microscope stage for 10 min. A final series of fluorescence images was acquired. Microscopy data were analyzed in ImageJ (version 1.50b) to quantify the average background corrected fluorescence intensity of each

cell in each ROI. These experiments were repeated multiple times using cells from at least two separate passages.

For some experiments, zinc pyrithione was added before irradiation with UV light using a procedure analogous to that described above. Here, the zinc pyrithione stock solution in DMEM (1 mL) was added before the plate was transferred to the microscope stage. After a 5 min incubation period, the medium was replaced with fresh dye free DMEM and cells were imaged as described above. In some cases, the zinc pyrithione solution was added before the cells were treated with the sensor. In these experiments, the zinc pyrithione solution was removed from the cells after a 5 min incubation period. A fresh solution of the sensor and Pluronic F-127 was added to the imaging dish and the cells were incubated for 15 min before the medium was replaced with fresh dye free DMEM. The cells were imaged as described above.

In separate experiments, the cells were incubated with the sensor and Pluronic F-127 in the presence of $50 \mu\text{M}$ ZnCl_2 for 15 min prior to imaging using the procedure described above. In some cases, a solution of zinc pyrithione was added to the cells before irradiation. Here, after the medium containing the sensor was removed, the cells were incubated with a fresh solution of zinc pyrithione in DMEM for 5 min. After this medium was replaced with dye free DMEM, the cells were imaged in the usual way.

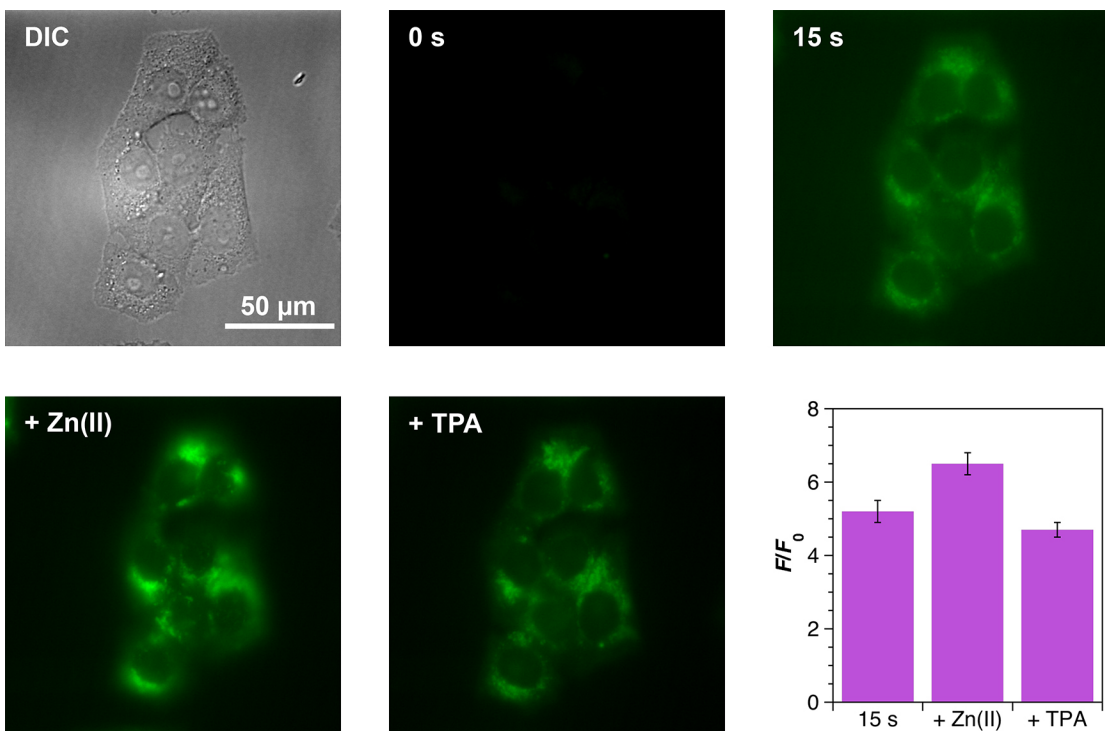


Figure S23. Representative differential interference contrast (DIC, upper left) and fluorescence microscopy images of HeLa cells treated with 1 μM **3** before and after irradiation with UV light for 15 s and after addition of 10 μM zinc pyrithione and subsequent addition of 13 μM TPA, as described in the text. Average integrated fluorescence turn-on for each condition is shown ($n = 51$). Error bars are standard error. $p = 1.3 \times 10^{-23}$ (15 s vs. Zn); $p = 2.9 \times 10^{-25}$ (Zn vs. TPA); $p = 4.6 \times 10^{-2}$ (15 s vs. TPA).

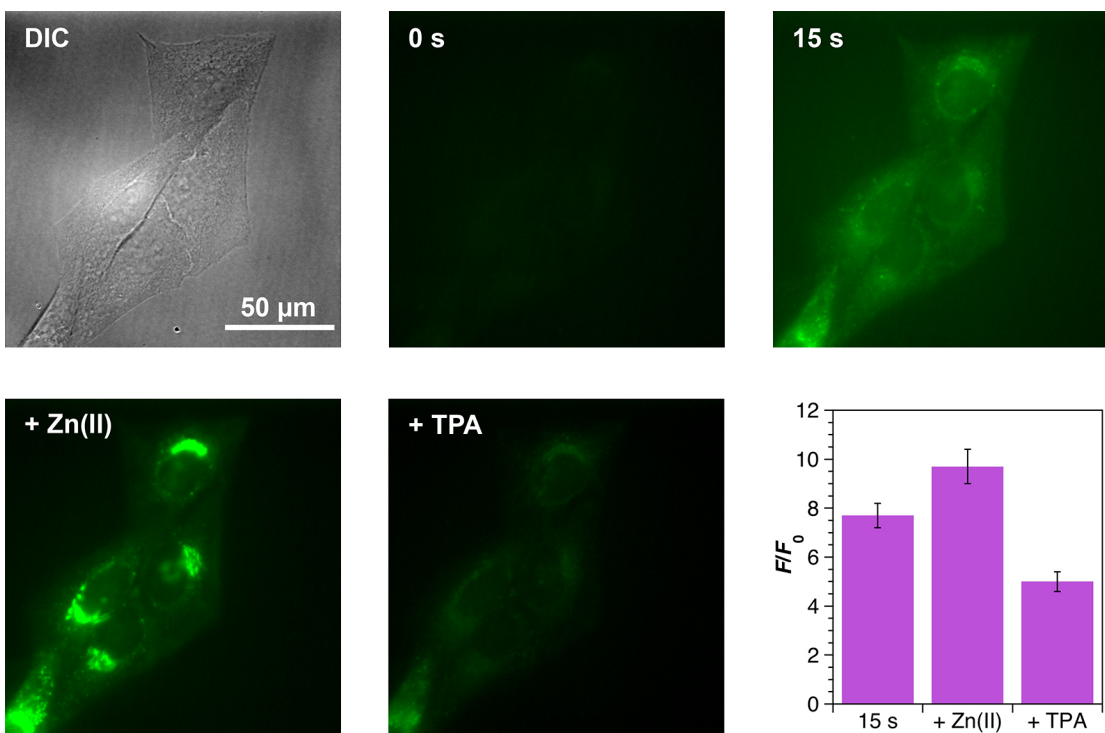


Figure S24. Representative differential interference contrast (DIC, upper left) and fluorescence microscopy images of HeLa cells treated with 1 μM **1** before and after irradiation with UV light for 15 s and after addition of 10 μM zinc pyrithione and subsequent addition of 13 μM TPA, as described in the text. Average integrated fluorescence turn-on for each condition is shown ($n = 52$). Error bars are standard error. $p = 4.5 \times 10^{-9}$ (15 s vs. Zn); $p = 8.7 \times 10^{-19}$ (Zn vs. TPA); $p = 1.3 \times 10^{-22}$ (15 s vs. TPA)

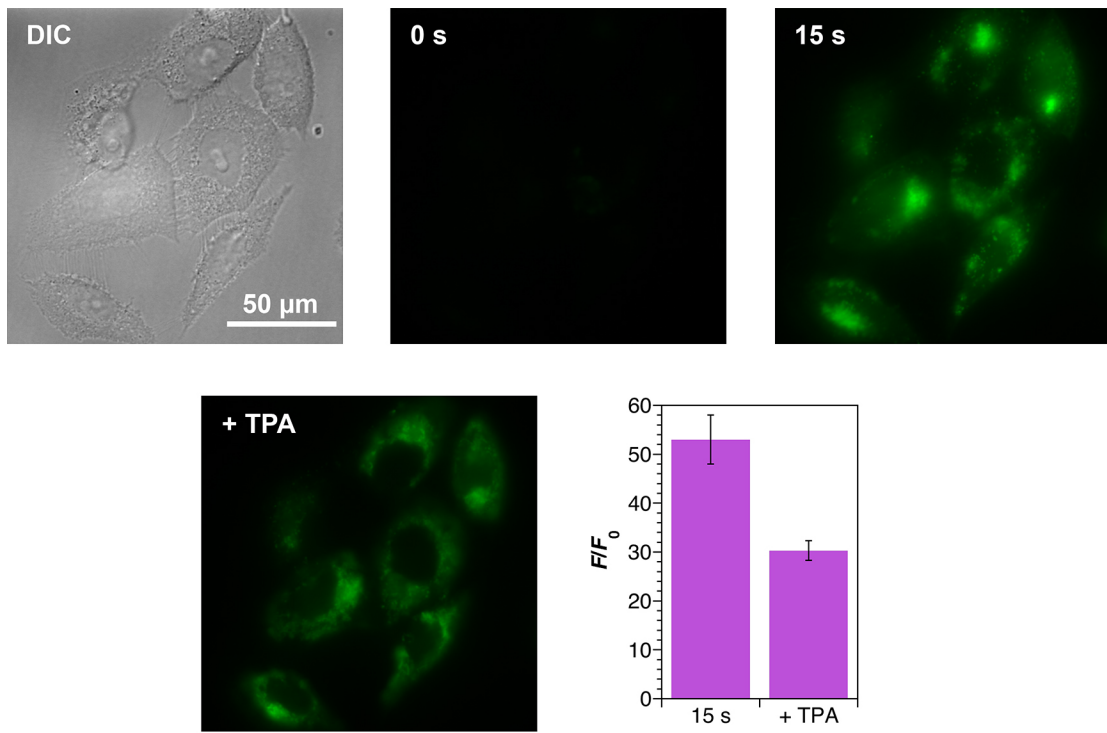


Figure S25. Representative differential interference contrast (DIC, upper left) and fluorescence microscopy images of HeLa cells treated with 1 μ M 1 and then incubated with 10 μ M zinc pyrithione before and after irradiation with UV light for 15 s and after subsequent addition of 13 μ M TPA, as described in the text. Average integrated fluorescence turn-on for each condition is shown ($n = 99$). Error bars are standard error. $p = 3.0 \times 10^{-11}$.

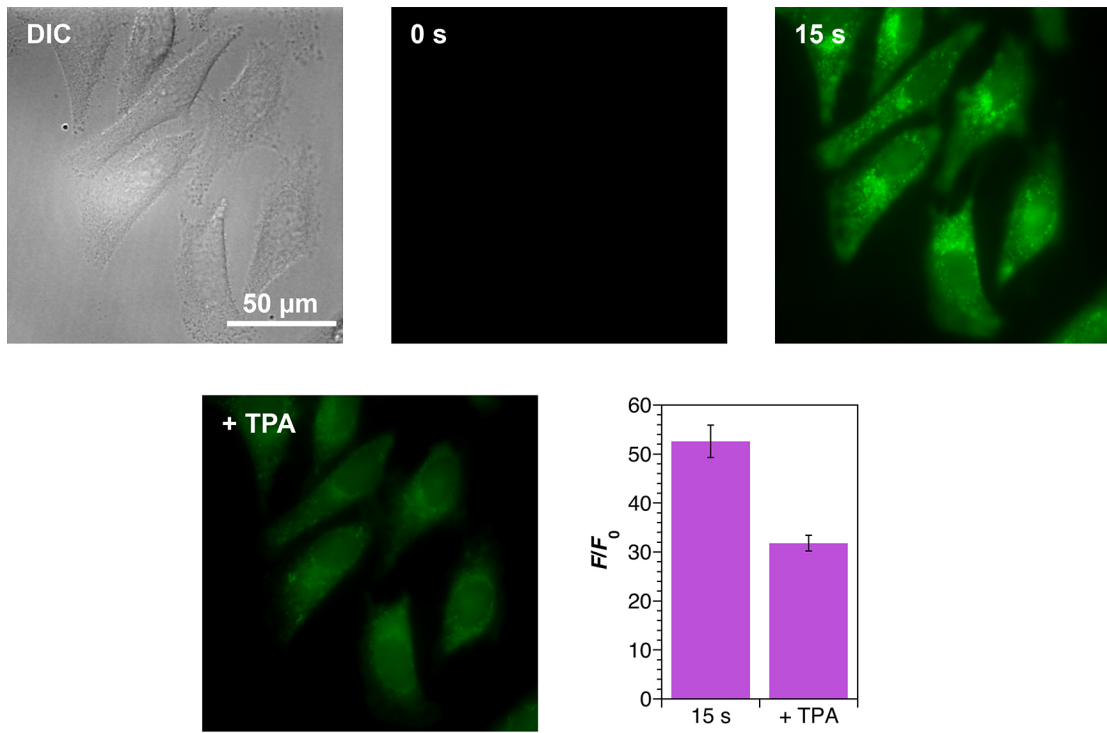


Figure S26. Representative differential interference contrast (DIC, upper left) and fluorescence microscopy images of HeLa cells incubated with a mixture of 1 μ M 3 and 50 μ M ZnCl₂ prior to treatment with 10 μ M zinc pyrithione before and after irradiation with UV light for 15 s and after subsequent addition of 13 μ M TPA, as described in the text. Average integrated fluorescence turn-on for each condition is shown ($n = 88$). Error bars are standard error. $p = 3.0 \times 10^{-23}$.

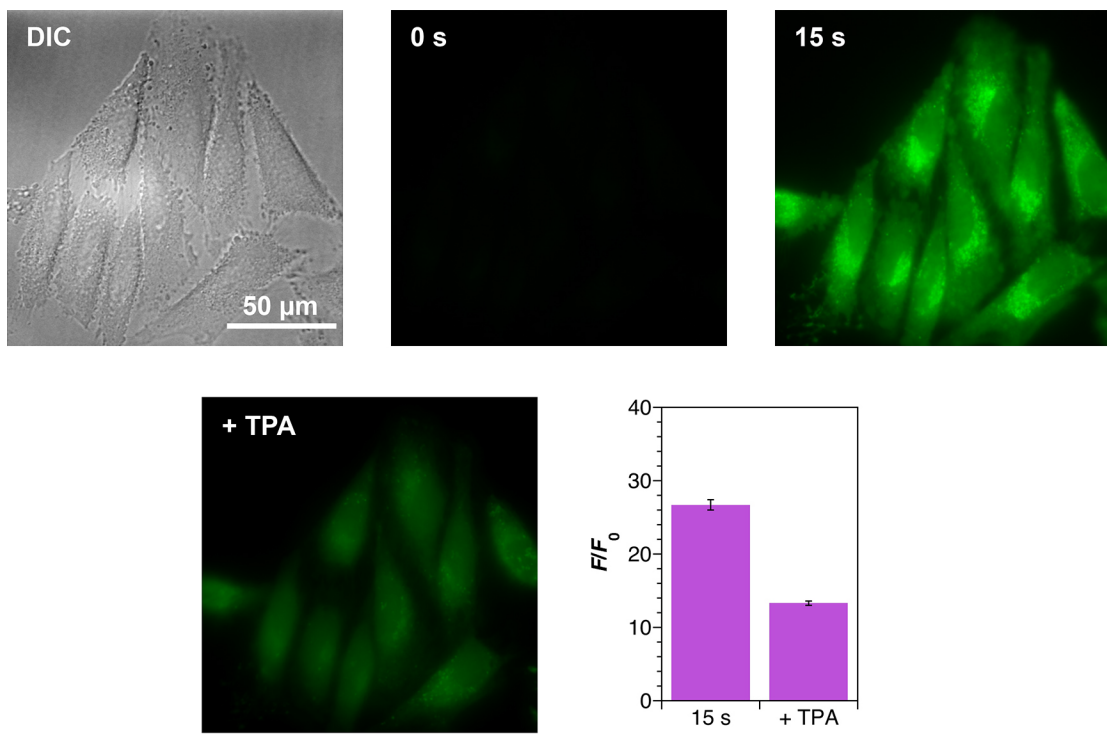


Figure S27. Representative differential interference contrast (DIC, upper left) and fluorescence microscopy images of HeLa cells incubated with 10 μ M zinc pyrithione prior to treatment with 1 μ M 3 before and after irradiation with UV light for 15 s and after subsequent addition of 13 μ M TPA, as described in the text. Average integrated fluorescence turn-on for each condition is shown ($n = 98$). Error bars are standard error. $p = 1.8 \times 10^{-54}$.

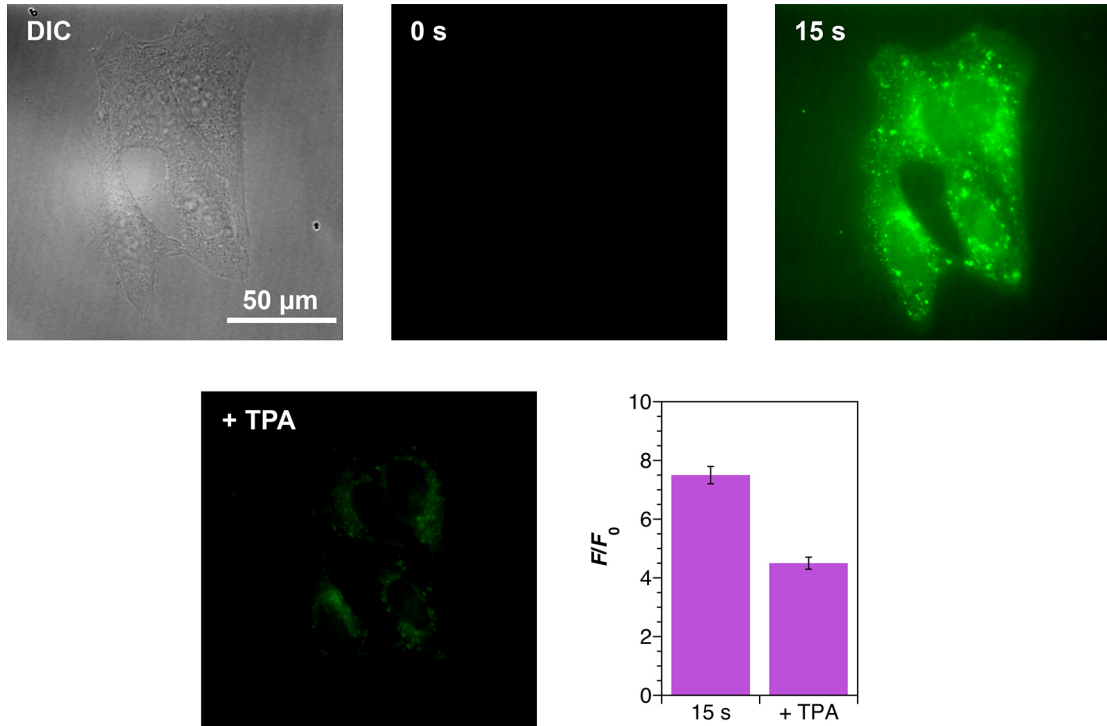


Figure S28. Representative differential interference contrast (DIC, upper left) and fluorescence microscopy images of HeLa cells incubated with a mixture of 1 μ M 3 and 50 μ M ZnCl₂ before and after irradiation with UV light for 15 s and after subsequent addition of 13 μ M TPA, as described in the text. Average integrated fluorescence turn-on for each condition is shown ($n = 88$). Error bars are standard error. $p = 8.4 \times 10^{-29}$.

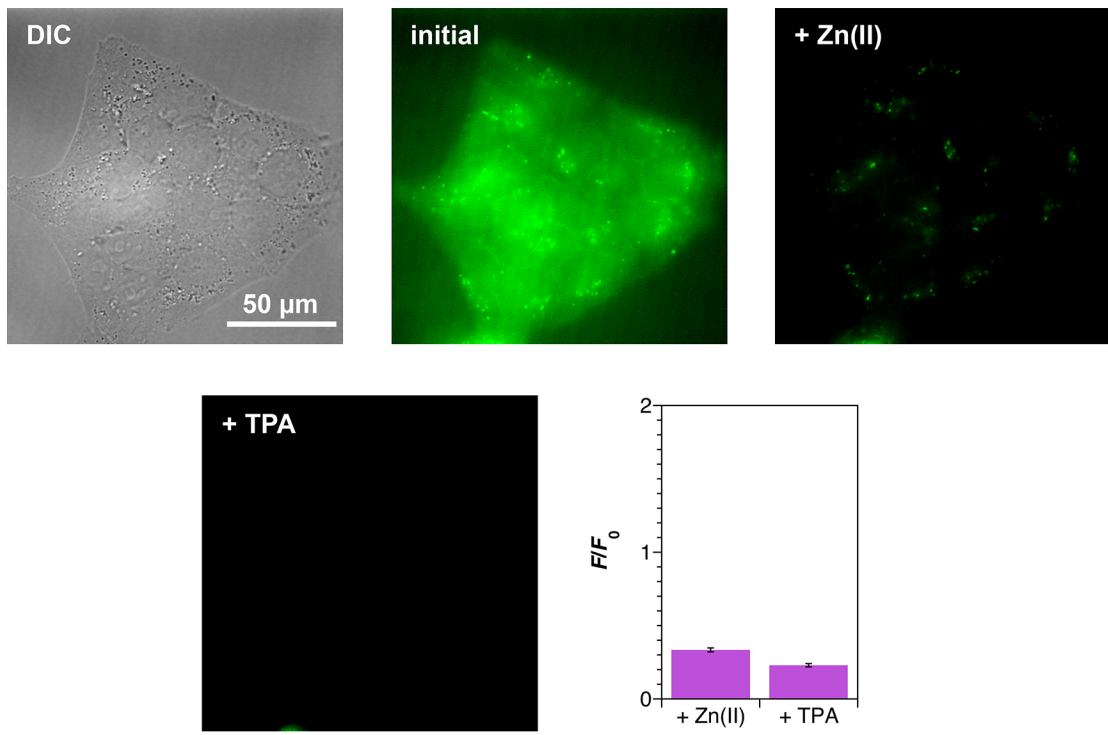


Figure S29. Representative differential interference contrast (DIC, upper left) and fluorescence microscopy images of HeLa cells incubated with a mixture of 1 μ M ZP1, 0.02% (w/v) Pluronic F-127, and 50 μ M ZnCl₂ before and after addition of 10 μ M zinc pyrithione, and after subsequent addition of 13 μ M TPA, as described in the text. Average integrated fluorescence turn-on for each condition is shown ($n = 75$). Error bars are standard error. $p = 1.2 \times 10^{-20}$. The decrease in fluorescence upon addition of Zn(II) is due to extracellular sensor being washed away during application of zinc pyrithione.

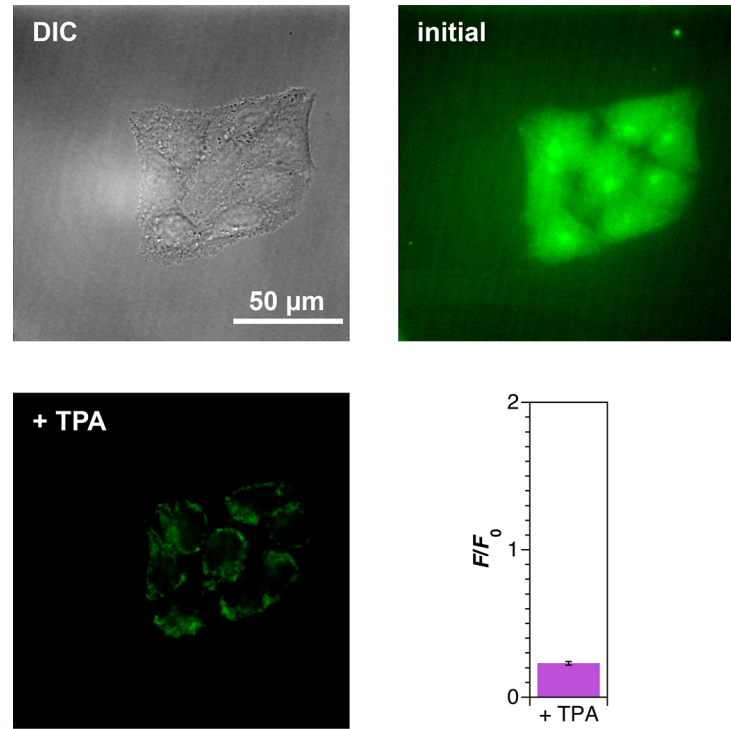


Figure S30. Representative differential interference contrast (DIC, upper left) and fluorescence microscopy images of HeLa cells incubated with 10 μ M zinc pyrithione prior to treatment with 1 μ M ZP1 and after subsequent addition of 13 μ M TPA, as described in the text. Average integrated fluorescence turn-on for each condition is shown ($n = 75$). Error bars are standard error.

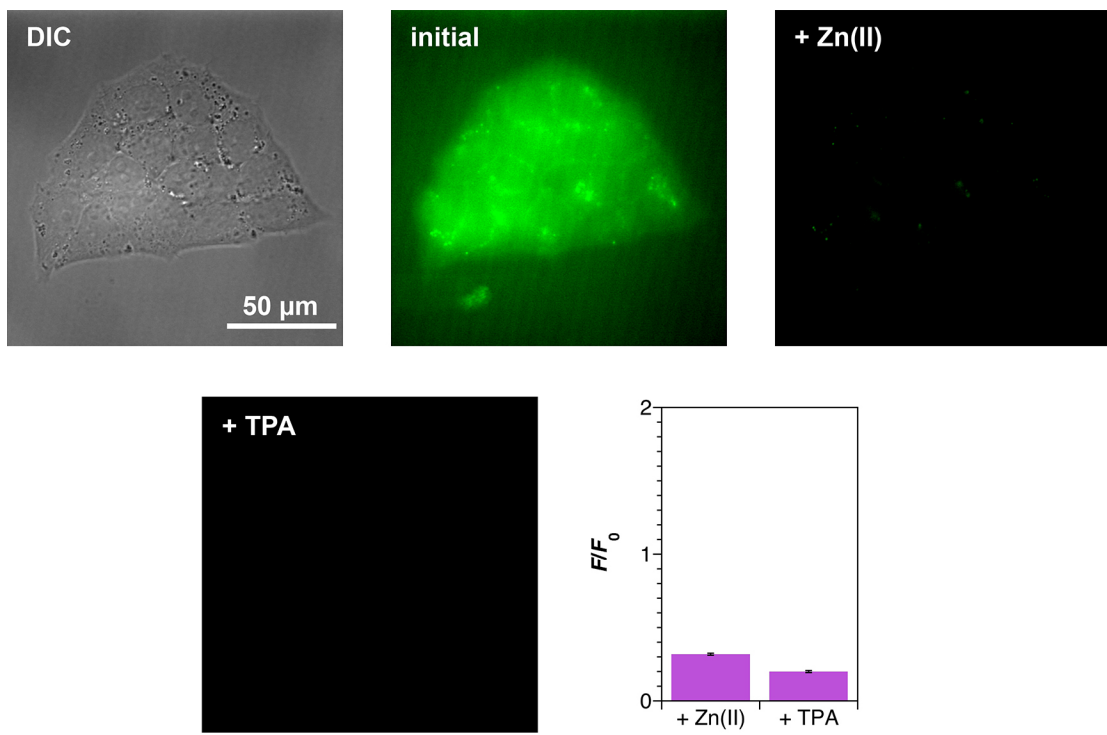


Figure S31. Representative differential interference contrast (DIC, upper left) and fluorescence microscopy images of HeLa cells incubated with a mixture of 1 μ M ZP1 and 50 μ M $ZnCl_2$ before and after treatment with 10 μ M zinc pyrithione before and after subsequent addition of 13 μ M TPA, as described in the text. Average integrated fluorescence turn-on for each condition is shown ($n = 72$). Error bars are standard error. $p = 1.1 \times 10^{-52}$. The decrease in fluorescence upon addition of Zn(II) is due to extracellular sensor being washed away during application of zinc pyrithione.

Experiments in DCN brain slices.

Animals. All procedures were approved by the Institutional Animal Care and Use Committee at the University of Pittsburgh, Pittsburgh, PA

Preparation of DCN brain slices. Male or female ICR mice (Harlan) aged between postnatal day 20 (P20) and P22 were used. Mice were anesthetized with isoflurane then immediately decapitated and brains were rapidly removed. Brain slices were prepared in warm (34 °C) artificial cerebrospinal fluid (ACSF) containing the following (in mM): 130 NaCl, 3 KCl, 1.2 CaCl₂·2H₂O, 1.3 MgCl₂·6H₂O, 20 NaHCO₃, 3 HEPES, and 10 D-glucose, saturated with 95% O₂/5% CO₂ (v/v), pH = 7.25-7.35, ~300 mOsm. Coronal slices (210 µm thickness) containing cross sections including the molecular and deep layers of the dorsal cochlear nucleus (DCN) were cut using a Vibratome (VT1200S; Leica), then transferred to a holding chamber containing warm ACSF and incubated for ~60 min at 34 °C before initiating imaging experiments. ACSF used for incubating and imaging had the same composition as cutting ACSF, except contaminating zinc was removed by stirring the ACSF with Chelex 100 resin (Bio-Rad) for 1 hour. Chelex resin was filtered using Nalgene rapid flow filters lined with polyethersulfone (0.2 µm pore size), then high purity CaCl₂·2H₂O and MgCl₂·6H₂O (99.995%; Sigma-Aldrich) were added to the ACSF. All plastic- and glassware were washed with 5% nitric acid.

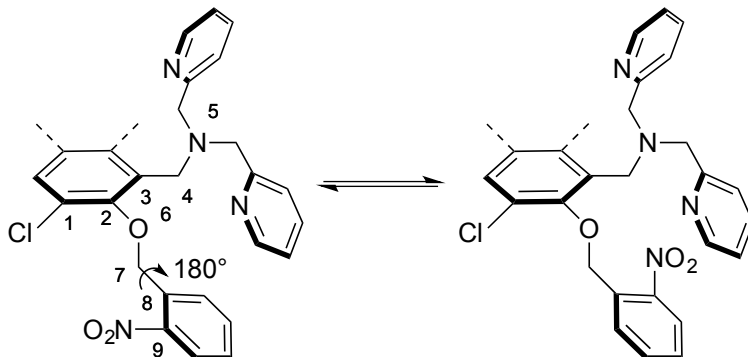
Fluorescence imaging and laser photoactivation. Slices were transferred to the imaging chamber and perfused with room temperature recirculating ACSF (1-2 mL/min). Prior to fluorescence imaging, 1 µL **3** (1 mM) was mixed with 1 µL 20% Pluronic F-127 (Invitrogen), then added to the ACSF for a final concentration of 1 µM **3**. Slices were allowed to incubate with **3** in the imaging chamber for 20 min before initiating fluorescence imaging. Images were acquired using an upright microscope (Olympus BX5) with a 20× water immersion objective and epifluorescence optics. The excitation source was a blue LED (470 nm wavelength, M470L3, Thorlabs), and green fluorescent signals were isolated using a GFP filter (U-N41017, Olympus) and acquired using a CCD camera (Retiga 2000R, QImaging). Images of fluorescent signals were captured before and after UV laser photostimulation. Photostimulation with UV laser light (355 nm, ~5.5 mW; DPSS Lasers) was performed under the 20× objective, and the photostimulation grid consisted of 8 × 8 sites (40 µm spacing) positioned to encompass the molecular layer and deep layer of the DCN. Each site was photostimulated with a 1 ms pulse of UV laser light (0.4 s between sites), and photostimulation of the entire grid was repeated 5 times.

Data analysis. All analysis was performed with custom routines in MATLAB (Mathworks) or with Prism 6 (GraphPad). For fluorescent images captured before and after photostimulation, a region of interest was selected containing the top row (molecular layer) or bottom row (deep layer) of the photostimulation grid. Fluorescence intensity was averaged within each region, and the change in intensity (ΔF) was calculated by subtracting the intensity before photostimulation from the intensity after photostimulation. $\Delta F/F$ was calculated by dividing ΔF by the intensity before photostimulation. Statistical comparison of $\Delta F/F$ in the molecular layer versus the deep layer was performed using an unpaired *t* test with Welch's correction.

Theoretical Calculations.

To examine the influence of the photocleavable protecting groups on the coordination environment of the zinc binding sites, we investigated the structures of **1**, **2**, and **3** with DFT calculations.⁷ Geometry optimization was performed at the CPCM(H₂O)-B3LYP/6-31G level of theory.⁸⁻⁹ The starting structural parameters of the ZP1 skeleton, in the lactone form, were adapted from previous calculations.¹⁰ To minimize steric interactions between the photocleavable protecting groups and the ZP1 backbone, the following sets of dihedral angle values were used in the initial structures. For the first set, we used $\phi_{C1-C2-O6-C7} = 90^\circ$ (*trans* with respect to the di(2-picoly)amine (DPA) arm), $\phi_{C2-O6-C7-C8} = 180^\circ$ (*trans* with respect to the fluorescein backbone), and $\phi_{O6-C7-C8-C9} = 90^\circ$. For the second set, we used $\phi_{C1-C2-O6-C7} = 90^\circ$ (*trans* with respect to the di(2-picoly)amine (DPA) arm), $\phi_{C2-O6-C7-C8} = 180^\circ$ (*trans* with respect to the fluorescein backbone), and $\phi_{O6-C7-C8-C9} = -90^\circ$.

With these initial structures, two local minima, confirmed by frequency analyses at the CPCM(H₂O)-B3LYP/6-31G level, were found for each sensor on the potential energy surface. To estimate better the relative energy of each conformer, free energies were calculated by combining single point calculations at the CPCM(H₂O)-B3LYP/6-311+G(d,p)//CPCM(H₂O)-B3LYP/6-31G level with thermal and entropic corrections obtained at the CPCM(H₂O)-B3LYP/6-31G level.



Scheme S4. Initial conformations considered in calculations.

To confirm that the 6-31G basis set is suitable for geometry optimization, we also investigated structures of **1** at the CPCM(H₂O)-B3LYP/6-31G(d) and CPCM(H₂O)-B3LYP/SVP levels of theory. As shown in Table S4, with the CPCM solvation model, the values of the key dihedral angle $\phi_{N5-C4-C3-C2}$ are nearly identical at different levels of theory. Compared to the structures predicted at the CPCM(H₂O)-B3LYP/6-31G level, slightly smaller $\phi_{N5-C4-C3-C2}$ values, -73° to -83° , were found at the CPCM(H₂O)-B3LYP/SVP level. As discussed below, these values are still significantly larger than the corresponding $\phi_{N5-C4-C3-C2}$ dihedral angle of ZP1 (-33°). We also performed geometry optimization of **1** in the gas phase to test the influence of the implicit CPCM model on the structure of **1**. The effect of the CPCM model is obvious when comparing the structures of **1-a** at the CPCM(H₂O)-B3LYP/6-31G(d) and B3LYP/6-31G(d) levels. Overall, these results suggested that the 6-31G

basis set, although rather small, is likely to provide reasonable geometric predictions. To balance computational efficiency and accuracy, we performed all calculations at the CPCM(H₂O)-B3LYP/6-31G(d) level of theory.

Table S4. Relative energies and $\phi_{N5-C4-C3-C2}$ of conformers of **1** at different levels of theory.

level		ΔE (kcal/mol)	ΔG (kcal/mol)	$\phi_{N5-C4-C3-C2}$ (°)
CPCM(H ₂ O)-B3LYP/6-31G	1-a	0.0	0.0	-78.9
	1-b	7.8	10.5	-83.3
CPCM(H ₂ O)-B3LYP/6-31G(d)	1-a	0.0	0.0	-76.4
	1-b	7.3	10.6	-80.3
B3LYP/6-31G(d)	1-a	0.0	0.0	-68.2
	1-b	13.8	15.9	-82.6
CPCM(H ₂ O)-B3LYP/SVP	1-a	0.0	0.0	-72.6
	1-b	8.7	12.0	-82.5
B3LYP/SVP	1-a	0.0	0.0	-69.5
	1-b	14.5	17.5	-83.4

As depicted in Figures S32-S37, the nitro groups of all three sensors point away from the DPA arms in the preferential conformations. As expected, the zinc binding sites of both the major and minor conformers exhibited a significant geometric deviation from the initial ZP1 coordination environment. The calculated dihedral angle $\phi_{N5-C4-C3-C2}$ in the lactone form of ZP1 is 33° (Figure S39). In comparison, this angle ranges from 77° to 85° in the protected sensors. This geometry does not allow for the trigonal bipyramidal zinc-binding mode of ZP1 that was previously determined in X-ray crystallography studies.¹¹ These results are consistent with our initial hypothesis that the introduction of protecting groups on the oxygen atoms diminishes the zinc binding affinities of the sensors compared to ZP1.

Table S5. Energies of conformers of protected ZP1 derivatives at the CPCM(H₂O)-B3LYP/6-31G level of theory.

	<i>E</i> (hartree)	ΔE (kcal/mol)	<i>G</i> (hartree)	ΔG (kcal/mol)	Thermal Correction (hartree)
1-a	-4348.28226382	0.0	-4347.43646600	0.0	0.845797
1-b	-4348.26987344	7.8	-4347.41975200	10.5	0.850122
2-a	-4806.22916340	0.0	-4805.26070100	0.0	0.968462
2-b	-4806.21112366	11.3	-4805.24488000	9.9	0.966244
3-a	-5022.17118093	0.0	-5021.32449300	0.0	0.846688
3-b	-5022.17302438	-1.2	-5021.32269600	1.1	0.850328

Table S6. Energies of conformers of protected ZP1 derivatives at the CPCM(H₂O)-B3LYP/6-311+G(d,p) level of theory.

	<i>E</i> (hartree)	ΔE (kcal/mol)	<i>G</i> (hartree)	ΔG (kcal/mol)
1-a	-4350.23524223	0.0	-4349.38944523	0.0
1-b	-4350.22326838	7.5	-4349.37314638	10.2
2-a	-4808.46242662	0.0	-4807.49396462	0.0
2-b	-4808.45270710	6.1	-4807.48646310	4.7
3-a	-5024.49347851	0.0	-5023.64679051	0.0
3-b	-5024.49314165	0.2	-5023.64281365	2.5

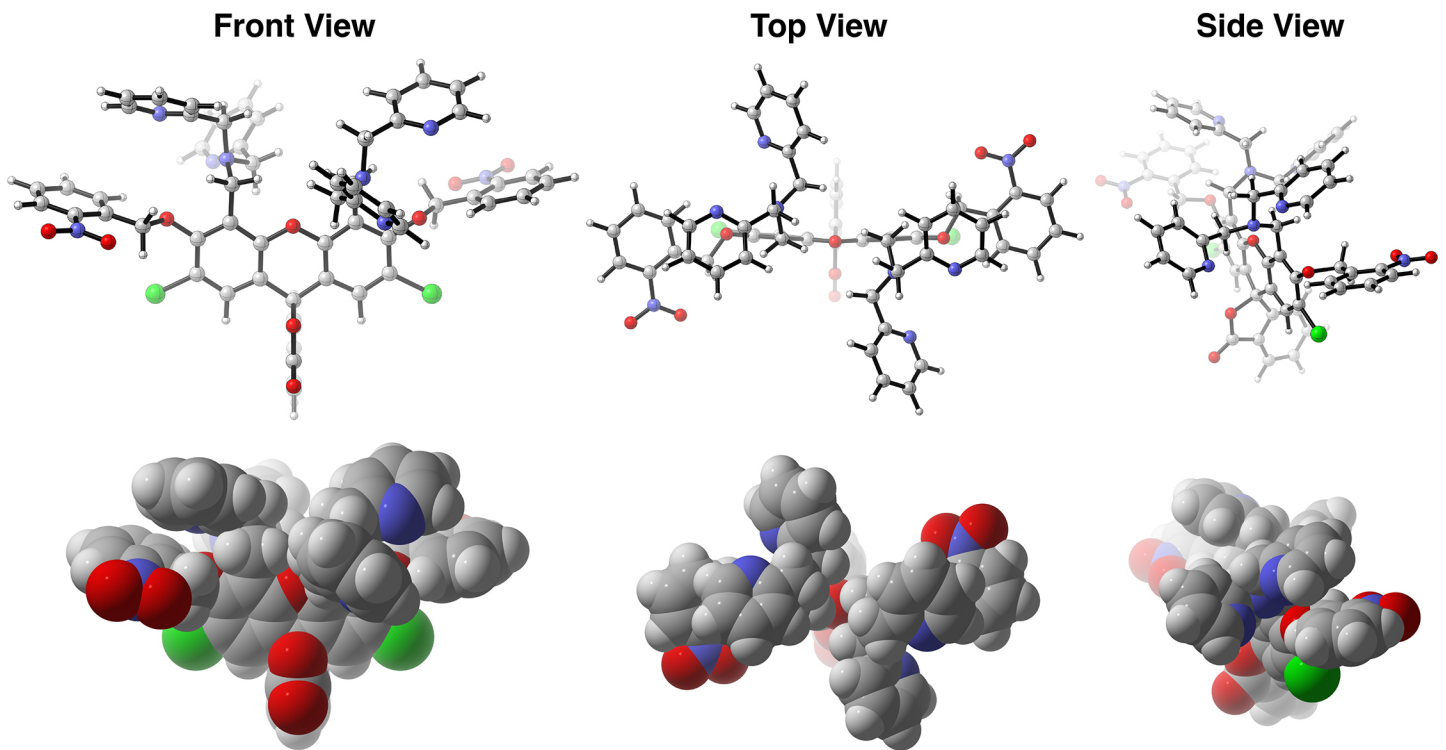


Figure S32. Ball and stick (top) and space filling (bottom) models of conformer **1-a** at the CPCM(H_2O)-B3LYP/6-31G level as viewed from the front, top, and side.

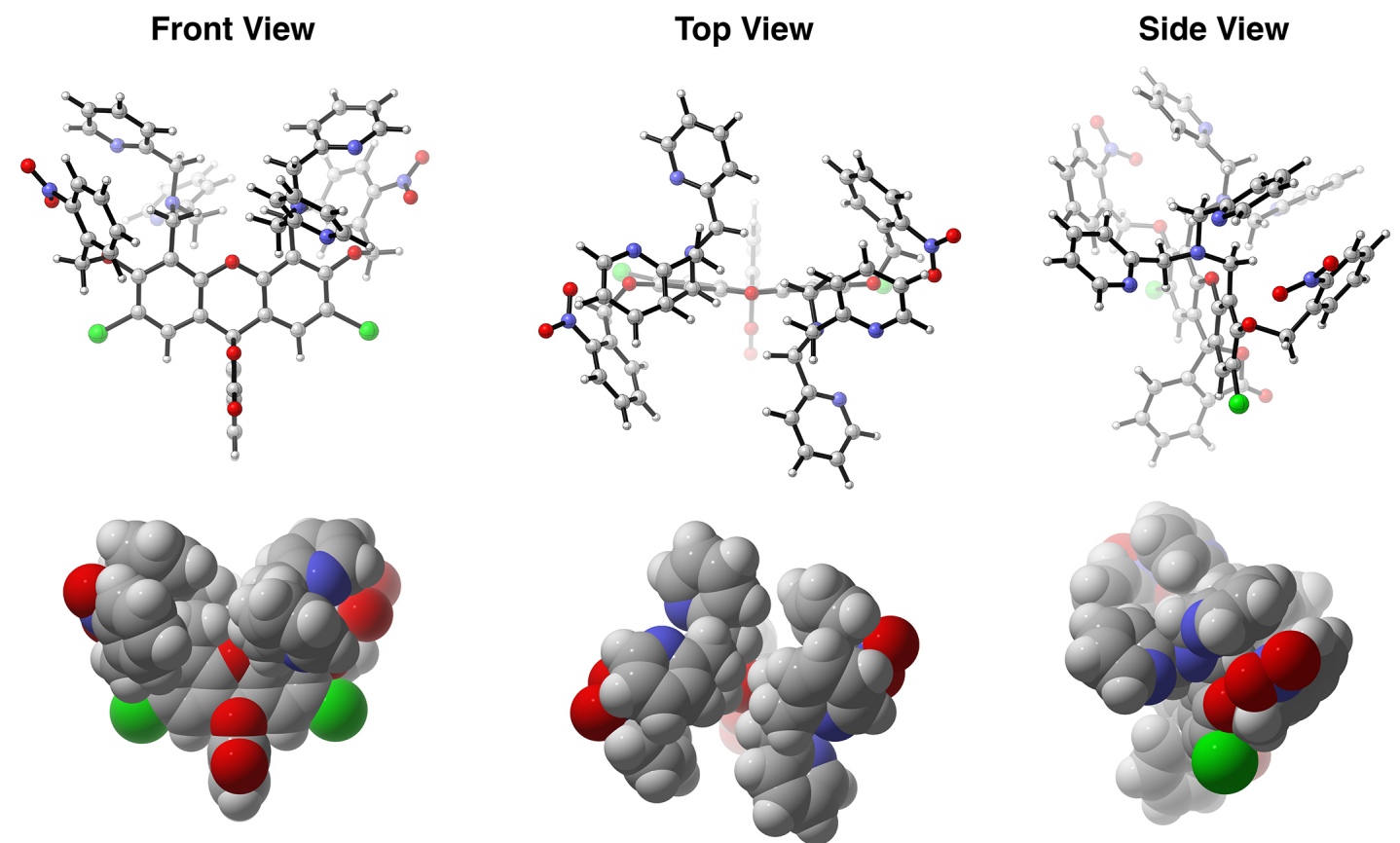


Figure S33. Ball and stick (top) and space filling (bottom) models of conformer **1-b** at the CPCM(H_2O)-B3LYP/6-31G level as viewed from the front, top, and side.

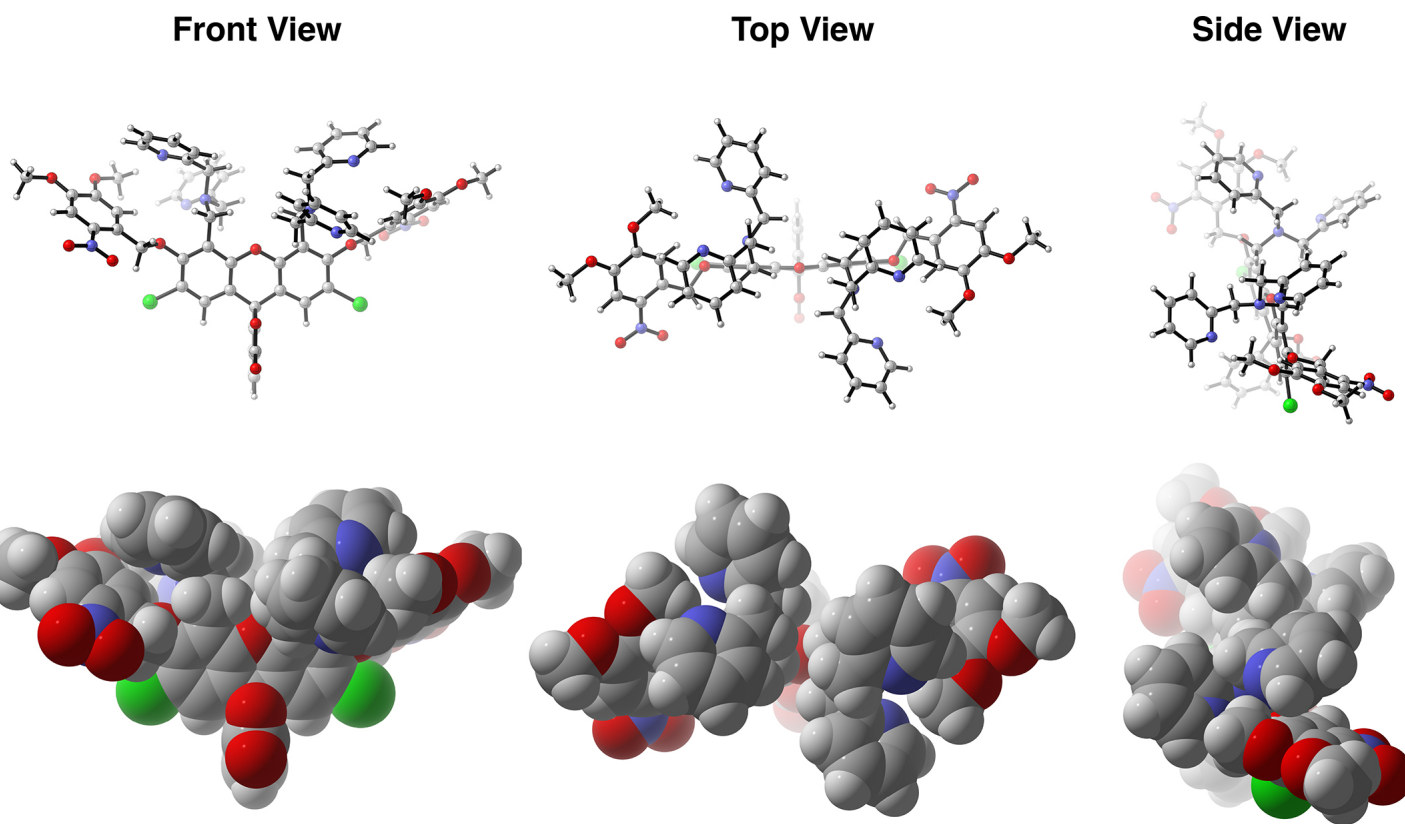


Figure S34. Ball and stick (top) and space filling (bottom) models of conformer **2-a** at the CPCM(H_2O)-B3LYP/6-31G level as viewed from the front, top, and side.

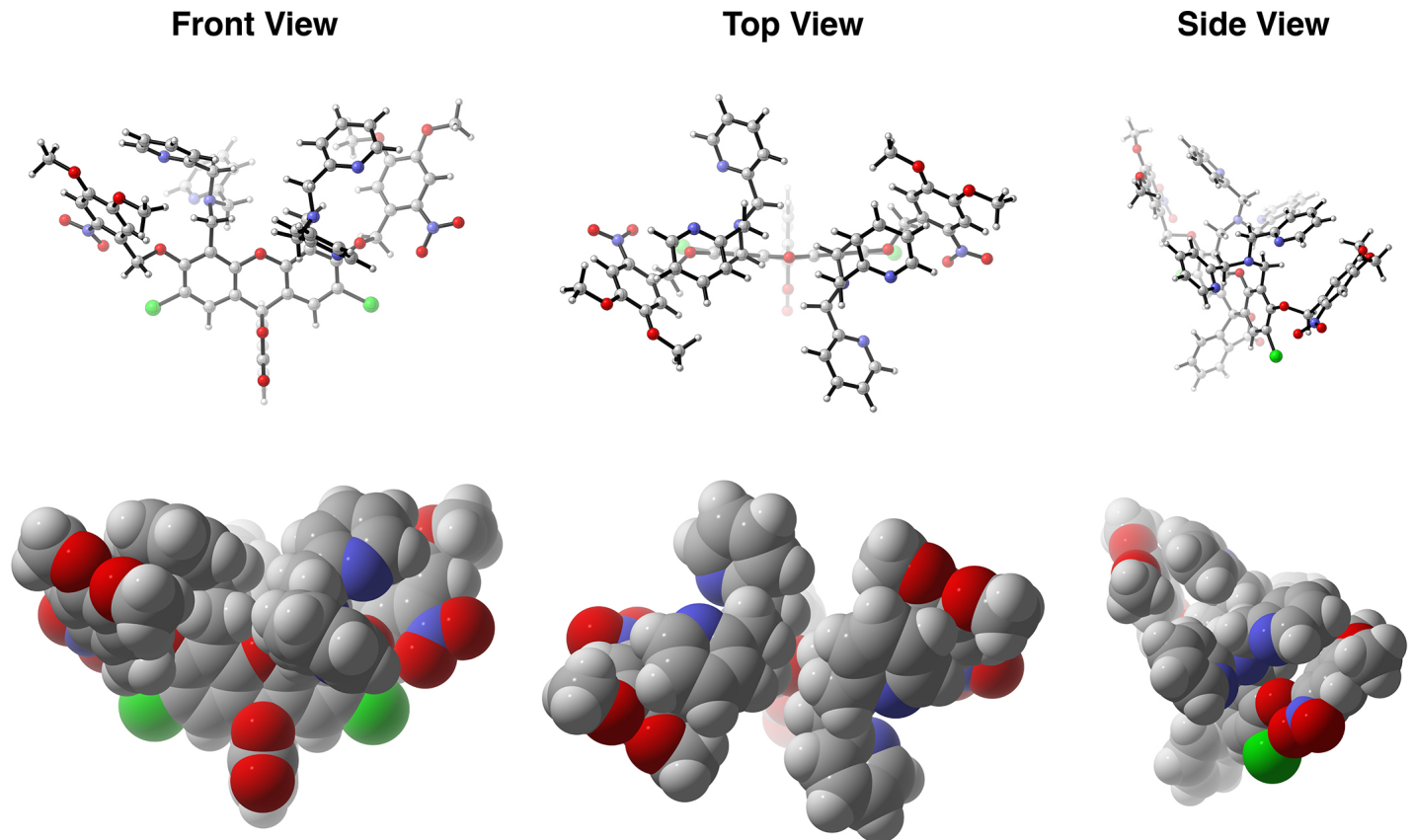


Figure S35. Ball and stick (top) and space filling (bottom) models of conformer **2-b** at the CPCM(H_2O)-B3LYP/6-31G level as viewed from the front, top, and side.

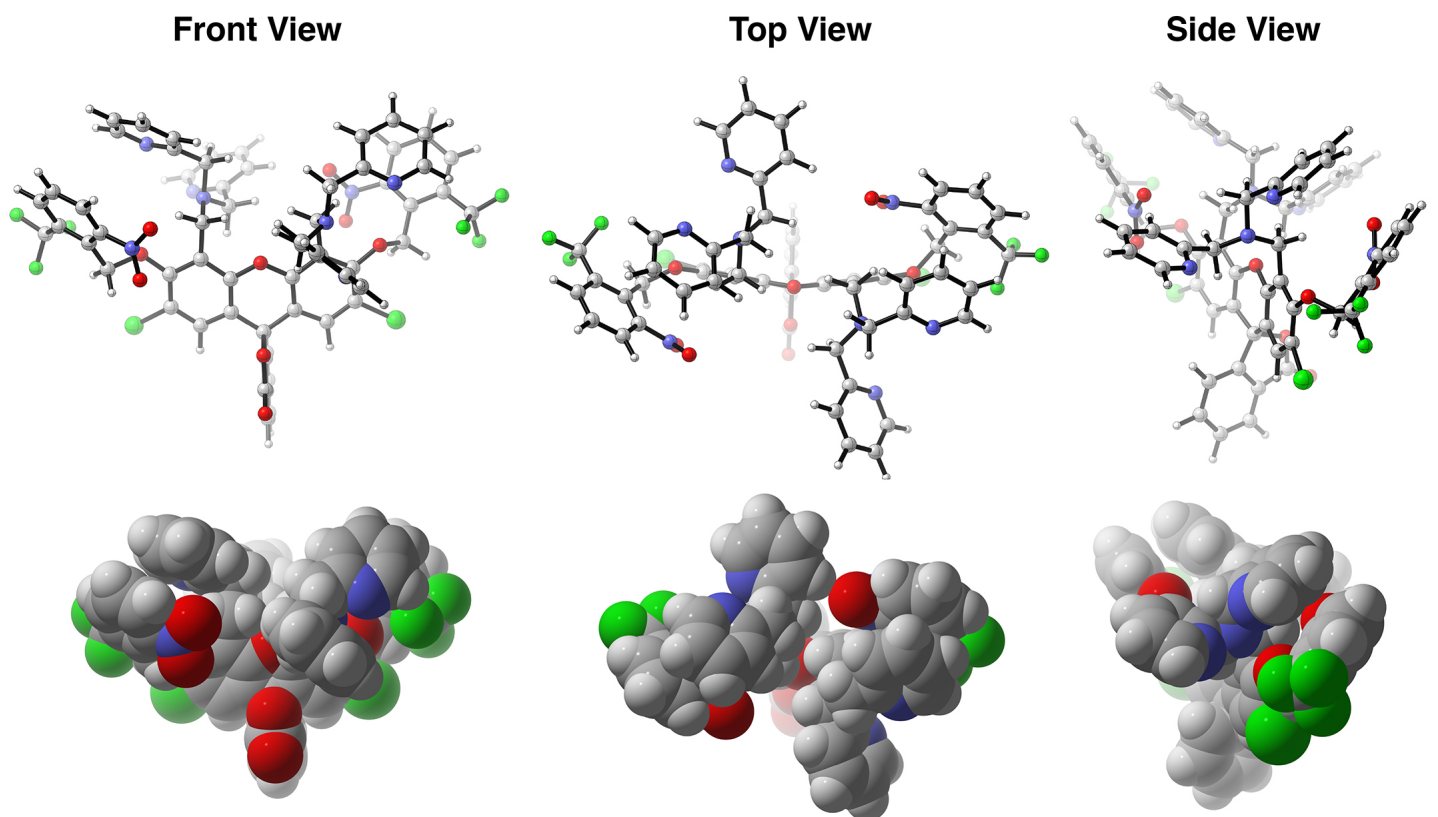


Figure S36. Ball and stick (top) and space filling (bottom) models of conformer **3-a** at the CPCM(H_2O)-B3LYP/6-31G level as viewed from the front, top, and side.

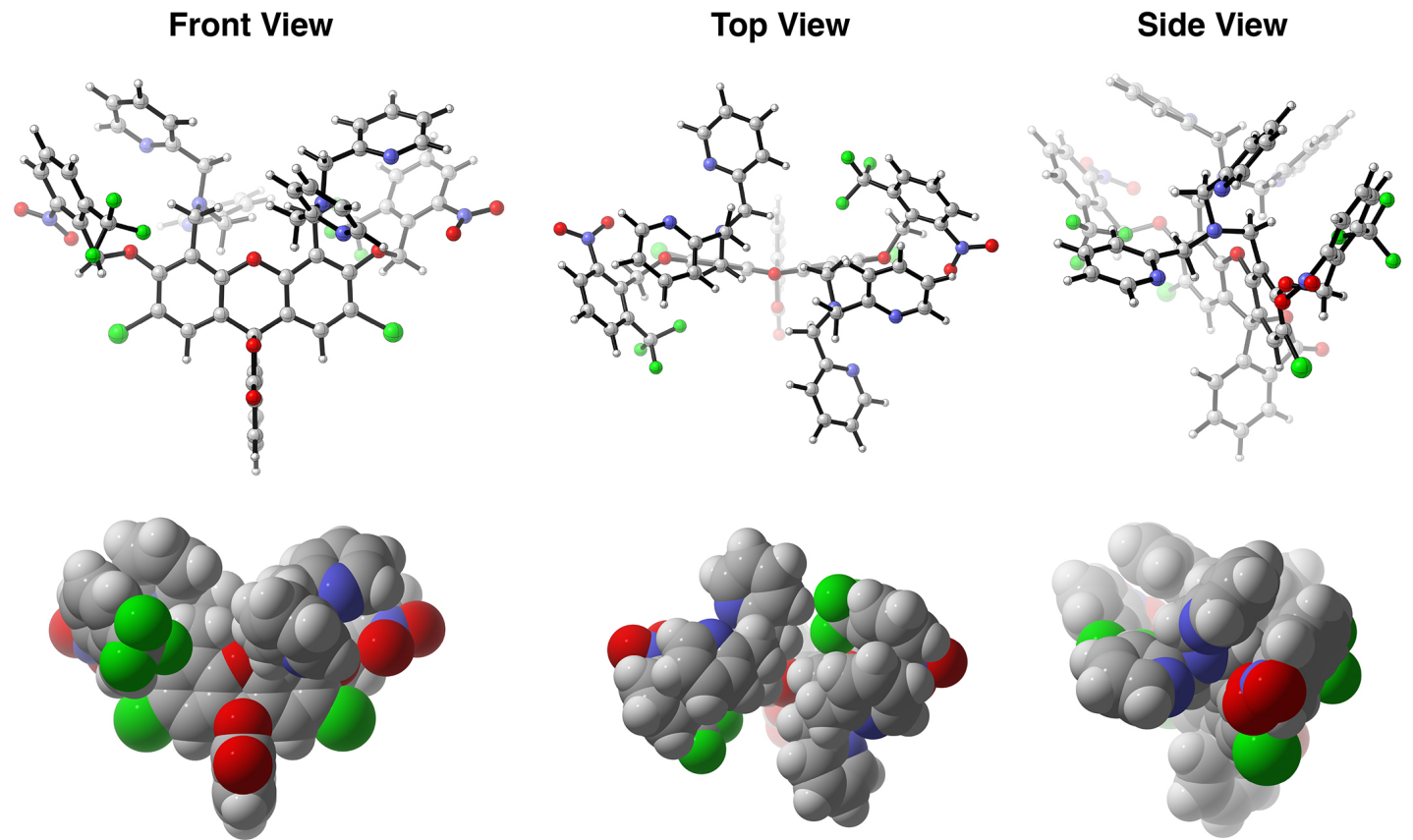
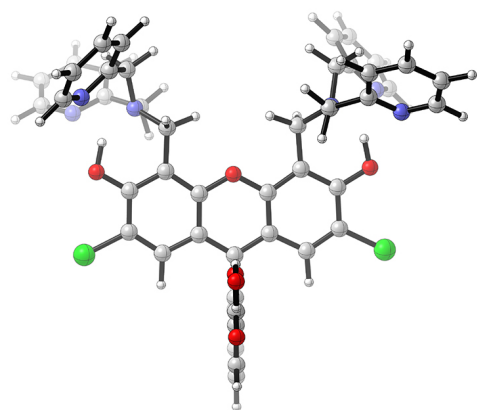
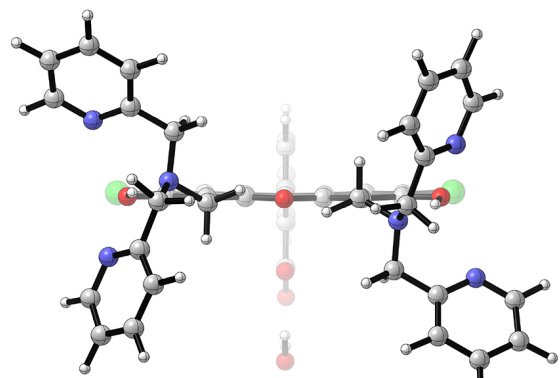


Figure S37. Ball and stick (top) and space filling (bottom) models of conformer **3-b** at the CPCM(H_2O)-B3LYP/6-31G level as viewed from the front, top, and side.

Front View



Top View



Side View

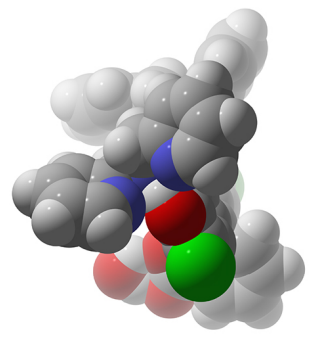
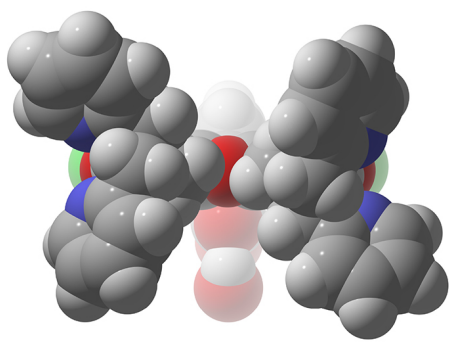
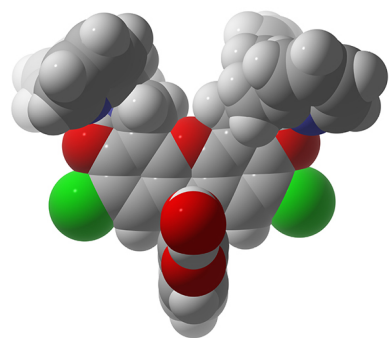
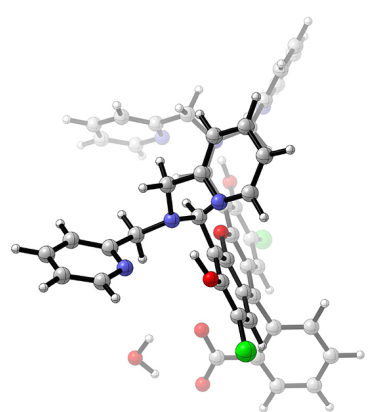


Figure S38. Ball and stick (top) and space filling (bottom) models of ZP1 as viewed from the front, top, and side.

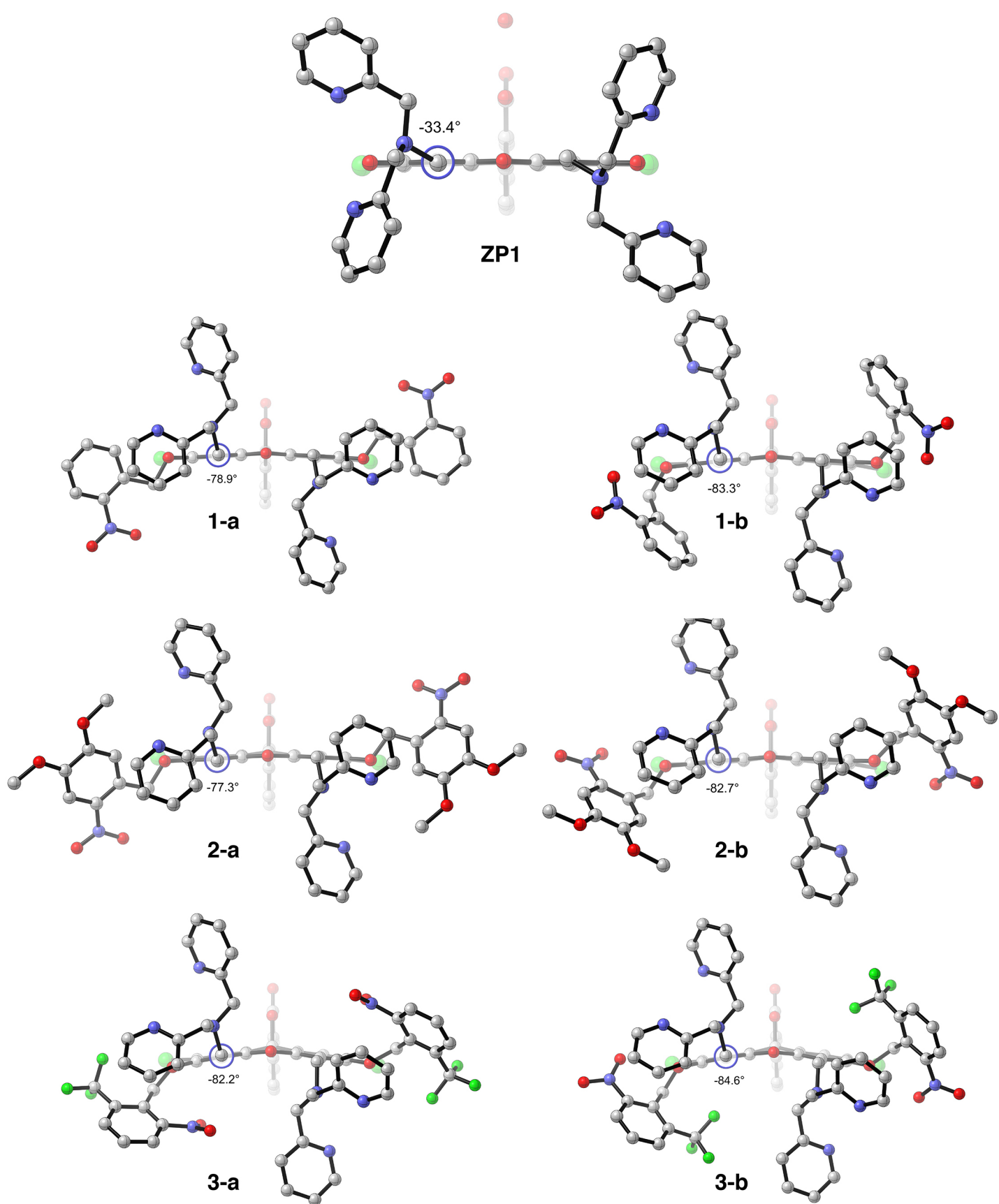
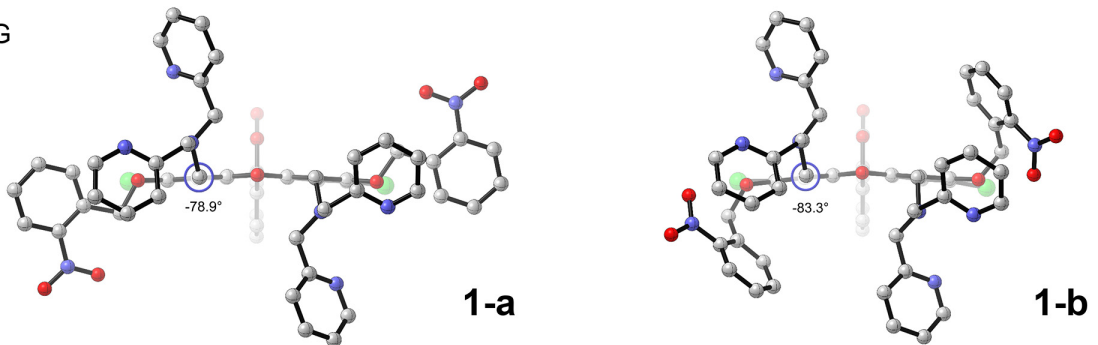
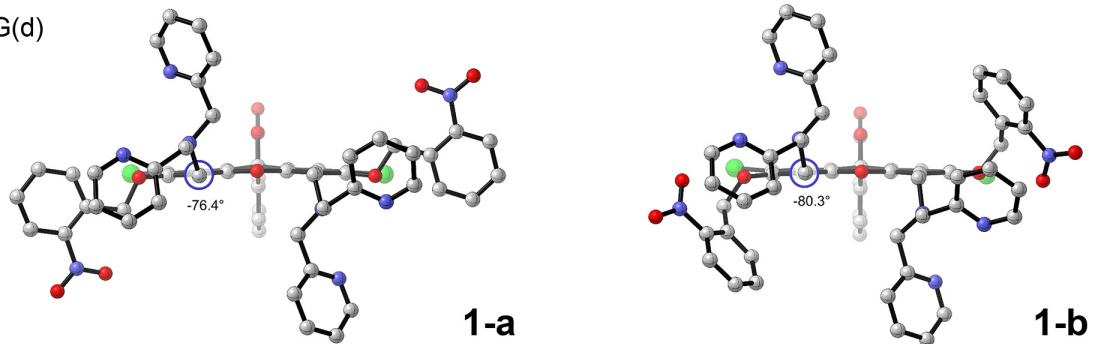


Figure S39. Orientation of the DPA arms in ZP1 and protected sensors. Dihedral angles ($\phi_{N5-C4-C3-C2}$) of the protected sensors calculated at the CPCM(H₂O)-B3LYP/6-31G level are indicated.

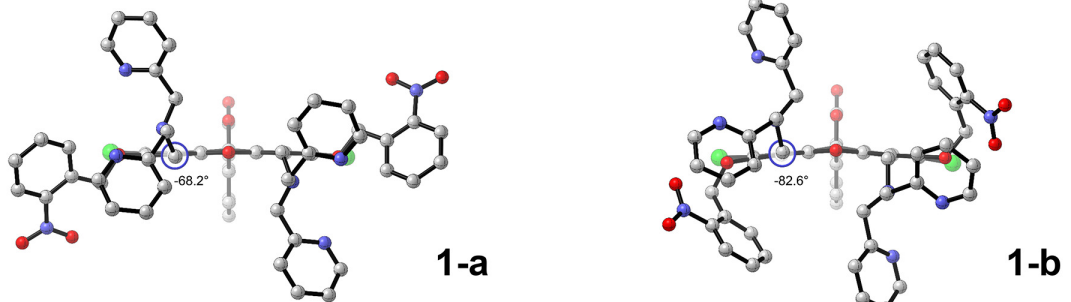
CPCM(H₂O)-B3LYP/6-31G



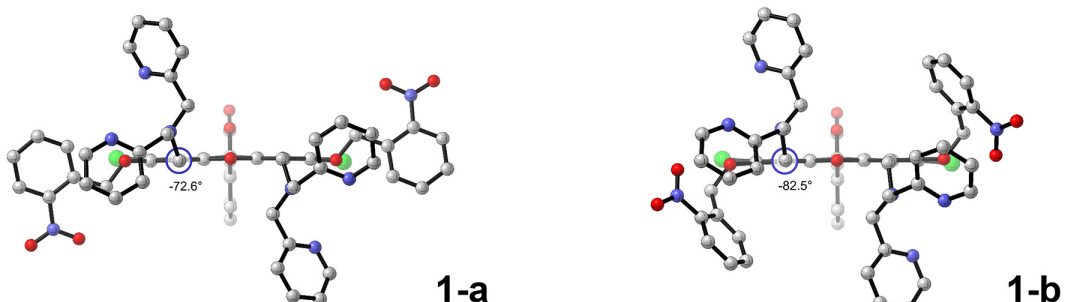
CPCM(H₂O)-B3LYP/6-31G(d)



B3LYP/6-31G(d)



CPCM(H₂O)-B3LYP/SVP



B3LYP/SVP

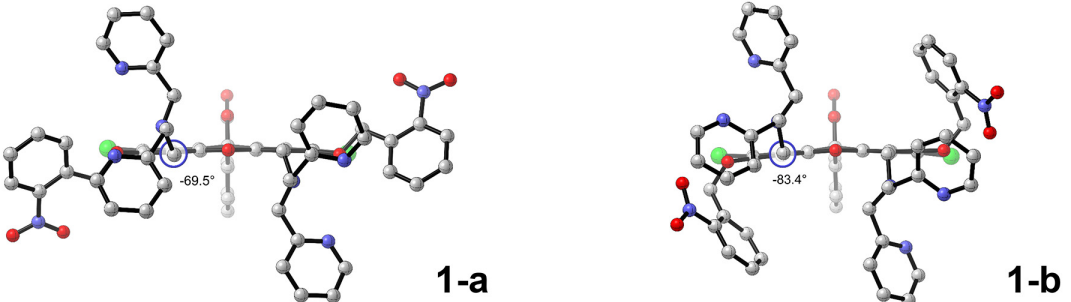


Figure S40. Comparison of **1-a** and **1-b** dihedral angles ($\phi_{N5-C4-C3-C2}$) calculated at different levels of theory, as indicated.

Optimized Coordinates of 1-a at the CPCM(H₂O)-B3LYP/6-31G level.

Standard orientation:							
Center Number	Atomic Number	Atomic Type	Coordinates (Angstroms)				
			X	Y	Z		
1	17	0	5.285626	3.298677	-0.389743	62	6
2	17	0	-5.240608	3.372817	0.254065	63	6
3	8	0	4.773524	0.297714	-0.284044	64	6
4	8	0	0.020383	0.550539	0.211874	65	6
5	8	0	-4.760486	0.362895	0.203945	66	6
6	6	0	0.133081	5.346318	1.852696	67	6
7	1	0	0.095970	7.998859	0.743421	68	6
8	1	0	-0.022542	8.425068	-1.721881	69	1
9	1	0	-0.112587	6.529595	-3.309973	70	1
10	1	0	-0.087210	4.180094	-2.498703	71	1
11	1	0	2.620606	4.320861	-0.059513	72	1
12	1	0	-2.541111	4.356965	0.244118	73	1
13	8	0	0.119734	3.949740	1.801464	74	1
14	8	0	0.190221	5.950739	2.926718	75	1
15	6	0	0.069380	5.854073	0.475074	76	1
16	6	0	0.056039	7.179590	0.034531	77	1
17	6	0	-0.010268	7.409412	-1.343247	78	1
18	6	0	-0.061402	6.331099	-2.245084	79	1
19	6	0	-0.047302	5.002769	-1.793560	80	1
20	6	0	0.018873	4.779934	-0.419381	81	1
21	6	0	0.046704	3.458697	0.337176	82	1
22	6	0	1.287556	2.629424	0.106703	83	1
23	6	0	2.541638	3.241833	-0.039117	84	1
24	6	0	3.680625	2.466056	-0.158574	85	1
25	6	0	3.622508	1.062347	-0.134700	86	1
26	6	0	2.378789	0.418996	-0.023516	87	1
27	6	0	1.233576	1.230224	0.101413	88	7
28	6	0	-1.188076	1.247432	0.215420	89	6
29	6	0	-2.351009	0.452405	0.197864	90	1
30	6	0	-3.590379	1.113165	0.182934	91	7
31	6	0	-3.631575	2.517552	0.202061	92	1
32	6	0	-2.475621	3.277018	0.221091	93	1
33	6	0	-1.221760	2.647062	0.223576	94	6
34	6	0	2.282813	-1.090949	-0.037226	95	1
35	6	0	1.431718	-1.221452	-2.378223	96	0
36	6	0	1.856013	-1.480407	-3.808679	97	0
37	6	0	1.161433	-2.380005	-4.630247	98	0
38	6	0	1.582575	-2.571924	-5.951827	99	0
39	6	0	2.689668	-1.857151	-6.418639	100	6
40	6	0	3.329501	-0.974599	-5.541019	101	6
41	6	0	2.511940	-3.166658	-1.329934	102	6
42	6	0	3.765483	-3.686574	-0.660102	103	6
43	1	0	6.977097	-3.876259	-1.365430	104	6
44	1	0	7.041333	-5.023834	0.854920	105	1
45	1	0	-0.562377	-3.040304	4.428315	106	6
46	1	0	-1.420931	-3.423277	6.747670	107	1
47	1	0	-3.404282	-2.092112	7.535924	108	1
48	1	0	-4.429003	-0.437415	5.966445	109	1
49	7	0	2.436603	-1.686084	-1.392468	110	7
50	7	0	-2.530333	-1.671341	1.529416	111	6
51	7	0	2.929488	-0.782281	-4.264569	112	8
52	7	0	-5.067408	-3.486728	1.398533	113	6
53	6	0	6.068824	-4.014790	-0.788033	114	6
54	6	0	6.103403	-4.656320	0.455028	115	6
55	6	0	4.903794	-4.811352	1.156361	116	6
56	6	0	-2.278730	-1.058867	0.196058	117	6
57	6	0	-2.645209	-3.148733	1.430643	118	1
58	6	0	-3.896894	-3.615000	0.719880	119	6
59	6	0	-3.849537	-4.180985	-0.562743	120	1
60	6	0	-5.033981	-4.622292	-1.164958	121	1
61	6	0	-6.237800	-4.488052	-0.466592	122	1
						123	7
						124	8
						125	8

Optimized Coordinates of 1-b at the CPCM(H₂O)-B3LYP/6-31G level.

Standard orientation:						
Center Number	Atomic Number	Atomic Type	Coordinates (Angstroms)			
			X	Y	Z	
1	17	0	5.268433	3.552205	-1.085668	62
2	17	0	-5.151692	3.788684	0.267125	63
3	8	0	4.787492	0.553520	-0.553504	64
4	8	0	0.076140	0.911555	0.202668	65
5	8	0	-4.705010	0.739661	0.210887	66
6	6	0	0.324171	5.737759	1.592626	67
7	1	0	0.247724	8.361040	0.417071	68
8	1	0	-0.013726	8.724562	-2.047152	69
9	1	0	-0.215607	6.789809	-3.576537	70
10	1	0	-0.163392	4.461639	-2.705424	71
11	1	0	2.666101	4.613743	-0.572718	72
12	1	0	-2.458968	4.730044	0.099360	73
13	8	0	0.291079	4.341101	1.580079	74
14	8	0	0.451032	6.370014	2.644598	75
15	6	0	0.185784	6.210411	0.207817	76
16	6	0	0.158395	7.524103	-0.266221	77
17	6	0	0.012003	7.718941	-1.643262	78
18	6	0	-0.102630	6.618415	-2.511731	79
19	6	0	-0.073727	5.302190	-2.026571	80
20	6	0	0.072208	5.114328	-0.653404	81
21	6	0	0.129645	3.813226	0.133948	82
22	6	0	1.344522	2.961120	-0.141955	83
23	6	0	2.584593	3.542267	-0.446140	84
24	6	0	3.706030	2.746074	-0.593116	85
25	6	0	3.652344	1.348356	-0.429310	86
26	6	0	2.408947	0.731929	-0.196333	87
27	6	0	1.283252	1.566493	-0.043346	88
28	6	0	-1.128350	1.615854	0.191920	89
29	6	0	-2.295536	0.827754	0.251026	90
30	6	0	-3.534848	1.491380	0.193102	91
31	6	0	-3.560509	2.899190	0.163028	92
32	6	0	-2.399855	3.649693	0.118441	93
33	6	0	-1.150051	3.012567	0.111888	94
34	6	0	2.269999	-0.772744	-0.145773	95
35	6	0	1.163557	-0.799090	-2.407554	96
36	6	0	1.378597	-1.196882	-3.853350	97
37	6	0	0.427086	-1.952120	-4.554741	98
38	6	0	0.657188	-2.274139	-5.897903	99
39	6	0	1.835431	-1.831584	-6.506532	100
40	6	0	2.735606	-1.079338	-5.743562	101
41	6	0	1.947110	-2.876623	-1.364972	102
42	6	0	3.152339	-3.639029	-0.860428	103
43	1	0	6.118125	-4.488179	-2.012958	104
44	1	0	6.247207	-5.673062	0.184751	105
45	1	0	-0.205426	-1.956134	4.773605	106
46	1	0	-0.991351	-2.205001	7.136252	107
47	1	0	-3.099455	-1.025846	7.837948	108
48	1	0	-4.316361	0.350149	6.141567	109
49	7	0	2.156097	-1.413695	-1.491663	110
50	7	0	-2.329252	-1.151506	1.808474	111
51	7	0	2.521093	-0.762458	-4.447462	112
52	7	0	-4.552618	-3.313811	2.005396	113
53	6	0	5.291520	-4.443666	-1.311472	114
54	6	0	5.362805	-5.106353	-0.080612	115
55	6	0	4.269926	-5.014835	0.787270	116
56	6	0	-2.210722	-0.674848	0.396692	117
57	6	0	-2.207390	-2.628925	1.877376	118
58	6	0	-3.387784	-3.385140	1.308815	119
59	6	0	-3.269474	-4.169932	0.152680	120
60	6	0	-4.373468	-4.904567	-0.296288	121
61	6	0	-5.571933	-4.830753	0.420673	122
						123
						124
						125

Optimized Coordinates of 2-a at the CPCM(H₂O)-B3LYP/6-31G level.

Standard orientation:							
Center Number	Atomic Number	Atomic Type	Coordinates (Angstroms)				
			X	Y	Z		
1	17	0	5.283023	3.767934	-0.260097	70	1
2	17	0	-5.250273	3.772903	0.067905	71	1
3	8	0	4.794505	0.753370	-0.032251	72	1
4	8	0	0.024970	0.980967	0.199276	73	1
5	8	0	-4.742772	0.750224	-0.015068	74	1
6	6	0	0.039453	5.815890	1.753377	75	1
7	1	0	0.025470	8.441236	0.578613	76	1
8	1	0	-0.000268	8.806187	-1.899110	77	1
9	1	0	-0.014078	6.872135	-3.442467	78	1
10	1	0	-0.002896	4.542751	-2.572582	79	1
11	1	0	2.603200	4.766529	-0.043649	80	1
12	1	0	-2.562541	4.767765	0.115114	81	1
13	8	0	0.037461	4.418248	1.735128	82	1
14	8	0	0.050958	6.445826	2.814017	83	1
15	6	0	0.025330	6.290291	0.362450	84	1
16	6	0	0.019261	7.604594	-0.110822	85	1
17	6	0	0.004877	7.800187	-1.495415	86	1
18	6	0	-0.002983	6.699928	-2.371868	87	1
19	6	0	0.003193	5.383135	-1.887532	88	7
20	6	0	0.017451	5.194593	-0.506884	89	6
21	6	0	0.025398	3.892062	0.281776	90	1
22	6	0	1.279868	3.067876	0.119967	91	7
23	6	0	2.533476	3.687960	0.008707	92	1
24	6	0	3.683309	2.921152	-0.040272	93	1
25	6	0	3.637730	1.518478	0.035772	94	6
26	6	0	2.395336	0.865748	0.107870	95	1
27	6	0	1.237481	1.668804	0.146084	96	1
28	6	0	-1.186915	1.669031	0.134759	97	6
29	6	0	-2.342789	0.865569	0.060581	98	1
30	6	0	-3.586458	1.517305	0.001488	99	1
31	6	0	-3.638047	2.921723	0.033831	100	6
32	6	0	-2.488615	3.688353	0.090613	101	6
33	6	0	-1.231037	3.067916	0.135645	102	6
34	6	0	2.304977	-0.644000	0.149521	103	6
35	6	0	1.734196	-0.769793	-2.285863	104	6
36	6	0	2.299795	-1.139699	-3.641145	105	6
37	6	0	1.603238	-1.979170	-4.522436	106	1
38	6	0	2.154300	-2.272127	-5.775906	107	7
39	6	0	3.390012	-1.714862	-6.117395	108	8
40	6	0	4.024392	-0.883825	-5.187106	109	8
41	6	0	2.389104	-2.783287	-1.049396	110	1
42	6	0	3.437430	-3.455160	-0.189697	111	7
43	1	0	6.607159	-4.306181	-0.468723	112	6
44	1	0	6.194300	-5.249336	1.811768	113	6
45	1	0	-0.912438	-2.410537	4.516255	114	6
46	1	0	-2.055159	-2.923376	6.682662	115	6
47	1	0	-4.297537	-1.880018	7.141339	116	1
48	1	0	-5.286927	-0.372647	5.409898	117	0
49	7	0	2.539894	-1.310614	-1.164269	118	8
50	7	0	-2.582850	-1.303908	1.332138	119	8
51	7	0	3.500895	-0.597086	-3.974149	120	1
52	7	0	-4.723494	-3.562189	0.786548	121	1
53	6	0	5.632021	-4.221720	-0.001068	122	8
54	6	0	5.398977	-4.746801	1.273795	123	8
55	6	0	4.121646	-4.608880	1.826012	124	8
56	6	0	-2.248470	-0.644384	0.037120	125	8
57	6	0	-2.445101	-2.778990	1.229724	126	6
58	6	0	-3.454329	-3.439319	0.316097	127	1
59	6	0	-3.087731	-3.942025	-0.941288	128	1
60	6	0	-4.046128	-4.584176	-1.733763	129	1
61	6	0	-5.350825	-4.711474	-1.246850	130	6
62	6	0	-5.643305	-4.185558	0.015389	131	1
63	6	0	-1.845445	-0.770472	2.503905	132	1
64	6	0	-2.504227	-1.131170	3.818753	133	1
65	6	0	-1.882254	-1.981724	4.744166	134	6
66	6	0	-2.521833	-2.266166	5.957014	135	1
67	6	0	-3.768761	-1.689192	6.214701	136	1
68	6	0	-4.325012	-0.847536	5.244857	137	1
69	1	0	3.069255	-1.023359	0.832658	138	6
						139	1
						140	1
						141	1

Optimized Coordinates of 2-b at the CPCM(H₂O)-B3LYP/6-31G level.

Standard orientation:								
Center Number	Atomic Number	Atomic Type	Coordinates (Angstroms)					
			X	Y	Z			
1	17	0	5.190870	4.025532	-0.824673	70	1	
2	17	0	-5.234706	4.034917	0.371992	71	1	
3	8	0	4.748014	0.948282	-0.417468	72	1	
4	8	0	0.027459	1.220209	0.219518	73	1	
5	8	0	-4.736465	0.944832	0.246249	74	1	
6	6	0	0.158491	6.053412	1.705085	75	1	
7	1	0	0.048353	8.678495	0.534983	76	1	
8	1	0	-0.177583	9.043489	-1.932554	77	1	
9	1	0	-0.312559	7.109296	-3.469993	78	1	
10	1	0	-0.227430	4.780127	-2.603718	79	1	
11	1	0	2.568598	4.992428	-0.346861	80	1	
12	1	0	-2.570669	4.996433	0.217143	81	1	
13	8	0	0.154373	4.656570	1.688322	82	1	
14	8	0	0.254126	6.685277	2.760759	83	1	
15	6	0	0.034349	6.527545	0.319374	84	1	
16	6	0	-0.011832	7.841824	-0.151831	85	1	
17	6	0	-0.138160	8.037483	-1.530700	86	1	
18	6	0	-0.214813	6.937204	-2.403773	87	1	
19	6	0	-0.167246	5.620563	-1.921437	88	7	
20	6	0	-0.041654	5.431858	-0.546391	89	6	
21	6	0	0.028873	4.129070	0.238060	90	1	
22	6	0	1.265196	3.304251	-0.020850	91	7	
23	6	0	2.502652	3.915586	-0.262969	92	1	
24	6	0	3.645174	3.147981	-0.407345	93	1	
25	6	0	3.616090	1.744292	-0.299968	94	6	
26	6	0	2.376206	1.100954	-0.108635	95	1	
27	6	0	1.228757	1.905948	0.031750	96	1	
28	6	0	-1.188502	1.905537	0.227687	97	6	
29	6	0	-2.343753	1.099702	0.259022	98	1	
30	6	0	-3.598189	1.742062	0.239424	99	1	
31	6	0	-3.644156	3.149316	0.241002	100	6	
32	6	0	-2.493252	3.917017	0.210916	101	6	
33	6	0	-1.233349	3.303599	0.190359	102	6	
34	6	0	2.272303	-0.406235	-0.066654	103	6	
35	6	0	1.316863	-0.453253	-2.396245	104	6	
36	6	0	1.673853	-0.810689	-3.823947	105	6	
37	6	0	0.852719	-1.637334	-4.604379	106	1	
38	6	0	1.221334	-1.926458	-5.923926	107	7	
39	6	0	2.403510	-1.378540	-6.430654	108	8	
40	6	0	3.168176	-0.558100	-5.593499	109	8	
41	6	0	2.054086	-2.516357	-1.302537	110	1	
42	6	0	3.196072	-3.257464	-0.643657	111	7	
43	1	0	6.293083	-4.084733	-1.397008	112	8	
44	1	0	6.165134	-5.211752	0.830582	113	8	
45	1	0	-0.270393	-1.852375	4.666572	114	6	
46	1	0	-1.094348	-2.256787	6.994326	115	6	
47	1	0	-3.258249	-1.193603	7.711118	116	1	
48	1	0	-4.491086	0.227163	6.063643	117	7	
49	7	0	2.254469	-1.051773	-1.414252	118	8	
50	7	0	-2.355608	-0.968608	1.700979	119	8	
51	7	0	2.820008	-0.273630	-4.319037	120	1	
52	7	0	-4.474614	-3.241050	1.626702	121	1	
53	6	0	5.384417	-4.038829	-0.805392	122	8	
54	6	0	5.308863	-4.676382	0.437985	123	8	
55	6	0	4.113266	-4.588889	1.157714	124	8	
56	6	0	-2.234797	-0.406195	0.321046	125	8	
57	6	0	-2.162646	-2.439070	1.690750	126	6	
58	6	0	-3.265487	-3.215939	1.006608	127	1	
59	6	0	-3.032813	-3.926233	-0.180426	128	1	
60	6	0	-4.065942	-4.685654	-0.742191	129	1	
61	6	0	-5.309444	-4.711882	-0.103325	130	6	
62	6	0	-5.467746	-3.972237	1.073779	131	1	
63	6	0	-1.493869	-0.320625	2.723193	132	1	
64	6	0	-1.953942	-0.610228	4.136703	133	1	
65	6	0	-1.202061	-1.413324	5.006606	134	6	
66	6	0	-1.663120	-1.636899	6.309745	135	1	
67	6	0	-2.865822	-1.048177	6.711328	136	1	
68	6	0	-3.557811	-0.254603	5.789419	137	1	
69	1	0	3.144015	-0.803213	0.458617	138	6	

Optimized Coordinates of 3-a at the CPCM(H₂O)-B3LYP/6-31G level.

Standard orientation:							
Center Number	Atomic Number	Atomic Type	Coordinates (Angstroms)				
			X	Y	Z		
1	17	0	5.231460	3.471361	-1.055814	65	6
2	17	0	-5.179010	3.553999	-0.454769	66	6
3	8	0	4.757677	0.420453	-0.239470	67	6
4	8	0	0.072465	0.844334	0.393496	68	6
5	8	0	-4.631198	0.448022	-0.146412	69	1
6	6	0	0.108263	5.705742	1.402447	70	1
7	1	0	0.079269	8.269319	0.098268	71	1
8	1	0	0.020970	8.511317	-2.393516	72	1
9	1	0	-0.013179	6.503032	-3.839347	73	1
10	1	0	0.009180	4.219520	-2.853633	74	1
11	1	0	2.634987	4.493044	-0.652165	75	1
12	1	0	-2.520075	4.531102	-0.427917	76	1
13	8	0	0.105066	4.310444	1.455210	77	1
14	8	0	0.133882	6.390505	2.428865	78	1
15	6	0	0.076615	6.110332	-0.010475	79	1
16	6	0	0.064229	7.399364	-0.548488	80	1
17	6	0	0.031557	7.526371	-1.940875	81	1
18	6	0	0.012120	6.384320	-2.761744	82	1
19	6	0	0.024616	5.093341	-2.212259	83	1
20	6	0	0.057336	4.973144	-0.824202	84	1
21	6	0	0.073878	3.712546	0.025989	85	1
22	6	0	1.319380	2.871972	-0.112812	86	1
23	6	0	2.560135	3.436446	-0.431858	87	1
24	6	0	3.698823	2.648040	-0.491199	88	7
25	6	0	3.658811	1.267769	-0.215950	89	6
26	6	0	2.410239	0.662604	0.043008	90	1
27	6	0	1.276465	1.490319	0.109523	91	7
28	6	0	-1.142590	1.501459	0.189403	92	1
29	6	0	-2.288841	0.689762	0.225081	93	1
30	6	0	-3.527505	1.290627	-0.082090	94	6
31	6	0	-3.581459	2.682035	-0.281851	95	1
32	6	0	-2.436619	3.463218	-0.275099	96	1
33	6	0	-1.182477	2.879422	-0.060329	97	6
34	6	0	2.271900	-0.835480	0.187226	98	1
35	6	0	1.255840	-1.008049	-2.103958	99	1
36	6	0	1.488849	-1.515388	-3.513346	100	6
37	6	0	0.458506	-2.137031	-4.235208	101	6
38	6	0	0.699427	-2.560687	-5.547551	102	6
39	6	0	1.965113	-2.353932	-6.105046	103	6
40	6	0	2.938505	-1.720580	-5.324710	104	6
41	6	0	2.038631	-3.011422	-0.918035	105	6
42	6	0	3.241756	-3.707220	-0.319363	106	1
43	1	0	6.293670	-4.497319	-1.272805	107	1
44	1	0	6.340437	-5.584106	0.978222	108	1
45	1	0	-0.695271	-1.601100	5.289479	109	7
46	1	0	-1.627482	-1.322243	7.595235	110	8
47	1	0	-3.566801	0.244052	7.931874	111	8
48	1	0	-4.474612	1.460818	5.945282	112	6
49	7	0	2.219974	-1.554838	-1.121088	113	6
50	7	0	-2.521323	-0.983618	2.063165	114	6
51	7	0	2.715401	-1.304246	-4.058117	115	6
52	7	0	-5.172693	-2.454049	2.370001	116	6
53	6	0	5.428937	-4.451568	-0.618346	117	6
54	6	0	5.454279	-5.058546	0.642179	118	1
55	6	0	4.314017	-4.968388	1.446439	119	1
56	6	0	-2.208272	-0.768726	0.620801	120	1
57	6	0	-2.723366	-2.419047	2.371173	121	7
58	6	0	-4.030734	-2.985610	1.860212	122	8
59	6	0	-4.059054	-4.049780	0.947376	123	8
60	6	0	-5.290873	-4.587879	0.556057	124	6
61	6	0	-6.465158	-4.039812	1.080717	125	6
62	6	0	-6.357576	-2.970473	1.976855	126	9
63	6	0	-1.560812	-0.341408	2.994028	127	9
64	6	0	-2.100252	-0.223041	4.403936	128	9
						129	9
						130	9
						131	9

Optimized Coordinates of 3-b at the CPCM(H₂O)-B3LYP/6-31G level.

Standard orientation:						
Center Number	Atomic Number	Atomic Type	Coordinates (Angstroms)			
			X	Y	Z	
1	17	0	5.210773	3.320454	-1.562511	65
2	17	0	-5.188490	3.534493	-0.839681	66
3	8	0	4.718350	0.382917	-0.552153	67
4	8	0	0.062558	0.926353	0.273557	68
5	8	0	-4.670254	0.543451	-0.086979	69
6	6	0	0.148736	5.821412	0.858165	70
7	1	0	0.110262	8.287522	-0.618788	71
8	1	0	0.009980	8.358118	-3.120120	72
9	1	0	-0.059957	6.255400	-4.423142	73
10	1	0	-0.034147	4.045724	-3.284225	74
11	1	0	2.624969	4.428324	-1.195926	75
12	1	0	-2.518390	4.518130	-0.925664	76
13	8	0	0.141200	4.433448	1.008147	77
14	8	0	0.196484	6.575662	1.833917	78
15	6	0	0.092720	6.126495	-0.578624	79
16	6	0	0.078600	7.375353	-1.203838	80
17	6	0	0.022534	7.406594	-2.600892	81
18	6	0	-0.017371	6.211006	-3.340458	82
19	6	0	-0.003276	4.960740	-2.703710	83
20	6	0	0.052361	4.935635	-1.311149	84
21	6	0	0.076058	3.737551	-0.375615	85
22	6	0	1.310490	2.875470	-0.477228	86
23	6	0	2.545909	3.395210	-0.884681	87
24	6	0	3.670145	2.585737	-0.910436	88
25	6	0	3.620904	1.232605	-0.526171	89
26	6	0	2.380254	0.672009	-0.160957	90
27	6	0	1.260629	1.521474	-0.124533	91
28	6	0	-1.152999	1.570569	0.033422	92
29	6	0	-2.304455	0.781196	0.194268	93
30	6	0	-3.542001	1.353750	-0.158777	94
31	6	0	-3.587732	2.705662	-0.543722	95
32	6	0	-2.440567	3.476664	-0.643177	96
33	6	0	-1.188319	2.911618	-0.370270	97
34	6	0	2.235574	-0.802007	0.136947	98
35	6	0	1.102801	-1.163526	-2.086452	99
36	6	0	1.270640	-1.820170	-3.443160	100
37	6	0	0.207282	-2.501437	-4.054426	101
38	6	0	0.389575	-3.065155	-5.322932	102
39	6	0	1.632810	-2.935103	-5.949092	103
40	6	0	2.642810	-2.235598	-5.279473	104
41	6	0	1.855397	-3.066424	-0.723821	105
42	6	0	3.079288	-3.766725	-0.174164	106
43	1	0	5.960241	-4.852106	-1.345455	107
44	1	0	6.200457	-5.688514	0.998588	108
45	1	0	-0.435770	-0.800681	5.401067	109
46	1	0	-1.278523	-0.316403	7.706646	110
47	1	0	-3.305825	1.149801	7.968004	111
48	1	0	-4.387168	2.065809	5.908195	112
49	7	0	2.080129	-1.647746	-1.084391	113
50	7	0	-2.455389	-0.670464	2.224821	114
51	7	0	2.475333	-1.684601	-4.056784	115
52	7	0	-4.984870	-2.204048	3.021614	116
53	6	0	5.178008	-4.678501	-0.613181	117
54	6	0	5.311593	-5.145612	0.699149	118
55	6	0	4.273970	-4.895718	1.602233	119
56	6	0	-2.224385	-0.621790	0.751906	120
57	6	0	-2.562476	-2.068836	2.704789	121
58	6	0	-3.891807	-2.727773	2.406593	122
59	6	0	-3.981675	-3.864325	1.590087	123
60	6	0	-5.223316	-4.485086	1.408940	124
61	6	0	-6.346895	-3.947431	2.044329	125
62	6	0	-6.180794	-2.804216	2.834209	126
63	6	0	-1.492046	0.123512	3.027326	127
64	6	0	-1.973886	0.370598	4.441477	128
						129
						130
						131

Optimized Coordinates of 1-a at the B3LYP/6-31G(d) level.

E = -4349.260154

Sum of electronic and thermal free energies = -4348.418465

Standard orientation:							
Center Number	Atomic Number	Atomic Type	Coordinates (Angstroms)				
			X	Y	Z		
1	17	0	-5.213268	3.567349	-0.011759	62	6
2	17	0	5.214317	3.506747	-0.510882	63	6
3	8	0	-4.727070	0.586811	0.106202	64	6
4	8	0	-0.014244	0.804778	-0.232598	65	6
5	8	0	4.710472	0.539780	-0.250915	66	6
6	6	0	-0.027884	5.689238	-1.776752	67	6
7	1	0	0.020202	8.244457	-0.431841	68	6
8	1	0	0.083146	8.440689	2.072032	69	1
9	1	0	0.103810	6.406790	3.475163	70	1
10	1	0	0.063596	4.143447	2.446692	71	1
11	1	0	-2.588896	4.577064	-0.306587	72	1
12	1	0	2.585407	4.549930	-0.512782	73	1
13	8	0	-0.035131	4.314317	-1.822038	74	1
14	8	0	-0.047986	6.374042	-2.767770	75	1
15	6	0	0.008255	6.088714	-0.350659	76	1
16	6	0	0.030074	7.366517	0.206902	77	1
17	6	0	0.064874	7.464097	1.597093	78	1
18	6	0	0.076628	6.307783	2.393534	79	1
19	6	0	0.054332	5.032440	1.822530	80	1
20	6	0	0.019981	4.943024	0.433945	81	1
21	6	0	-0.007341	3.717847	-0.471254	82	1
22	6	0	-1.259345	2.880686	-0.304920	83	1
23	6	0	-2.515034	3.496241	-0.262677	84	1
24	6	0	-3.671801	2.744268	-0.148915	85	1
25	6	0	-3.610876	1.337985	-0.092919	86	1
26	6	0	-2.365773	0.692507	-0.130898	87	1
27	6	0	-1.205122	1.487262	-0.228373	88	7
28	6	0	1.181091	1.478291	-0.265642	89	6
29	6	0	2.338468	0.676276	-0.189074	90	1
30	6	0	3.588785	1.310069	-0.236402	91	7
31	6	0	3.659706	2.711405	-0.361549	92	1
32	6	0	2.505078	3.473336	-0.412396	93	1
33	6	0	1.243700	2.870282	-0.358208	94	6
34	6	0	-2.280262	-0.821149	-0.095978	95	1
35	6	0	-2.015980	-0.866883	2.352882	96	1
36	6	0	-2.719502	-1.224806	3.650117	97	6
37	6	0	-2.073598	-1.963365	4.647807	98	1
38	6	0	-2.749465	-2.240693	5.836485	99	1
39	6	0	-4.050607	-1.769905	5.988962	100	6
40	6	0	-4.611673	-1.039202	4.938237	101	6
41	6	0	-2.478184	-2.894998	1.129824	102	6
42	6	0	-3.337921	-3.604352	0.100443	103	6
43	1	0	-6.488099	-4.385698	-0.241464	104	6
44	1	0	-5.650854	-5.416728	-2.356625	105	1
45	1	0	1.292336	-2.776831	-4.540080	106	6
46	1	0	2.636106	-3.546810	-6.505901	107	1
47	1	0	5.047167	-2.839035	-6.659030	108	1
48	1	0	5.975694	-1.400863	-4.842666	109	1
49	7	0	-2.672142	-1.443709	1.179432	110	7
50	7	0	2.715042	-1.602849	-1.201219	111	8
51	7	0	-3.974244	-0.766214	3.796929	112	8
52	7	0	4.605840	-3.749407	-0.004956	113	6
53	6	0	-5.431329	-4.335601	-0.498939	114	6
54	6	0	-4.965314	-4.910725	-1.683514	115	6
55	6	0	-3.605113	-4.815437	-1.967044	116	6
56	6	0	2.244478	-0.829831	-0.040865	117	6
57	6	0	2.497681	-3.035704	-0.992081	118	1
58	6	0	3.279629	-3.623511	0.168001	119	6
59	6	0	2.637108	-4.041875	1.339700	120	1
60	6	0	3.393145	-4.604696	2.367628	121	1
61	6	0	4.769150	-4.729345	2.192688	122	1
						123	7
						124	8
						125	8

Optimized Coordinates of 1-b at the B3LYP/6-31G(d) level.

E = -4349.238096

Sum of electronic and thermal free energies = -4348.393169

Standard orientation:						
Center Number	Atomic Number	Atomic Type	Coordinates (Angstroms)			
			X	Y	Z	
1	17	0	5.251123	3.349197	-1.139648	62
2	17	0	-5.034753	3.720641	0.236458	63
3	8	0	4.752618	0.392534	-0.578814	64
4	8	0	0.102549	0.840763	0.229849	65
5	8	0	-4.637404	0.704280	0.229263	66
6	6	0	0.411457	5.678074	1.459753	67
7	1	0	0.342437	8.262859	0.177494	68
8	1	0	0.070729	8.522805	-2.306838	69
9	1	0	-0.146474	6.525499	-3.745765	70
10	1	0	-0.104959	4.237616	-2.771626	71
11	1	0	2.731013	4.475125	-0.613824	72
12	1	0	-2.388875	4.661994	0.081525	73
13	8	0	0.364257	4.305972	1.479321	74
14	8	0	0.556215	6.341951	2.455415	75
15	6	0	0.261327	6.111307	0.050481	76
16	6	0	0.241979	7.401923	-0.476383	77
17	6	0	0.091015	7.534880	-1.855968	78
18	6	0	-0.033289	6.399540	-2.672533	79
19	6	0	-0.012347	5.110707	-2.132077	80
20	6	0	0.135824	4.985907	-0.753360	81
21	6	0	0.191200	3.740605	0.118855	82
22	6	0	1.384609	2.853884	-0.162473	83
23	6	0	2.629564	3.403794	-0.483730	84
24	6	0	3.742838	2.596519	-0.644048	85
25	6	0	3.655198	1.197523	-0.470682	86
26	6	0	2.398967	0.611906	-0.238214	87
27	6	0	1.291347	1.464545	-0.055832	88
28	6	0	-1.075081	1.547173	0.219852	89
29	6	0	-2.250682	0.774372	0.312000	90
30	6	0	-3.485919	1.437930	0.221690	91
31	6	0	-3.511589	2.849039	0.164865	92
32	6	0	-2.336985	3.579595	0.111329	93
33	6	0	-1.093506	2.939432	0.110271	94
34	6	0	2.235499	-0.894034	-0.225533	95
35	6	0	0.963828	-0.909448	-2.351874	96
36	6	0	1.103036	-1.175967	-3.839570	97
37	6	0	0.313774	-2.129539	-4.494586	98
38	6	0	0.484816	-2.330459	-5.865008	99
39	6	0	1.435078	-1.566974	-6.537449	100
40	6	0	2.163814	-0.628614	-5.801539	101
41	6	0	1.942062	-2.938116	-1.487900	102
42	6	0	3.211282	-3.667146	-1.092872	103
43	1	0	6.053186	-4.414638	-2.510393	104
44	1	0	6.438667	-5.582353	-0.338601	105
45	1	0	-0.329053	-2.007526	4.910057	106
46	1	0	-1.107793	-2.022524	7.290101	107
47	1	0	-3.006283	-0.502223	7.937139	108
48	1	0	-4.008115	0.957040	6.176171	109
49	7	0	2.069538	-1.479290	-1.571619	110
50	7	0	-2.325423	-1.105141	1.957631	111
51	7	0	2.007762	-0.426248	-4.491002	112
52	7	0	-4.640274	-3.145475	2.236454	113
53	6	0	5.290136	-4.397074	-1.734006	114
54	6	0	5.506780	-5.057634	-0.521422	115
55	6	0	4.501828	-5.005968	0.440299	116
56	6	0	-2.187574	-0.722218	0.540052	117
57	6	0	-2.284925	-2.562835	2.104763	118
58	6	0	-3.493423	-3.293789	1.553181	119
59	6	0	-3.392522	-4.125945	0.432210	120
60	6	0	-4.519487	-4.829206	0.004237	121
61	6	0	-5.712570	-4.668402	0.703585	122
						123
						124
						125

Optimized Coordinates of 1-a at the CPCM(H₂O)-B3LYP/SVP level.

E = -4346.563925

Sum of electronic and thermal free energies = -4345.725283

Standard orientation:							
Center Number	Atomic Number	Atomic Type	Coordinates (Angstroms)				
			X	Y	Z		
1	17	0	-5.250020	3.154829	-0.228180	61	6
2	17	0	5.200494	3.172469	-0.486159	62	6
3	8	0	-4.735910	0.187338	-0.033727	63	6
4	8	0	-0.015676	0.459436	-0.170352	64	6
5	8	0	4.707487	0.220478	-0.074364	65	6
6	6	0	-0.034945	5.253100	-1.942062	66	6
7	1	0	-0.046997	7.892097	-0.729387	67	6
8	1	0	-0.049482	8.211947	1.765259	68	6
9	1	0	-0.041737	6.245544	3.274897	69	1
10	1	0	-0.031456	3.925151	2.362194	70	1
11	1	0	-2.628895	4.200607	-0.464340	71	1
12	1	0	2.568782	4.212155	-0.559170	72	1
13	8	0	-0.027228	3.890135	-1.915599	73	1
14	8	0	-0.037904	5.874576	-2.974735	74	1
15	6	0	-0.037810	5.731013	-0.541295	75	1
16	6	0	-0.043651	7.038531	-0.048109	76	1
17	6	0	-0.044991	7.206771	1.338003	77	1
18	6	0	-0.040602	6.090243	2.193368	78	1
19	6	0	-0.034746	4.784379	1.687893	79	1
20	6	0	-0.033440	4.623748	0.303264	80	1
21	6	0	-0.027529	3.354198	-0.538191	81	1
22	6	0	-1.276460	2.511688	-0.367844	82	1
23	6	0	-2.540396	3.116609	-0.384887	83	1
24	6	0	-3.694529	2.353902	-0.284973	84	1
25	6	0	-3.620327	0.947458	-0.175173	85	1
26	6	0	-2.366115	0.316927	-0.131665	86	1
27	6	0	-1.208141	1.119658	-0.229156	87	1
28	6	0	1.170910	1.131579	-0.211489	88	7
29	6	0	2.334892	0.341155	-0.089353	89	6
30	6	0	3.584248	0.980962	-0.139191	90	1
31	6	0	3.648246	2.380356	-0.321620	91	7
32	6	0	2.487704	3.133671	-0.419160	92	1
33	6	0	1.227912	2.522860	-0.360251	93	1
34	6	0	-2.280940	-1.186047	0.036296	94	6
35	6	0	-1.846217	-1.083866	2.457130	95	1
36	6	0	-2.547690	-1.139865	3.803006	96	1
37	6	0	-1.993549	-1.838289	4.885615	97	6
38	6	0	-2.660807	-1.835724	6.113751	98	1
39	6	0	-3.862591	-1.135722	6.220930	99	1
40	6	0	-4.338601	-0.468126	5.086493	100	6
41	6	0	-2.694858	-3.114104	1.445795	101	6
42	6	0	-3.840691	-3.734258	0.667914	102	6
43	1	0	-7.107948	-3.880294	0.917220	103	6
44	1	0	-6.858023	-5.297836	-1.126148	104	6
45	1	0	1.157504	-3.384704	-4.307926	105	1
46	1	0	2.418106	-3.846632	-6.429699	106	6
47	1	0	4.571652	-2.592973	-6.845953	107	1
48	1	0	5.342071	-0.948580	-5.129165	108	1
49	7	0	-2.644395	-1.655302	1.377027	109	1
50	7	0	2.652530	-1.903757	-1.137801	110	7
51	7	0	-3.704953	-0.465564	3.911436	111	8
52	7	0	5.146687	-3.638527	-0.647524	112	8
53	6	0	-6.112370	-4.074177	0.500531	113	6
54	6	0	-5.977253	-4.868676	-0.643712	114	6
55	6	0	-4.692290	-5.093344	-1.138727	115	6
56	6	0	2.262779	-1.163529	0.065573	116	6
57	6	0	2.740589	-3.340430	-0.884724	117	6
58	6	0	3.945239	-3.746962	-0.056373	118	1
59	6	0	3.803036	-4.238948	1.249553	119	6
60	6	0	4.942059	-4.625559	1.961177	120	1
						121	1
						122	1
						123	7
						124	8
						125	8

Optimized Coordinates of 1-b at the CPCM(H₂O)-B3LYP/SVP level.

E = -4346.550117

Sum of electronic and thermal free energies = -4345.706139

Standard orientation:							
Center Number	Atomic Number	Atomic Type	Coordinates (Angstroms)			62	63
			X	Y	Z	64	6
1	17	0	-5.200795	3.649725	-0.026668	68	6
2	17	0	5.207087	3.549574	-0.875404	69	0
3	8	0	-4.727610	0.656205	0.064308	70	1
4	8	0	-0.002907	0.899825	-0.204169	71	1
5	8	0	4.725695	0.611078	-0.295964	72	1
6	6	0	-0.067556	5.702079	-1.977798	73	1
7	1	0	0.021277	8.330793	-0.745203	74	1
8	1	0	0.164369	8.628611	1.747994	75	1
9	1	0	0.231121	6.649211	3.238986	76	1
10	1	0	0.158962	4.336800	2.308481	77	1
11	1	0	-2.595355	4.658845	-0.387939	78	1
12	1	0	2.597994	4.609455	-0.803593	79	0
13	8	0	-0.073491	4.338632	-1.962493	80	1
14	8	0	-0.121089	6.331980	-3.003881	81	1
15	6	0	0.013099	6.168104	-0.575412	82	1
16	6	0	0.052065	7.471258	-0.072176	83	1
17	6	0	0.131436	7.627240	1.313097	84	1
18	6	0	0.169271	6.503322	2.157912	85	1
19	6	0	0.129129	5.201969	1.642486	86	1
20	6	0	0.050518	5.053629	0.258755	87	1
21	6	0	-0.004524	3.791240	-0.592089	88	7
22	6	0	-1.251050	2.960807	-0.358829	89	6
23	6	0	-2.510191	3.574115	-0.314618	90	1
24	6	0	-3.664130	2.820167	-0.165309	91	7
25	6	0	-3.602555	1.408931	-0.064023	92	1
26	6	0	-2.346605	0.776688	-0.034711	93	1
27	6	0	-1.190036	1.571688	-0.206767	94	6
28	6	0	1.186141	1.556608	-0.328155	95	1
29	6	0	2.343984	0.746574	-0.279335	96	1
30	6	0	3.601008	1.371379	-0.369207	97	6
31	6	0	3.665258	2.769154	-0.588077	98	1
32	6	0	2.510886	3.535435	-0.635640	99	1
33	6	0	1.248971	2.944789	-0.488479	100	6
34	6	0	-2.230186	-0.709700	0.224817	101	6
35	6	0	-1.410674	-0.323227	2.539099	102	6
36	6	0	-1.847970	-0.391420	3.991619	103	6
37	6	0	-1.028037	-0.963190	4.975654	104	6
38	6	0	-1.467956	-0.985158	6.302241	105	1
39	6	0	-2.714400	-0.435620	6.602997	106	6
40	6	0	-3.460260	0.116457	5.554848	107	1
41	6	0	-2.151432	-2.517973	1.831784	108	1
42	6	0	-3.380239	-3.330881	1.470167	109	1
43	1	0	-6.425001	-3.707448	2.629838	110	7
44	1	0	-6.532854	-5.429122	0.822739	111	8
45	1	0	0.070049	-2.524950	-4.343432	112	8
46	1	0	0.849579	-3.152443	-6.646161	113	6
47	1	0	3.091981	-2.294393	-7.431898	114	6
48	1	0	4.422418	-0.851316	-5.885093	115	6
49	7	0	-2.296075	-1.074397	1.650151	116	6
50	7	0	2.303490	-1.453824	-1.479620	117	6
51	7	0	-3.044460	0.143095	4.286929	118	1
52	7	0	4.488107	-3.583994	-1.536686	119	6
53	6	0	-5.553972	-3.884990	1.987931	120	1
54	6	0	-5.619925	-4.850445	0.976257	121	1
55	6	0	-4.491854	-5.041675	0.177740	122	1
56	6	0	2.228680	-0.759185	-0.182989	123	7
57	6	0	2.162297	-2.898669	-1.306216	124	8
58	6	0	3.392203	-3.599717	-0.760406	125	8
59	6	0	3.359056	-4.285304	0.462759		
60	6	0	4.495395	-4.981059	0.884917		
61	6	0	5.631431	-4.962722	0.075099		

Optimized Coordinates of 1-a at the B3LYP/SVP level.

E = -4346.521105

Sum of electronic and thermal free energies = -4345.682251

Standard orientation:						
Center Number	Atomic Number	Atomic Type	Coordinates (Angstroms)			
			X	Y	Z	
1	17	0	-5.208320	3.528335	-0.083745	63
2	17	0	5.228143	3.470364	-0.370554	64
3	8	0	-4.715085	0.532082	0.006342	65
4	8	0	-0.005127	0.773513	-0.221531	66
5	8	0	4.709184	0.489088	-0.132410	67
6	6	0	0.015453	5.644337	-1.763649	68
7	1	0	0.026985	8.217975	-0.431031	69
8	1	0	0.029440	8.429021	2.081964	70
9	1	0	0.020809	6.396050	3.500569	71
10	1	0	0.009297	4.119956	2.480354	72
11	1	0	-2.587050	4.545235	-0.321633	73
12	1	0	2.608483	4.520022	-0.408452	74
13	8	0	0.010964	4.275677	-1.791382	75
14	8	0	0.018698	6.317465	-2.755573	76
15	6	0	0.016621	6.055673	-0.335653	77
16	6	0	0.022978	7.338418	0.216705	78
17	6	0	0.024257	7.444077	1.609064	79
18	6	0	0.019282	6.290366	2.412721	80
19	6	0	0.012850	5.010161	1.846860	81
20	6	0	0.011542	4.912131	0.456132	82
21	6	0	0.006505	3.684379	-0.448038	83
22	6	0	-1.248963	2.844266	-0.305326	84
23	6	0	-2.508164	3.458102	-0.286649	85
24	6	0	-3.671084	2.705865	-0.204505	86
25	6	0	-3.610910	1.294724	-0.156505	87
26	6	0	-2.359657	0.652487	-0.171388	88
27	6	0	-1.193651	1.447031	-0.237388	89
28	6	0	1.188128	1.438622	-0.220220	90
29	6	0	2.347252	0.636676	-0.125112	91
30	6	0	3.603677	1.267907	-0.138711	92
31	6	0	3.677121	2.674925	-0.248799	93
32	6	0	2.519786	3.436849	-0.317731	94
33	6	0	1.254864	2.834584	-0.298975	95
34	6	0	-2.279477	-0.859918	-0.134855	96
35	6	0	-2.091106	-0.895294	2.326939	97
36	6	0	-2.853535	-1.238163	3.595944	98
37	6	0	-2.223759	-1.890385	4.666824	99
38	6	0	-2.951822	-2.152234	5.829998	100
39	6	0	-4.287554	-1.755822	5.885642	101
40	6	0	-4.828683	-1.111976	4.766451	102
41	6	0	-2.514849	-2.930673	1.097251	103
42	6	0	-3.371776	-3.636565	0.062435	104
43	1	0	-6.545009	-4.341897	-0.334188	105
44	1	0	-5.687546	-5.441209	-2.415005	106
45	1	0	1.426775	-2.559675	-4.685646	107
46	1	0	2.859007	-3.259733	-6.625040	108
47	1	0	5.318393	-2.684775	-6.572209	109
48	1	0	6.205576	-1.442394	-4.588007	110
49	7	0	-2.671391	-1.483466	1.131477	111
50	7	0	2.717118	-1.623224	-1.172968	112
51	7	0	-4.137464	-0.858237	3.656268	113
52	7	0	4.612091	-3.704447	0.076315	114
53	6	0	-5.473944	-4.323072	-0.569005	115
54	6	0	-4.998609	-4.936955	-1.733595	116
55	6	0	-3.628476	-4.884369	-1.989787	117
56	6	0	2.254852	-0.870407	-0.004953	118
57	6	0	2.526251	-3.056033	-1.006946	119
58	6	0	3.275531	-3.665994	0.163806	120
59	6	0	2.590314	-4.193978	1.269356	121
60	6	0	3.319270	-4.773883	2.309977	122
61	6	0	4.710524	-4.805712	2.215078	123
62	6	0	5.304313	-4.253650	1.074078	124
						125

Optimized Coordinates of 1-b at the B3LYP/SVP level.

E = -4346.497978

Sum of electronic and thermal free energies = -4345.654287

Standard orientation:						
Center Number	Atomic Number	Atomic Type	Coordinates (Angstroms)			
			X	Y	Z	
1	17	0	5.225217	3.460224	-0.678511	62
2	17	0	-5.106765	3.591228	0.632648	63
3	8	0	4.740837	0.460786	-0.379712	64
4	8	0	0.054251	0.796855	0.204100	65
5	8	0	-4.674856	0.588982	0.283409	66
6	6	0	0.278957	5.588828	1.779889	67
7	1	0	0.182128	8.229013	0.592119	73
8	1	0	-0.066977	8.576766	-1.893495	74
9	1	0	-0.235377	6.623702	-3.411059	75
10	1	0	-0.166101	4.295201	-2.517544	76
11	1	0	2.673140	4.520288	-0.181274	77
12	1	0	-2.484511	4.584254	0.487793	78
13	8	0	0.253480	4.222547	1.738235	79
14	8	0	0.398487	6.210501	2.798454	80
15	6	0	0.138562	6.075518	0.382546	81
16	6	0	0.103065	7.386193	-0.098250	82
17	6	0	-0.034965	7.567589	-1.475927	83
18	6	0	-0.131279	6.459138	-2.335549	84
19	6	0	-0.094090	5.150132	-1.841049	85
20	6	0	0.041142	4.976258	-0.464152	86
21	6	0	0.108888	3.702085	0.368434	87
22	6	0	1.323023	2.846702	0.066390	88
23	6	0	2.576330	3.434757	-0.145455	89
24	6	0	3.711571	2.656621	-0.318190	90
25	6	0	3.638146	1.243295	-0.263563	91
26	6	0	2.378164	0.628562	-0.135335	92
27	6	0	1.243758	1.449622	0.049986	93
28	6	0	-1.125959	1.480917	0.271453	94
29	6	0	-2.296521	0.690485	0.294520	95
30	6	0	-3.544965	1.340381	0.315436	96
31	6	0	-3.585081	2.753008	0.413710	97
32	6	0	-2.415882	3.499221	0.403238	98
33	6	0	-1.163465	2.879326	0.308539	99
34	6	0	2.238134	-0.874454	-0.239527	100
35	6	0	1.167445	-0.712612	-2.484991	101
36	6	0	1.547192	-0.805709	-3.951955	102
37	6	0	0.881749	-1.666292	-4.837918	103
38	6	0	1.289977	-1.717503	-6.173414	104
39	6	0	2.345162	-0.902431	-6.581075	105
40	6	0	2.934405	-0.062956	-5.627421	106
41	6	0	2.018318	-2.824040	-1.663040	107
42	6	0	3.278501	-3.585714	-1.298952	108
43	1	0	6.152576	-4.235342	-2.724937	109
44	1	0	6.508755	-5.545457	-0.621893	110
45	1	0	-0.430385	-2.438264	4.704950	111
46	1	0	-1.372353	-2.667885	7.022792	112
47	1	0	-3.375909	-1.264998	7.649154	113
48	1	0	-4.313786	0.302678	5.936456	114
49	7	0	2.138001	-1.371951	-1.617398	115
50	7	0	-2.282610	-1.372075	1.706387	116
51	7	0	2.548063	-0.010059	-4.354451	117
52	7	0	-4.524182	-3.513415	1.996052	118
53	6	0	5.370437	-4.269443	-1.957022	119
54	6	0	5.571908	-5.009913	-0.785988	120
55	6	0	4.551368	-5.025057	0.163070	121
56	6	0	-2.211081	-0.819204	0.349427	122
57	6	0	-2.212942	-2.827794	1.699789	123
58	6	0	-3.456560	-3.529039	1.186528	124
59	6	0	-3.465837	-4.205570	-0.042765	125
60	6	0	-4.623416	-4.882652	-0.437324	
61	6	0	-5.735266	-4.851569	0.402624	

Analytical HPLC Chromatograms of Purified Sensors.

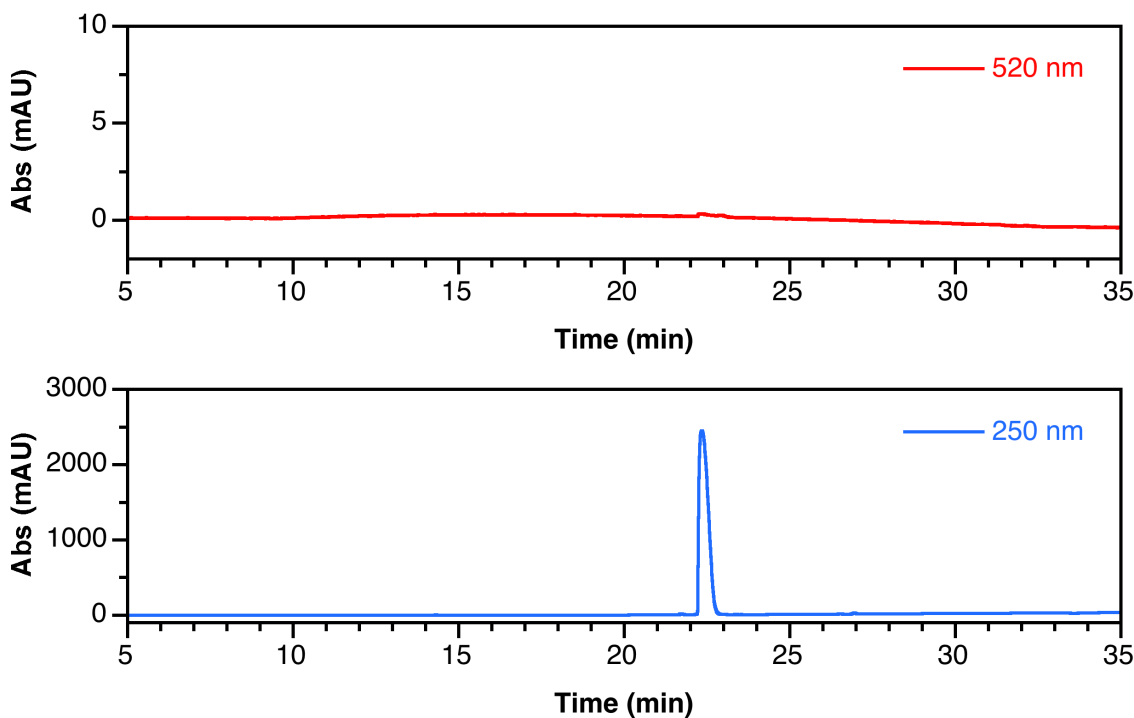


Figure S41. Analytical HPLC traces of purified **1**. Absorbance monitored at 520 nm (top) and 250 nm (bottom) using solvent gradient 8 (Table S1).

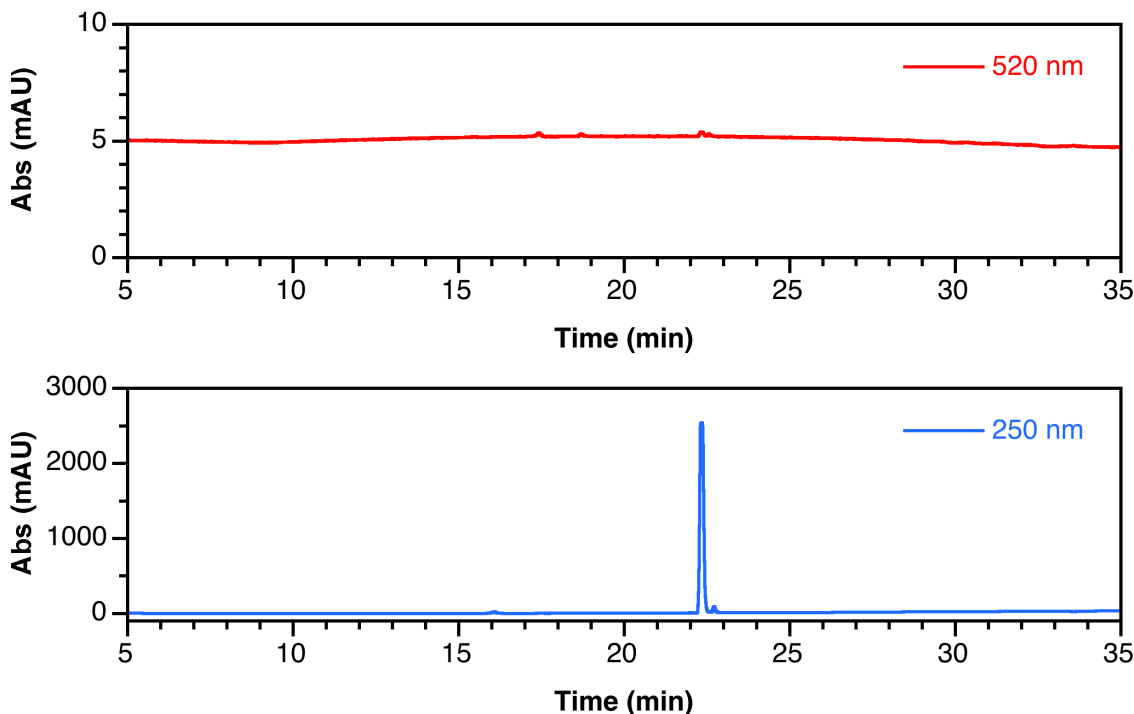


Figure S42. Analytical HPLC traces of purified **2**. Absorbance monitored at 520 nm (top) and 250 nm (bottom) using solvent gradient 8 (Table S1).

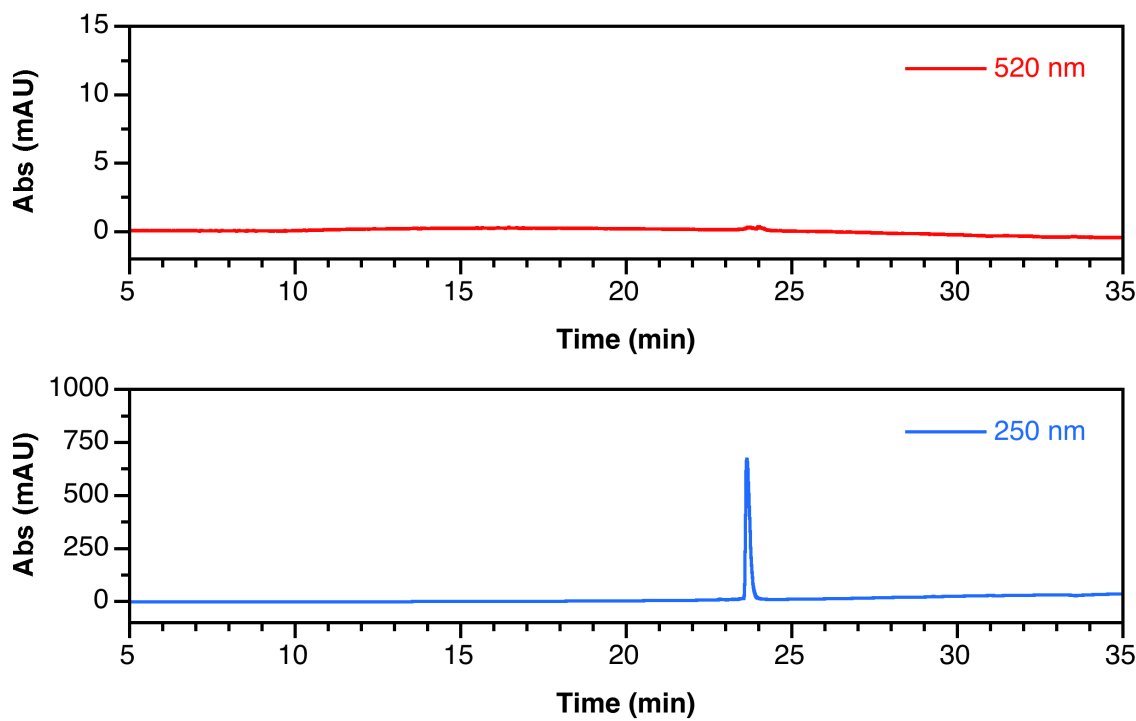


Figure S43. Analytical HPLC traces of purified **3**. Absorbance monitored at 520 nm (top) and 250 nm (bottom) using solvent gradient 8 (Table S1).

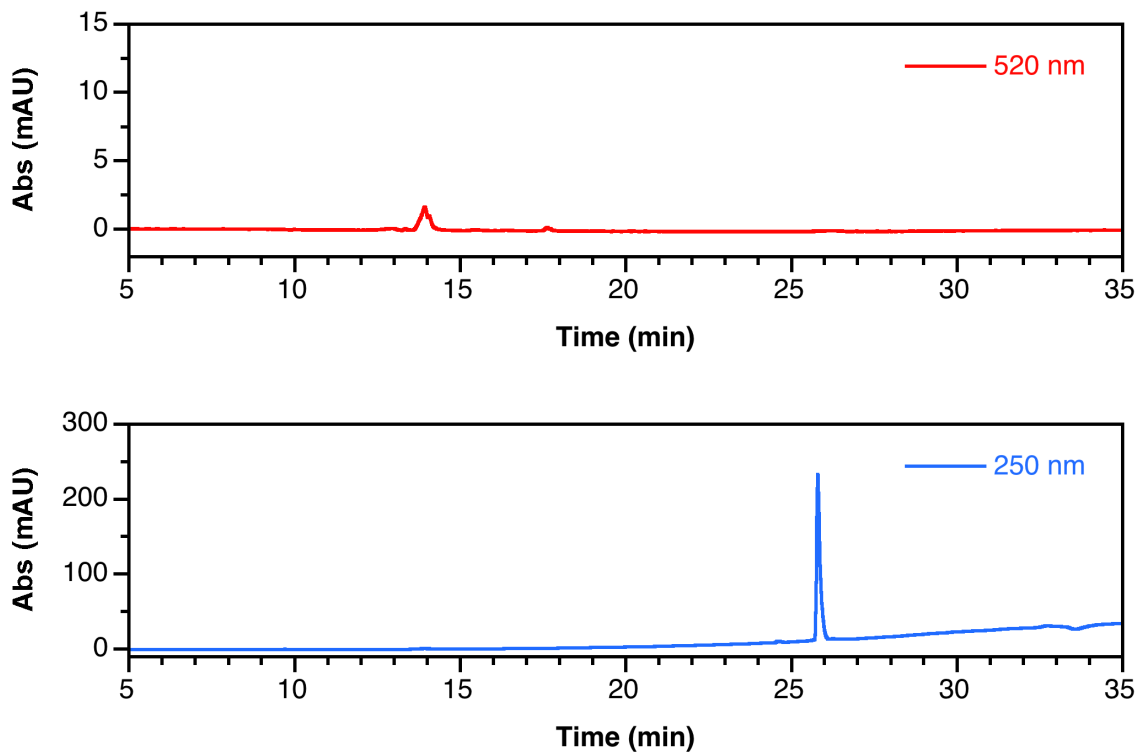


Figure S44. Analytical HPLC traces of purified **4**. Absorbance monitored at 520 nm (top) and 250 nm (bottom) using solvent gradient 8 (Table S1).

NMR Spectra.

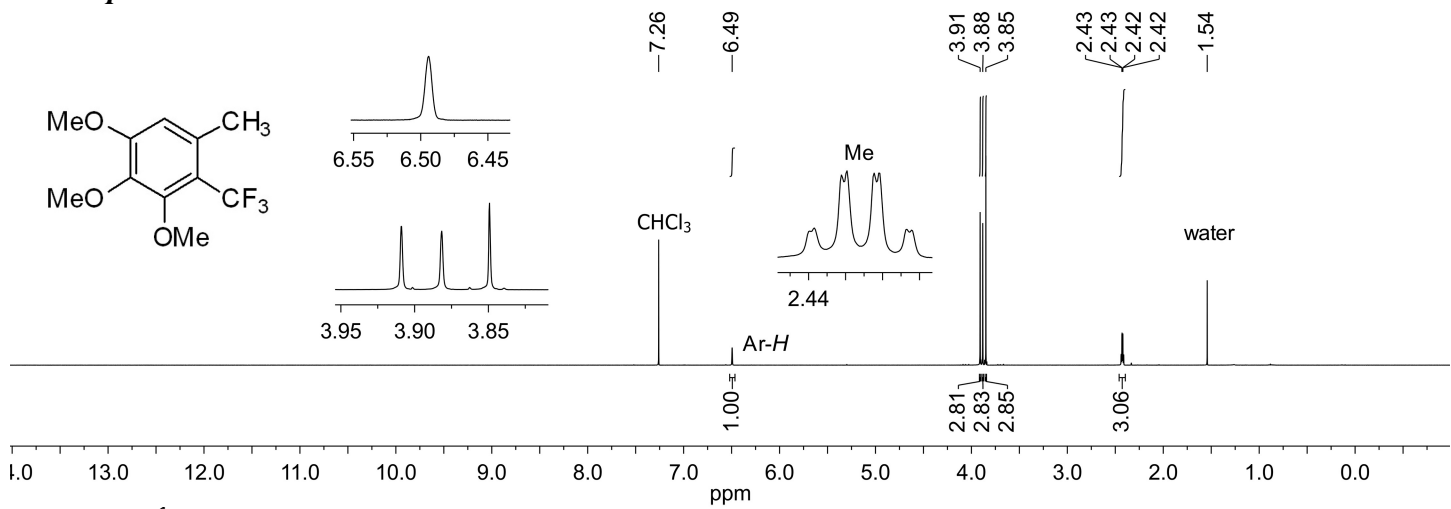


Figure S45. ¹H NMR spectrum of S2.

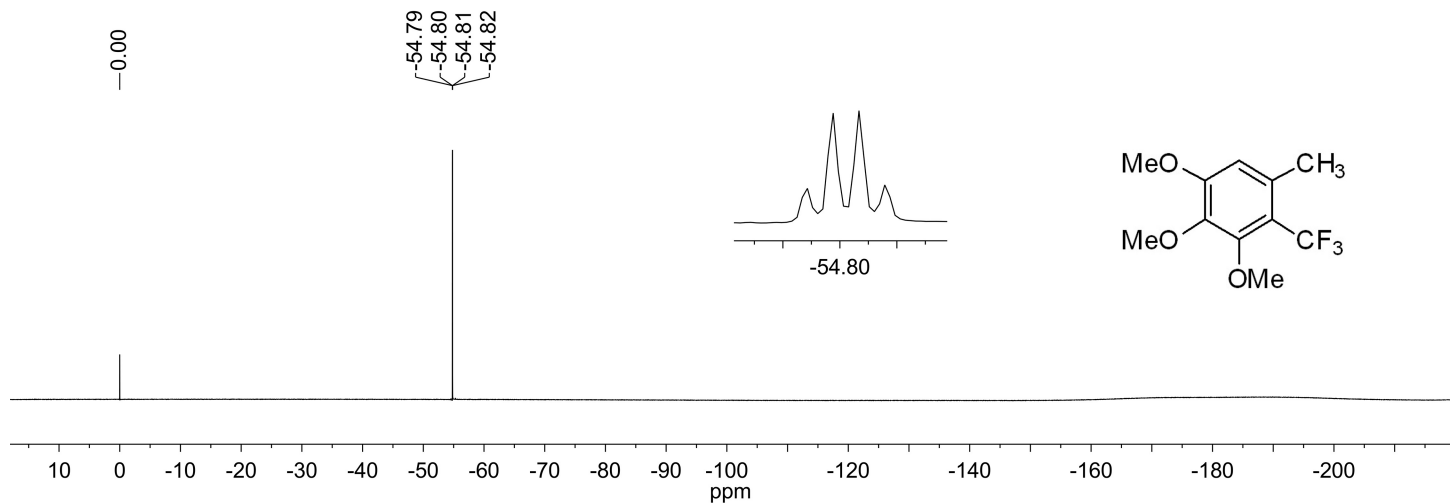


Figure S46. ¹⁹F NMR spectrum of S2.

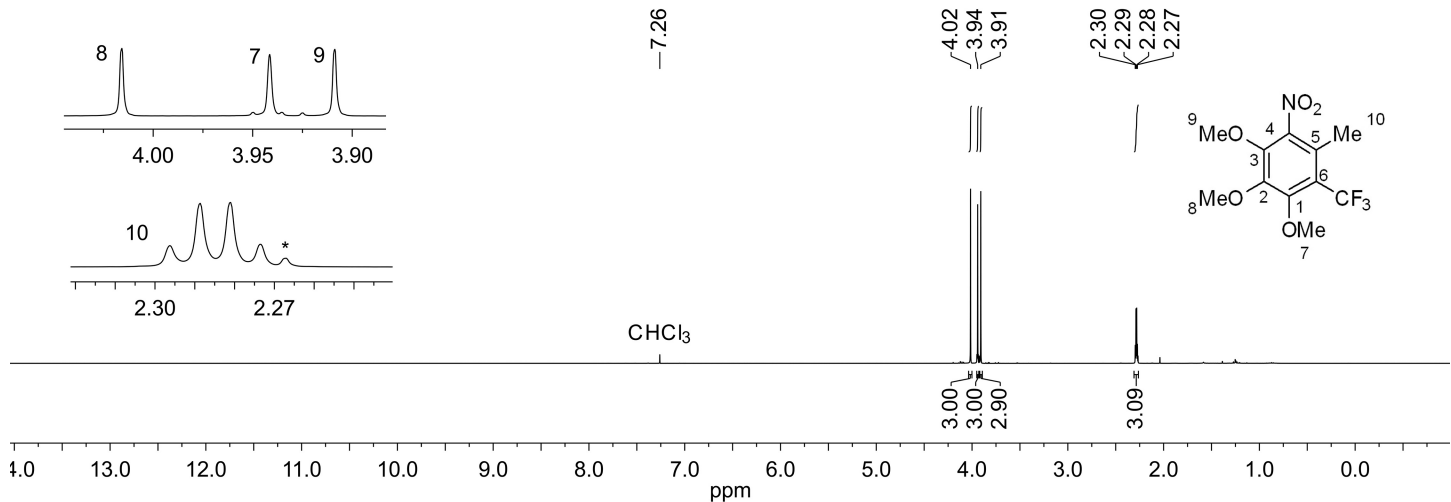


Figure S47. ¹H NMR spectrum of S3.

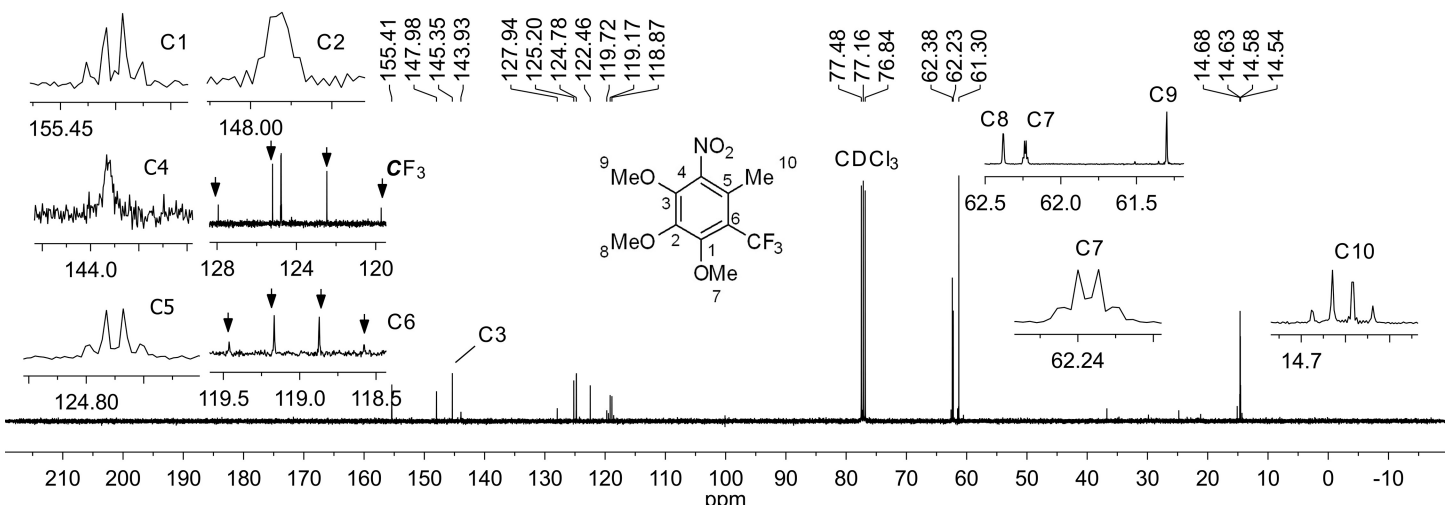


Figure S48. $^{13}\text{C}\{\text{H}\}$ NMR spectrum of **S3**.

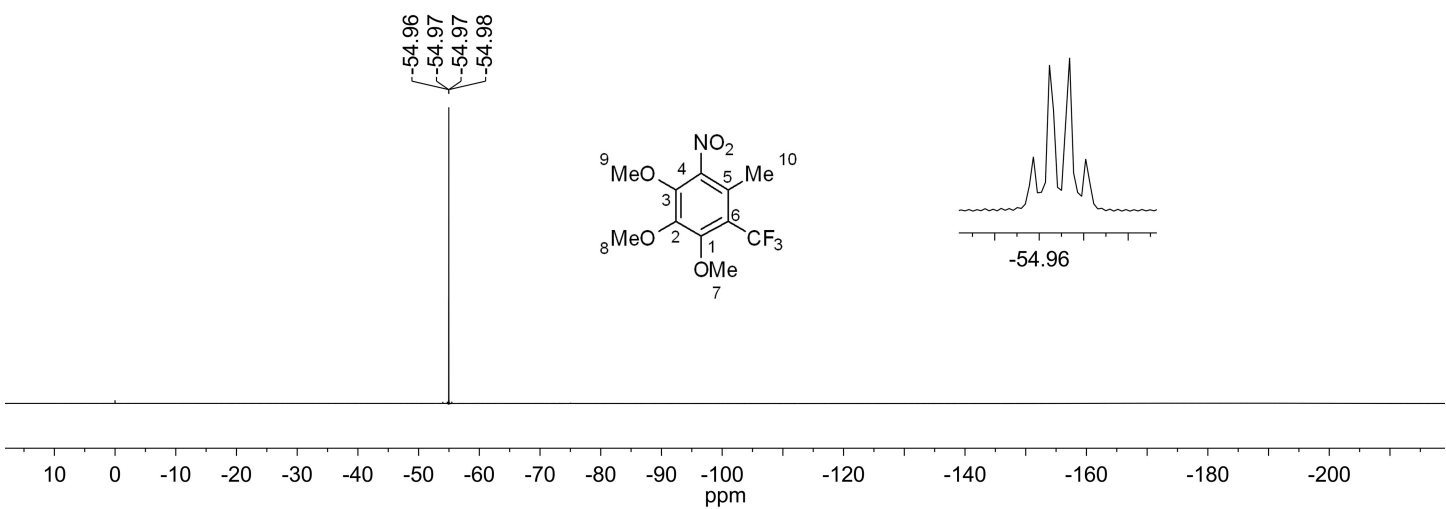


Figure S49. ^{19}F NMR spectrum of **S3**.

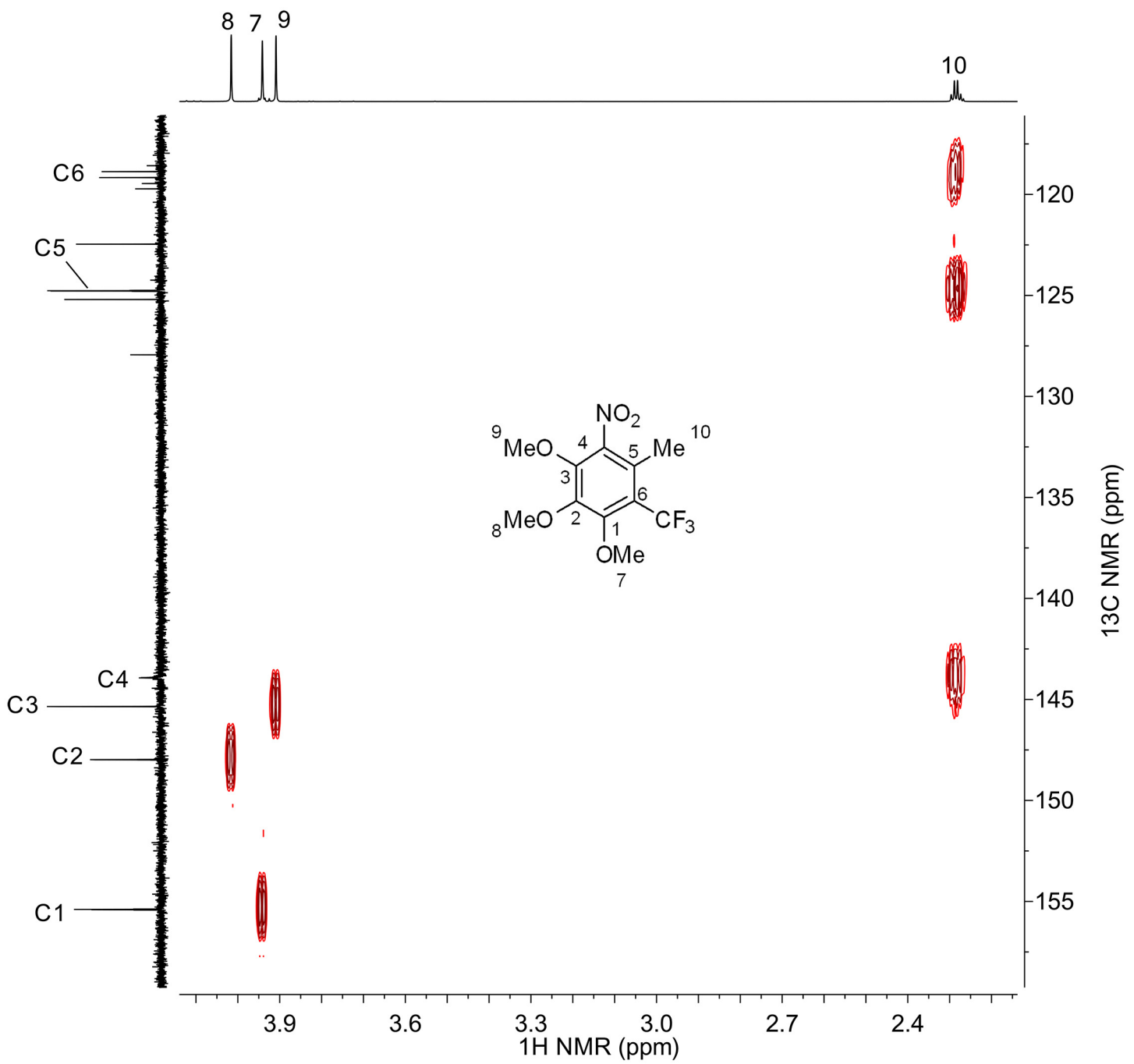


Figure S50. ^1H - ^{13}C HMBC spectrum of S3.

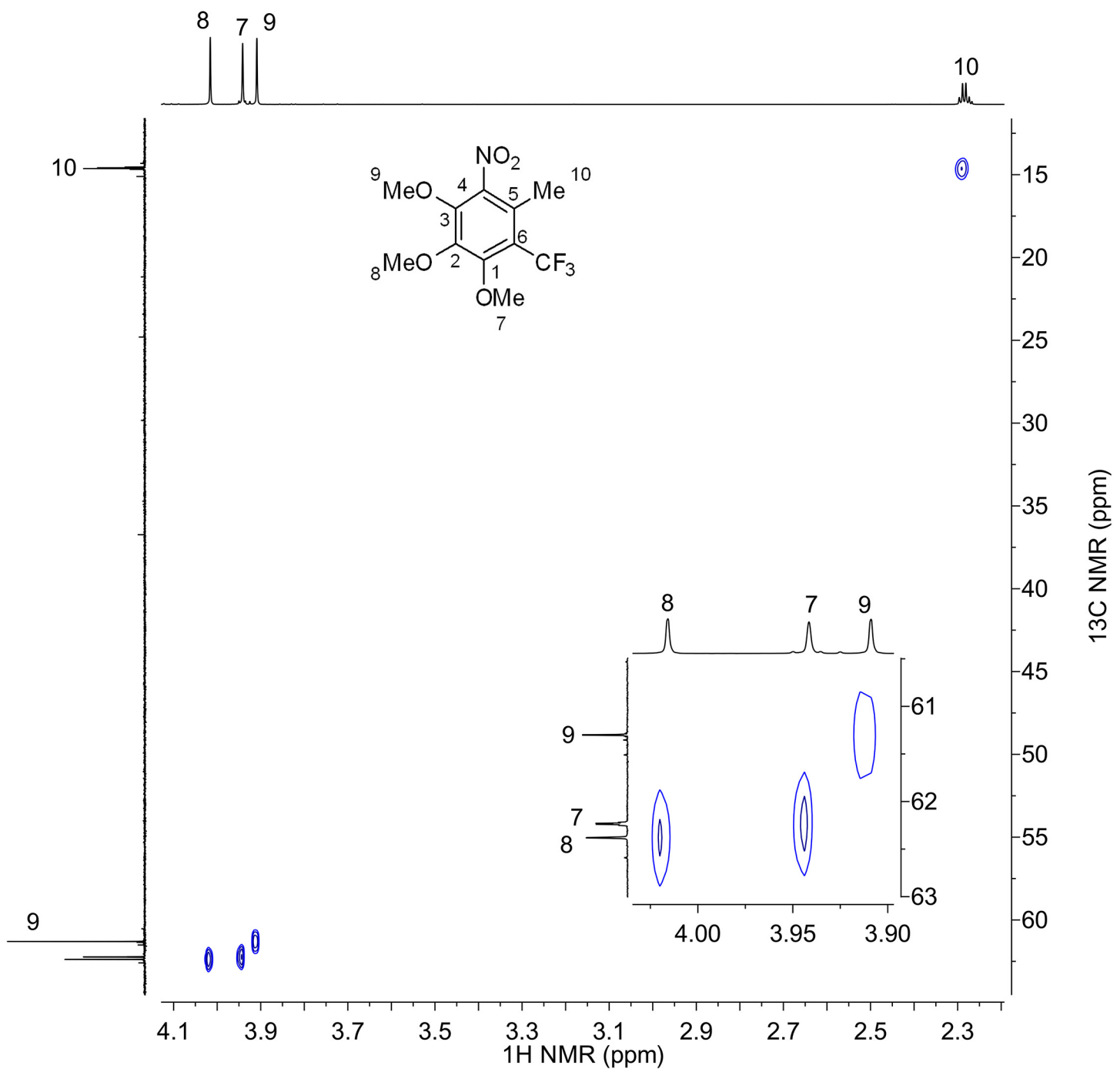


Figure S51. ^1H - ^{13}C HSQC spectrum of **S3**.

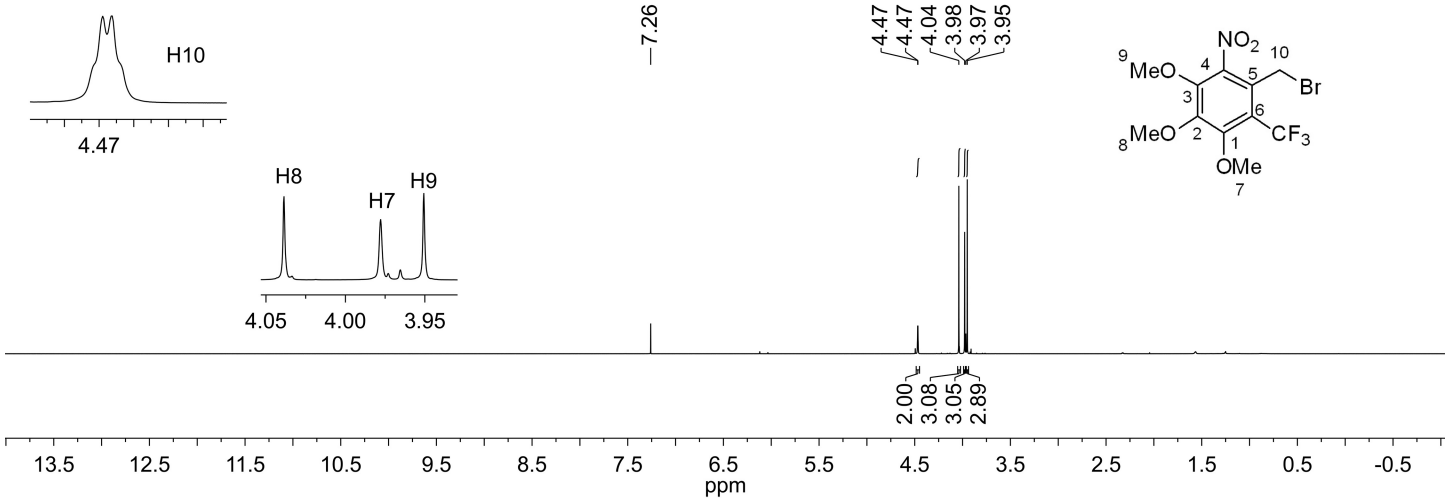


Figure S52. ^1H NMR spectrum of **S4**.

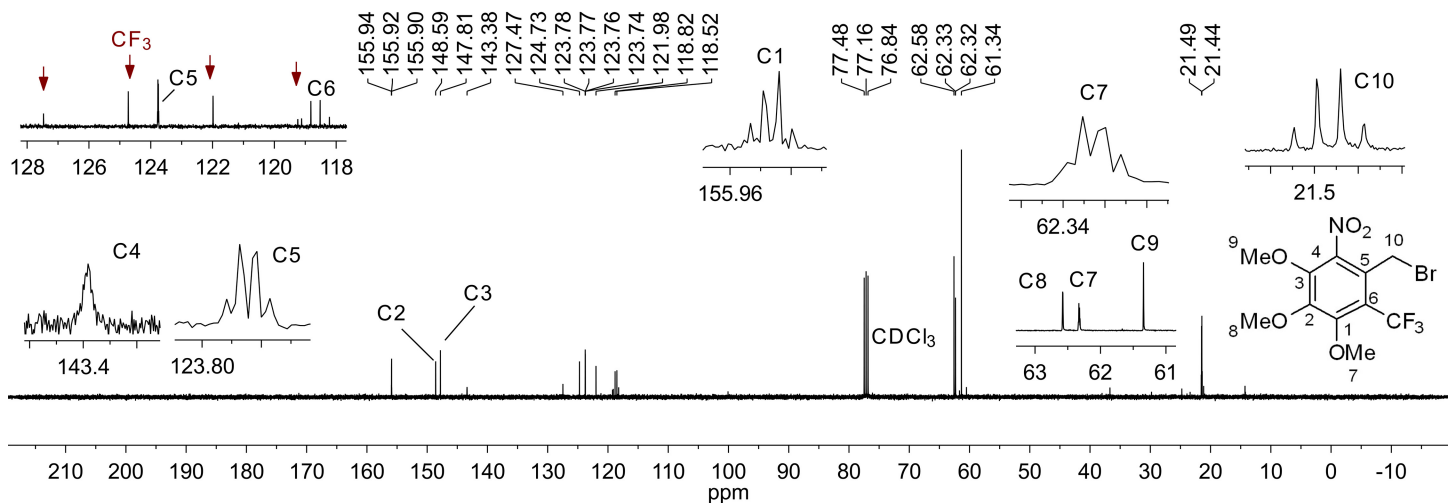


Figure S53. $^{13}\text{C}\{\text{H}\}$ NMR spectrum of **S4**.

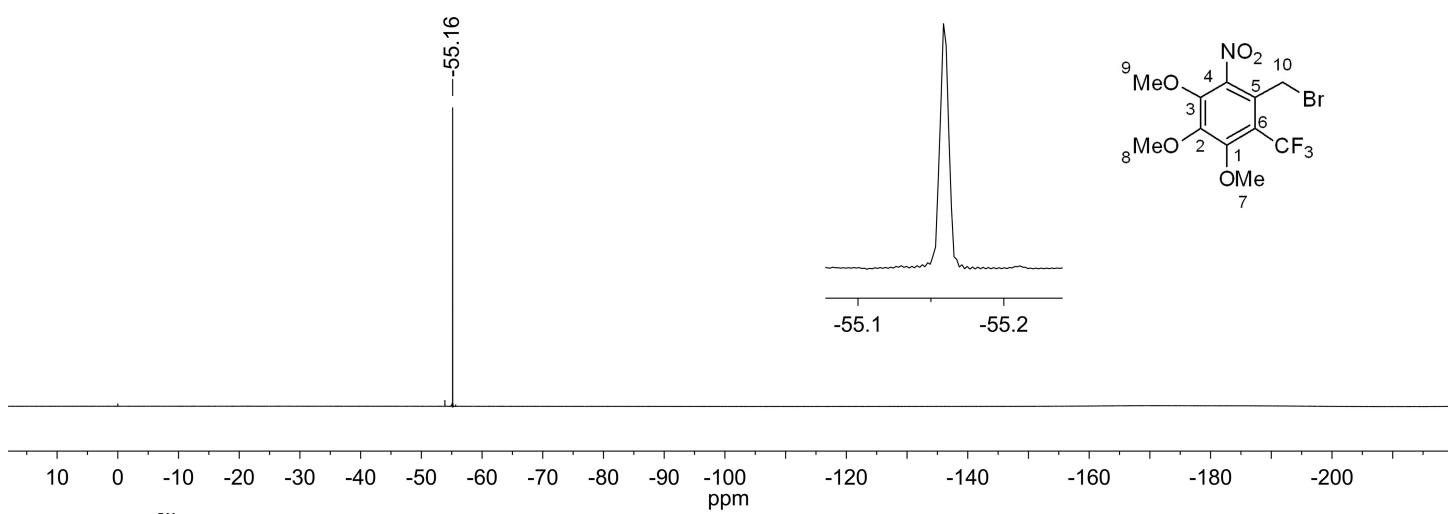


Figure S54. ^{19}F NMR spectrum of **S4**.

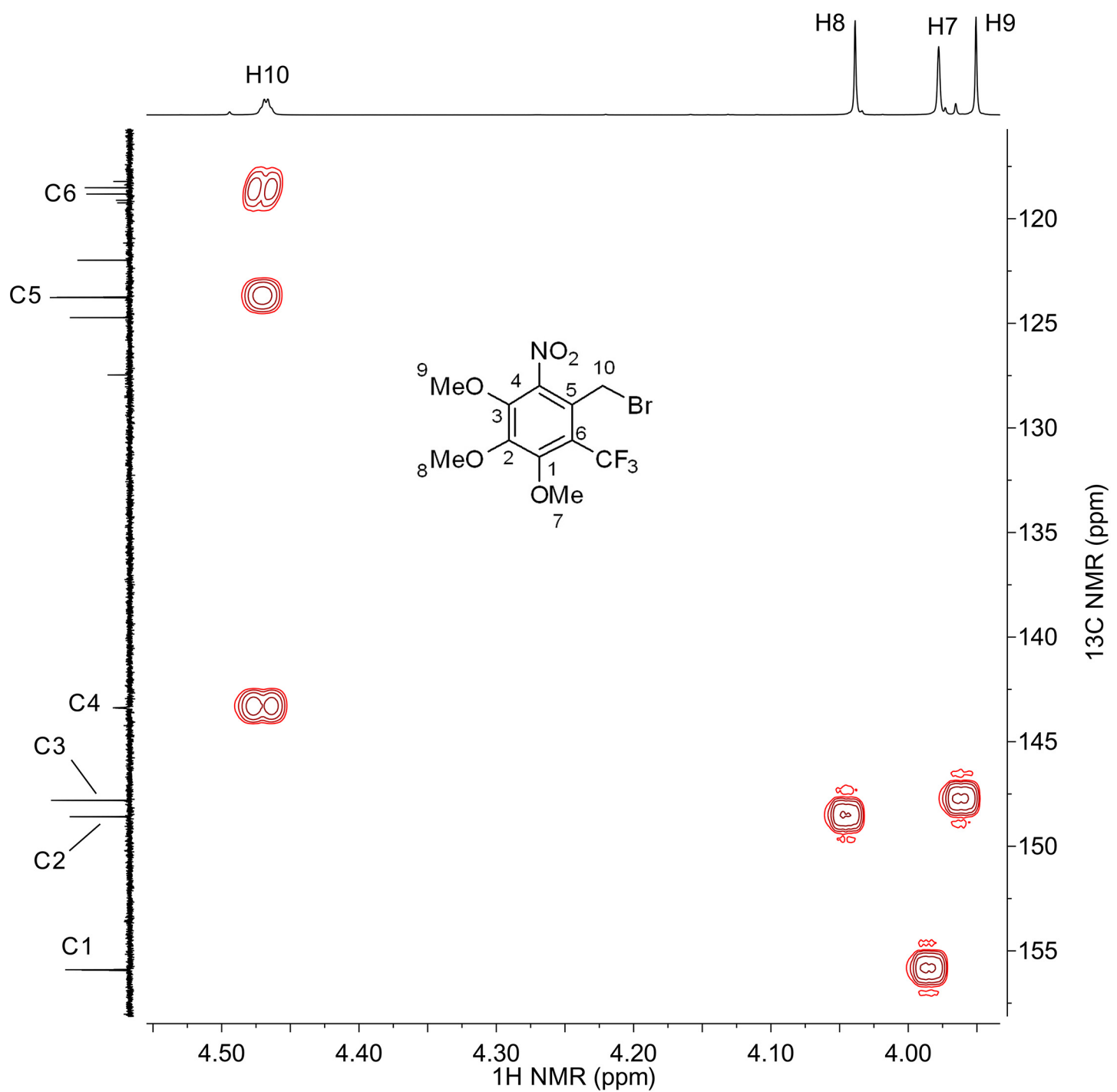


Figure S55. ^1H - ^{13}C HMBC spectrum of **S4**.

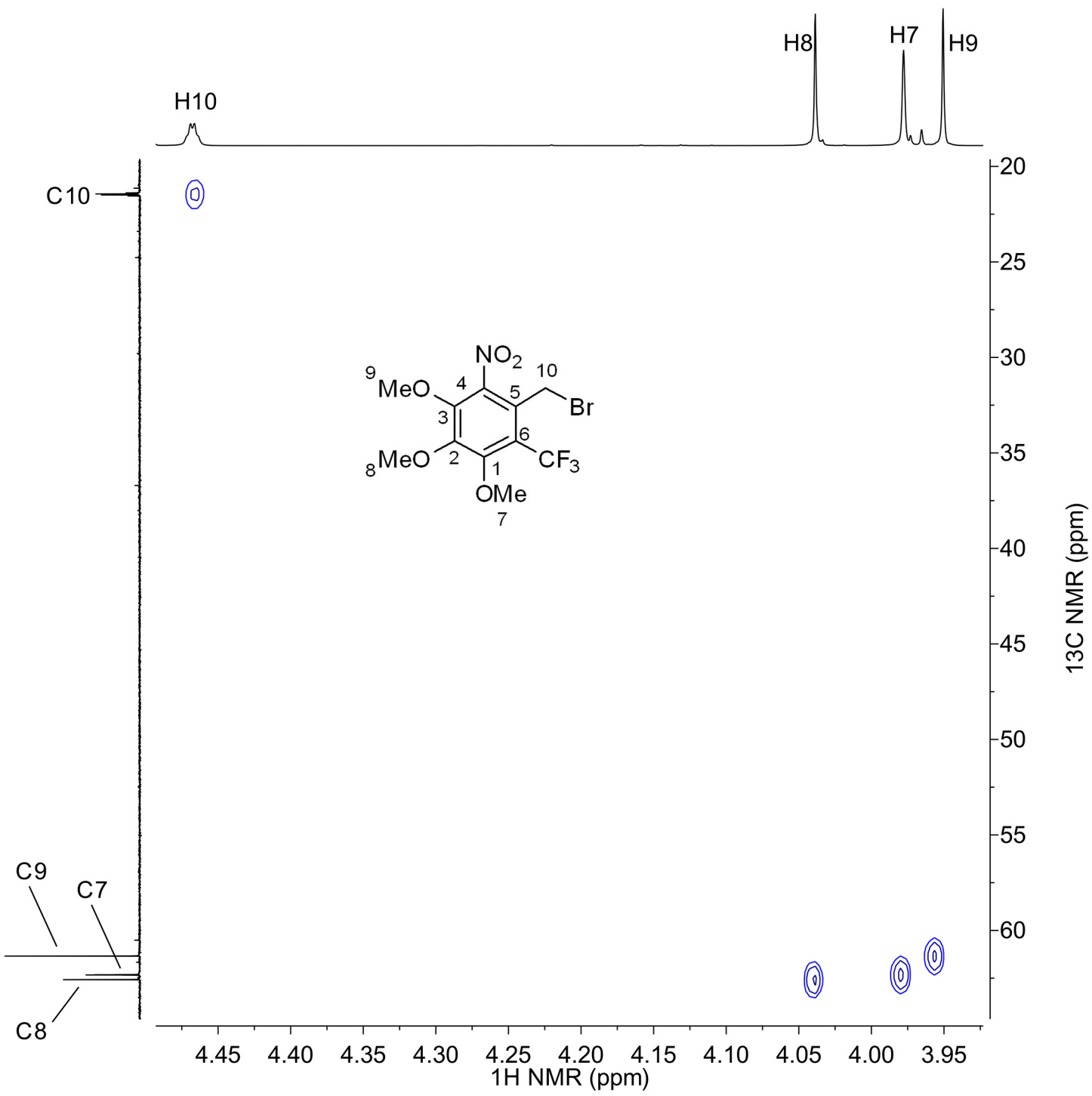


Figure S56. ^1H - ^{13}C HSQC spectrum of **S4**.

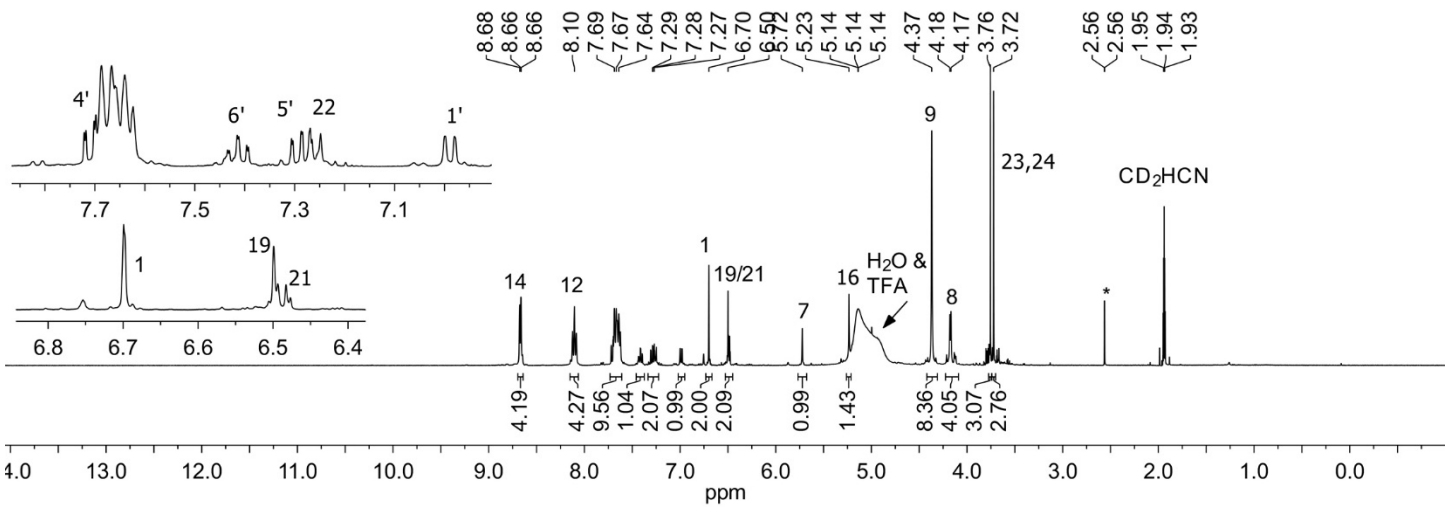


Figure S57. ^1H NMR spectrum of **S5**.

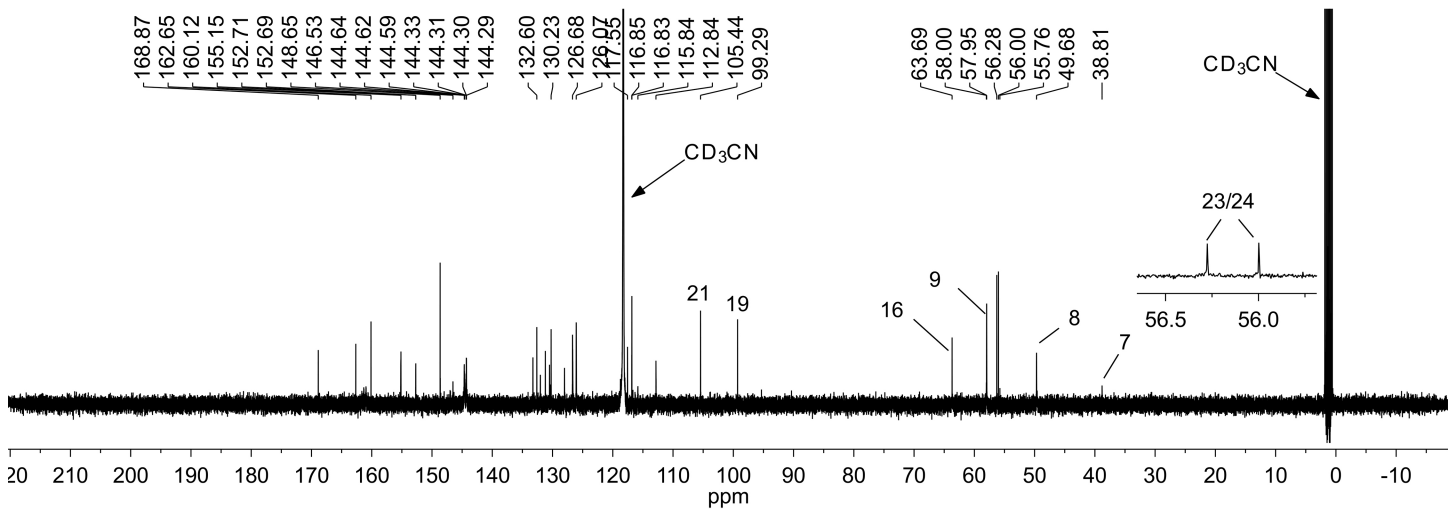


Figure S58. $^{13}\text{C}\{^1\text{H}\}$ NMR spectrum of **S5**.

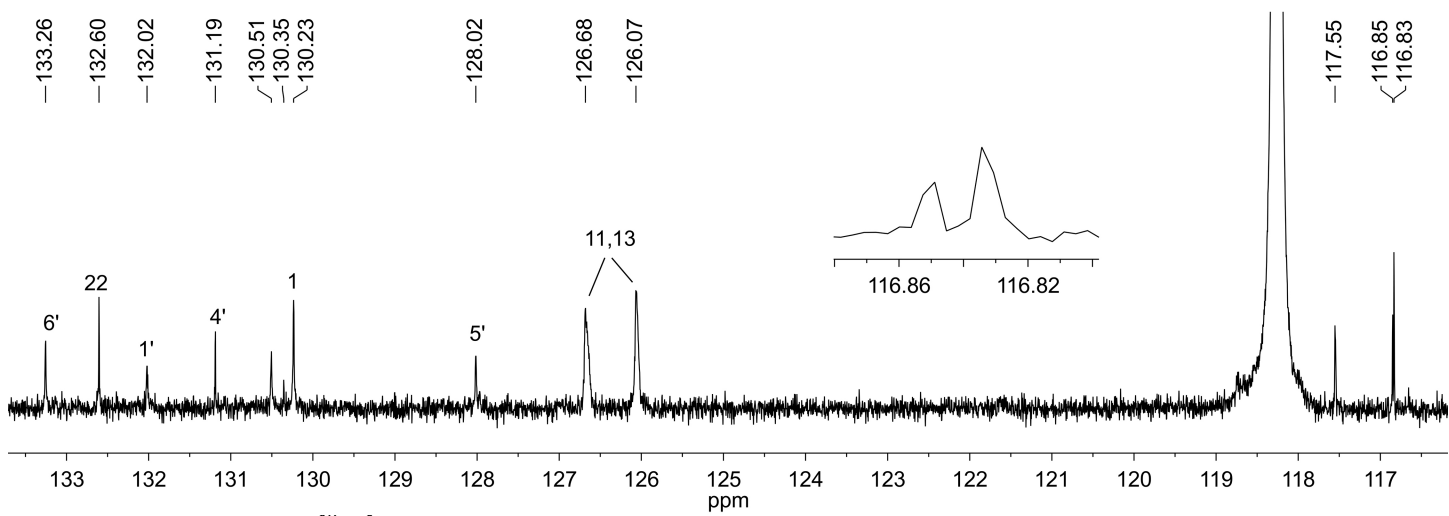


Figure S59. Expansion of $^{13}\text{C}\{^1\text{H}\}$ NMR spectrum of **S5** from 116 to 134 ppm.

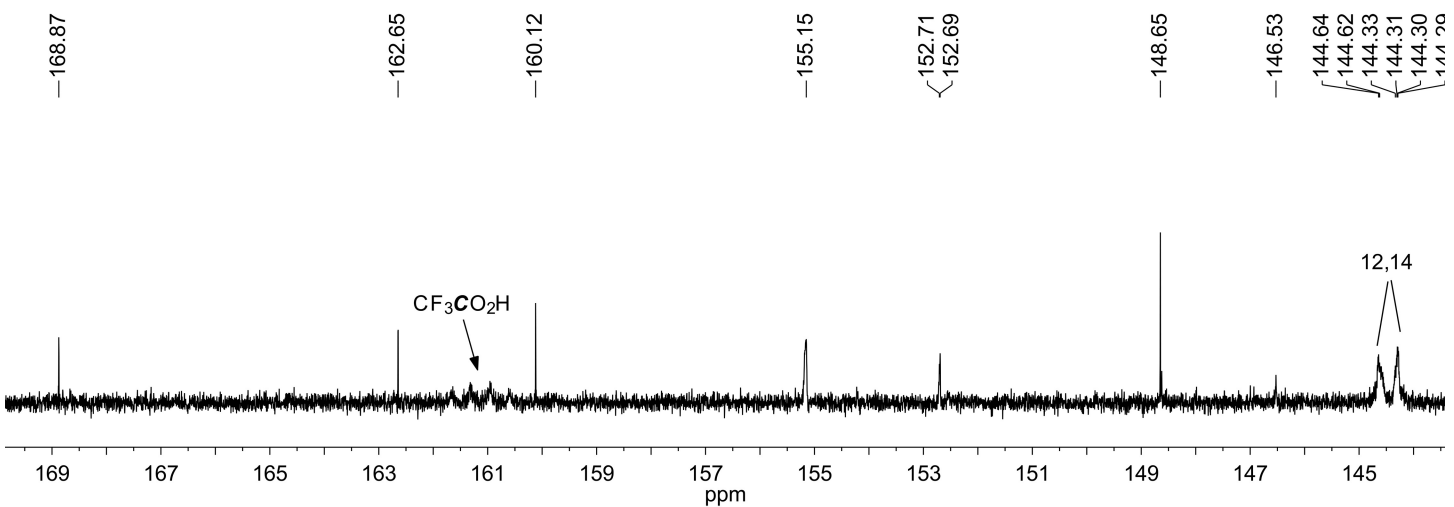


Figure S60. Expansion of $^{13}\text{C}\{\text{H}\}$ NMR spectrum of **S5** from 144 to 170 ppm.

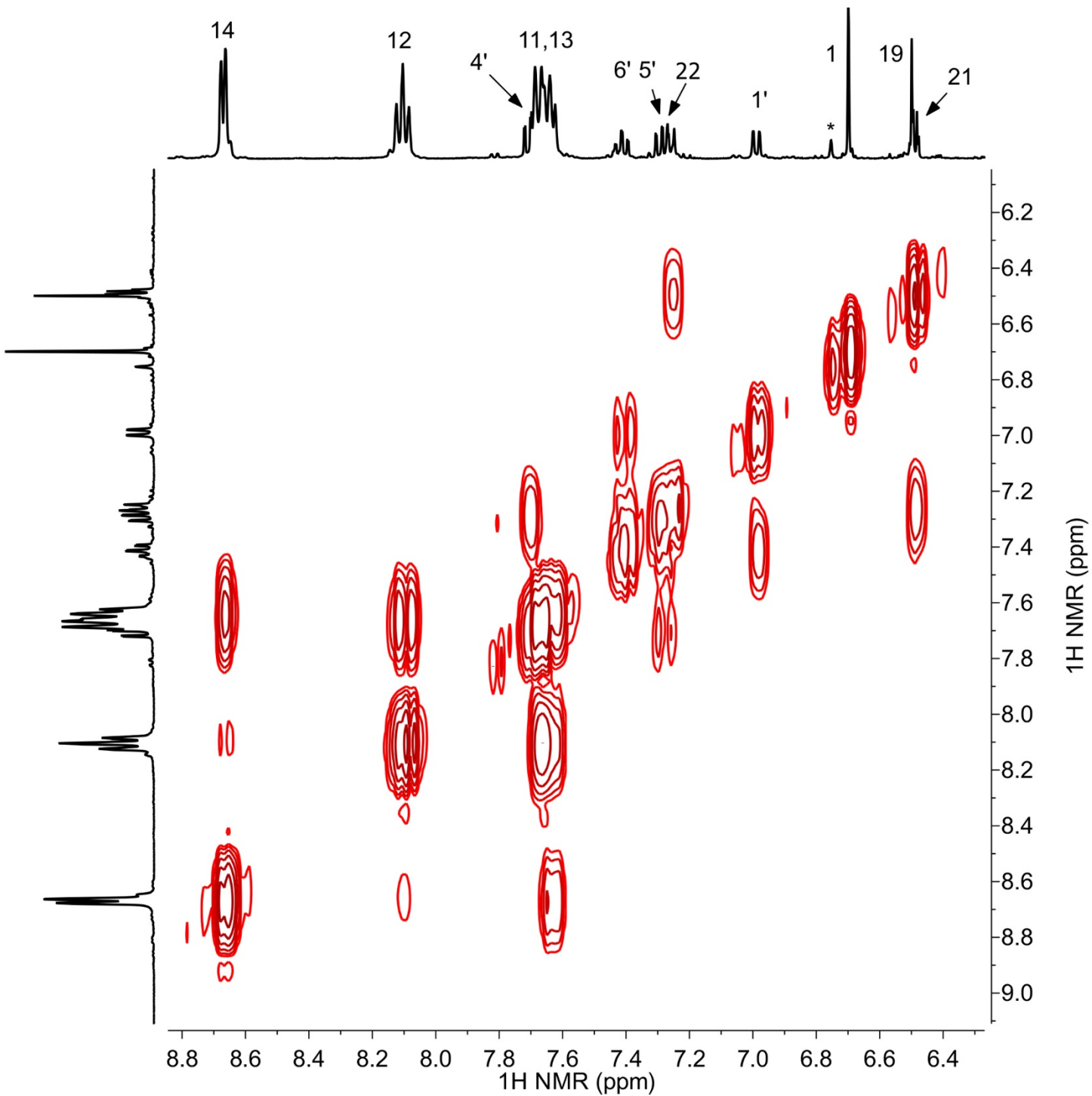


Figure S61. ^1H - ^1H COSY spectrum of **S5** aromatic region.

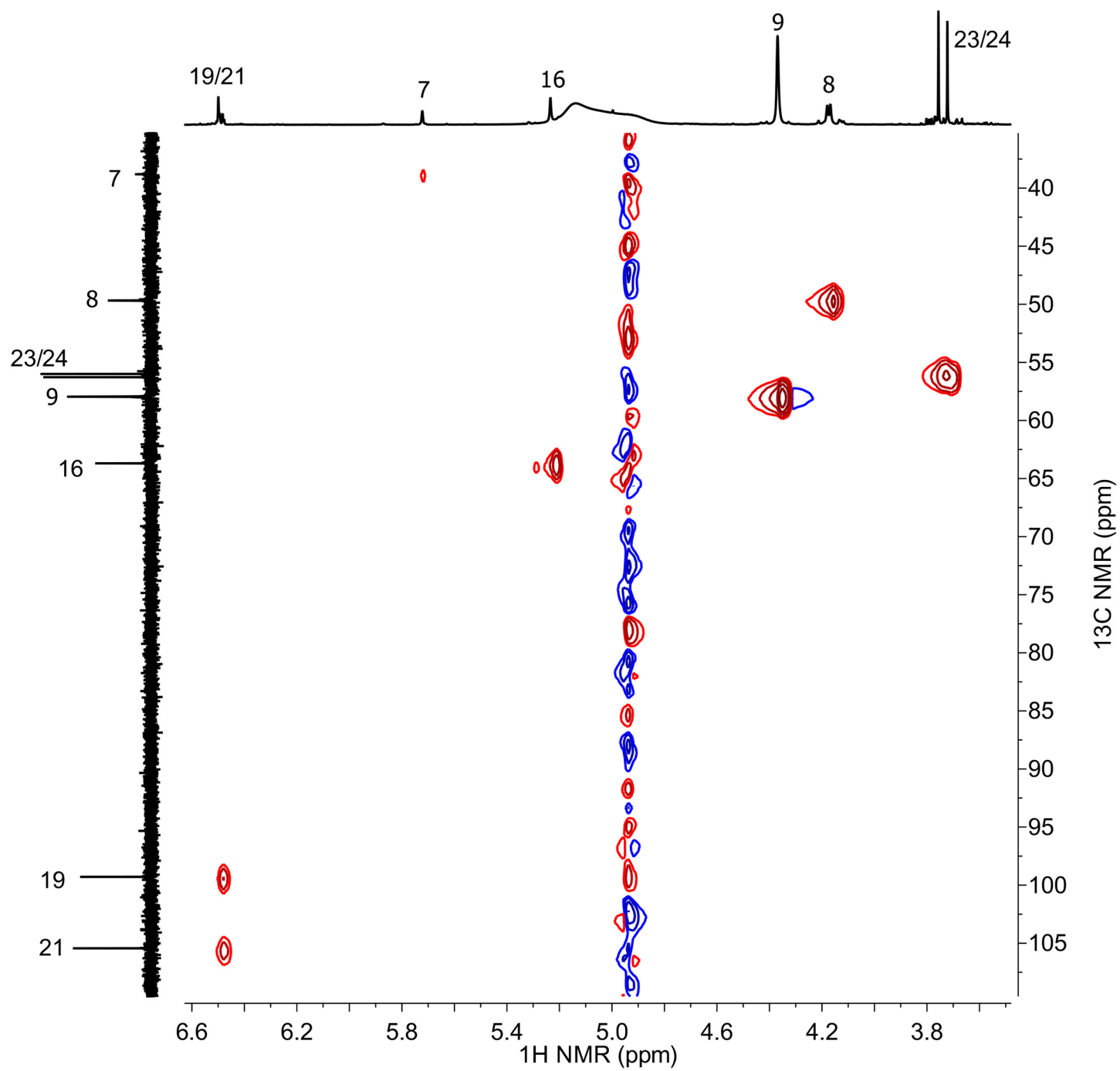


Figure S62. ^1H - ^{13}C HSQC spectrum of **S5** aliphatic region.

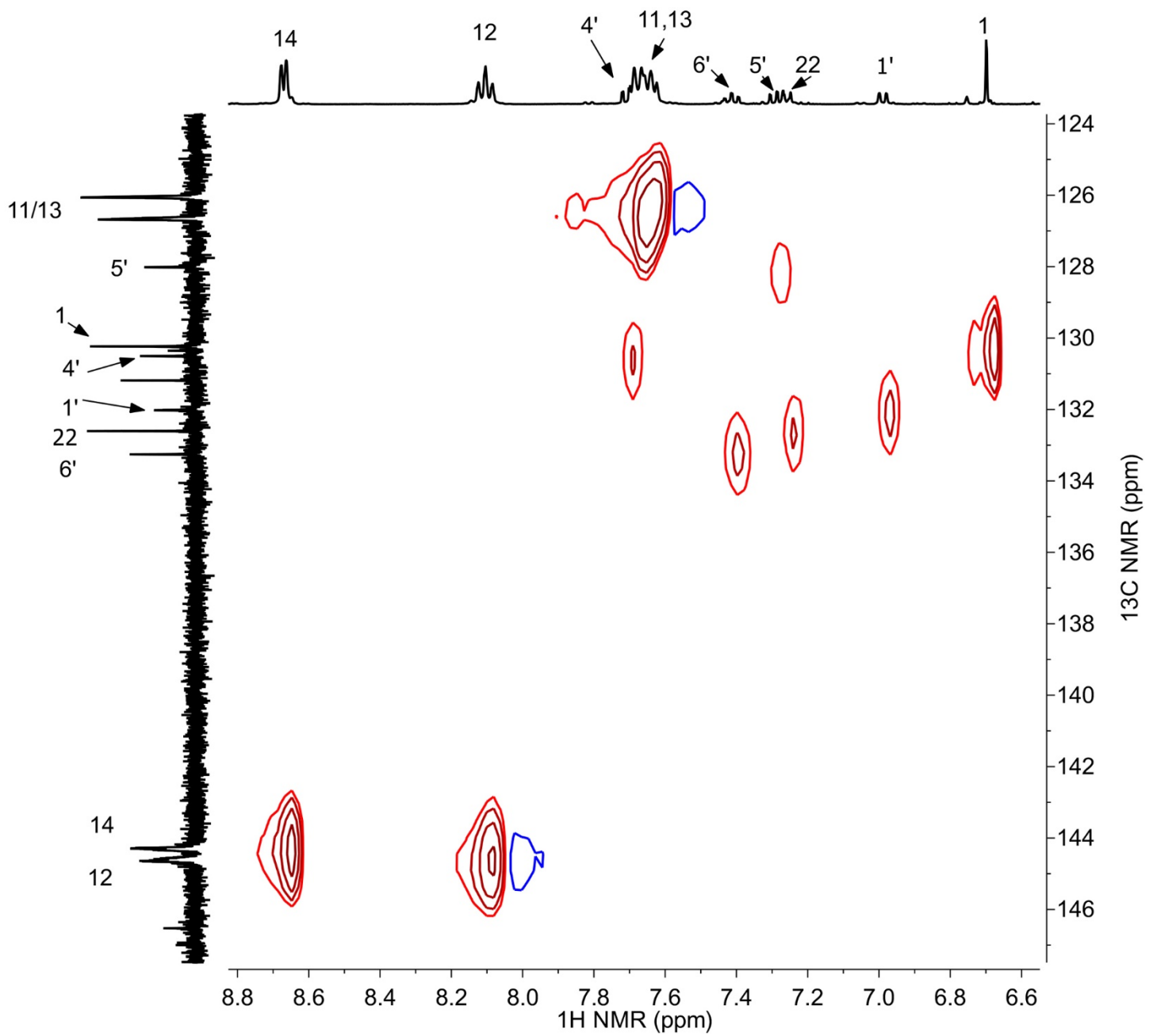


Figure S63. ^1H - ^{13}C HSQC spectrum of **S5** aromatic region.

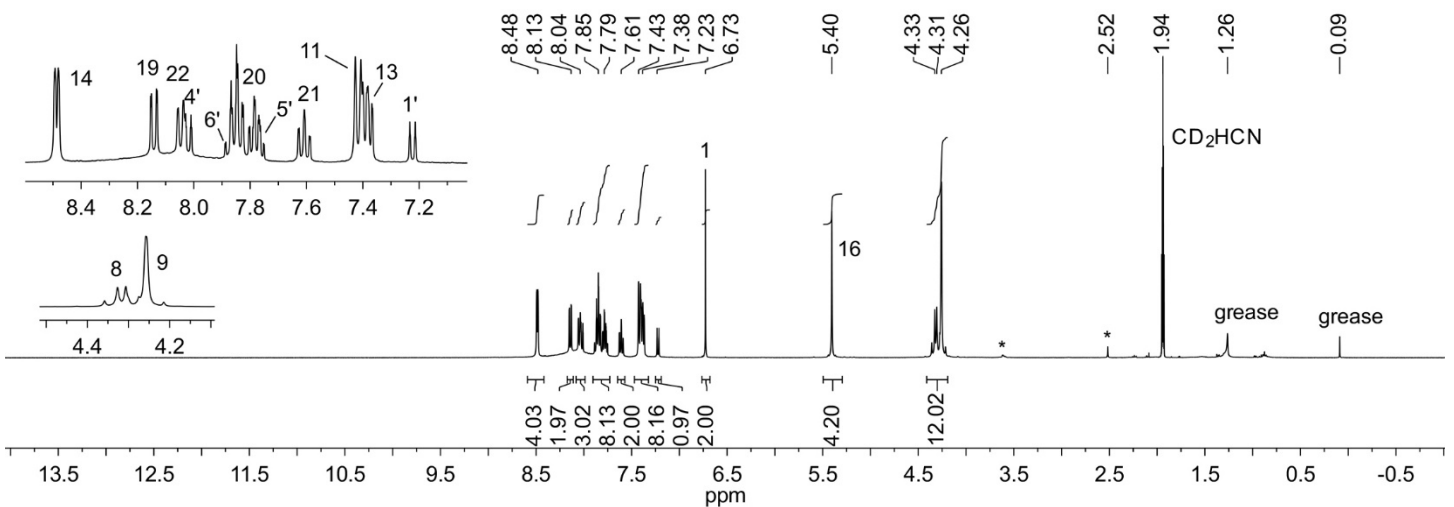


Figure S64. ^1H NMR spectrum of **1**.

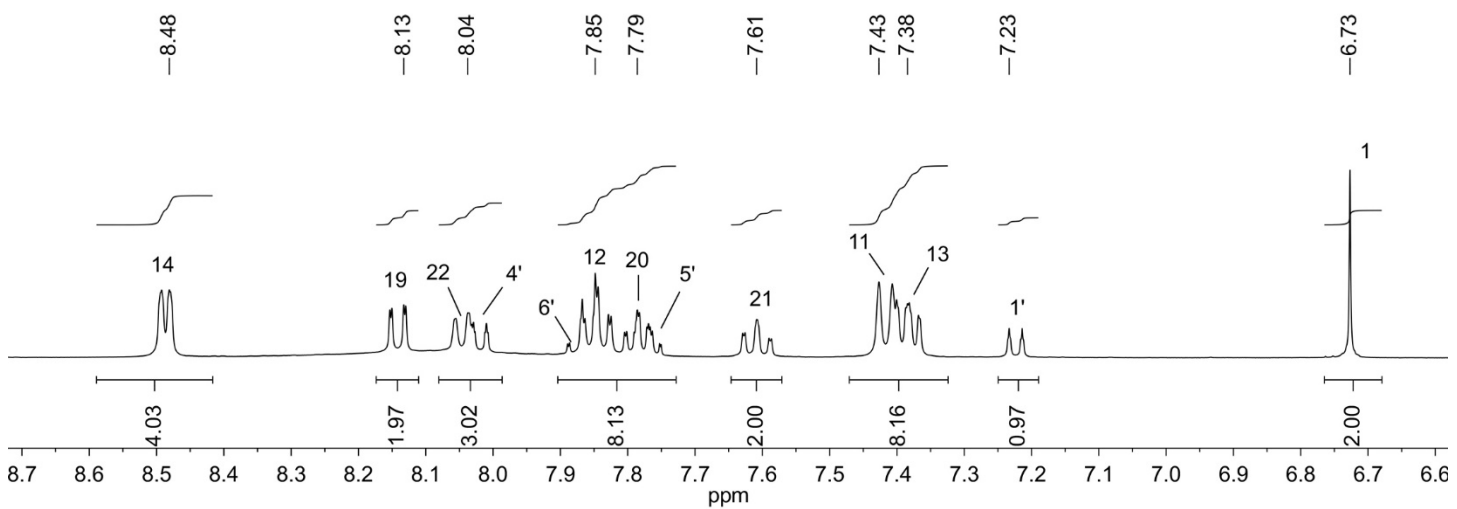


Figure S65. Expansion of ^1H NMR spectrum of **1**.

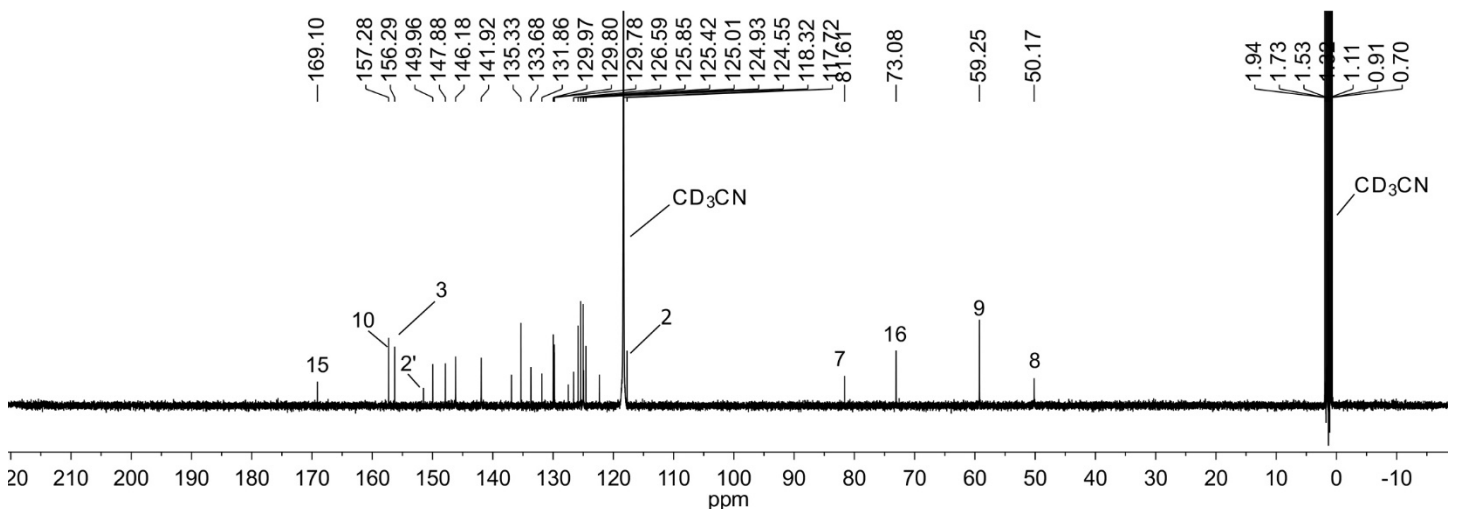


Figure S66. $^{13}\text{C}\{^1\text{H}\}$ NMR spectrum of **1**.

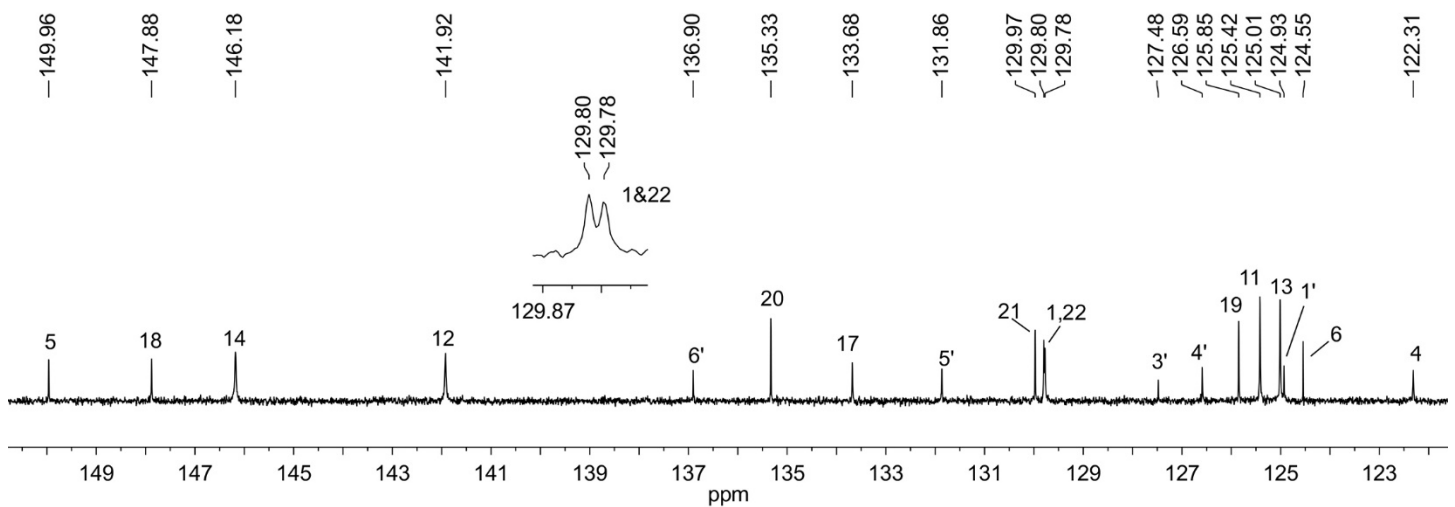


Figure S67. Expansion of $^{13}\text{C}\{^1\text{H}\}$ NMR spectrum of **1**.

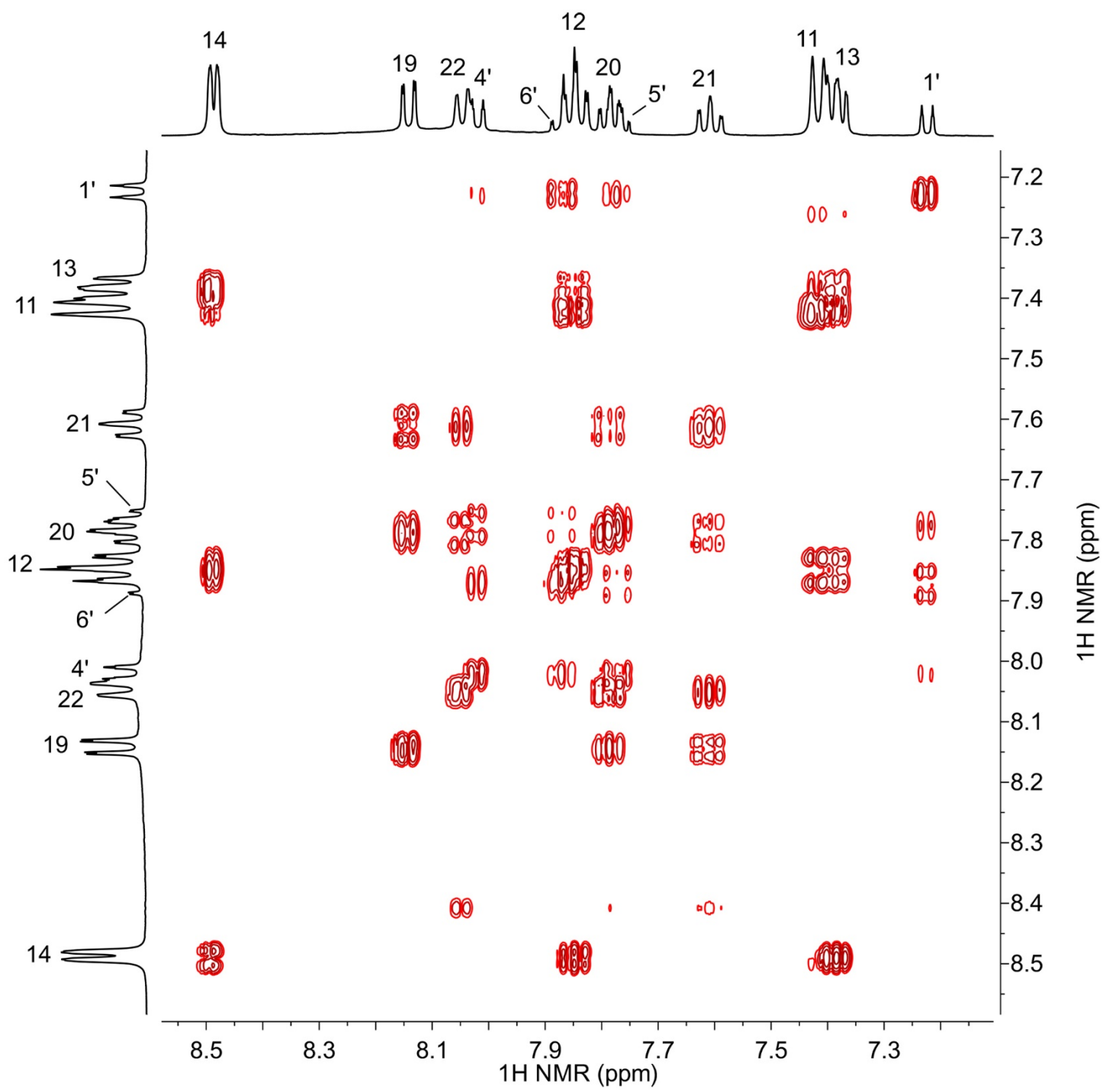


Figure S68. ^1H - ^1H COSY spectrum of **1**.

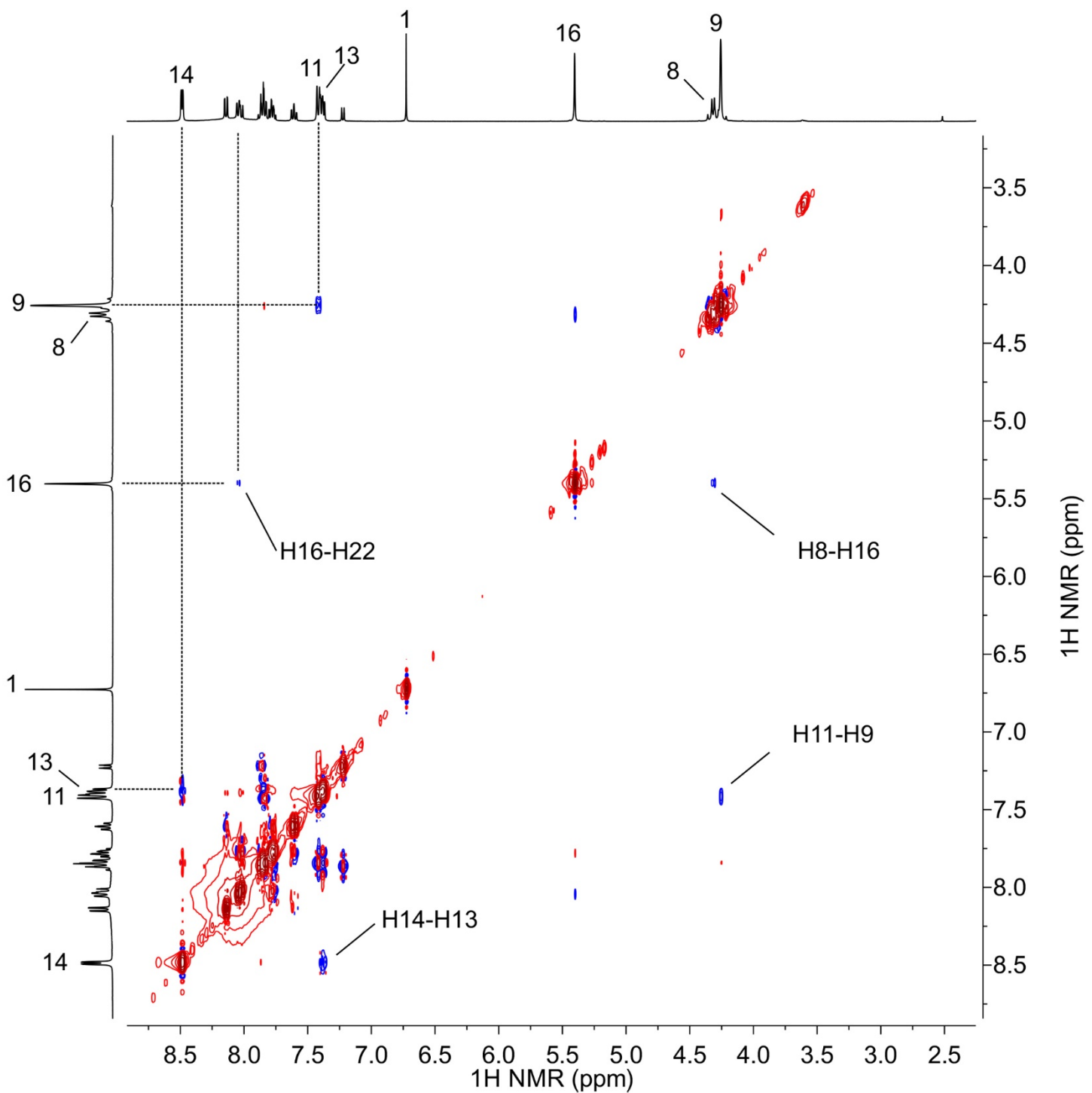


Figure S69. ^1H - ^1H NOESY spectrum of **1**.

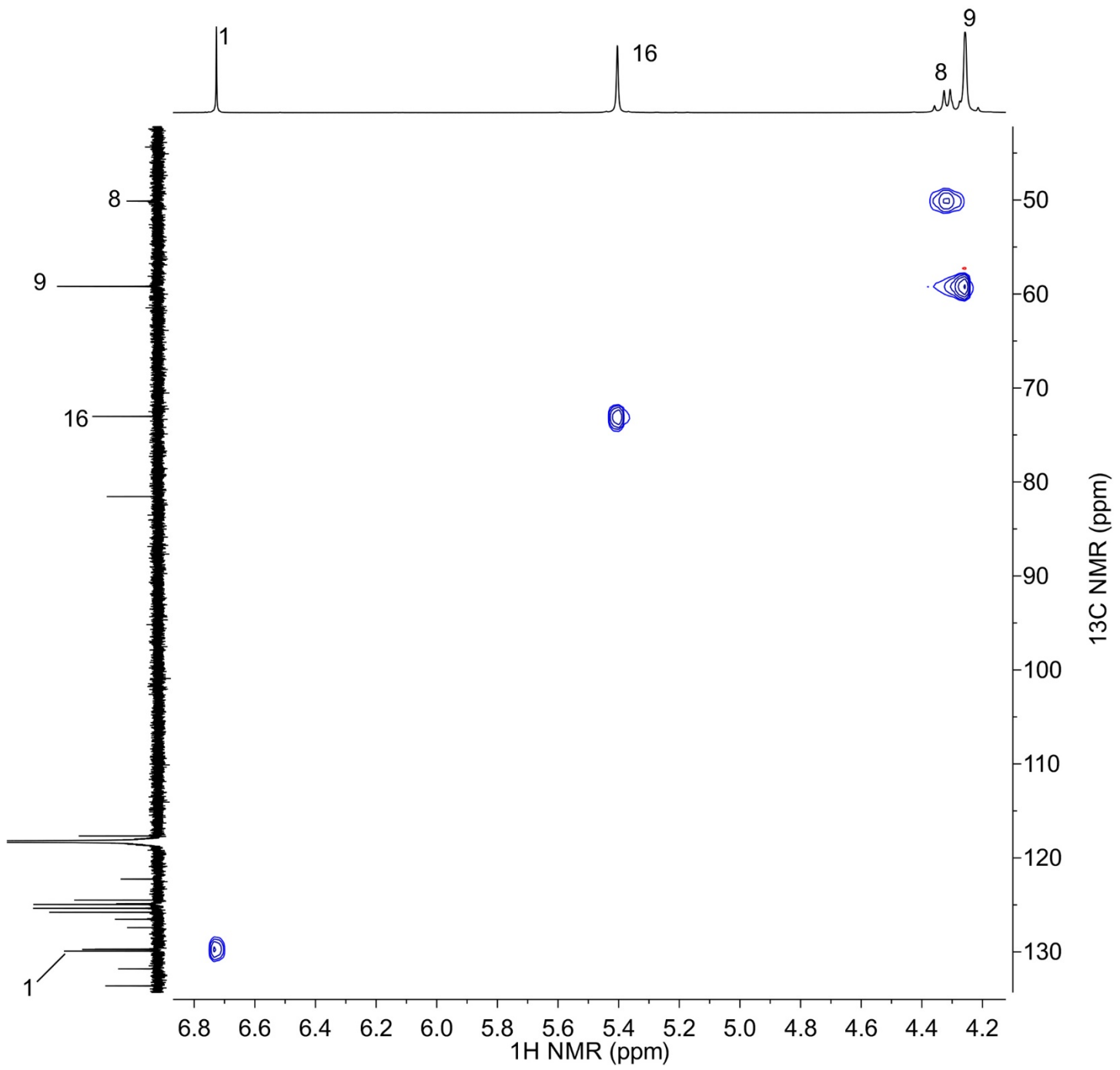


Figure S70. ^1H - ^{13}C HSQC spectrum of **1** from 4.2 to 6.8 ppm (^1H) and 40 to 135 ppm (^{13}C).

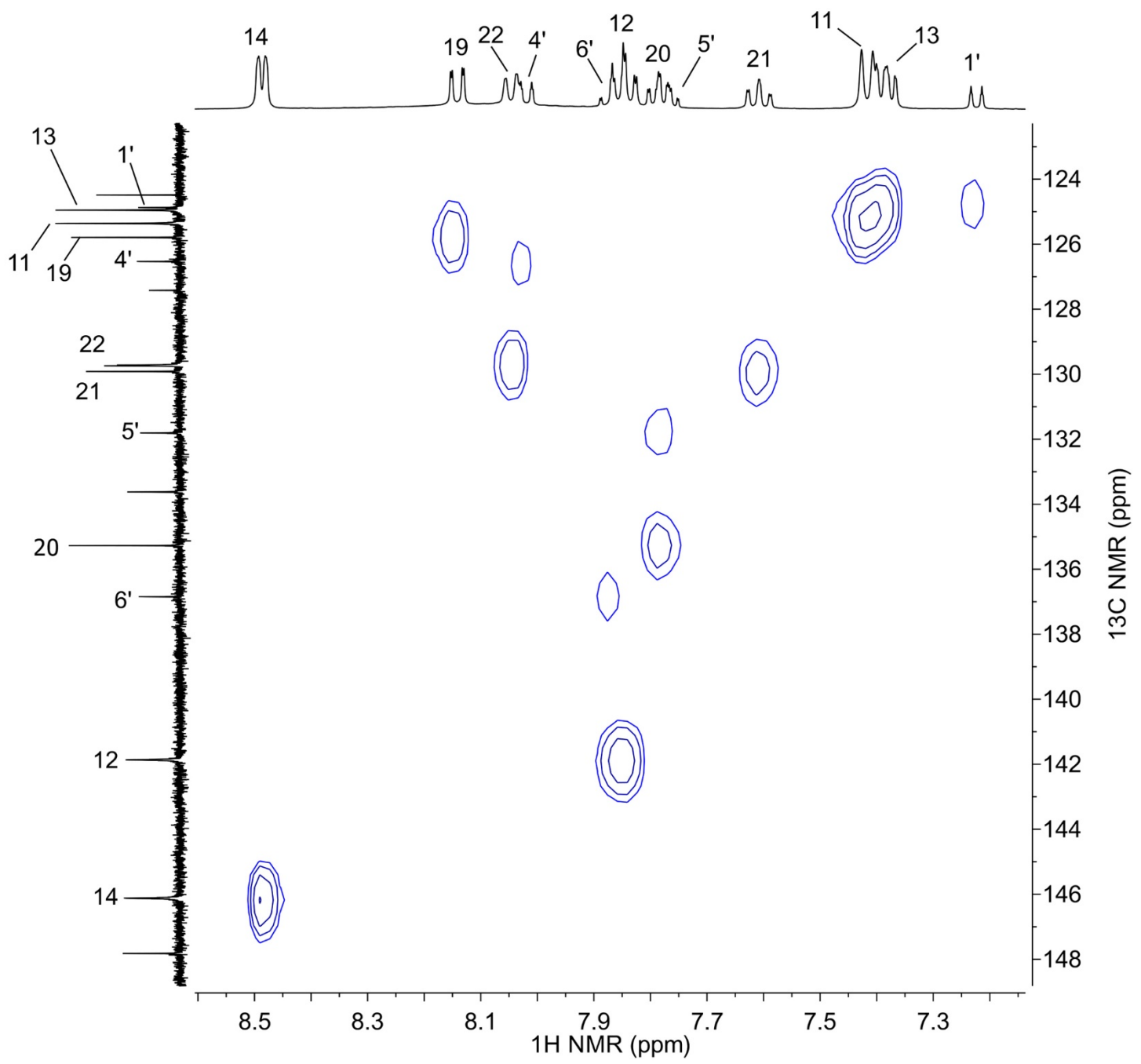


Figure S71. ^1H - ^{13}C HSQC spectrum of **1** from 7.2 to 8.6 ppm (^1H) and 123 to 148 ppm (^{13}C).

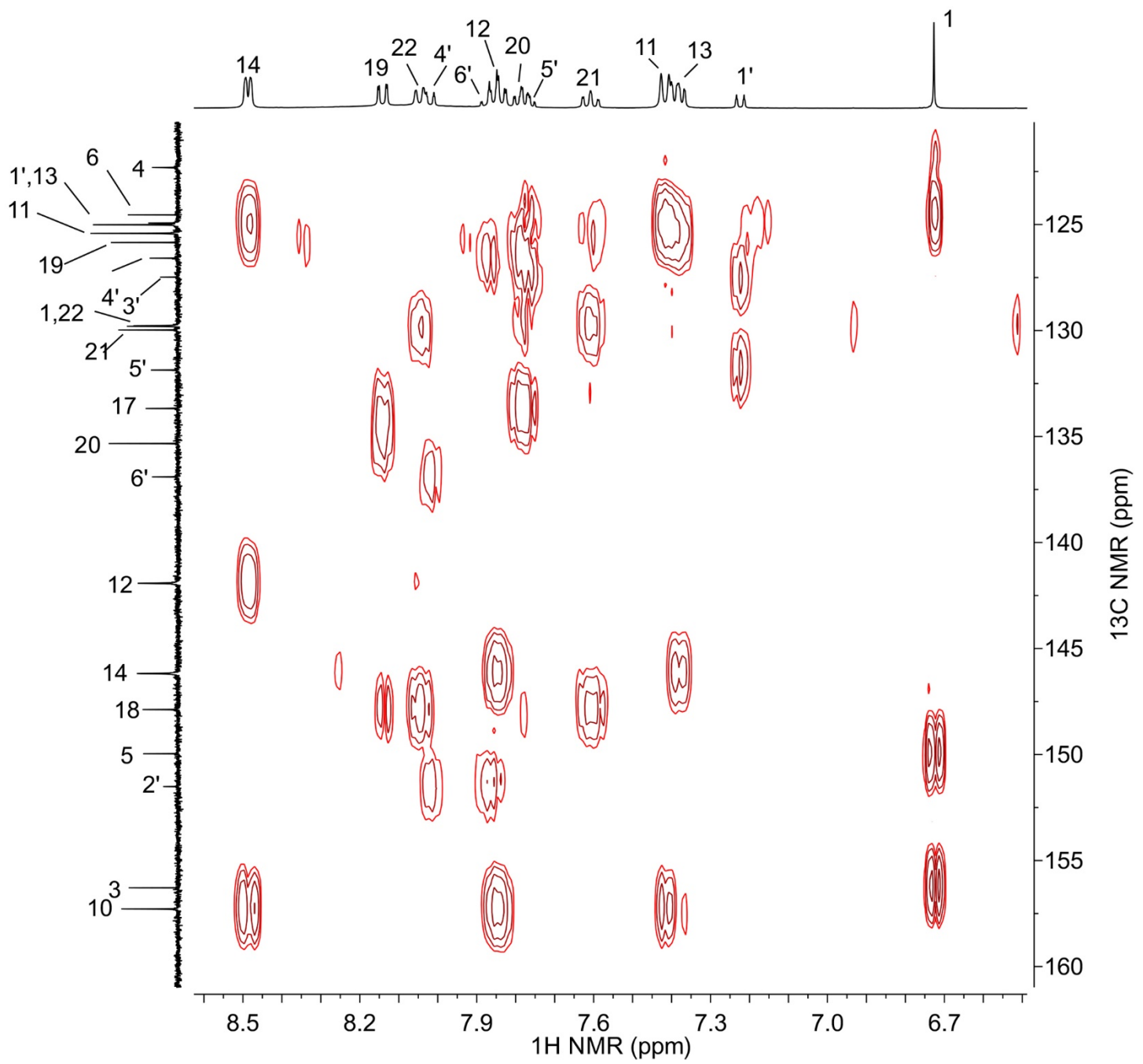


Figure S72. ^1H - ^{13}C HMBC spectrum of **1** from 6.5 to 8.6 ppm (^1H) and 120 to 160 ppm (^{13}C).

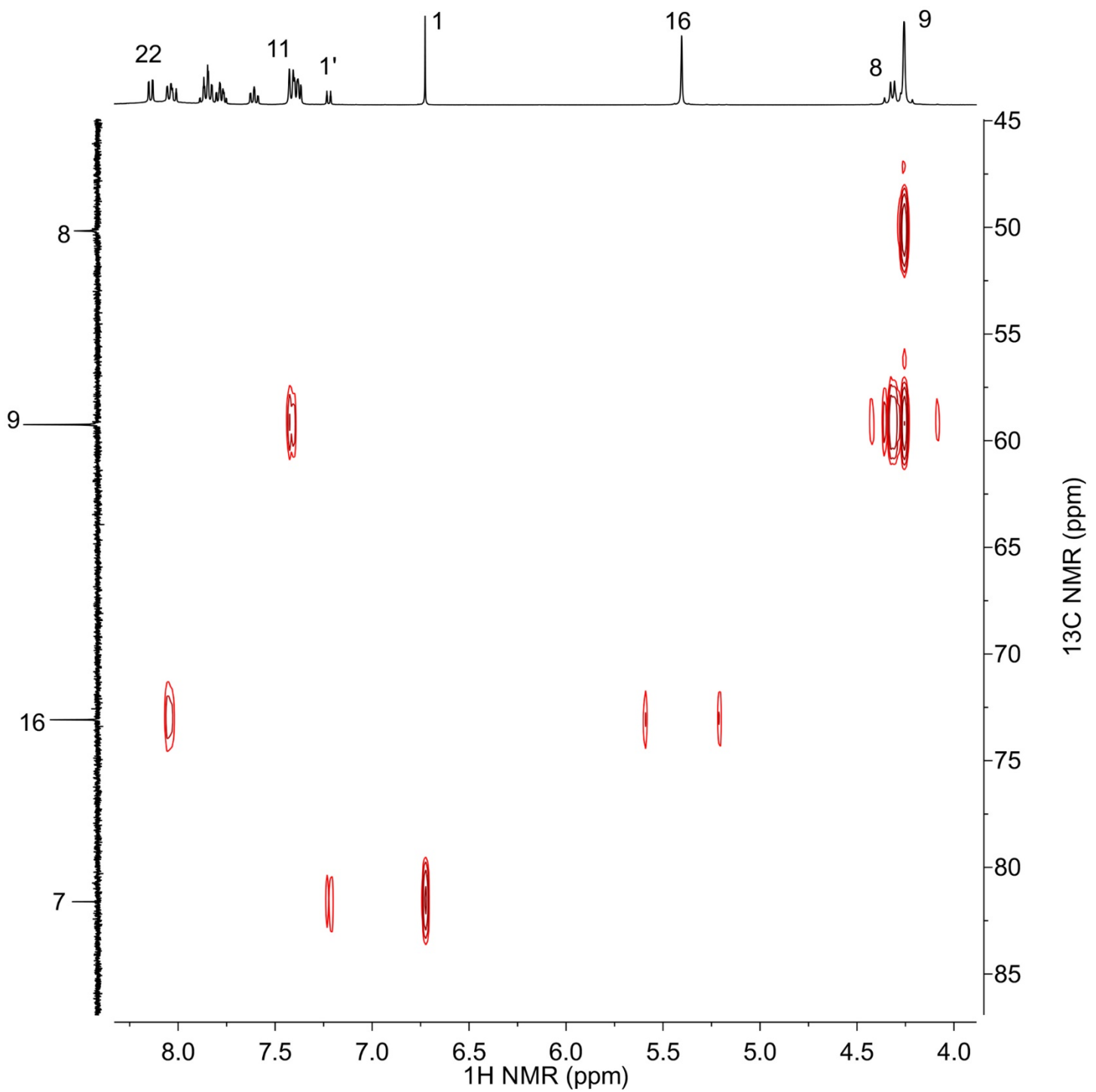


Figure S73. ^1H - ^{13}C HMBC spectrum of **1** from 4.0 to 8.3 ppm (^1H) and 45 to 85 ppm (^{13}C).

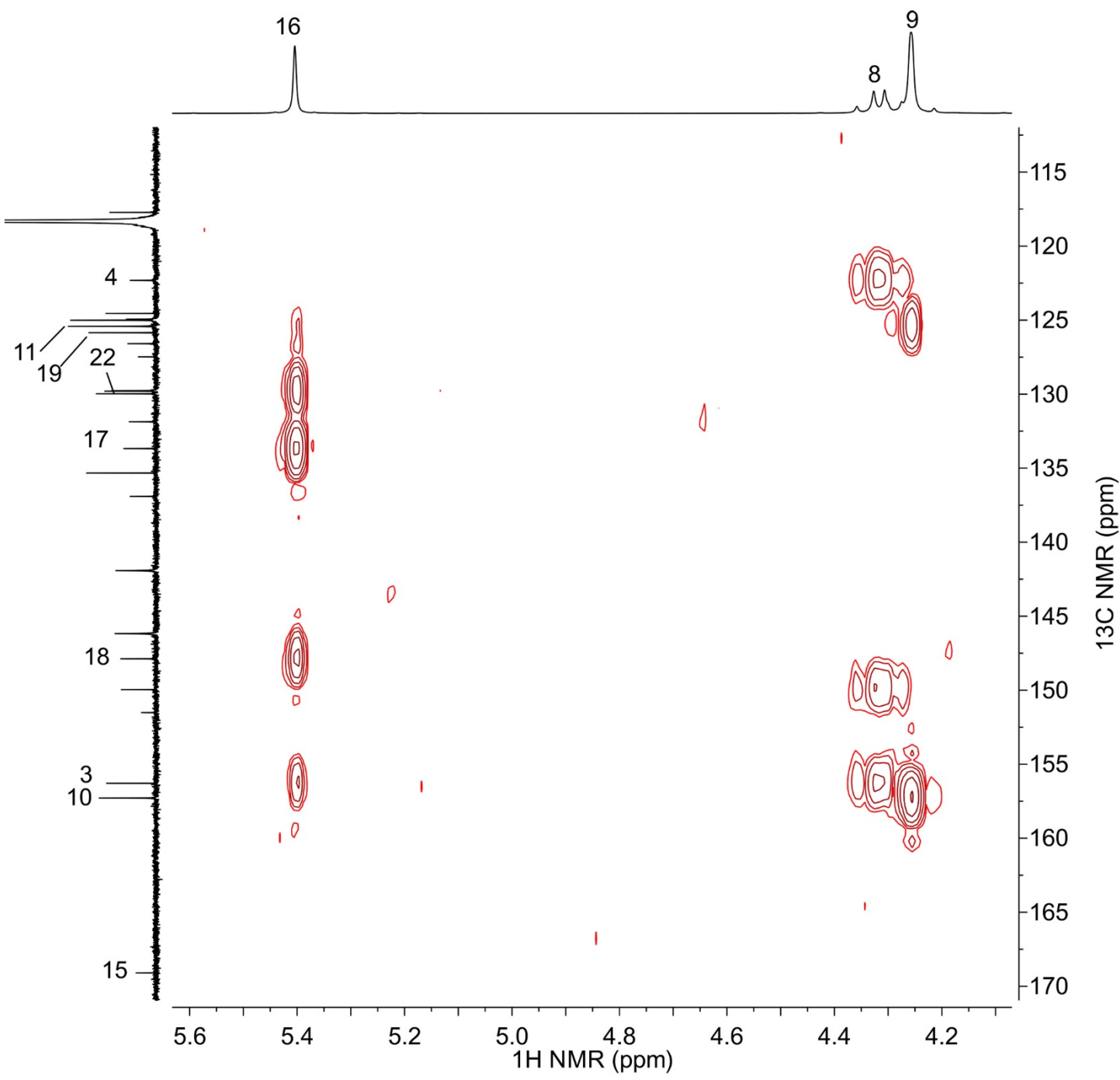


Figure S74. ^1H - ^{13}C HMBC spectrum of **1** from 4.1 to 5.6 ppm (^1H) and 110 to 170 ppm (^{13}C).

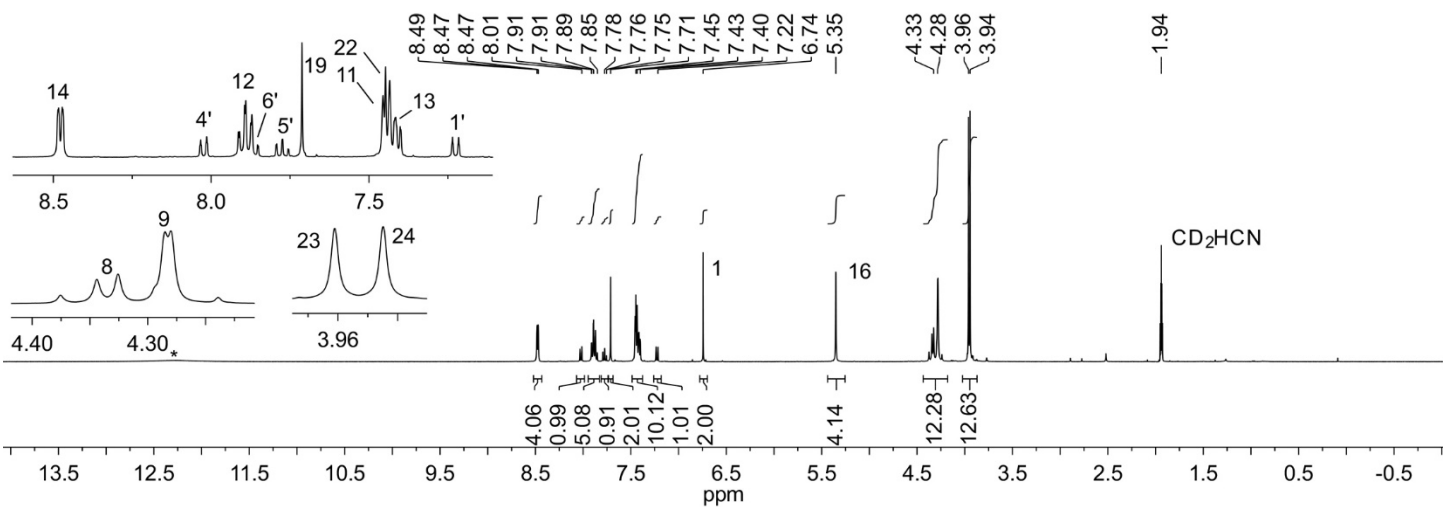


Figure S75. ^1H NMR spectrum of **2**.

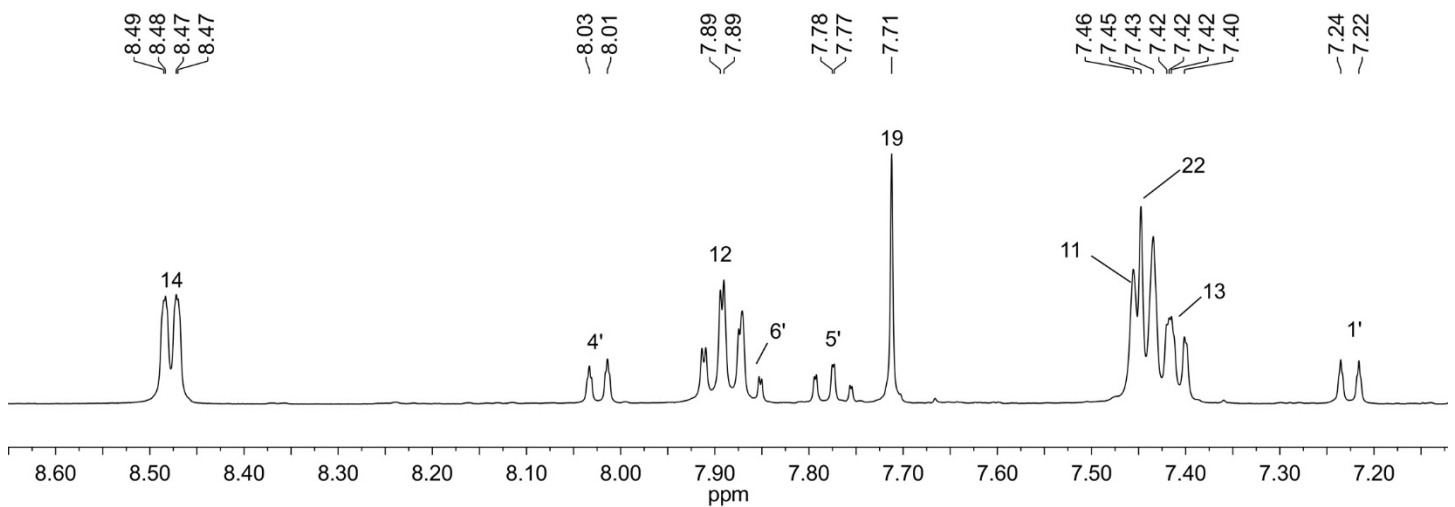


Figure S76. Expansion of ^1H NMR spectrum of **2**.

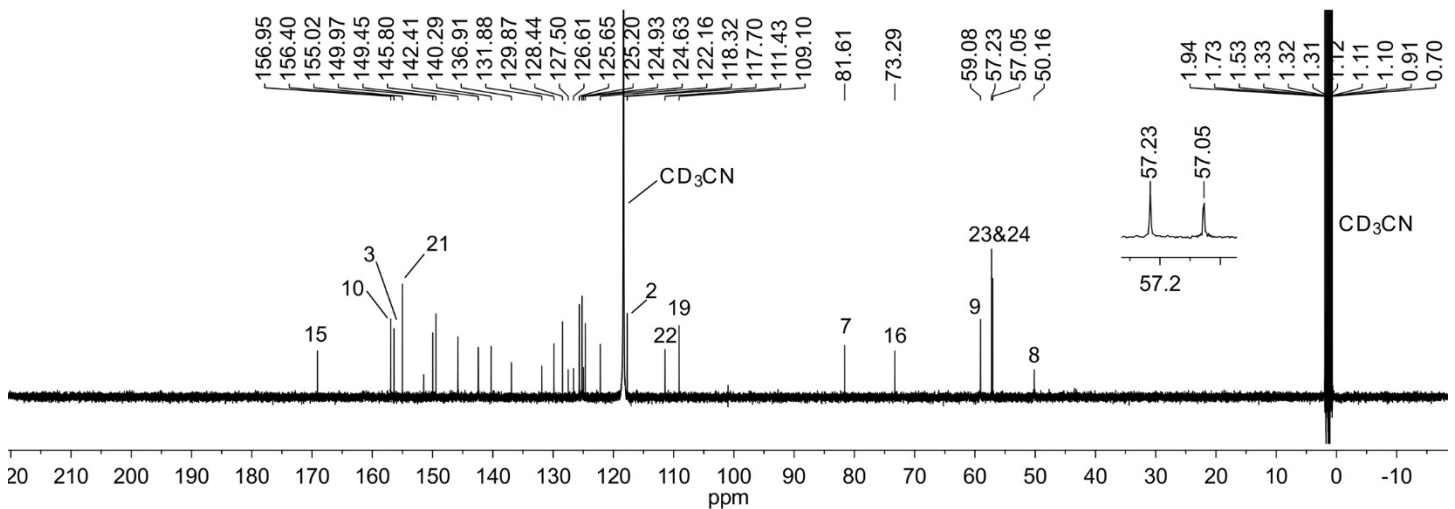


Figure S77. $^{13}\text{C}\{^1\text{H}\}$ NMR spectrum of **2**.

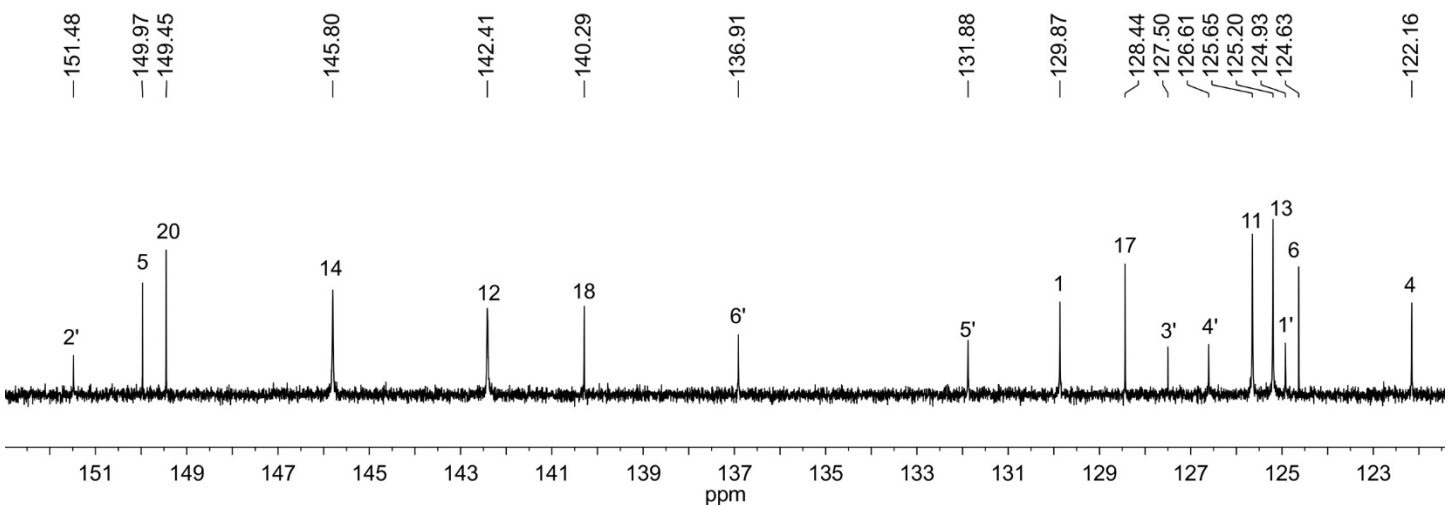


Figure S78. Expansion of $^{13}\text{C}\{\text{H}\}$ NMR spectrum of **2**.

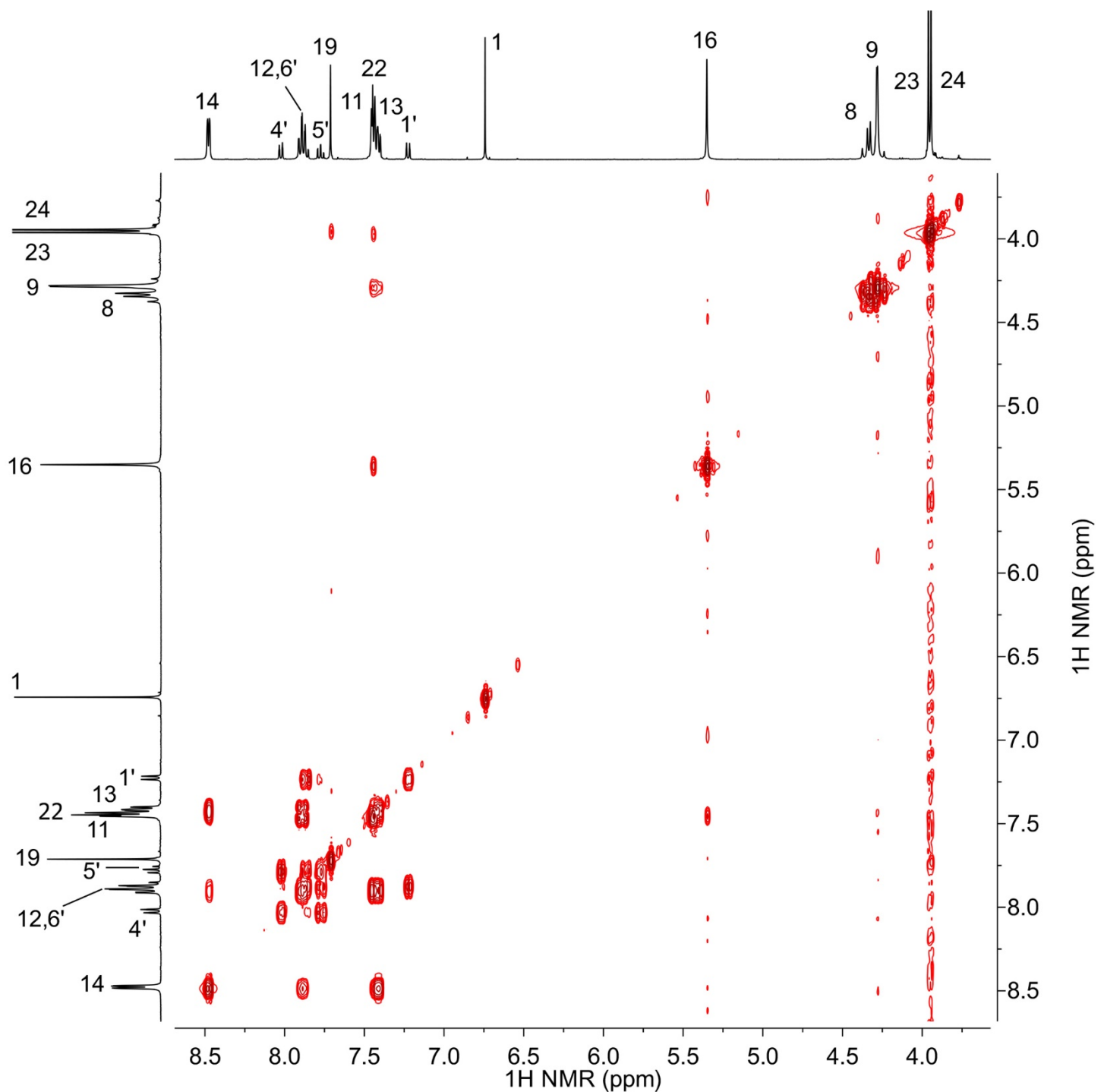


Figure S79. ^1H - ^1H COSY spectrum of **2**.

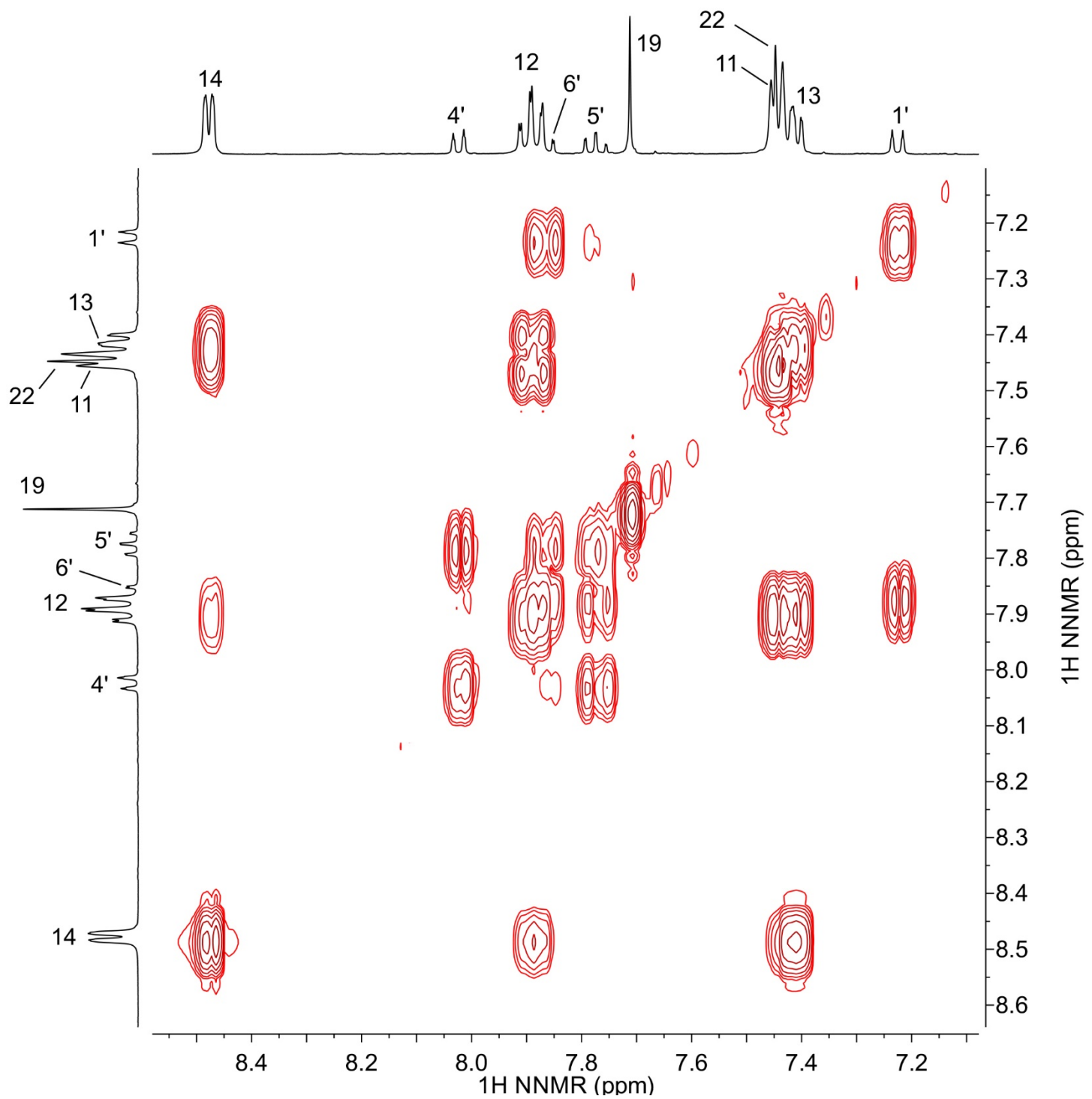


Figure S80. Expansion of ^1H - ^1H COSY spectrum of **2**.

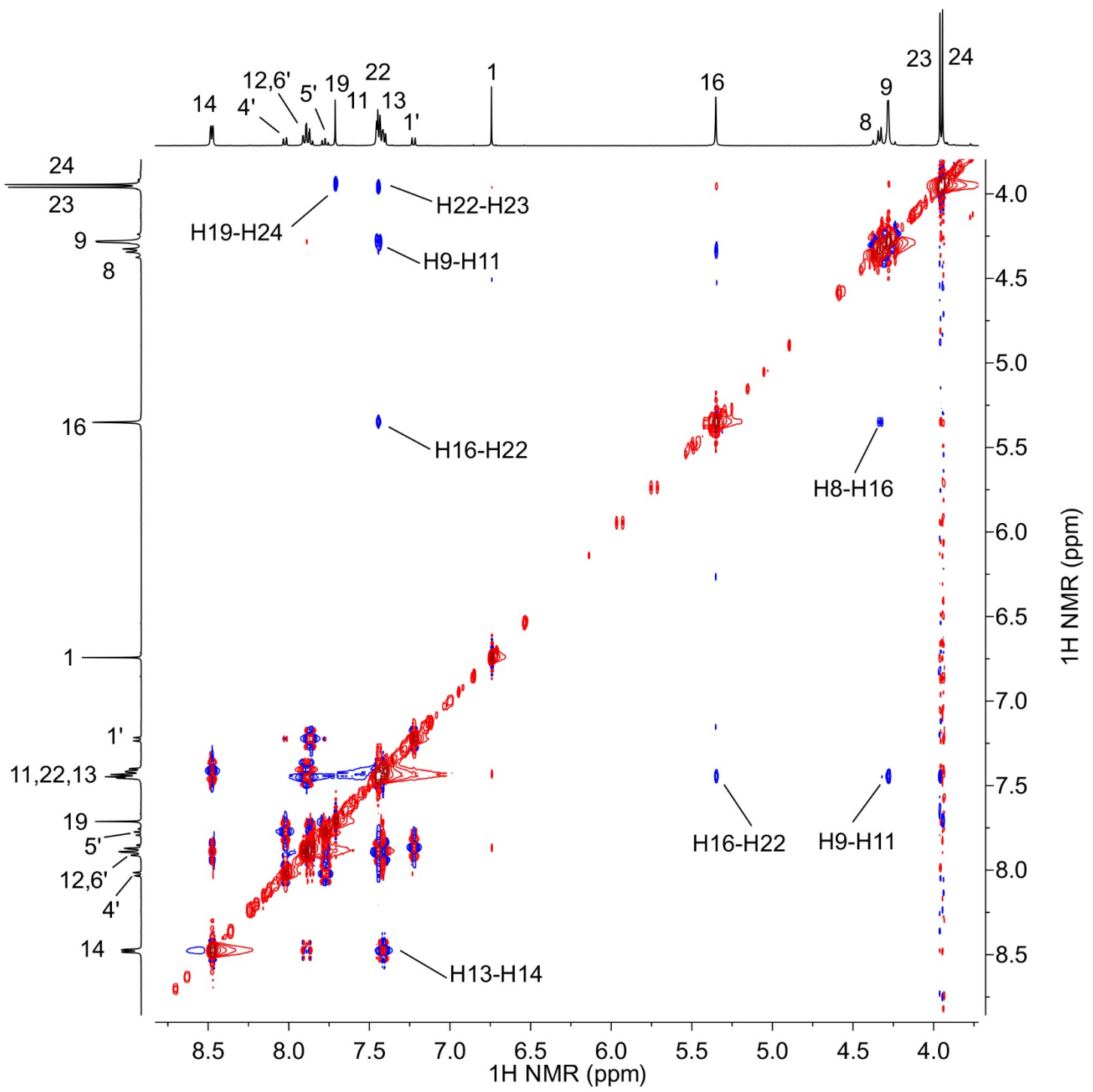


Figure S81. ^1H - ^1H NOESY spectrum of **2**.

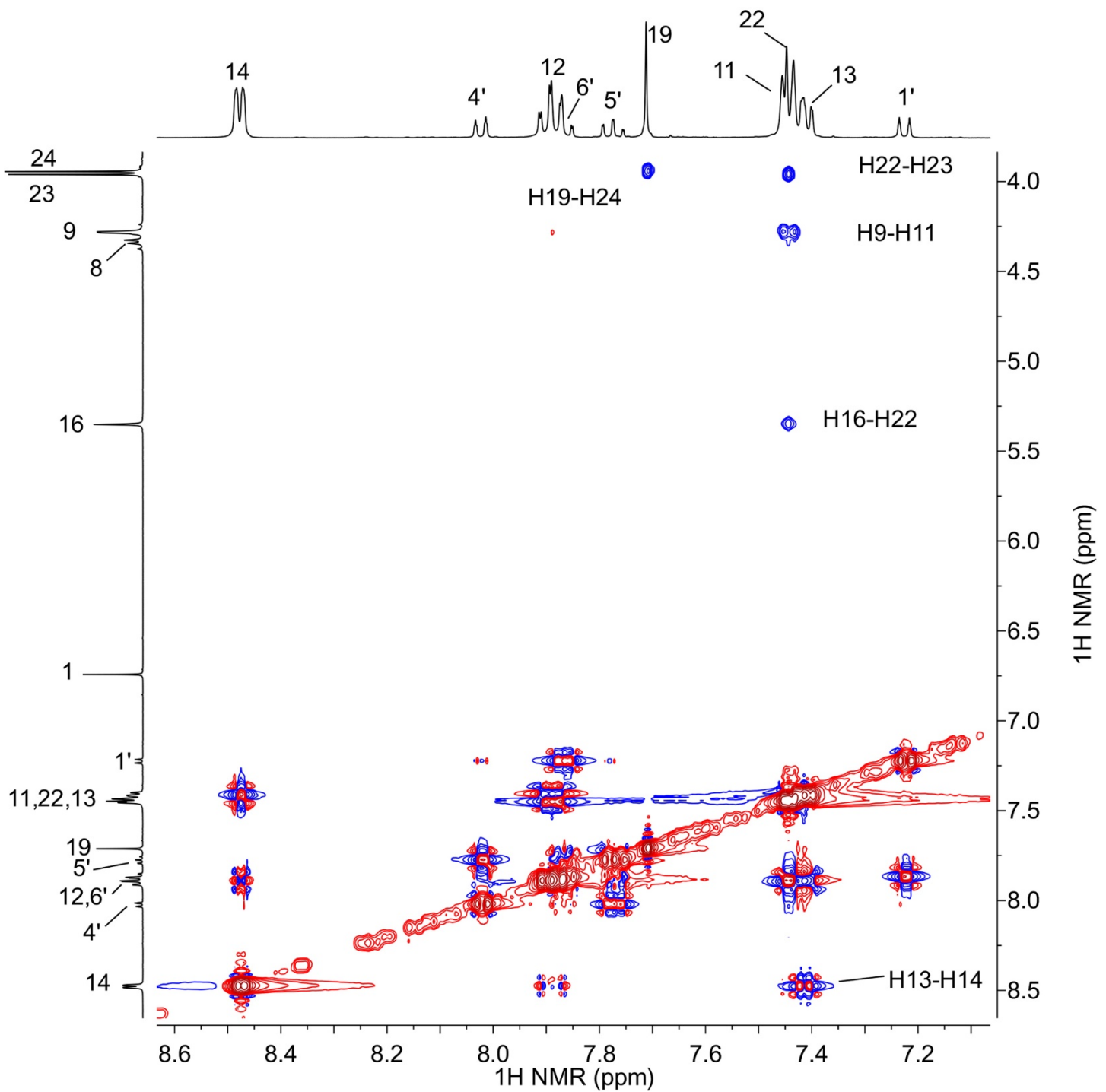


Figure S82. Expansion of ^1H - ^1H NOESY spectrum of **2**.

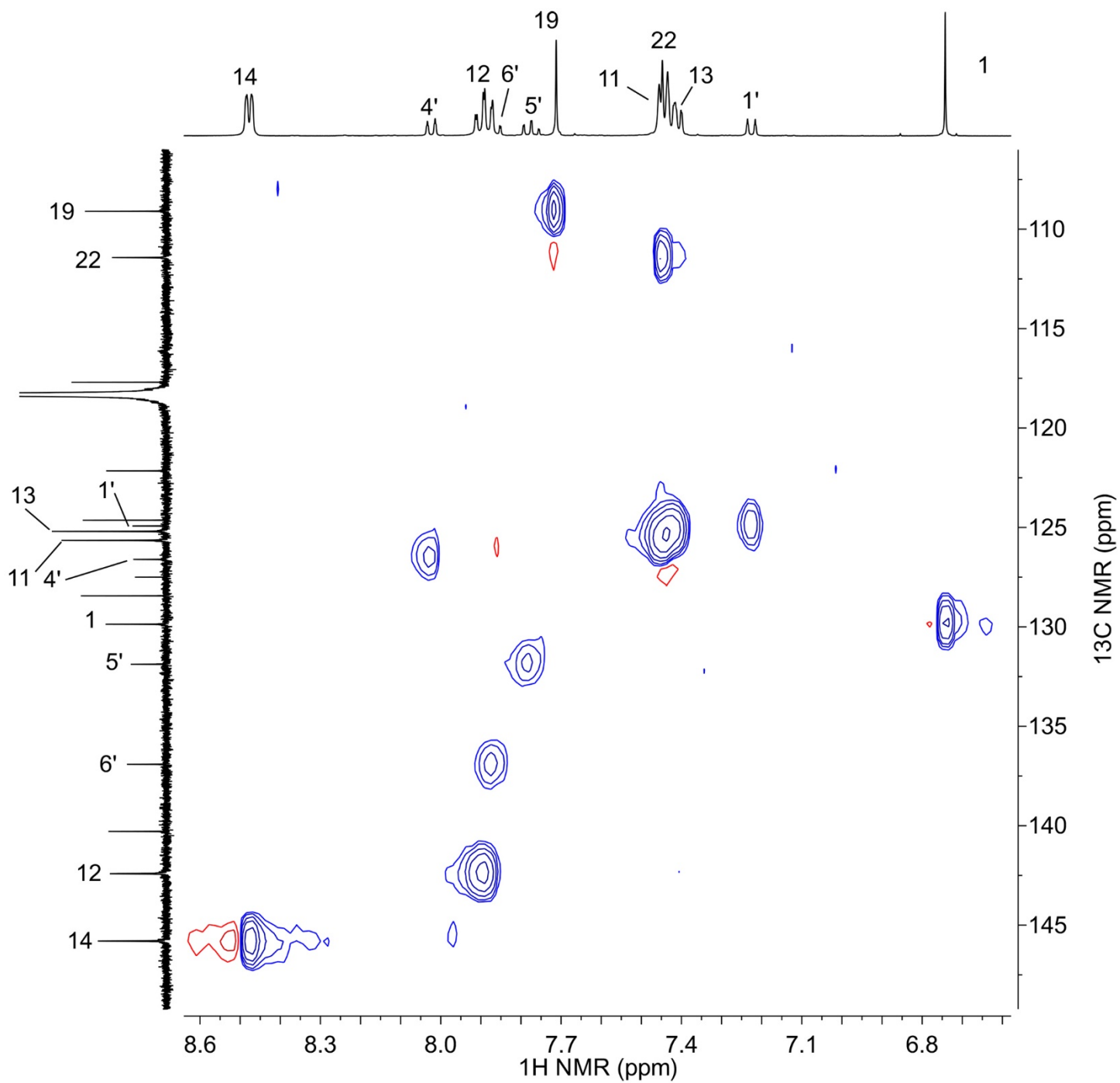


Figure S83. ^1H - ^{13}C HSQC spectrum of **2** from 6.6 to 8.6 ppm (^1H) and 100 to 150 ppm (^{13}C).

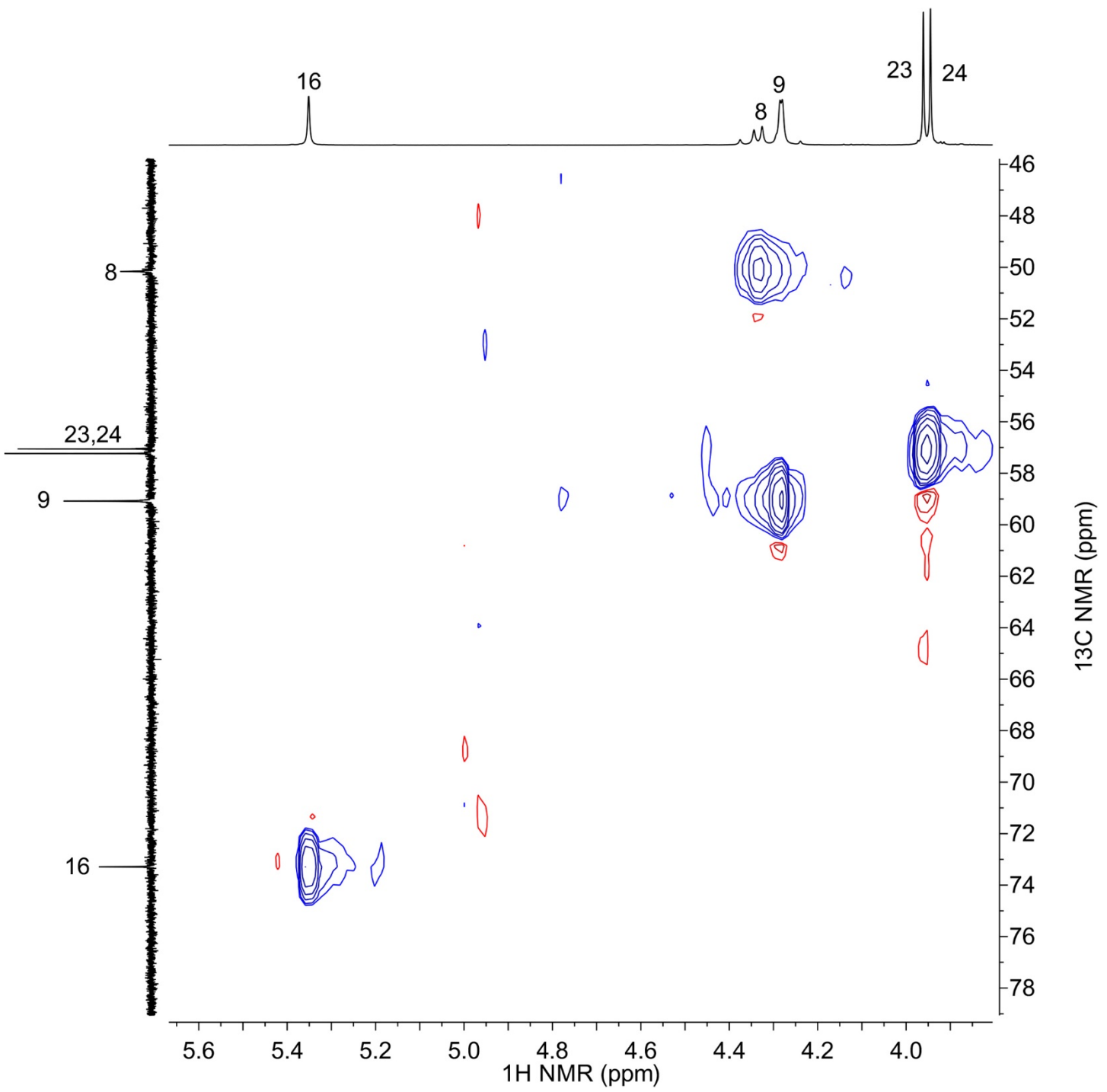


Figure S84. ^1H - ^{13}C HSQC spectrum of **2** from 3.8 to 5.7 ppm (^1H) and 46 to 78 ppm (^{13}C).

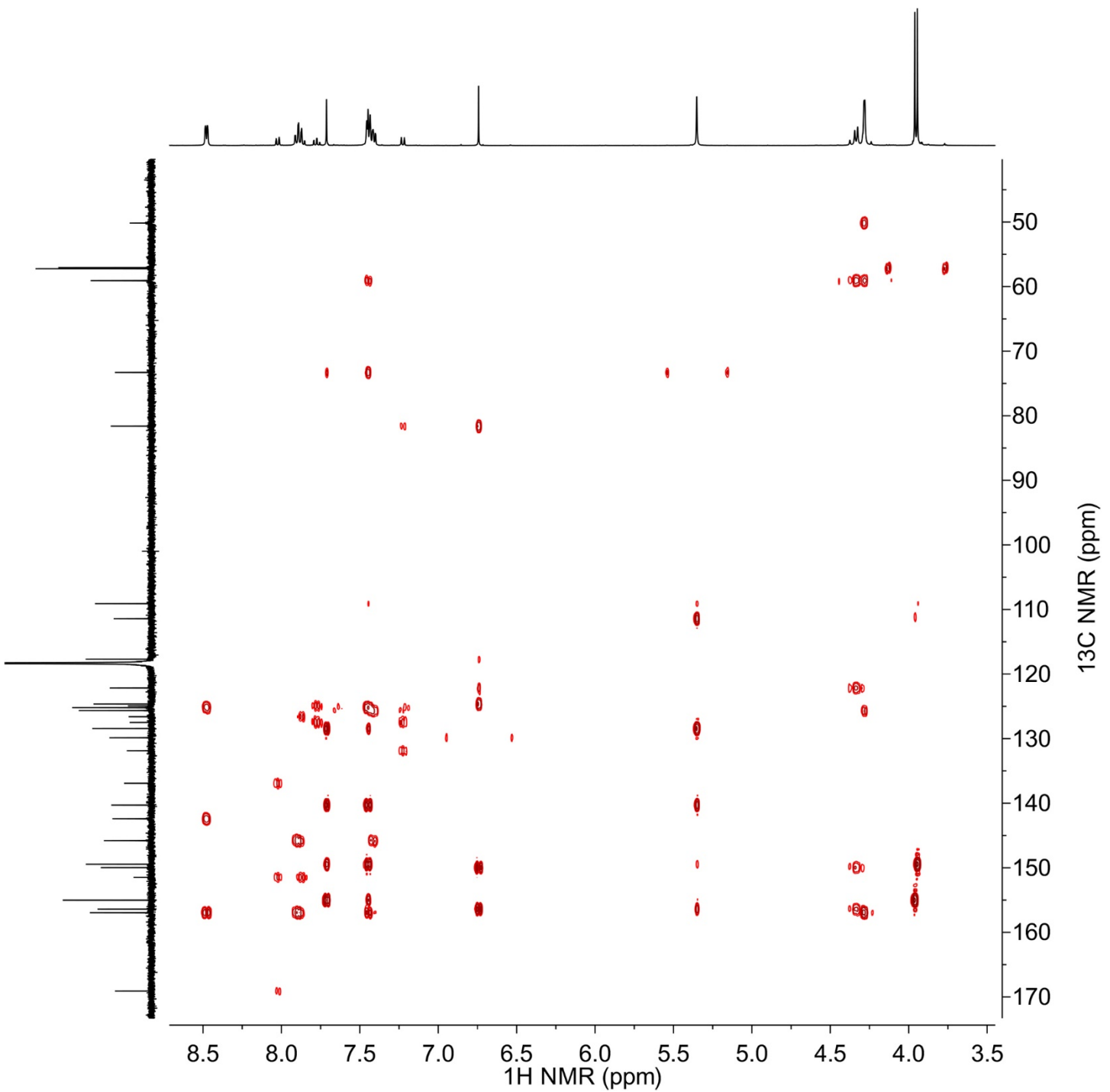


Figure S85. ^1H - ^{13}C HMBC spectrum of **2**.

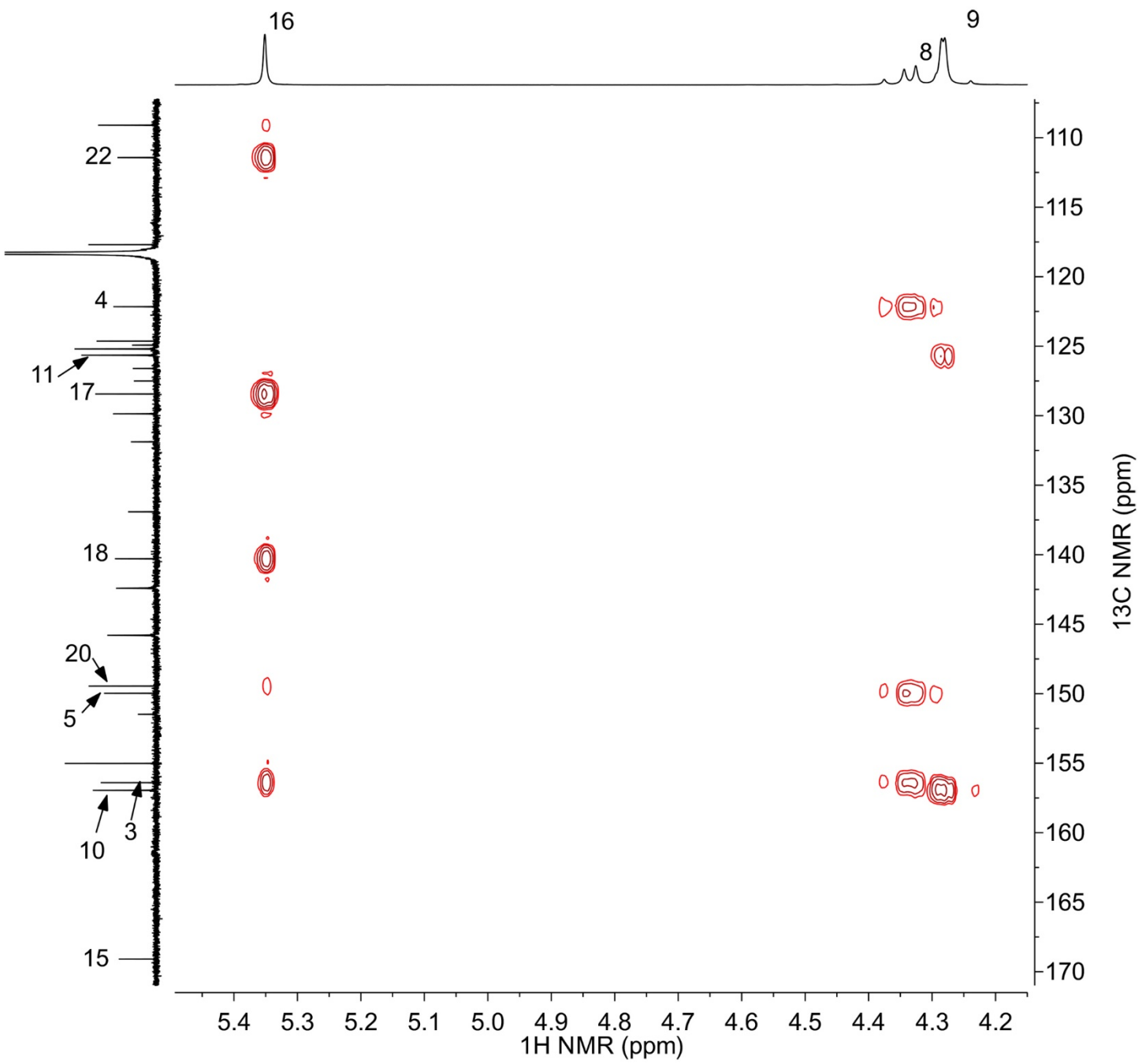


Figure S86. Expansion of ^1H - ^{13}C HMBC spectrum of **2** from 4.2 to 5.5 ppm (^1H) and 105 to 170 ppm (^{13}C).

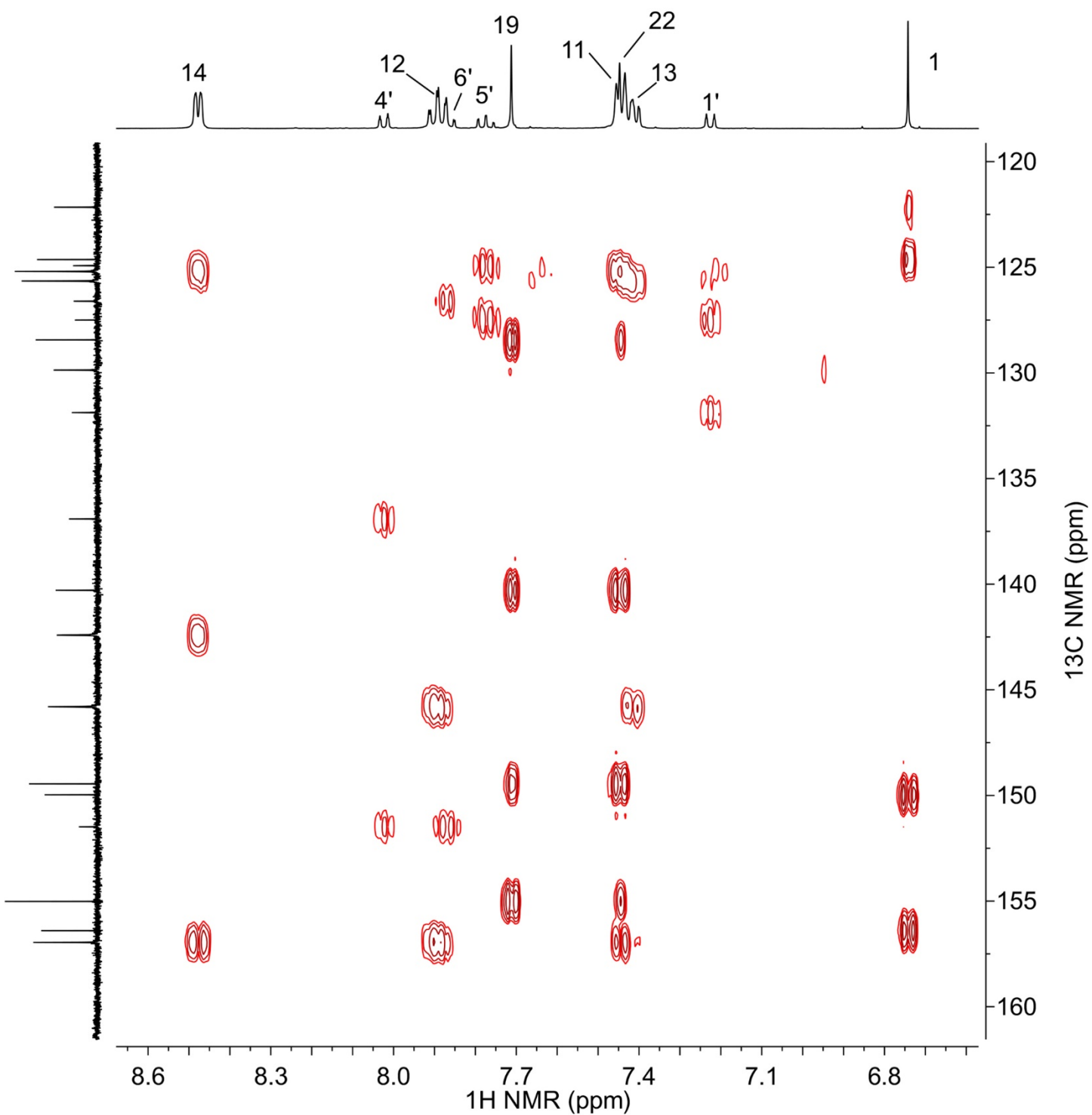


Figure S87. Expansion of ¹H-¹³C HMBC spectrum of **2** from 6.6 to 8.7 ppm (¹H) and 120 to 160 ppm (¹³C).

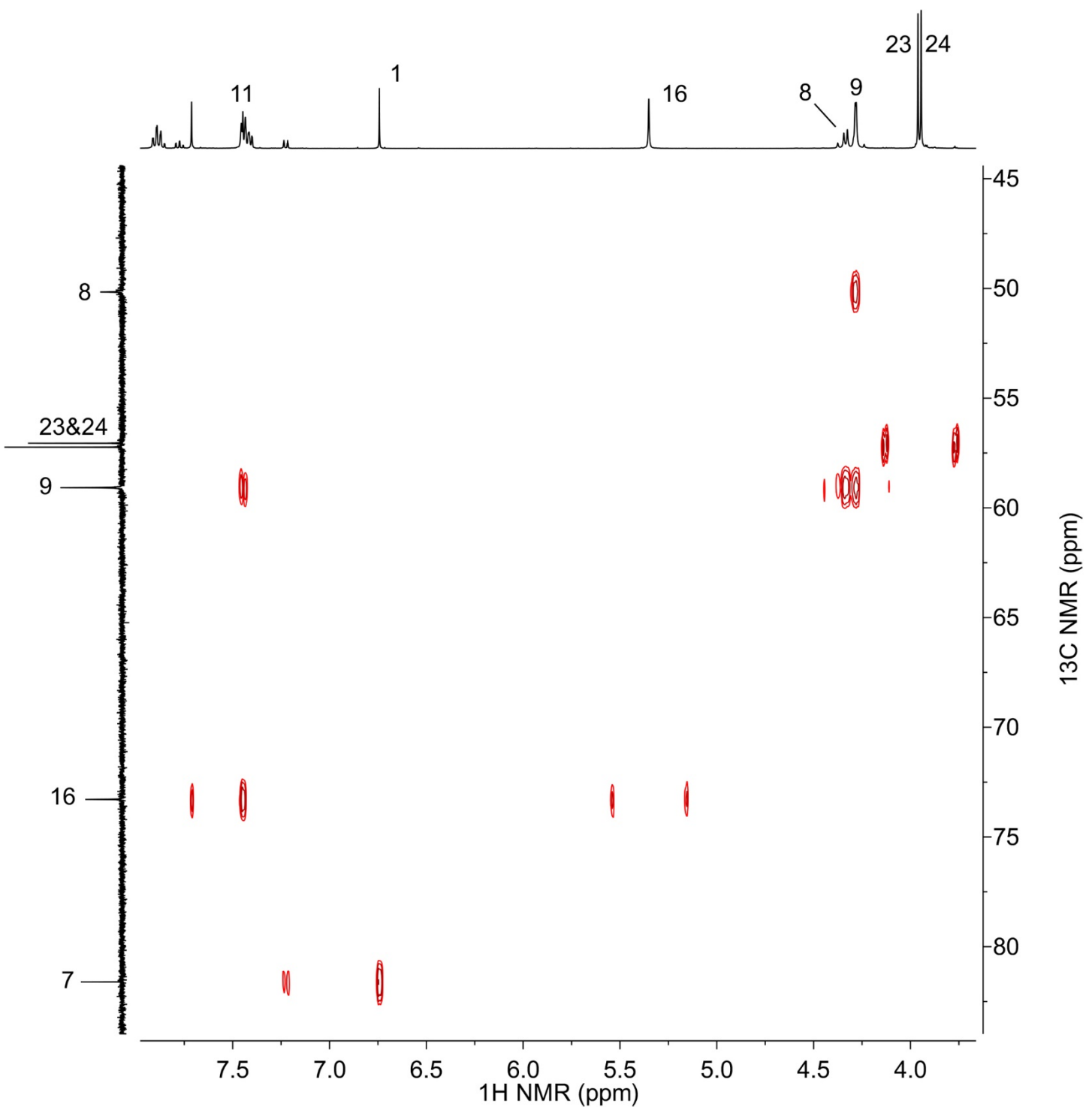


Figure S88. Expansion of ^1H - ^{13}C HMBC spectrum of **2** from 3.7 to 8.0 ppm (^1H) and 45 to 90 ppm (^{13}C).

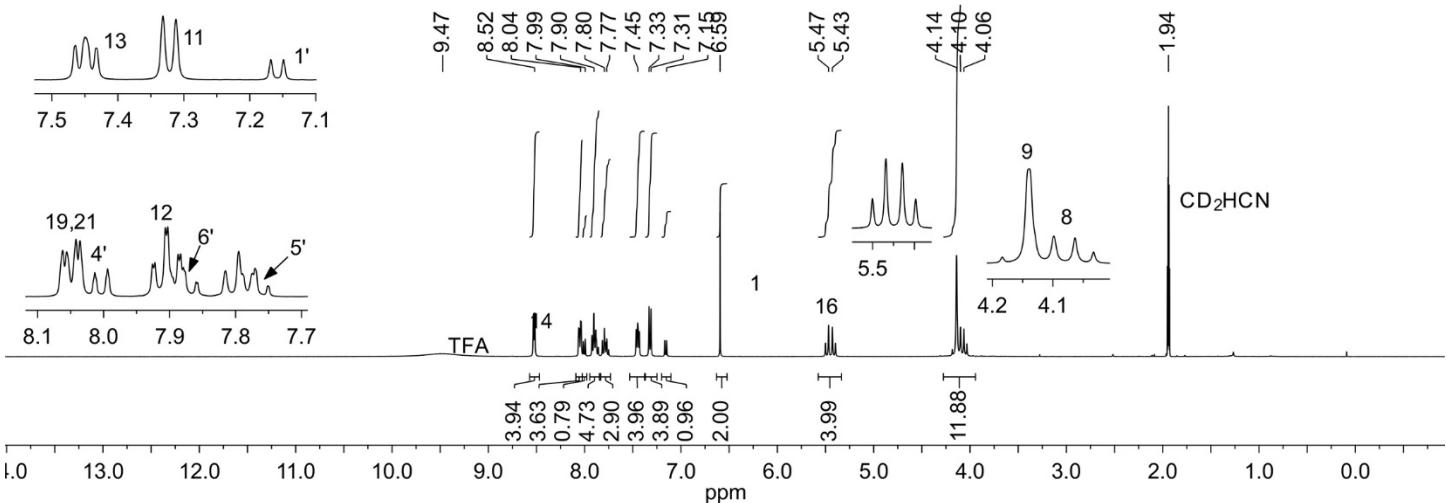


Figure S89. ^1H NMR spectrum of **3**.

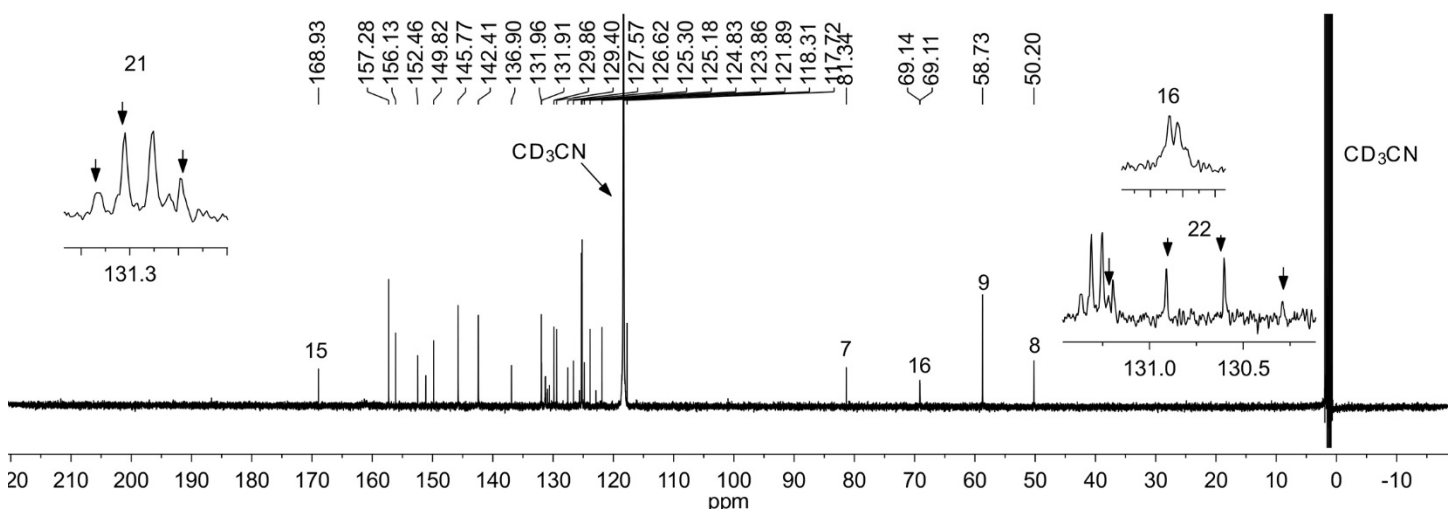


Figure S90. $^{13}\text{C}\{^1\text{H}\}$ NMR spectrum of **3**.

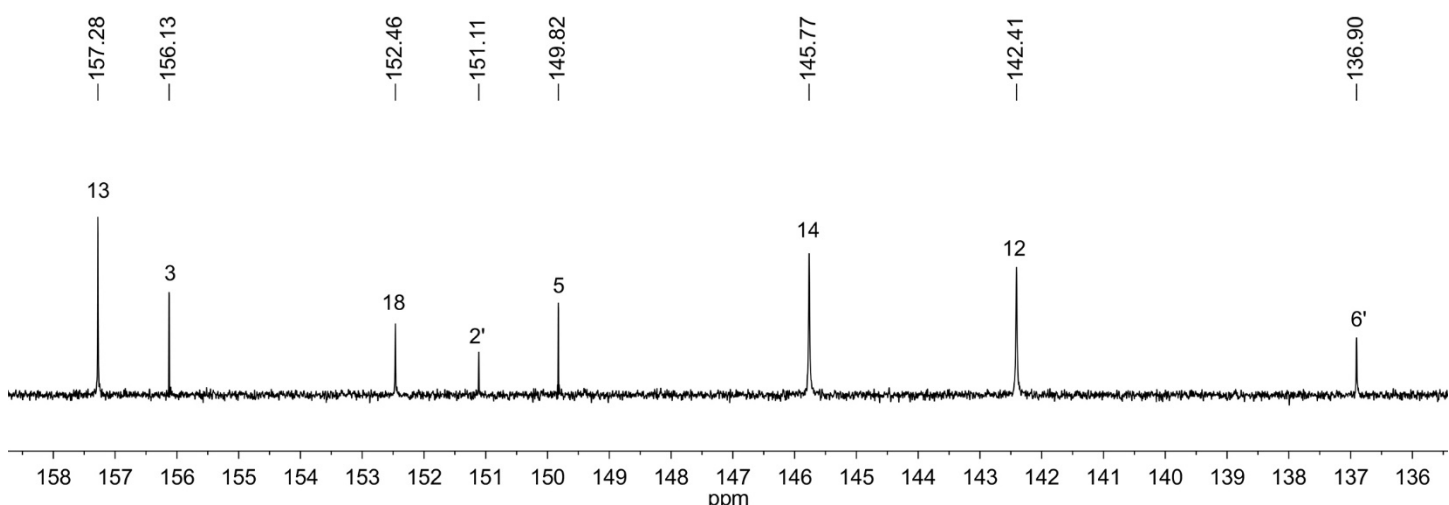


Figure S91. Expansion of $^{13}\text{C}\{^1\text{H}\}$ NMR spectrum of **3** from 136 to 159 ppm.

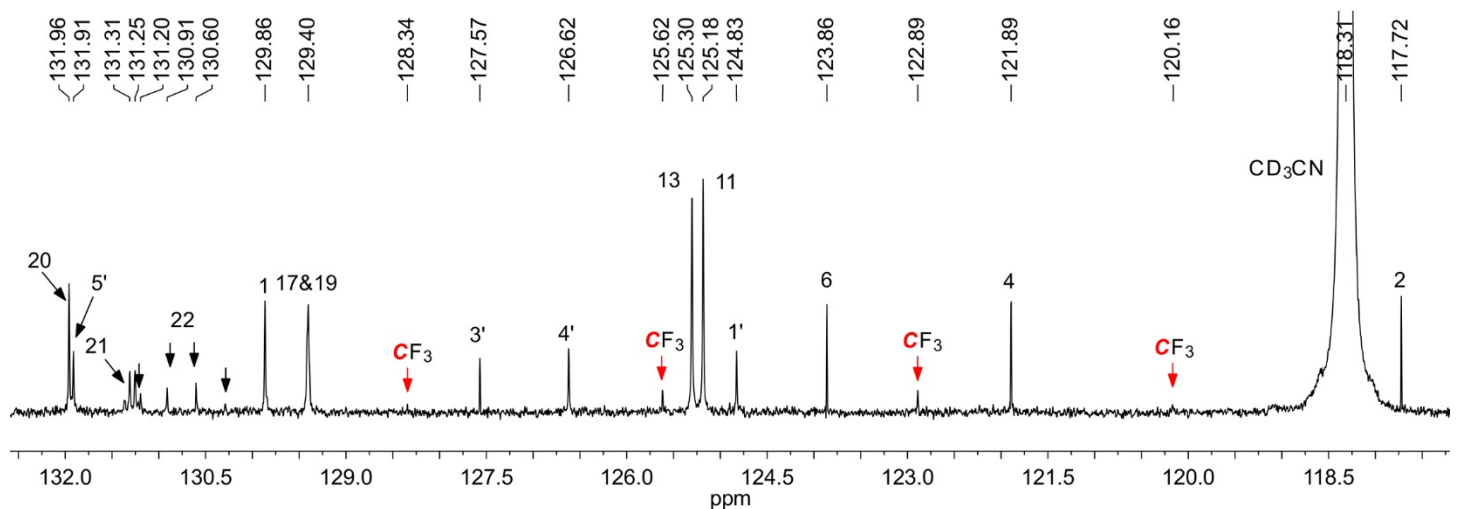


Figure S92. Expansion of $^{13}\text{C}\{^1\text{H}\}$ NMR spectrum of **3** from 117 to 132 ppm.

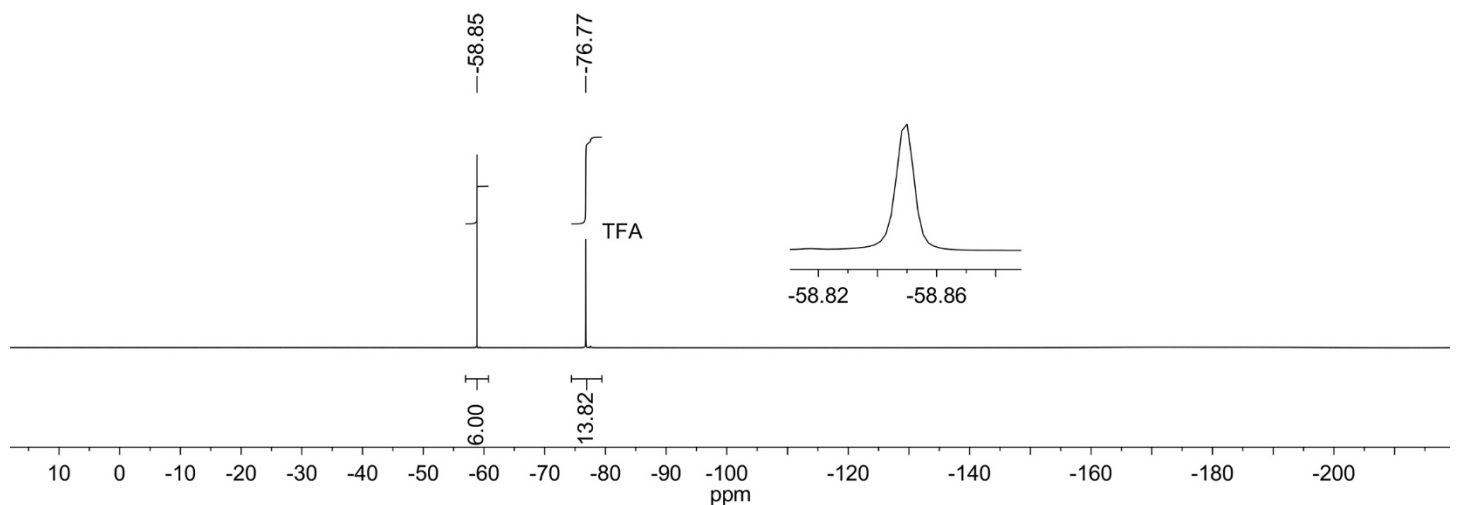


Figure S93. ^{19}F NMR spectrum of **3**.

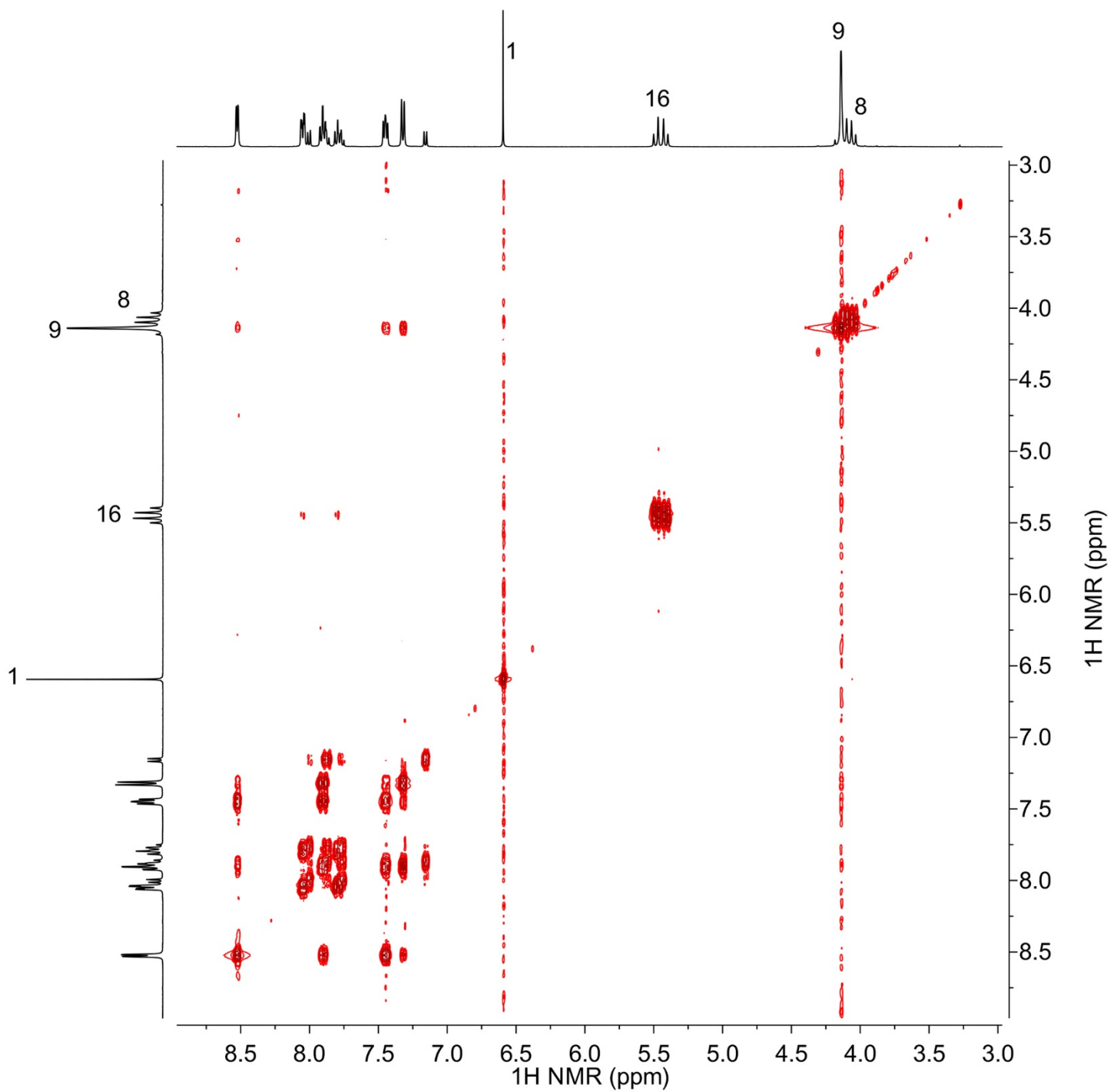


Figure S94. ^1H - ^1H COSY spectrum of **3**.

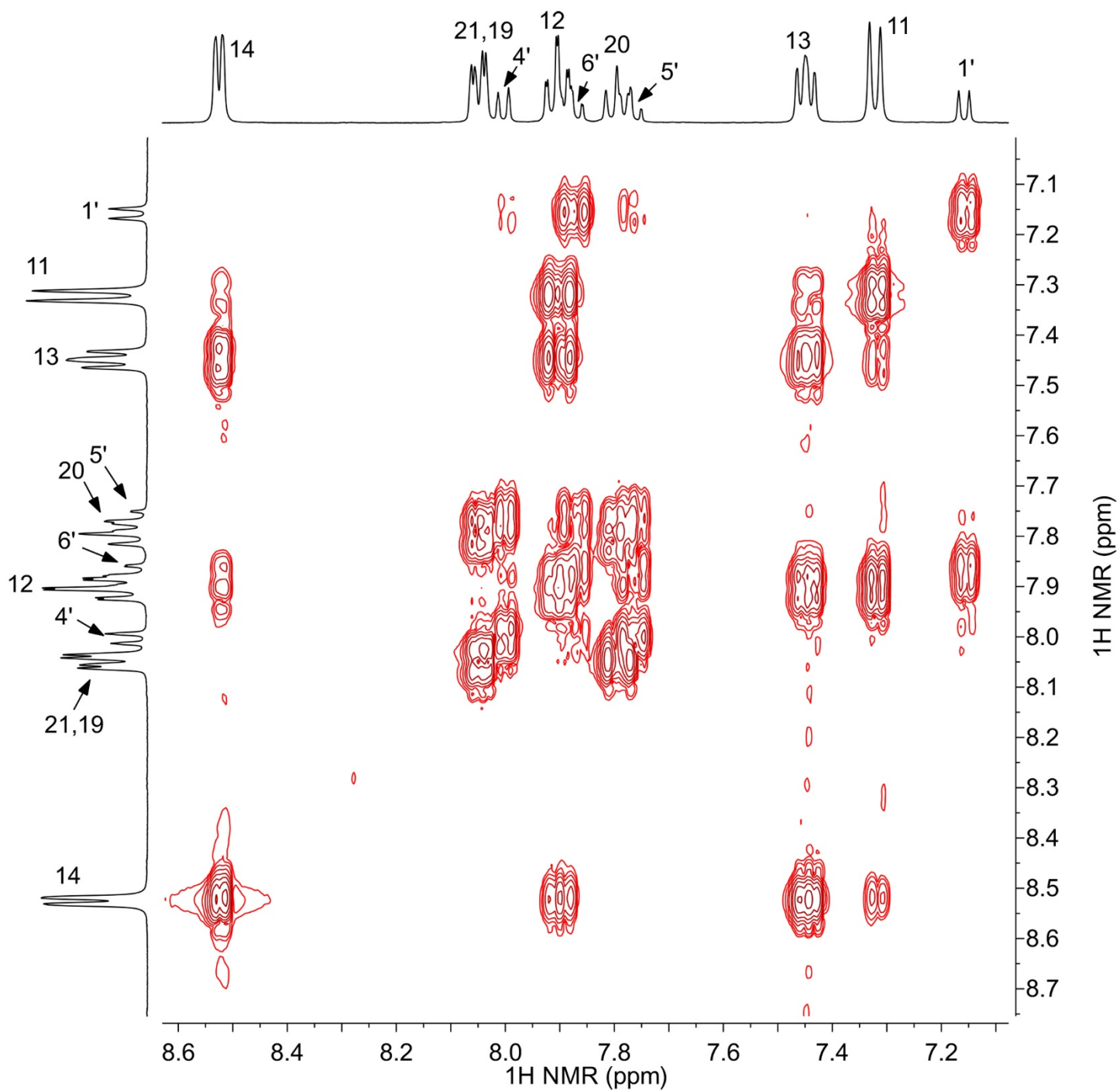


Figure S95. Expansion of ^1H - ^1H COSY spectrum of **3**.

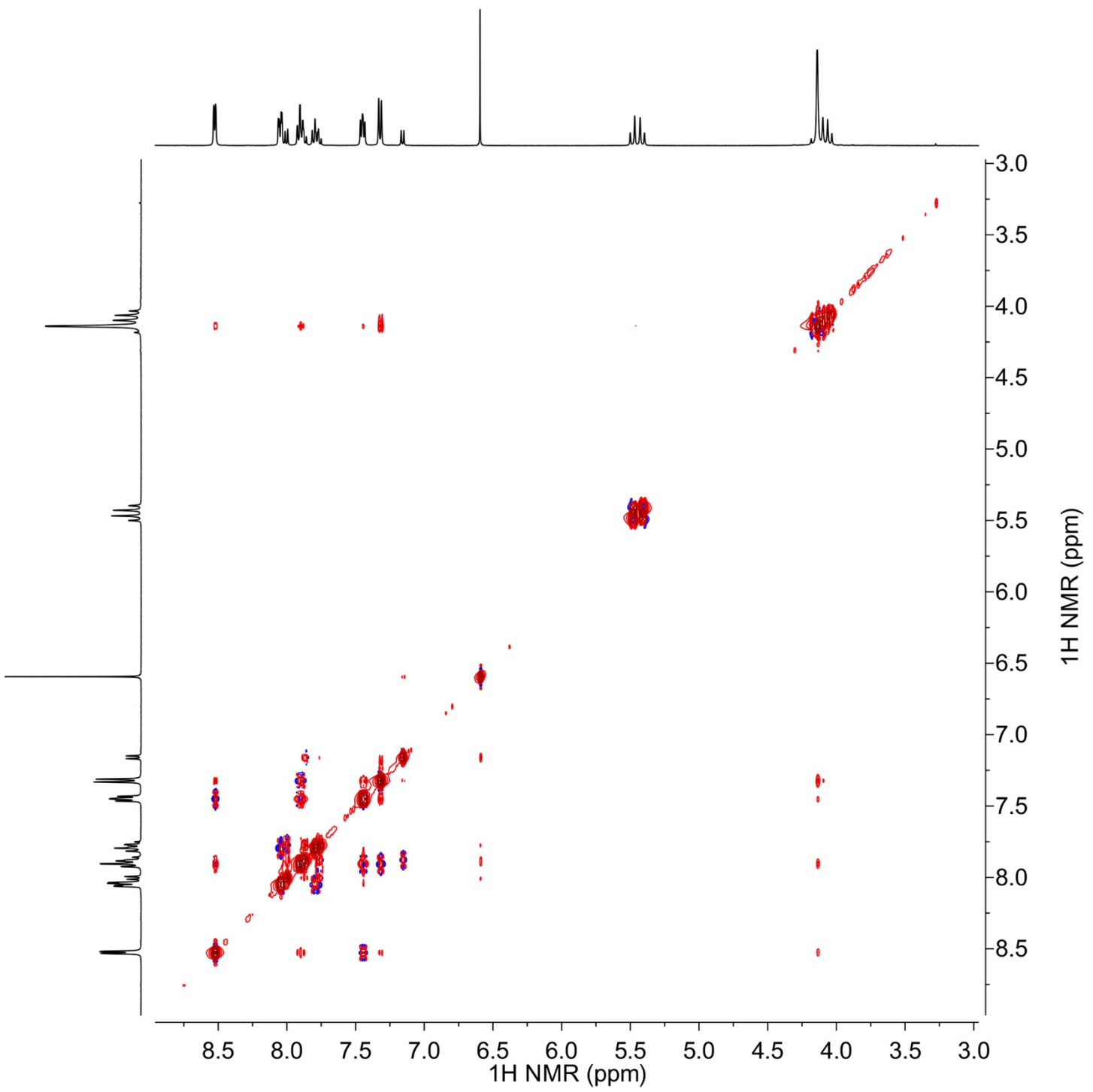


Figure S96. ^1H - ^1H NOESY spectrum of 3.

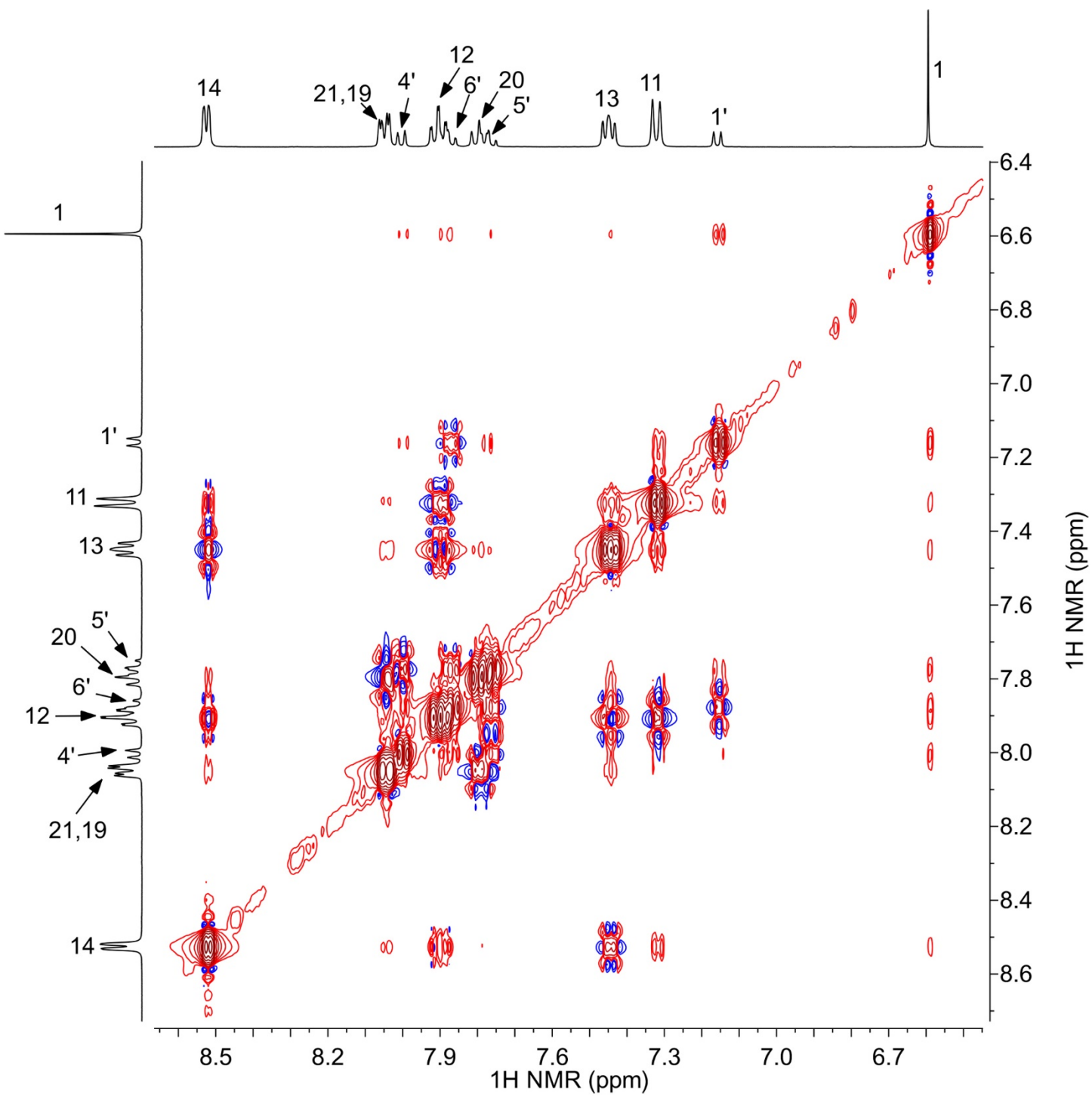


Figure S97. Expansion of ^1H - ^1H NOESY spectrum of **3** from 6.4 to 8.7 ppm.

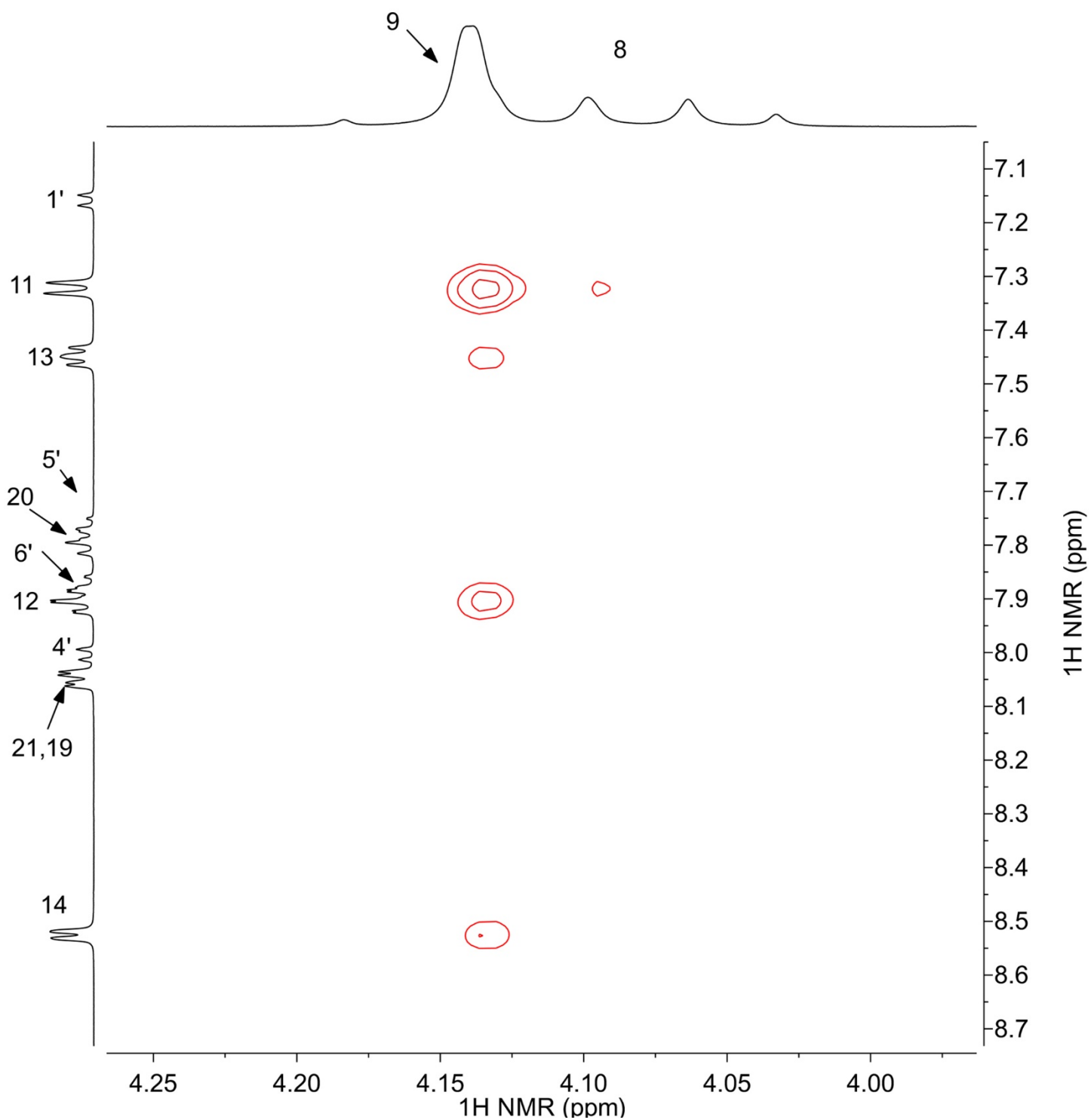


Figure S98. Expansion of ^1H - ^1H NOESY spectrum of **3** from 4.0 to 4.3 ppm.

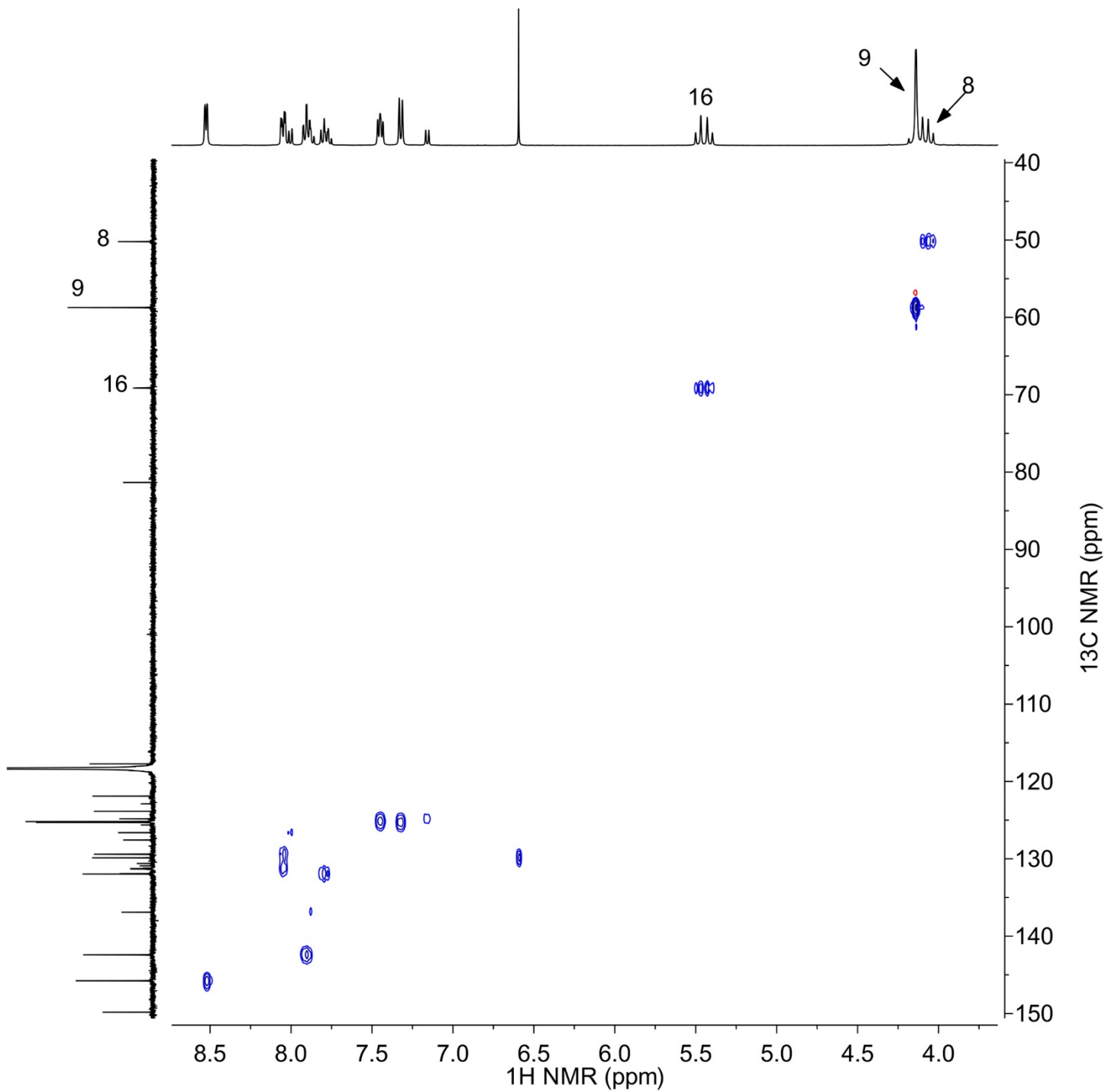


Figure S99. ^1H - ^{13}C HSQC spectrum of 3.

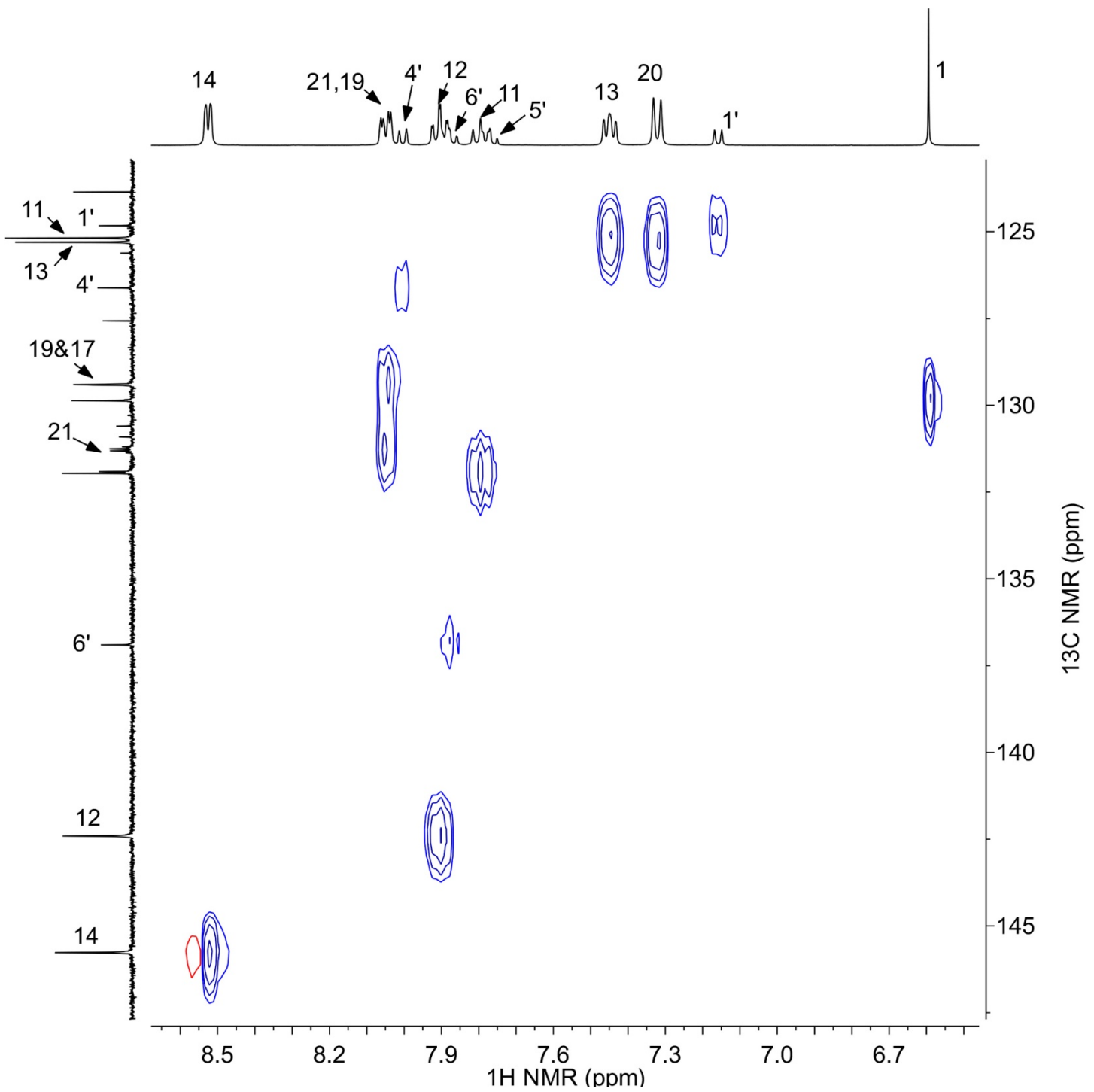


Figure S100. Expansion of ^1H - ^{13}C HSQC spectrum of 3.

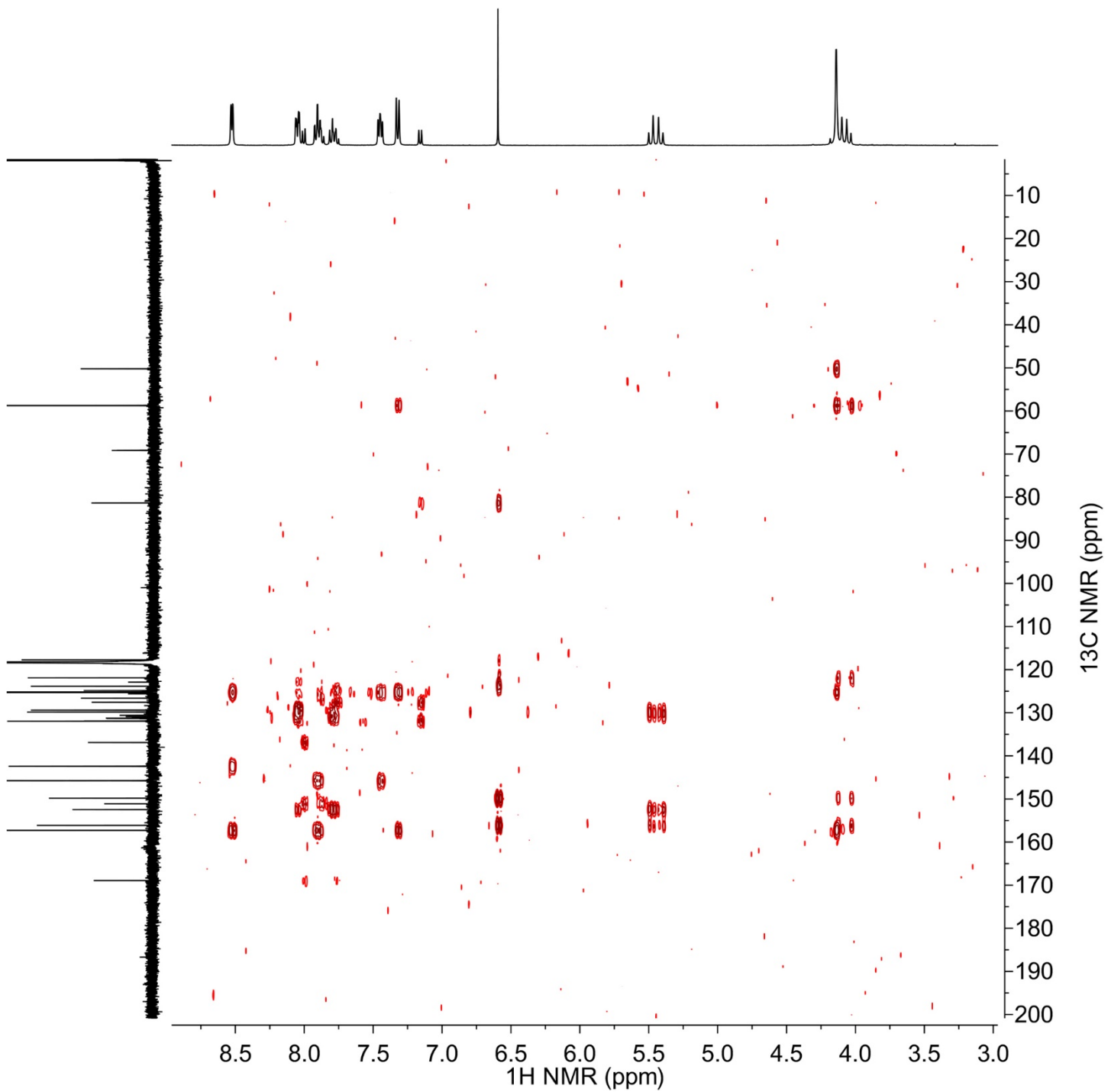


Figure S101. ^1H - ^{13}C HMBC spectrum of **3**.

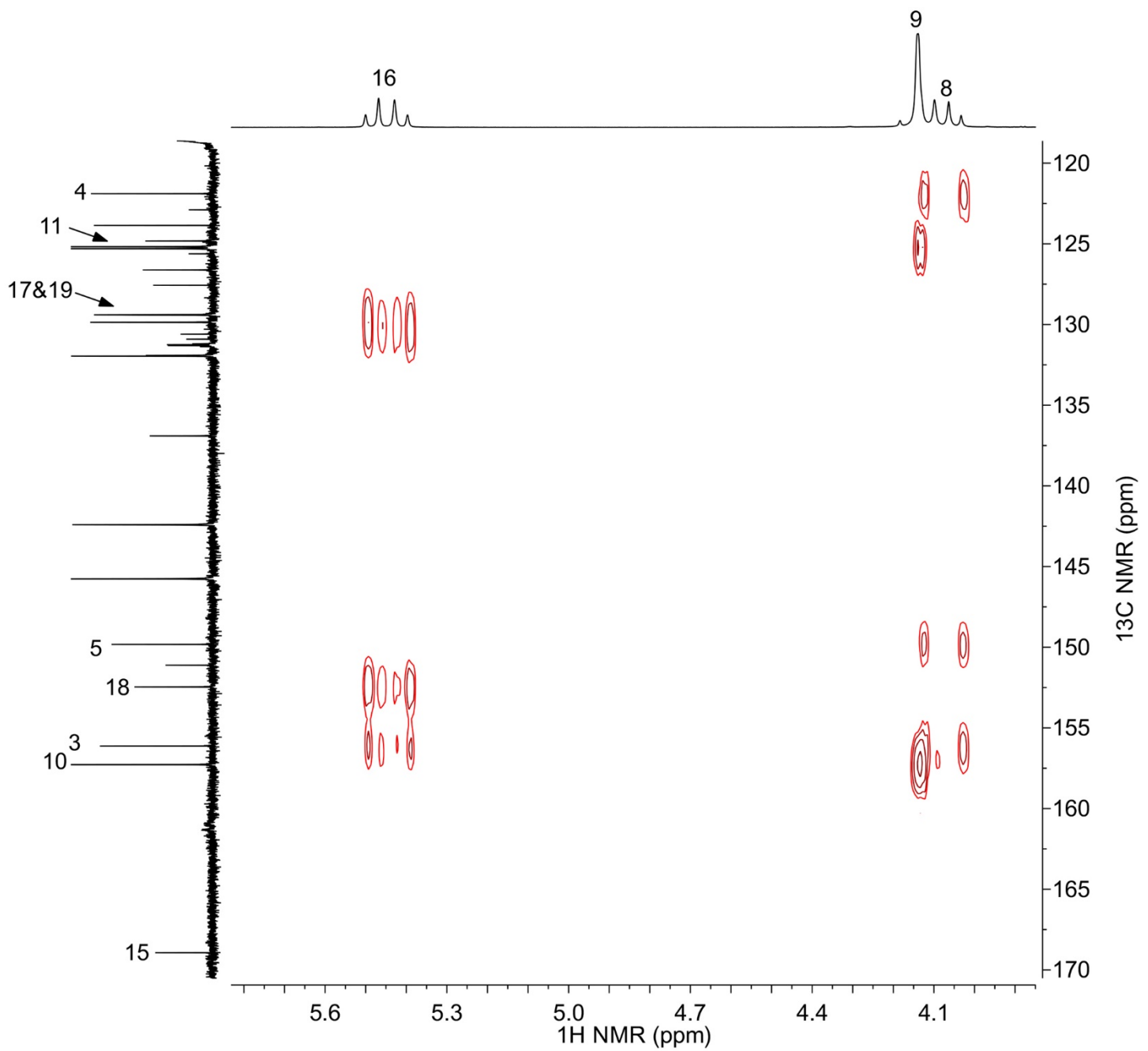


Figure S102. Expansion of ^1H - ^{13}C HMBC spectrum of **3** from 3.9 to 5.8 ppm (^1H) and 120 to 170 ppm (^{13}C).

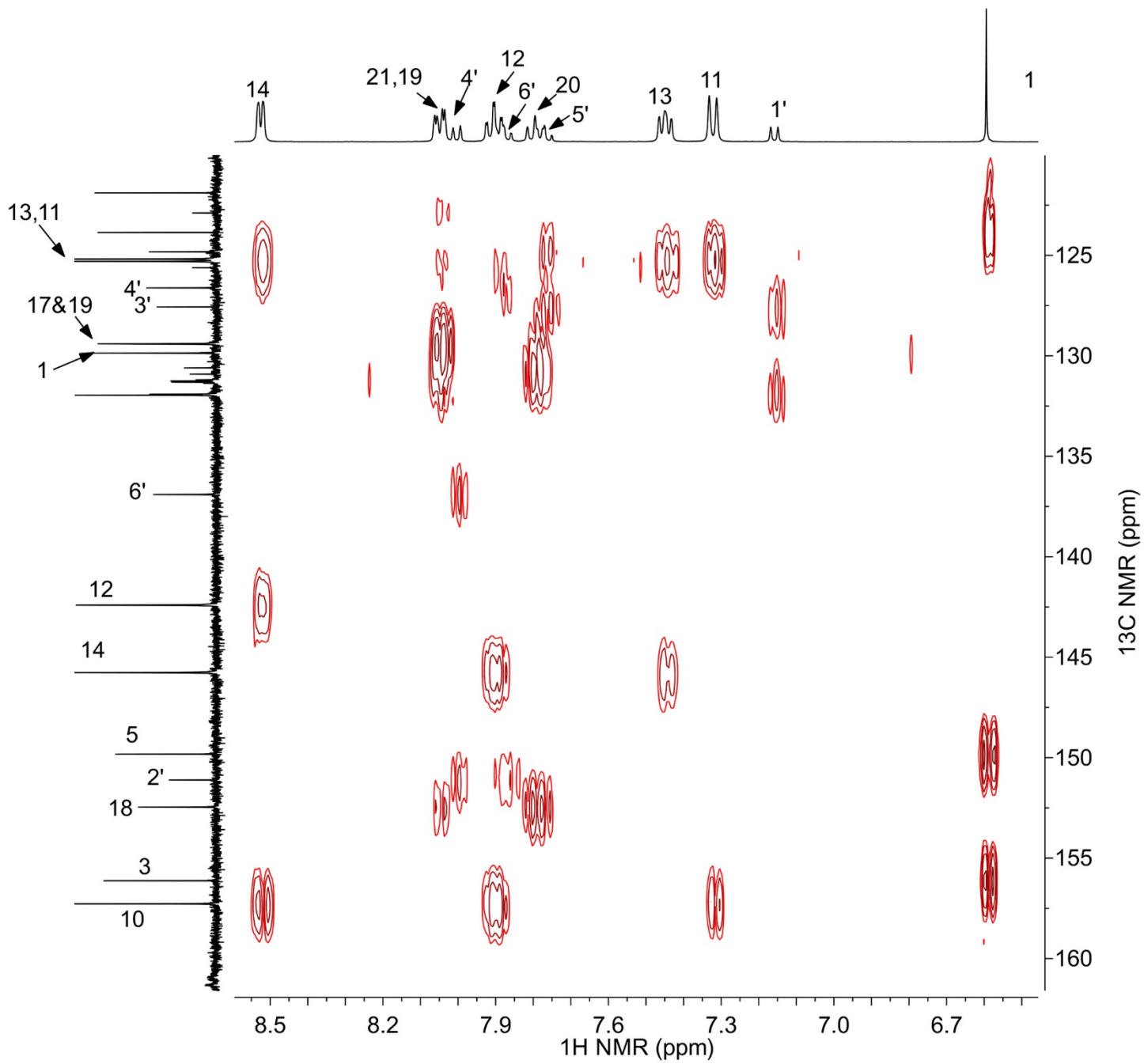


Figure S103. Expansion of ^1H - ^{13}C HMBC spectrum of **3** from 6.5 to 8.6 ppm (^1H) and 120 to 160 ppm (^{13}C).

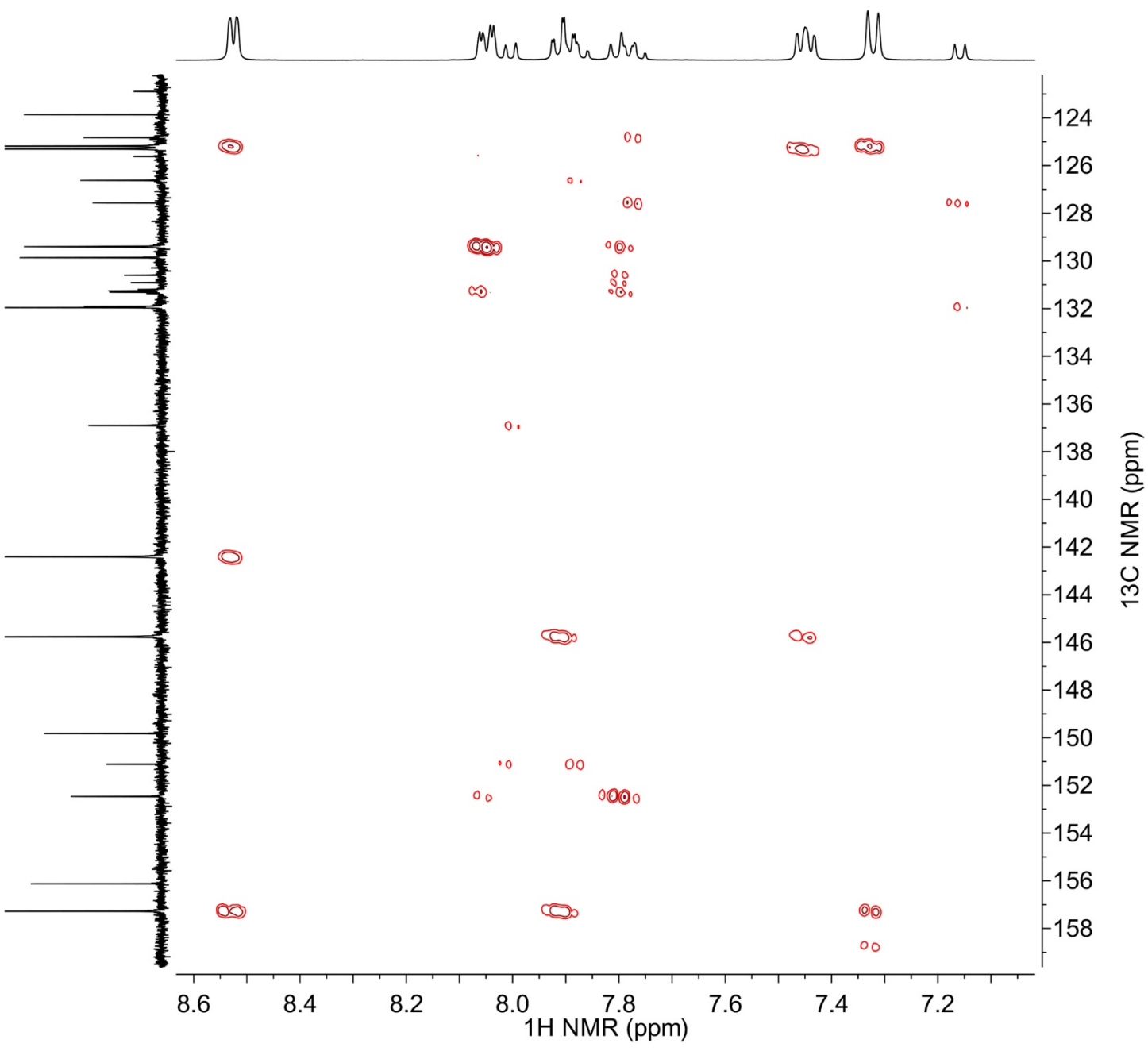


Figure S104. Expansion of high-resolution ^1H - ^{13}C HMBC spectrum of **3** from 7.1 to 8.6 ppm (^1H) and 122 to 160 ppm (^{13}C).

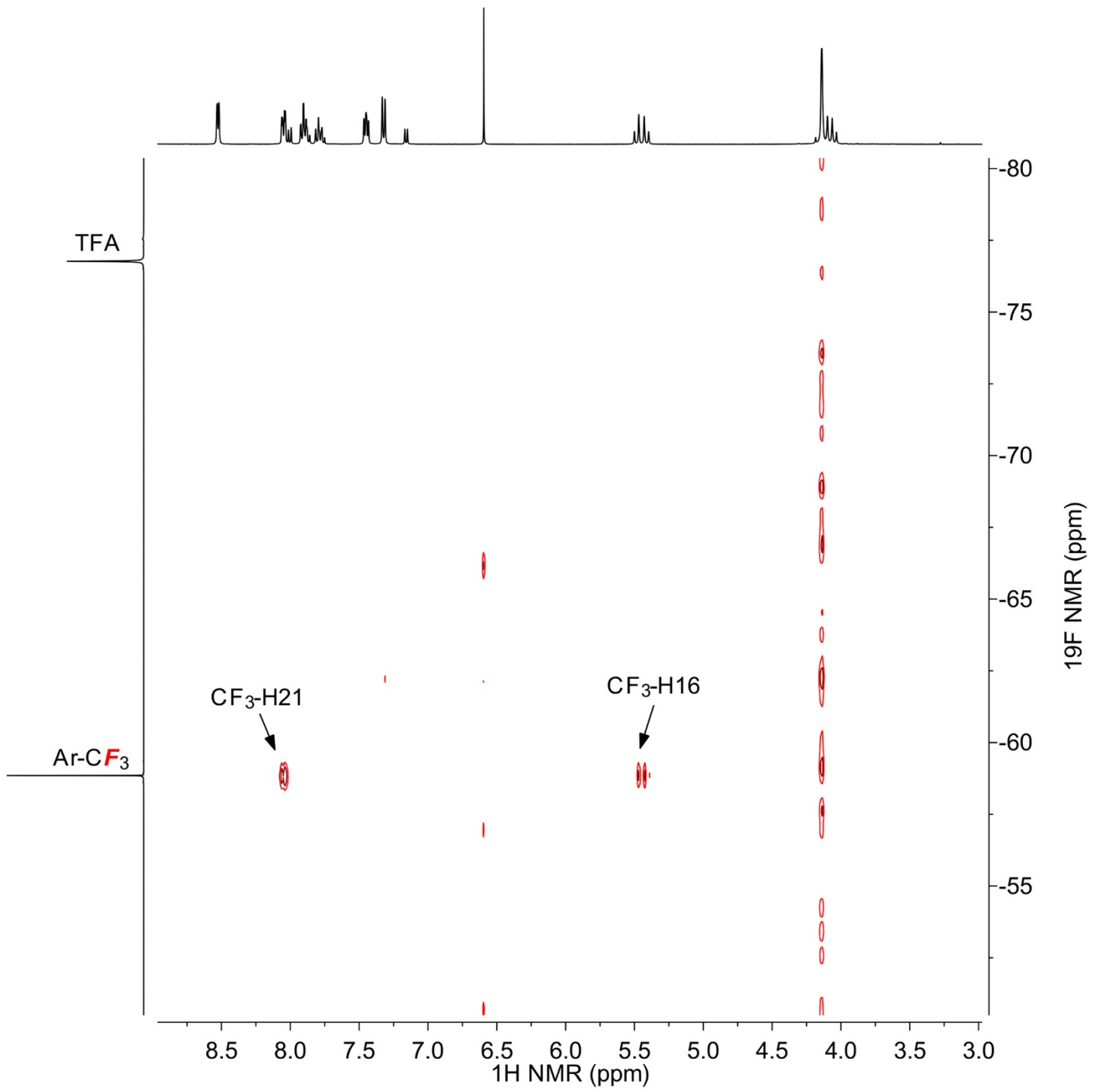


Figure S105. ^1H - ^{19}F HOESY spectrum of 3.

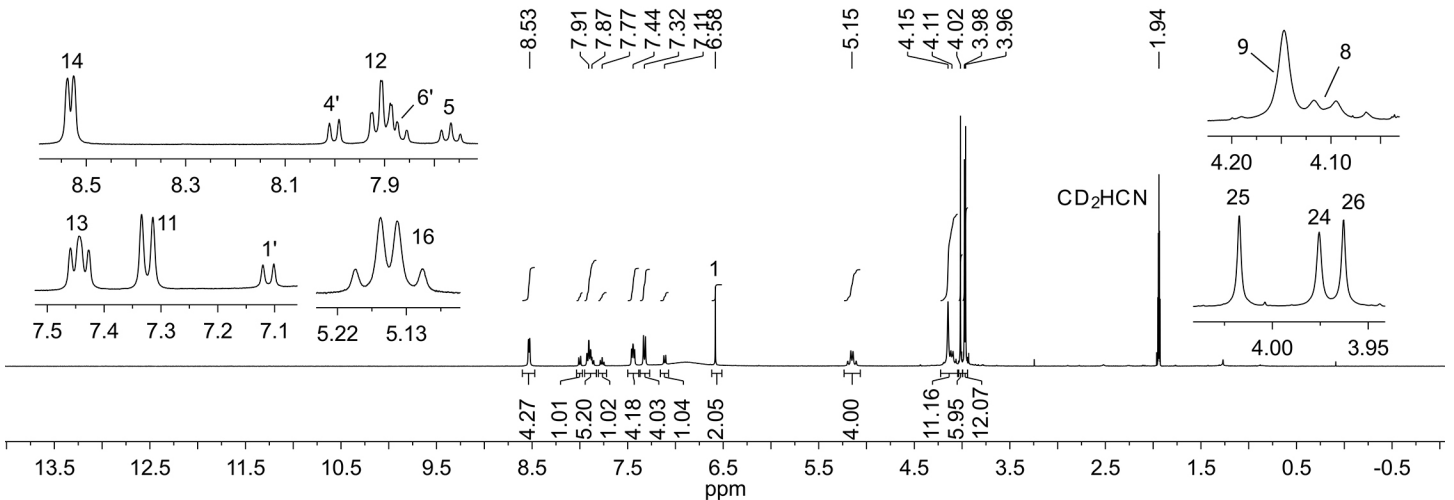


Figure S106. ¹H NMR spectrum of **4**.

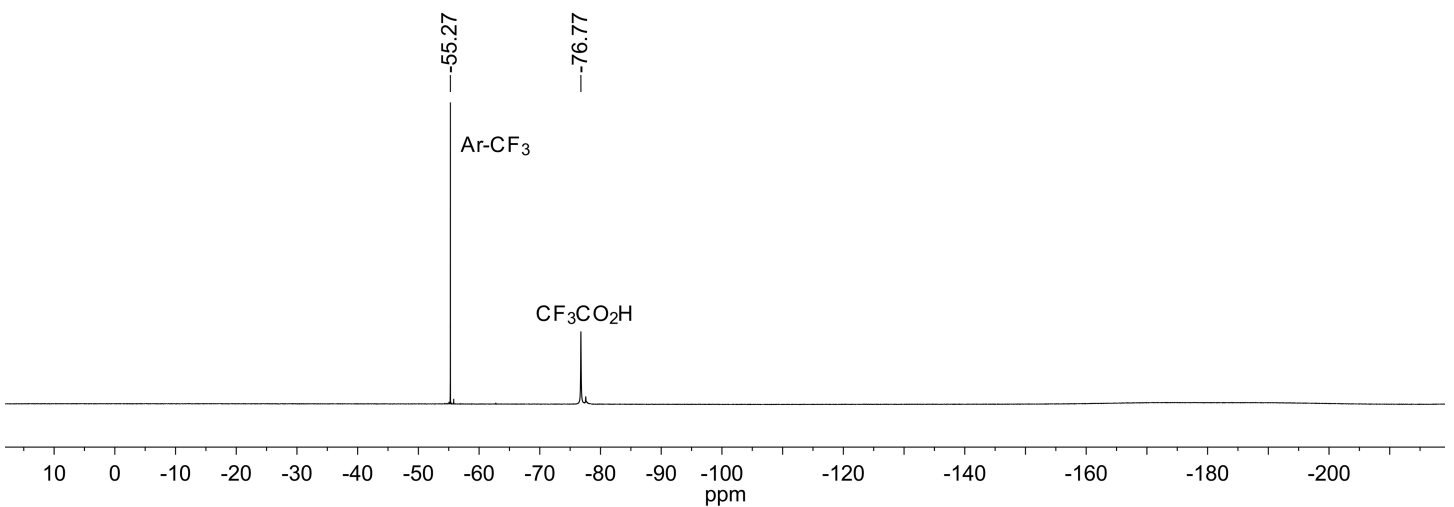


Figure S107. ¹⁹F NMR spectrum of **4**.

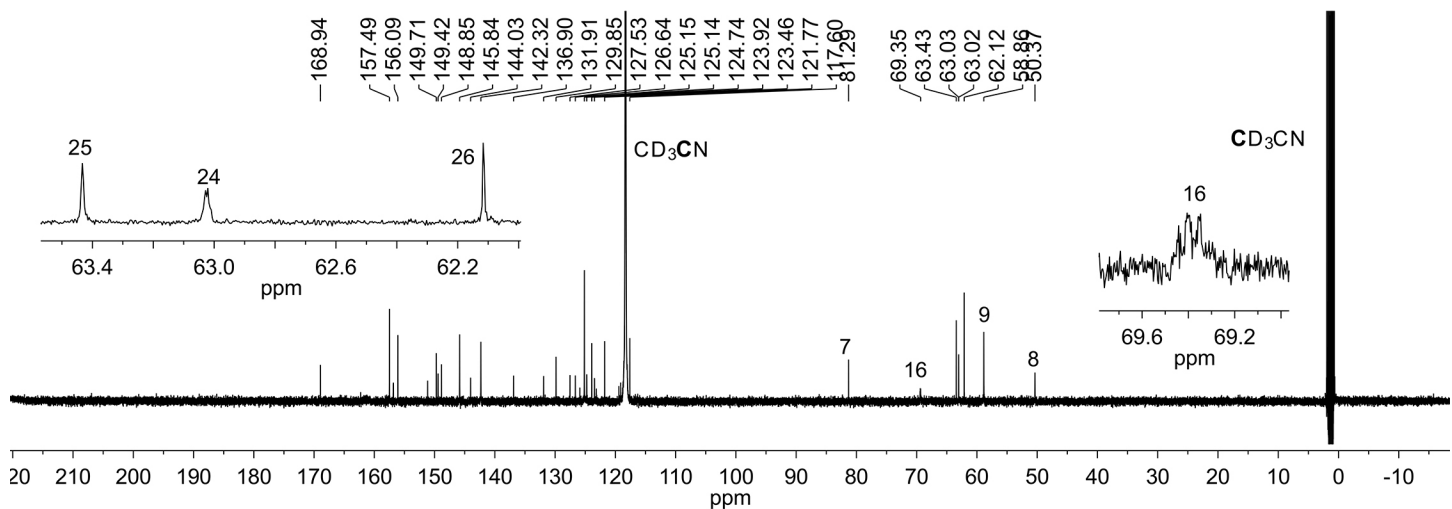


Figure S108. $^{13}\text{C}\{^1\text{H}\}$ NMR spectrum of **4**.

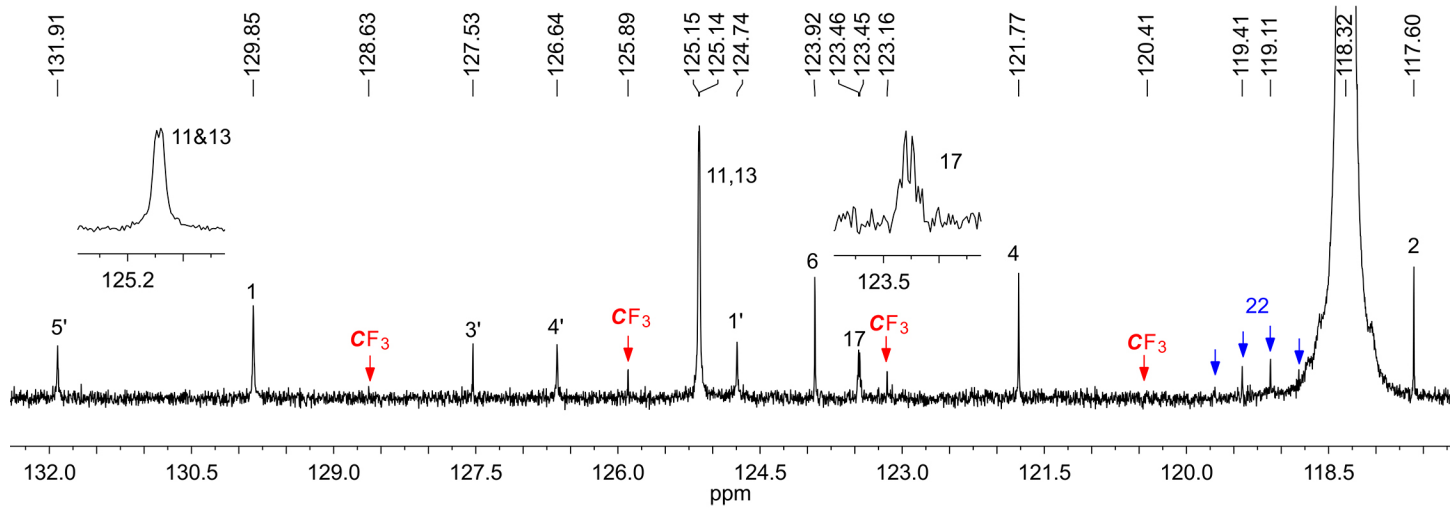


Figure S109. Expansion of $^{13}\text{C}\{^1\text{H}\}$ NMR spectrum of **4** from 117 to 132 ppm.

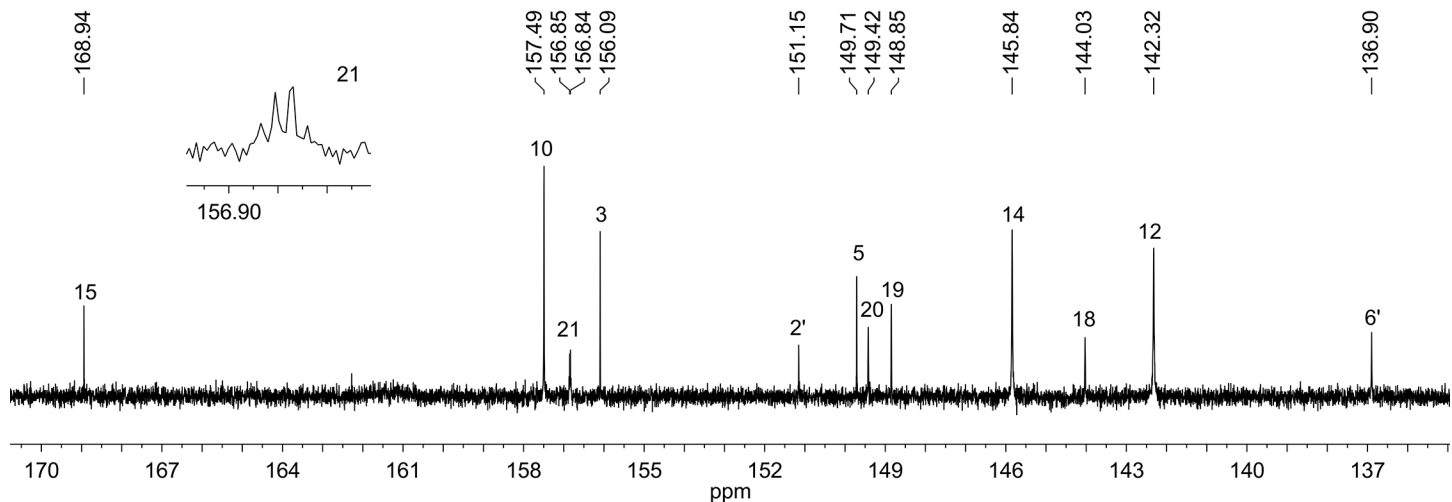


Figure S110. Expansion of $^{13}\text{C}\{^1\text{H}\}$ NMR spectrum of **4** from 135 to 171 ppm.

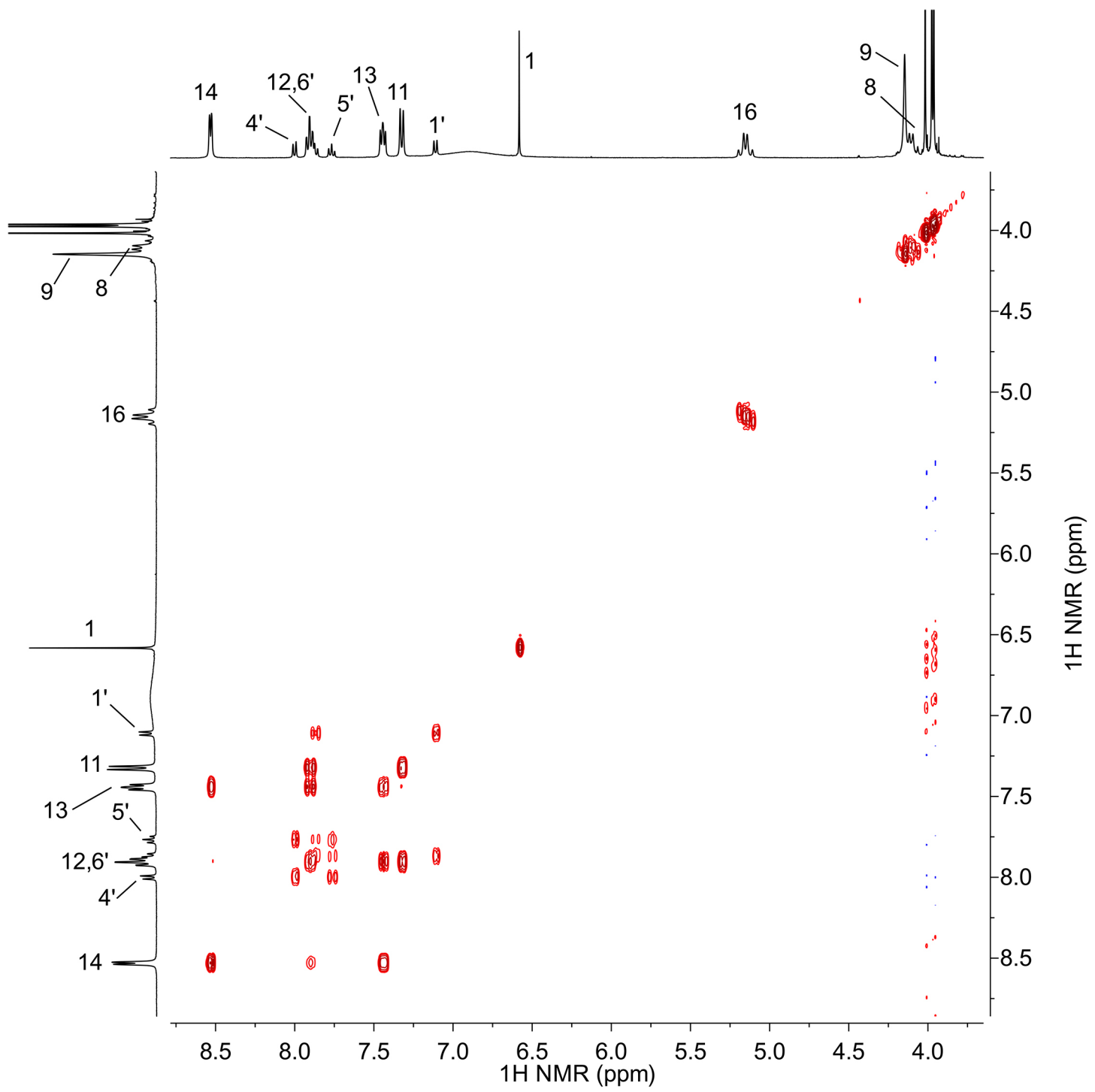


Figure S111. ^1H - ^1H COSY spectrum of **4**.

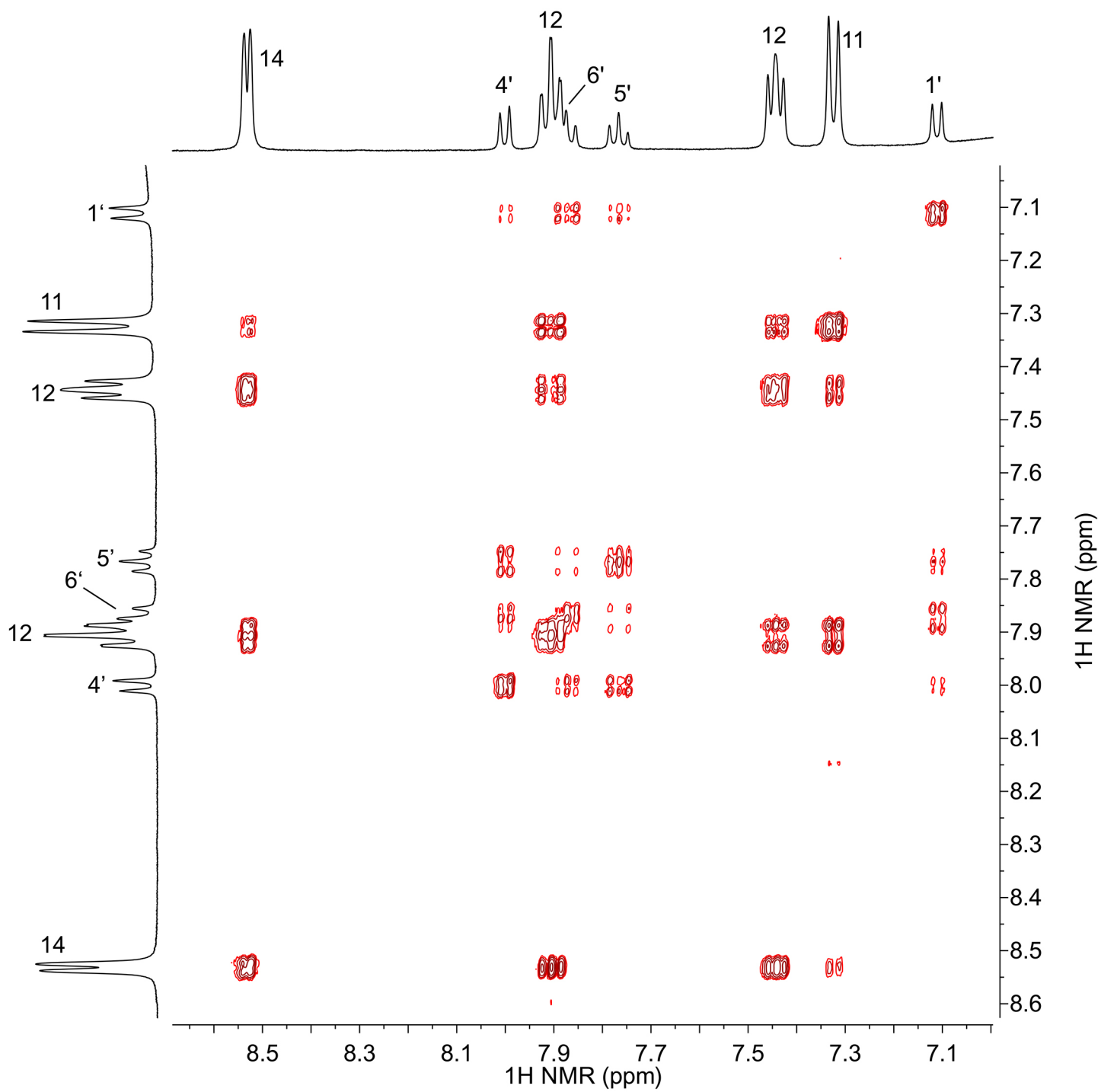


Figure S112. Expansion of ^1H - ^1H COSY spectrum of **4**.

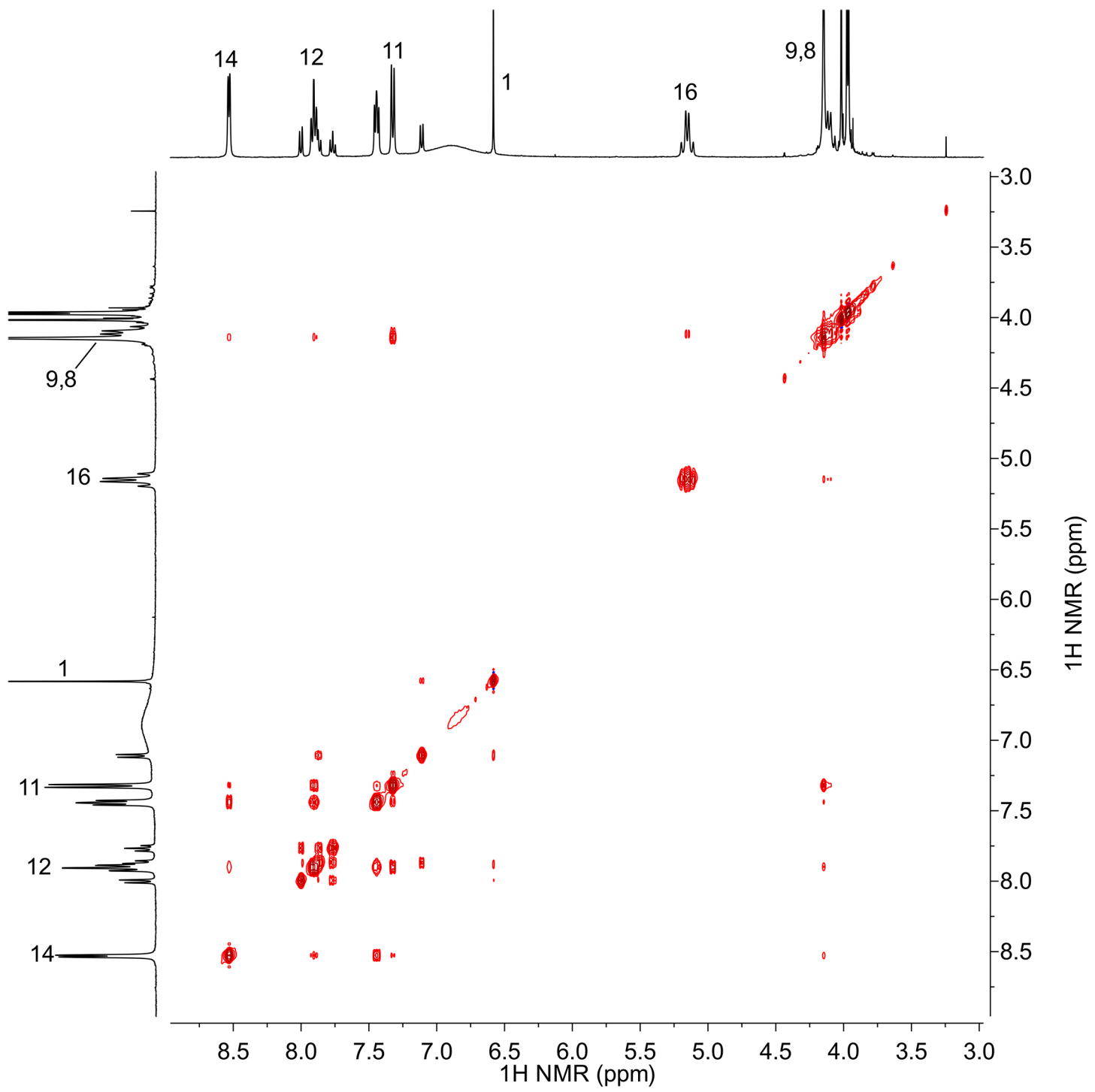


Figure S113. ^1H - ^1H NOESY spectrum of **4**.

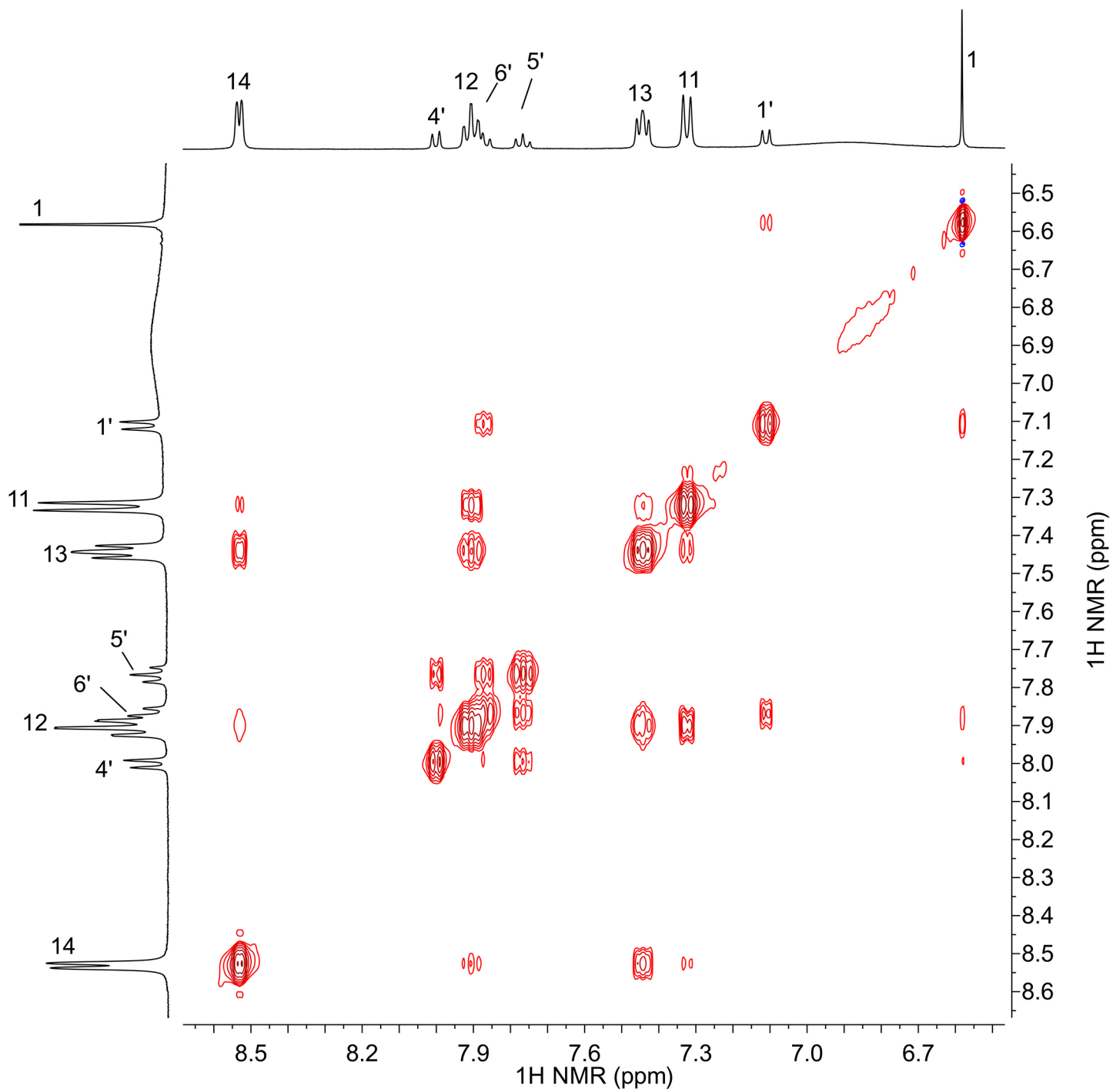


Figure S114. Expansion of ^1H - ^1H NOESY spectrum of **4**.

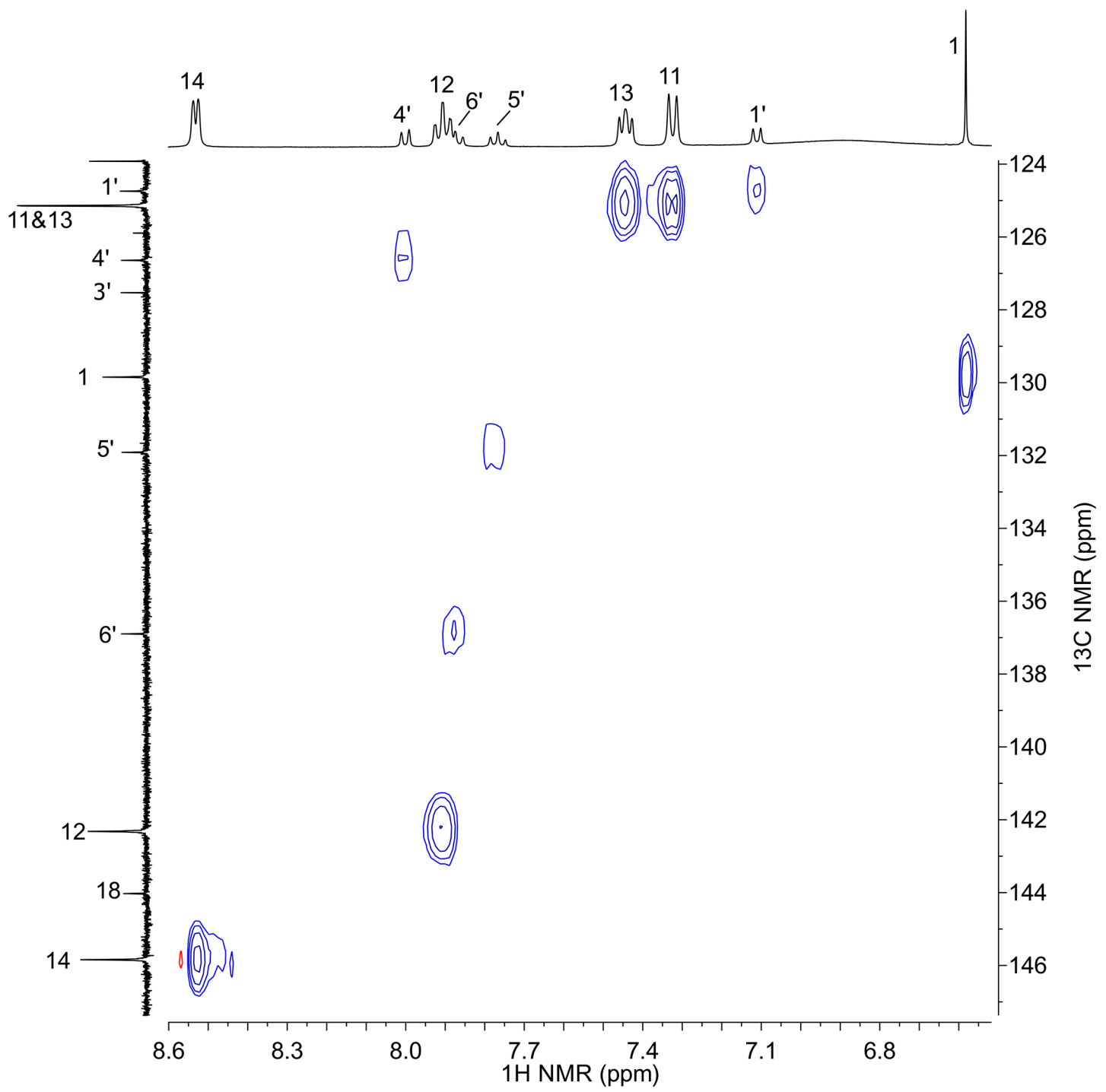


Figure S115. Expansion of ^1H - ^{13}C HSQC spectrum of **4** from 6.5 to 8.6 ppm (^1H) and 124 to 147 ppm (^{13}C).

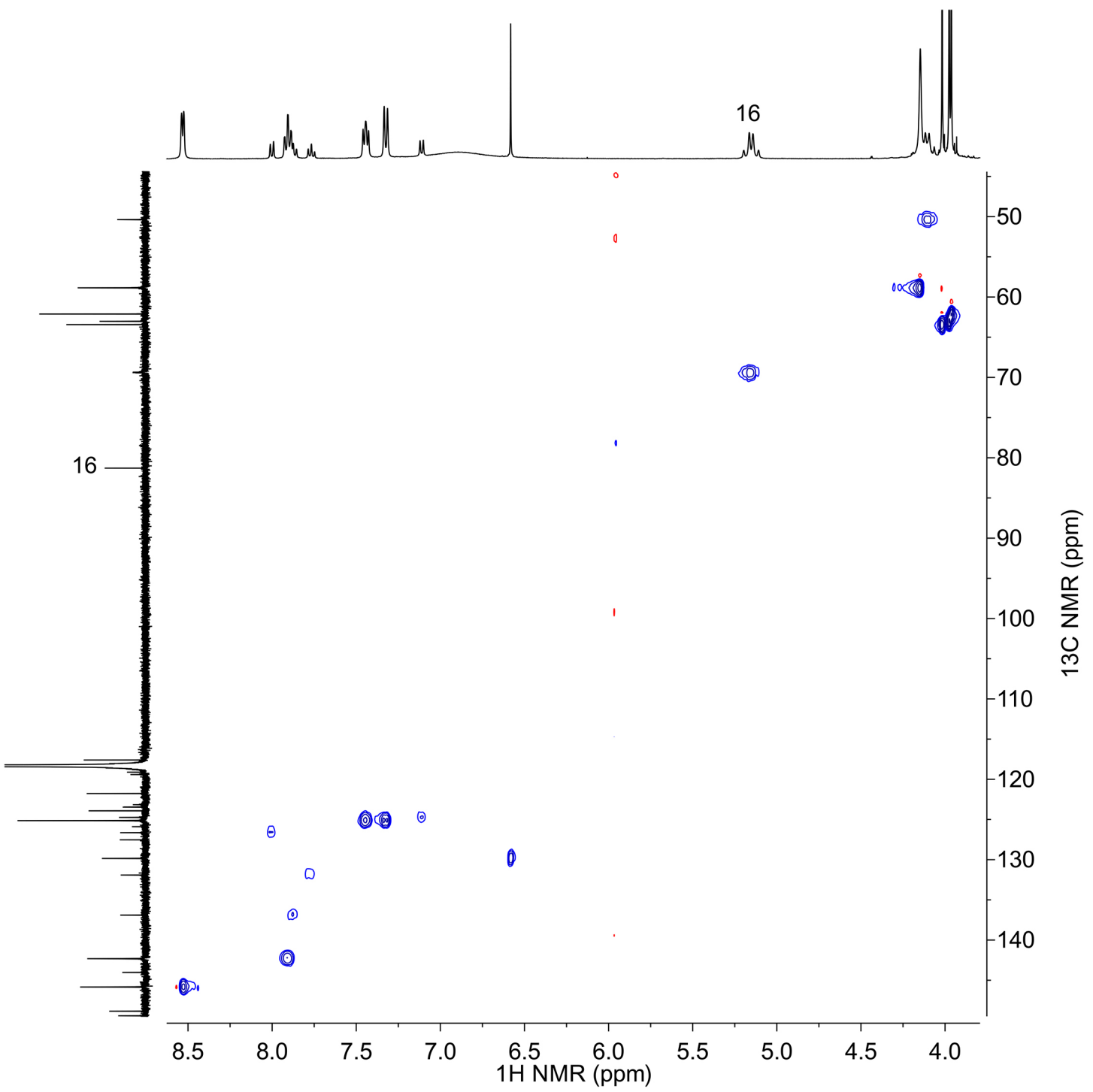


Figure S116. Expansion of ^1H - ^{13}C HSQC spectrum of **4** from 3.9 to 8.6 ppm (^1H) and 45 to 150 ppm (^{13}C).

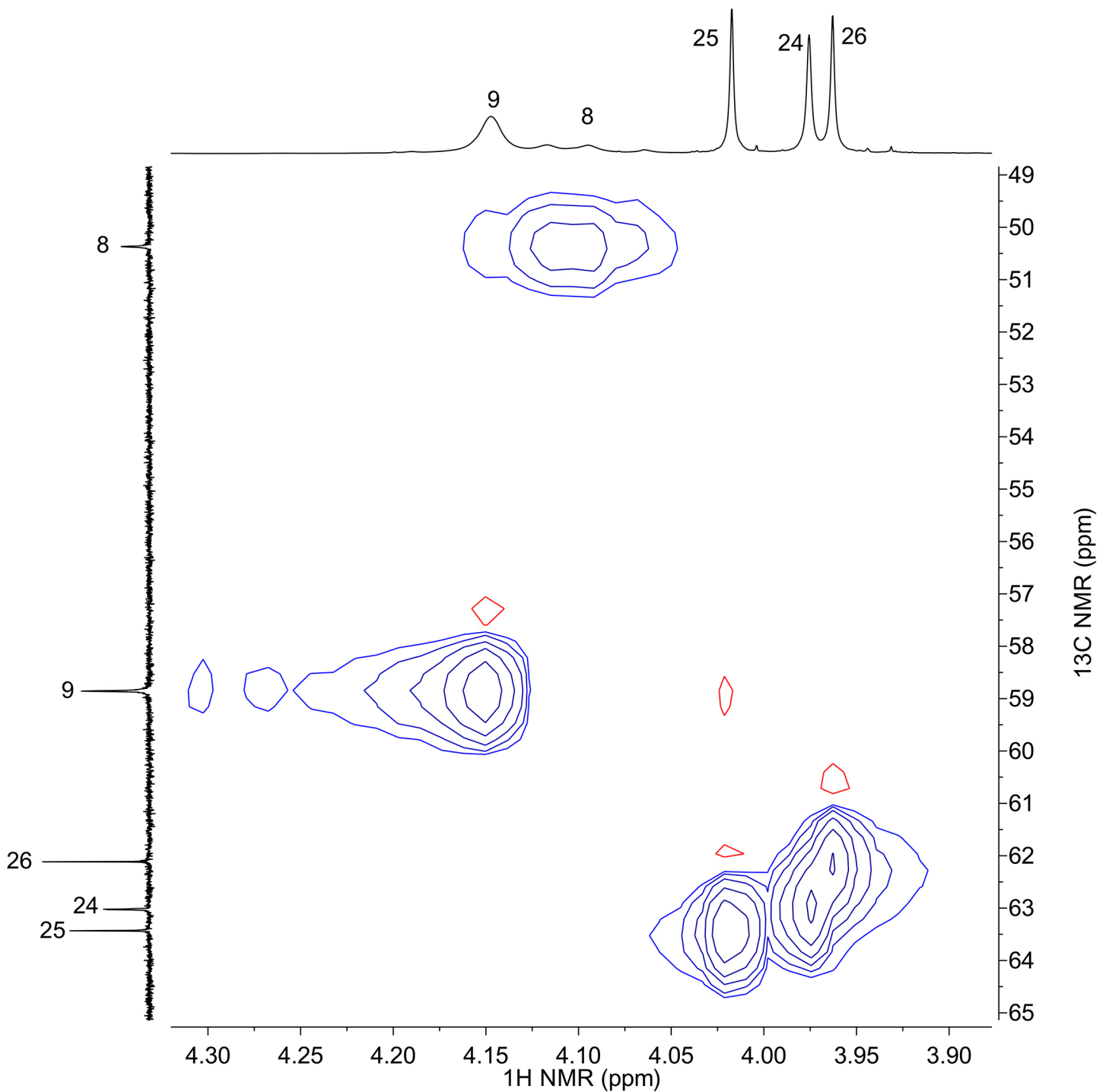


Figure S117. Expansion of ^1H - ^{13}C HSQC spectrum of **4** from 3.9 to 4.3 ppm (^1H) and 49 to 65 ppm (^{13}C).

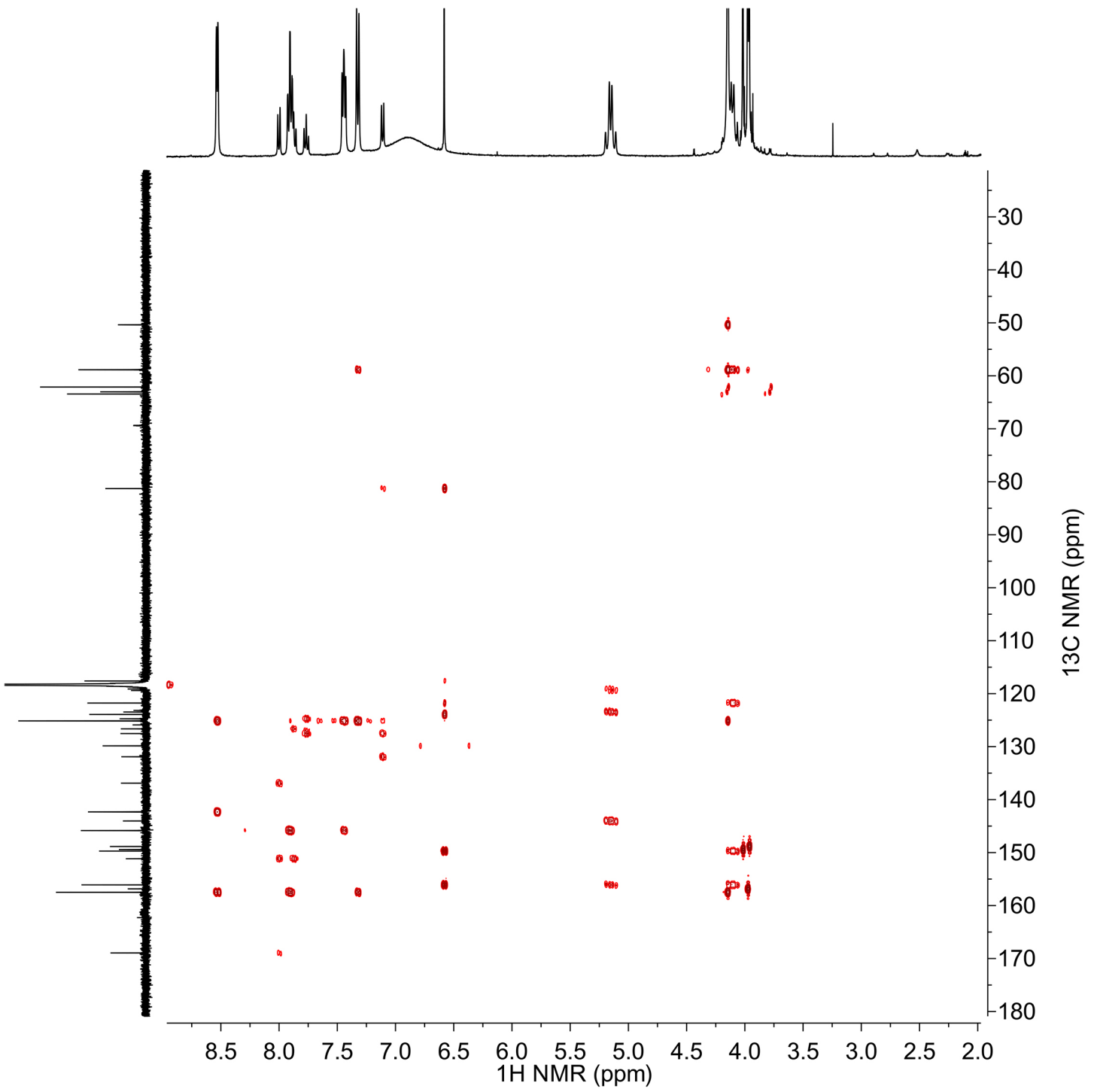


Figure S118. ^1H - ^{13}C HMBC spectrum of **4**.

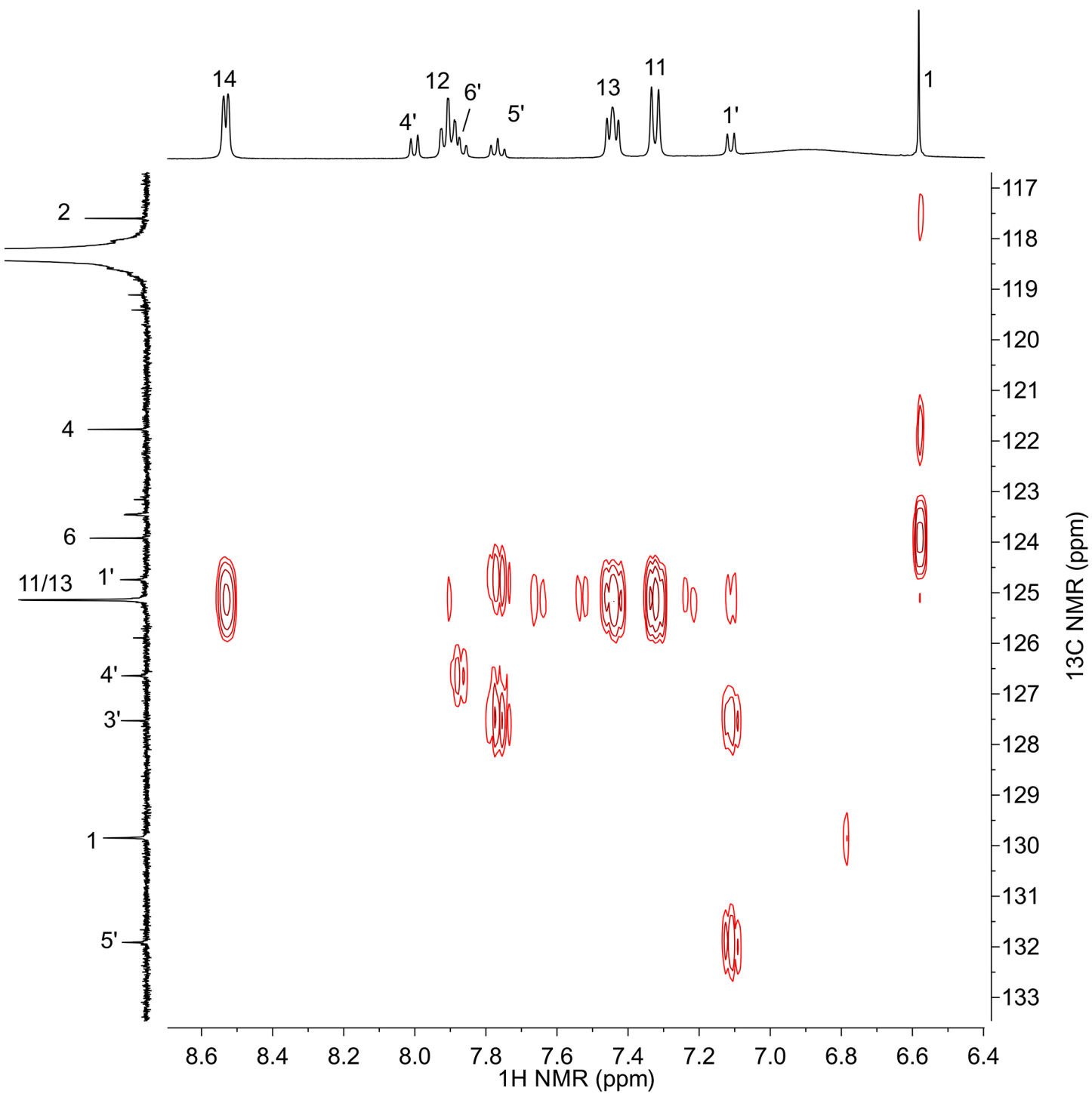


Figure S119. Expansion of ^1H - ^{13}C HMBC spectrum of **4** from 6.4 to 8.6 ppm (^1H) and 117 to 133 ppm (^{13}C).

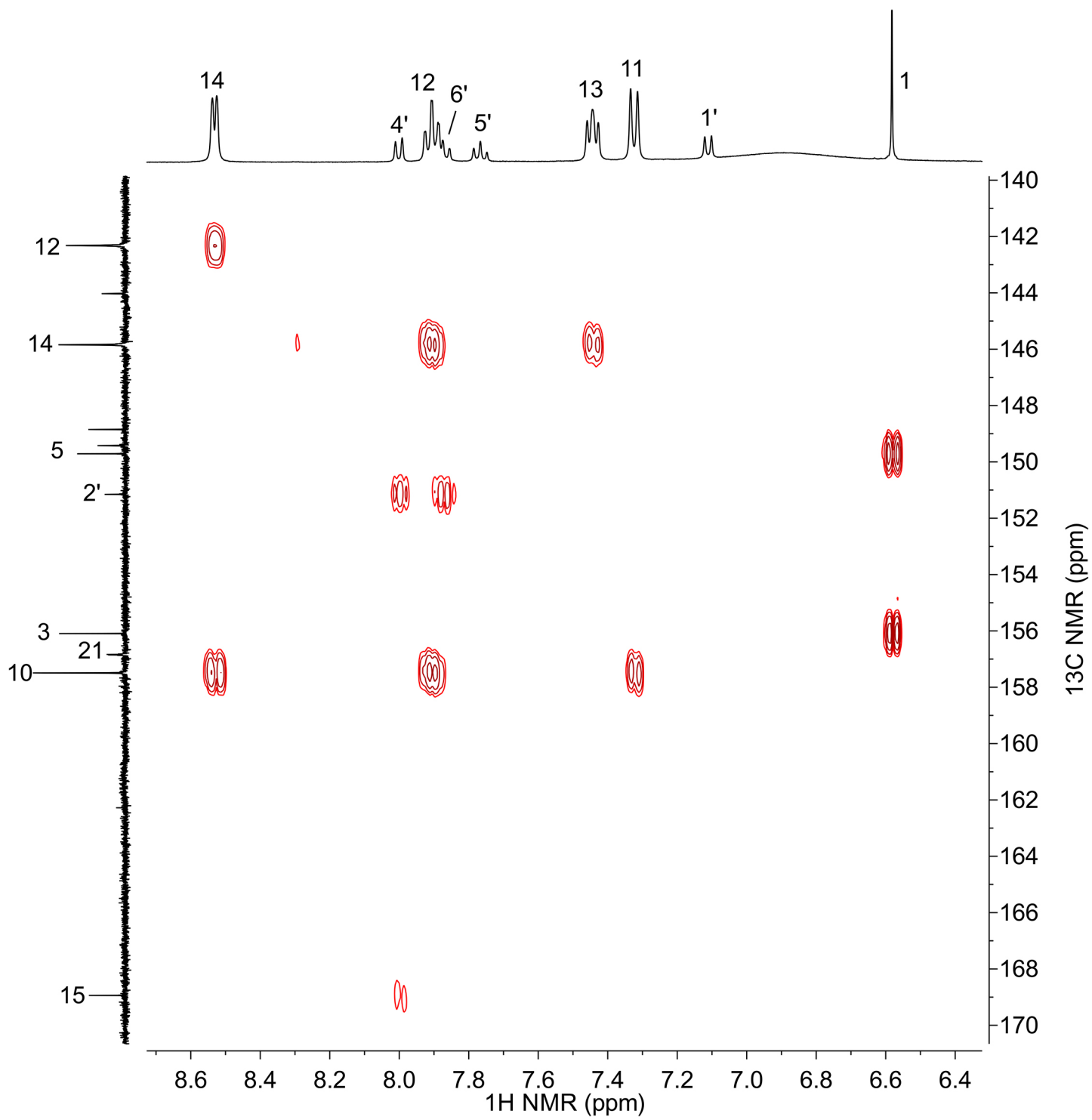


Figure S120. Expansion of ^1H - ^{13}C HMBC spectrum of **4** from 6.4 to 8.6 ppm (^1H) and 140 to 170 ppm (^{13}C).

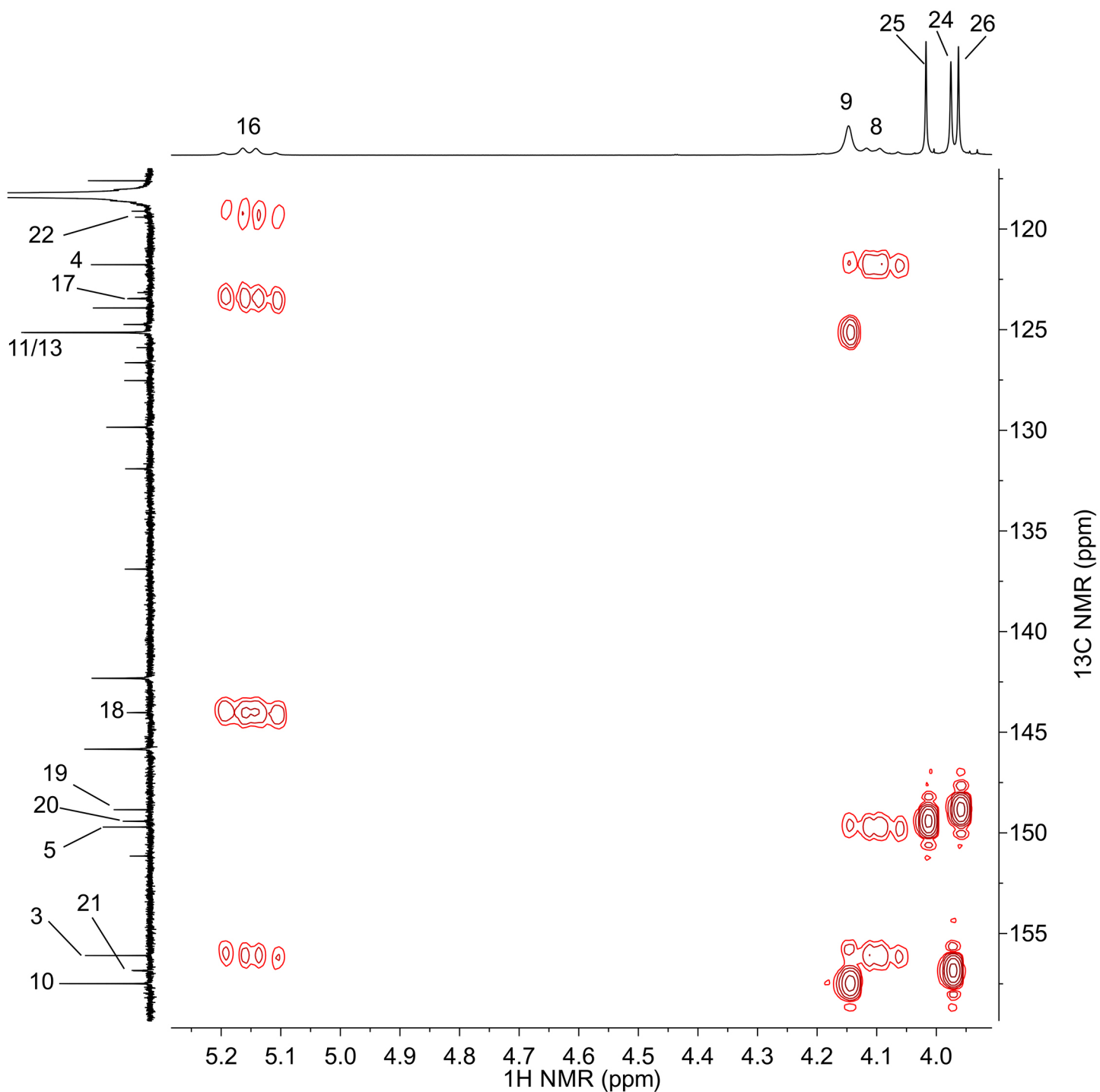


Figure S121. Expansion of ^1H - ^{13}C HMBC spectrum of **4** from 3.9 to 5.3 ppm (^1H) and 115 to 160 ppm (^{13}C).

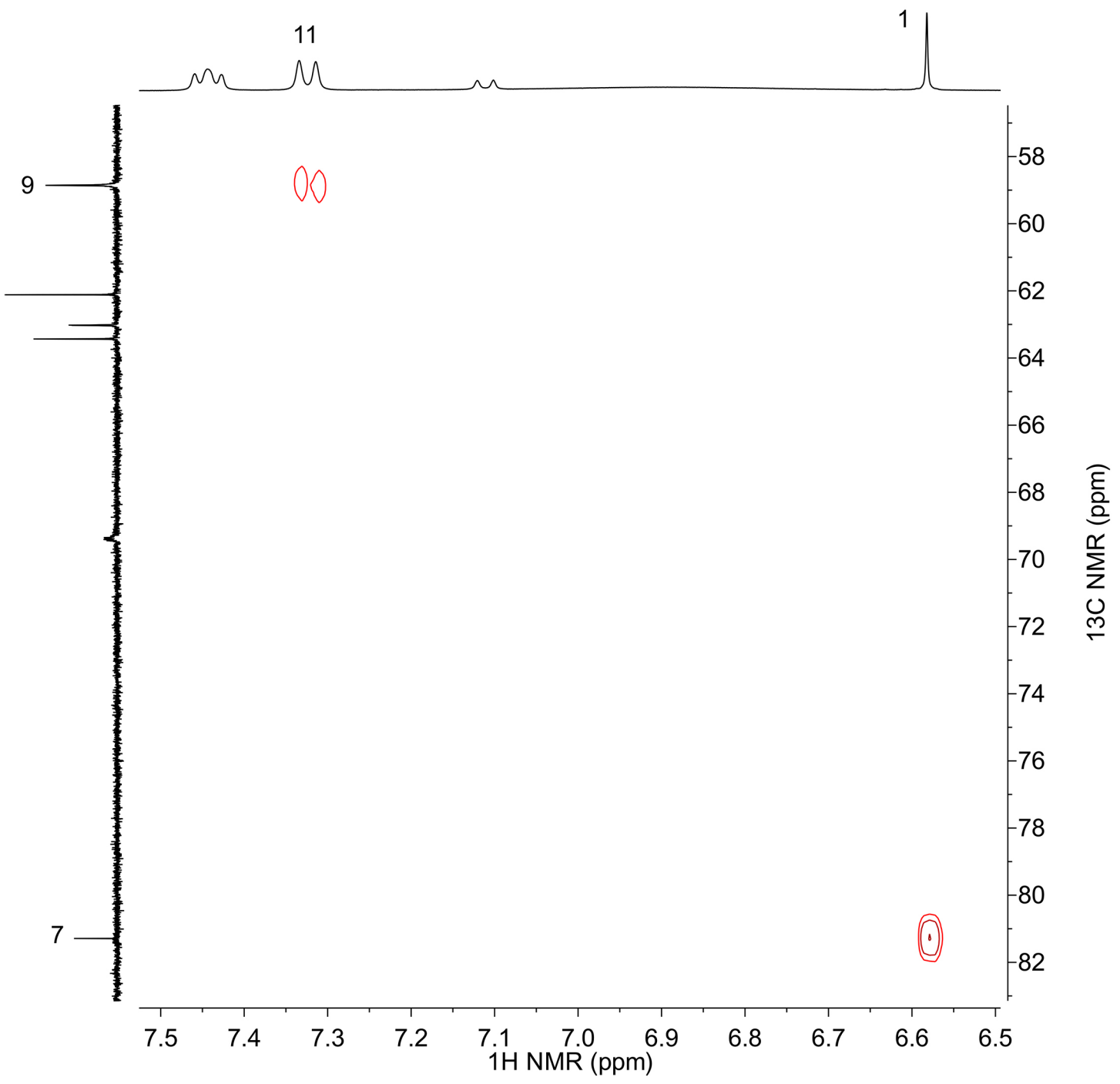


Figure S122. Expansion of ^1H - ^{13}C HMBC spectrum of **4** from 6.5 to 7.5 ppm (^1H) and 57 to 83 ppm (^{13}C).

References.

1. Walkup, G. K.; Burdette, S. C.; Lippard, S. J.; Tsien, R. Y., *J. Am. Chem. Soc.* **2000**, *122*, 5644-5645.
2. Zastrow, M. L.; Radford, R. J.; Chyan, W.; Anderson, C. T.; Zhang, D. Y.; Loas, A.; Tzounopoulos, T.; Lippard, S. J., *ACS Sens.* **2016**, *1*, 32-39.
3. Gottlieb, H. E.; Kotlyar, V.; Nudelman, A., *J. Org. Chem.* **1997**, *62*, 7512-7515.
4. Apfel, C.; Banner, D. W.; Bur, D.; Dietz, M.; Hubschwerlen, C.; Locher, H.; Marlin, F.; Masciadri, R.; Pirson, W.; Stalder, H., *J. Med. Chem.* **2001**, *44*, 1847-1852.
5. Li, L.; Mu, X.; Liu, W.; Wang, Y.; Mi, Z.; Li, C.-J., *J. Am. Chem. Soc.* **2016**, *138*, 5809-5812.
6. Pincioli, V.; Biancardi, R.; Visentin, G.; Rizzo, V., *Org. Process Res. Dev.* **2004**, *8*, 381-384.
7. Frisch, M. J.; Trucks, G. W.; Schlegel, H. B.; Scuseria, G. E.; Robb, M. A.; Cheeseman, J. R.; Scalmani, G.; Barone, V.; Mennucci, B.; Petersson, G. A.; Nakatsuji, H.; Caricato, M.; Li, X.; Hratchian, H. P.; Izmaylov, A. F.; Bloino, J.; Zheng, G.; Sonnenberg, J. L.; Hada, M.; Ehara, M.; Toyota, K.; Fukuda, R.; Hasegawa, J.; Ishida, M.; Nakajima, T.; Honda, Y.; Kitao, O.; Nakai, H.; Vreven, T.; Montgomery Jr., J. A.; Peralta, J. E.; Ogliaro, F.; Bearpark, M. J.; Heyd, J.; Brothers, E. N.; Kudin, K. N.; Staroverov, V. N.; Kobayashi, R.; Normand, J.; Raghavachari, K.; Rendell, A. P.; Burant, J. C.; Iyengar, S. S.; Tomasi, J.; Cossi, M.; Rega, N.; Millam, N. J.; Klene, M.; Knox, J. E.; Cross, J. B.; Bakken, V.; Adamo, C.; Jaramillo, J.; Gomperts, R.; Stratmann, R. E.; Yazyev, O.; Austin, A. J.; Cammi, R.; Pomelli, C.; Ochterski, J. W.; Martin, R. L.; Morokuma, K.; Zakrzewski, V. G.; Voth, G. A.; Salvador, P.; Dannenberg, J. J.; Dapprich, S.; Daniels, A. D.; Farkas, Ö.; Foresman, J. B.; Ortiz, J. V.; Cioslowski, J.; Fox, D. J. *Gaussian 09*, Gaussian, Inc.: Wallingford, CT, USA, 2009.
8. Barone, V.; Cossi, M., *J. Phys. Chem. A* **1998**, *102*, 1995-2001.
9. Cossi, M.; Rega, N.; Scalmani, G.; Barone, V., *J. Comput. Chem.* **2003**, *24*, 669-681.
10. Kowalczyk, T.; Lin, Z.; Voorhis, T. V., *J. Phys. Chem. A* **2010**, *114*, 10427-10434.
11. Burdette, S. C.; Walkup, G. K.; Spangler, B.; Tsien, R. Y.; Lippard, S. J., *J. Am. Chem. Soc.* **2001**, *123*, 7831-7841.